DOCTOR OF PHILOSOPHY

Investigating the role of MyD88 signalling pathway in immune mediated diseases

Petrova, Tsvetana

Award date:
2019

Investigating the role of MyD88 signalling pathway in immune mediated diseases

Tsvetana Petrova

A thesis submitted for the degree of Doctor of Philosophy

University of Dundee, May 2019

Table of Contents

List of figures

List of tables

Acknowledgments

I would like to thank Simon Arthur for all the help and advice during my PhD, for giving me enough balance of supervision and freedom and for patiently listening to my ideas, which were not very reasonable most of the time. I am very grateful to Sambit Nanda for all the help with the ABIN1 project and for proofreading my thesis, and also for the support he gave me during stressful moments and when the science was not going the way I wanted. I am very grateful to all the people I met in Simon Arthur lab for making the work a lot more enjoyable and for sharing many cakes together, especially Rangeetha, Iain and Manuel. I would like to thank Momchil Razsolkov, who helped a lot with some of the experiments during his PhD rotation project and Linda Sinclair for introducing to me the area of immunometabolism and proofreading a chapter of this thesis. I am also grateful to Rhucha Sutavini, Bettina Meier and Manjula Nagala for their supervision during my rotation projects. I would like to acknowledge my thesis committee members Paul Crocker and Marios Stavridis. I would also like to thank Professor Philip Cohen for giving me the opportunity to continue working on the ABIN1 project.

My work has been supported by many people in the Cell Signalling and Immunology Division. I would like to acknowledge Sarah Thomson, Manuel and Sambit for helping with the *in vivo* experiments. The research carried out would not be possible without the members of the Flow cytometry services and the Resource Units and the generous support from the Wellcome Trust.

Finally I would like to thank my partner for all the support during my PhD and for the last minute Microsoft word formatting advices and my family and friends for all the help during the last four years. I am very happy that I had the chance to meet Tamara and I promise at some point I will do a postdoc in Madrid.

Declaration

I hereby declare that the following thesis is based on the results of investigations conducted by myself, and that this thesis is of my own composition. Work other than my own is clearly indicated in the text by reference to the researchers or their publications. This dissertation has not in whole or in part been previously presented for a higher degree.

Tsvetana Petrova

I certify that Tsvetana Petrova has spent the equivalent of at least nine terms in research work in the Division of Cell Signalling and Immunology, School of Life Sciences, University of Dundee and that she has fulfilled the conditions of the Ordinance General No. 14 of the University of Dundee and is qualified to submit the accompanying thesis in application for the degree of Doctor of Philosophy.

Professor J. Simon C. Arthur

Summary

The Myeloid differentiation primary response protein (MyD88) plays a central role in innate immune signalling by acting as an adaptor protein downstream of most of the Toll-like receptor (TLR) family and all the IL-1 receptor family members. Activation of MyD88 dependent signalling is critical for the immune response during infections, however dysregulation of these pathways can contribute to the development of immune mediated diseases.

The first aim of my thesis was to understand the role IL-33 signalling type 2 innate lymphoid cells and to identify potential targets to modulate their response. Stimulation of ILC2 cells with IL-33 induced phosphorylation of p38 and ERK1/2 and secretion of IL-13, IL-5, IL-6, IL-9 and GM-CSF. Inhibition of p38 using the specific inhibitor VX745 showed that p38 is crucial for cytokine production in ILC2s. MK2 and MK3, two kinases downstream of p38, were also found to regulate production of IL-6 and IL-13. In addition to cytokine production, stimulation of ILC2 cells with IL-33 induced an increase in ILC2 size and granularity. Moreover, IL-33 stimulated ILC2 cells had a higher uptake of the tryptophan metabolite kynurenine in comparison to unstimulated cells, which was dependent on the amino acid transporter Slc7a5.

The second aim in my thesis was to understand the role of the A20 binding inhibitor of NF-κB (ABIN1) in the development of lupus like autoimmunity in mice. Mice carrying a mutation of Asp485 to Asn in the ubiquitin binding domain of ABIN1 develop spontaneous autoimmunity with hallmarks of SLE including splenomegaly, presence of autoreactive antibodies against nuclear antigens and glomerulonephritis. Characterisation of innate immune populations in ABIN1[D485N] mice showed that these mice have a massive increase of Ly6C^{-ve} patrolling monocytes. Crossing ABIN1[D485N] mice to TLR7, MyD88 knock out mice or to mice with catalytically inactive IRAK1 or IRAK4 kinases prevented the increase in the monocytes, suggesting that a TLR7-MyD88-IRAK4-IRAK1 pathway not only drives lupus in ABIN1[D485N] mice but also increases the number of patrolling monocytes. Targeting this pathway using an IRAK4 specific inhibitor blocked the expansion of the Ly6C^{-ve} patrolling monocytes and the disease development in ABIN1[D485N] mice. Therefore, inhibition of the IRAK4 kinase could have beneficial effect in SLE patients with mutation in the *tnip1* genes or dysregulation of the TLR pathways.

Abbreviations

2-DG	2-deoxy-d-glucose
ABIN	A20 binding inhibitor of NF-κB
Alox	arachidonate 5-lipoxygenase
Alt	*Alternaria alternata*
AMPK	5' AMP-activated protein kinase
Areg	Amphiregulin
Arg1	Arginase I
ATP	Adenosine triphosphate
BCH	2-aminobicyclo-(2,2,1)-heptane-2carboxylic acid
Bcl	B cell lymphoma
BMMC	Bone marrow derived mast cells
BMDM	Bone marrow derived macrophages
CaMKKβ	Ca2+/Calmodulin-dependent protein kinase kinase beta
CCL	Chemokine ligand
CD	Cluster of differentiation
CDK	Cyclin-dependent kinase
CHILP	Common helper innate lymphoid progenitor
CLP	Common lymphoid progenitor
COPD	Chronic obstructive pulmonary disease
CRTH2	Prostaglandin D2 receptor 2
CXCL	Chemokine (C-X-C motif) ligand
cysLT	cysteinyl leukotrienes
DAMP	Danger associated molecular pattern

DAPI	4′,6-diamidino-2-phenylindole
DEPTOR	DEP-domain containing mTOR-interacting protein
DMSO	Dimethyl sulfoxide
DNA	Deoxyribonucleic acid
DSS	Dextran sulfate sodium
DUB	Deubiquitinase
ECAR	Extracellular acidification rate
eIF4E	Eukaryotic translation initiation factor 4E
ERK	Extracellular signal-regulated kinases
eWAT	Epididymal white adipose tissue
FADD	Fas-associated protein with death domain
FAK	Focal adhesion kinase
FALC	Fat-associated lymphoid clusters
FSC-A	Forward side scatter-area
GDP	Guanosine diphosphate
Gfi	Growth factor independent 1 transcriptional repressor
GM-CSF	Granulocyte-macrophage colony-stimulating factor
Grb2	Growth factor receptor-bound protein
GSK	Glycogen synthase kinase
GTP	Guanosine triphosphate
H&E	Haematoxylin & Eosin
HIF1α	Hypoxia-inducible factors
IBD	Inflammatory bowel disease
ICOS	Inducible T-cell co-stimulator
ICOSL	Inducible T-cell co-stimulator ligand
IFN	Interferon

Ig	Immunoglobulin
IKK	IκB kinase
IL-1RAcP	IL-1 receptor accessory protein
IL-33	Interleukine-33
ILC	Innate lymphoid cells
ILCP	Innate lymphoid cells progenitor
IRAK	Interleukin-1 receptor associated kinases
ITIM	intracellular immunoreceptor tyrosine based inhibitory motif
JNK	c-Jun N-terminal kinases
KLRG1	Killer cell lectin-like receptor subfamily G
Kyn	kynurenine
LAT	Large neutral amino acid transporter
Lin	Lineage
LPS	Lipopolysaccharide
LSEC	Liver sinusoidal endothelial cells
LTC	Leukotriene C
LTD4	Leukotriene D4
LTi	Lymphoid tissue induces
LUBAC	Linear ubiquitin assembly complex
MAPK	Mitogen activated protein kinase
MCP-1	Monocyte Chemoattractant Protein-1
M-CSF	Macrophage colony-stimulating factor
MetEnk	Methionine Enkephalin
MMP	Multipotent progenitor cells
mRNA	Messenger ribonucleic acid
mTOR	Mechanistic target of rapamycin

MyD88	myeloid differentiation primary response 88
NEMO	NF-κB
NET	Neutrophils extracellular traps
NF-HEV	nuclear factor from high endothelial venules
NF-κB	Nuclear factor kappa-light-chain-enhancer of activated B cells
NKT	natural killer T cells
NLR	Nucleotide oligomerization domain (NOD)-like receptor
NLS	Nuclear localisation sequence
NMU	Neuromedin
nor-NOHA	Nω-hydroxy-nor-arginine
OCR	oxygen consumption rate
OVA	Ovalbumin
PAMP	Pathogen-associated molecular pattern
PBS	Phosphate-buffered saline
PDK1	Phosphoinositide-dependent kinase-1
PGD	Prostaglandin
PI3K	Phosphoinositide 3-kinase
PIN	prolyl-csi-trans isomerase
PIP3	phosphatidylinositol-3,4,5-triphosphate (PI(3,4,5,)P3)
PPAR	peroxisome proliferator-activated receptor
PRR	Pattern recognition receptors
RA	Rheumatoid Arthirtis
Raptor	Regulatory protein associated with mTOR
Rictor	Rapamycin insensitive companion of mTOR
RIG	Retinoic acid-inducible gene
RIPK	Receptor-interacting serine/threonine-protein kinase 1

RLR	RIG-I-like receptor
ROR-γ	RAR-related orphan receptor gamma
RSK	Ribosomal S6 kinase
RXR	Retinoid X receptor
SCF	Stem cell factor
SCF	Stem cell factor
SEM	Standard error of the mean
SH	Src homology
SIGIRR	Single Ig IL-1-related receptor
SLE	Systemic lupus erythematosus
SNEC	Sinonasal epithelial cells
SPC	Surfactant protein C
SSC-A	Side scatter area
ST2	Suppressor of tumorogenicity
TAB	TAK1 binding protein
TAK1	Transforming growth factor beta-activated kinase 1
TCR	T cell receptor
TGF-β	Transforming growth factor beta
TIR	Toll-IL-1-intracellular domain
TLR	Toll-like receptor
TNF	Tumor Necrosis Factor
TNFAIP3	TNF-α induced protein 3
TNFR	Tumor necrosis factor receptor
TRADD	Tumor necrosis factor receptor type 1-associated DEATH domain
TRAF	TNF receptor associated factors
TSC2	Tuberos Sclerosis Complex

TSLP	Thymic stromal lymphopoietin
TTP	Tristetraprolin
Ub	Ubiquitin
Ucp1	Uncoupling protein 1
VHL	Von Hippel–Lindau tumor suppressor
WT	Wild type
β2AR	β2-adrenergic receptor

I. Introduction

1.1. Innate immune system

The immune system evolved to protect the organisms from infectious microorganisms and other pathogens and also plays a role in tissue homeostasis and tumour surveillance. There are two branches of the immune system: innate and adaptive immunity. While the innate immune system is conserved and present in all multicellular organisms, the adaptive immunity is characterised in higher vertebrates (Pancer and Cooper, 2006). The innate immune system is divided into a cellular and humoral components. Innate immune cells include granulocytes such as neutrophils, eosinophils and mast cells, macrophages and dendritic cells and the recently identified group of innate lymphoid cells (Eberl et al., 2015). The humoral component is represented by the complement system, which is made of plasma proteins involved in the opsonisation of pathogens and their removal by phagocytosis (Sarma and Ward, 2011). Innate immunity provides the first line of host defence and innate immune cells rely on a variety of germline-encoded receptors to recognise conserved molecular structures expressed by the pathogens (Turvey and Broide, 2010). This concept was first introduced in 1989 by Charles Janeway who described these receptors as Pattern Recognition Receptors (PRRs) and correspondingly their ligands as Pathogen-Associated Molecular Patterns (PAMPs) (Janeway, 1989). The PRRs include Toll-like receptors (TLR), Nucleotide Oligomerization Domain (NOD)-like receptors (NLR), Retinoic acid-Inducible Gene I (RIG-I)-like receptors and C-type lectins (Takeuchi and Akira, 2010). In addition to the PAMPs, innate immune cells can sense the so called danger signals or Danger Associated Molecular Patterns (DAMPs), also referred as alarmins, which are released upon tissue damage or necrosis. DAMPs include endogenous molecules such as the high mobility group box1 protein (HMGB-1), IL-33, IL-1α, uric acid, ROS, DNA and ATP (Bianchi, 2007). Finally, innate immune such as NK cells can recognise “altered self” or missing structures. For example virus infected cells or cancer cells which lose the expression of MHC I are then recognised and killed by NK cells (Jaeger and Vivier, 2012).

1.2. Receptors utilising MyD88 adaptor protein

The MyD88 protein plays a central role in the inflammatory pathways and acts as an adaptor protein downstream of members of the TLR family (with the exception of TLR3) and the IL-1 receptor family. MyD88 signalling is involved in both innate and adaptive immune responses to a variety of pathogens (Deguine and Barton, 2014). The MyD88 protein is made up of a C-terminal TIR domain (Toll/IL-1R homology domain), which mediates the interaction with TLRs and IL-1R members, an intermediate domain and N-terminal death domain (DD) (Bonnert et al., 1997). The last associates with the DD of the IL-1 associated kinases (IRAKs) (Neumann et al., 2007, George et al., 2011). The importance of MyD88 has been highlighted by studies using MyD88 deficient animals. These mice are susceptible to a large number of pathogens and have been extensively used as a model of TLR deficiency (Takeuchi et al., 2000, Feng et al., 2003).

1.2.1. Toll-like receptors

The discovery of the TLR4 in the mid-1990s was a key event in the innate immunity field (Lemaitre et al., 1996). The Toll protein was initially described in Drosophila where it was required for the establishment of dorsal-ventral polarity during development (Anderson et al., 1985). Subsequently it was found that it also mediated survival in response to infection with the fungal pathogen Aspergillus (Lemaitre et al., 1996). In 1997, Medzhitov et al discovered TLR4 as the first mammalian homologous of the Drosophila Toll protein and demonstrated that TLR4 is involved in the activation of NF-κB singling and production of inflammatory cytokines such as IL-1, IL-6 and IL-8 (Medzhitov et al., 1997). The importance of TLR4 in immunity was confirmed by the observation that C3H/HeJ mice, which are resistant to the bacterial endotoxin LPS, had a mutation in the TLR4 gene (Poltorak et al., 1998). In agreement with this, TLR4 knockout mice were also found to be resistant to LPS induced endotoxic shock (Hoshino et al., 1999). 13 TLRs have been described in mice and 10 TLRs in humans, with TLR11/12 and 13 not found in humans (Kawai and Akira, 2010). TLR1, TLR2, TLR4, TLR5 and TLR6 are expressed on the cell surface, whereas TLR3, TLR7, TLR8, TLR9, TLR11, TLR12 and TLR13 have intracellular localisation and are expressed in the endosomes, lysosomes and

endoplasmic reticulum (ER) (Kawai and Akira, 2010, Raetz et al., 2013). The TLRs and their ligands are illustrated in Figure 1.1.

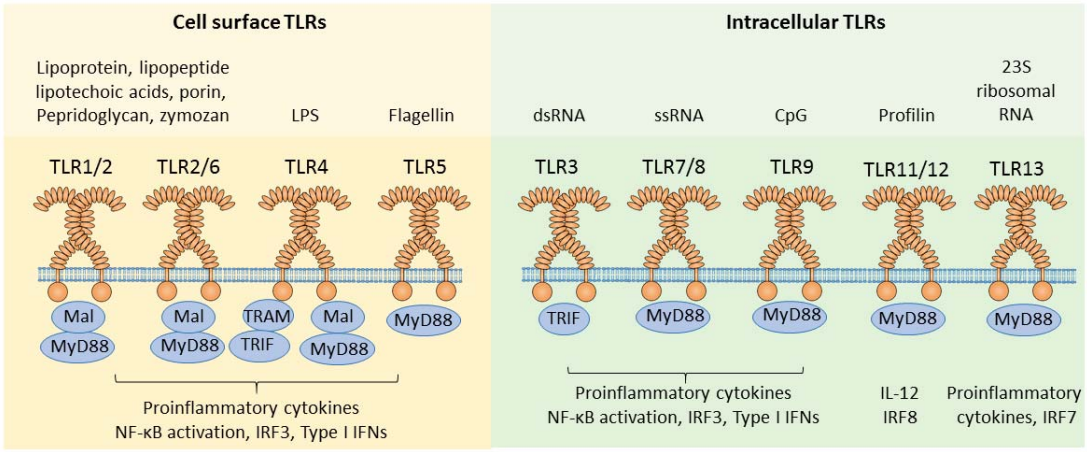

Figure 1.1 Toll-like Receptors.
TLR1/2/4 and 5 are expressed on the cell surface and recognise bacterial and fungal pathogens. TLR2 forms a heterodimeric complex with either TLR1 or TLR6 and recruits MyD88 adaptor protein via a 2nd adaptor Mal. TLR4 recognises LPS and could signals both using TRIF and MyD88 adaptor proteins. The ligand for TLR5 is flagellin. TLR3 binds dsRNA, TLR7/8 recognise ssRNA and TLR9 recognises unmethylated CpG DNAmotifs. TLR11/12 have been shown to bind profilin protein in parasites and TLR13 binds to 23S ribosomal RNA. All intracellular TLR recruit MyD88 adaptor protein apart from TLR3, which binds to TRIF. Activation of the TLRs triggers production of proinflammatory cytokines and NF-κB activation.

TLR2 forms heterodimeric complexes with either TLR1 or TLR6 and recognises lipoproteins, peptidoglycans, zymosan, mannans and others (West et al., 2006). In addition, TLR2 can act as a homodimer and recognise ligands such as the lipoteichoic acids or lipoarabinomannan (Triantafilou et al., 2004, Bhattacharya et al., 2010). TLR3 is recognising double-stranded RNA (dsRNA) and triggers responses mediating anti-viral immunity. Studies with TLR3 deficient mice show variable roles of TLR3 in mediating resistance to viral infections. This may reflect a role for other PRRs (eg RIG-1 and MDA5) which can also recognise viral RNA. $TLR3^{-/-}$ mice were more resistant to intraperitoneal administration of West Nile virus due to enhanced viral load in the periphery, but had lower viral load in the brain. However, upon intracerebroventricular administration of the virus, wild type (WT) and $TLR3^{-/-}$ deficient animals had similar responses (Wang et al., 2004). In humans TLR3 deficiency has been associated with impaired immunity to herpes simplex virus 1 and viral dissemination (Zhang et al., 2007).

TLR4 is one of the most extensively studied TLRs. TLR4 binds to bacterial lipopolysaccharide (LPS, a component of gram negative bacterial cell walls) in complex with the protein MD2 (Park et al., 2009). LPS/TLR4 interaction elicits production of proinflammatory cytokines such as TNF-α, IL-1 and IL-6 (Perera et al., 2001, Kawai and Akira, 2010). TLR4 can bind other ligands such as viral proteins (Kurt-Jones et al., 2000) or antimicrobial peptides such as beta-defensin 2 (Biragyn et al., 2002). TLR5 binds to a specific site of the protein flagellin, which is a component from the bacterial flagellum (Smith et al., 2003). This binding leads to the activation of NF-κB and the production of TNF-α (Hayashi et al., 2001). TLR7 and TLR8 recognise single stranded RNA (ssRNA) and similar to TLR3 have intracellular localisation and mediate responses to RNA viruses and bacterial nucleic acids (Heil et al., 2004). Ligation of these receptors in plasmacytoid dendritic cells leads to activation of pathways regulating IFN production (Diebold et al., 2004). Deficiency of TLR7 and TLR8 in humans are associated with susceptibility to hepatitis C virus infections (Wang et al., 2011). TLR9 binds to unmethylated CpG DNA motifs in the endosomal compartment. TLR9 recognises viral and bacterial DNA and, similar to TLR7/8, induces IFN production in plasmacytoid dendritic cells. (Lund et al., 2003, Stetson and Medzhitov, 2006). TLR7, 8 and 9 are also expressed on macrophages where their activation is able to induce the production of pro-inflammatory cytokines such as TNF, IL-6 and IL-12 (Pauls et al., 2013). Although the endosomal location of TLR7/8/9 prevents them to interact with host DNA and RNA, uptake of Immunoglobulin complexes conjugated to nucleic acids could trigger activation of these receptors in the absence of pathogens leading to the so called sterile inflammation (Leadbetter et al., 2002, Wang et al., 2007). The TLR11/12 and 13 are less well characterised. TLR11 and TLR12 recognise the profilin protein in parasites (Raetz et al., 2013), whereas ligand for TLR13 is the 23S ribosomal RNA, which is found in bacteria, but not in eukaryotic cells (Li and Chen, 2012).

The TLRs are made of an extracellular N-terminal ligand binding domain, a transmembrane domain and a conserved cytoplasmic C-terminal Toll/IL-1R homology (TIR) domain, which is required to trigger downstream signalling (Botos et al., 2011). The extracellular domain contains leucine-rich repeat motifs and forms a horseshoe structure. Ligand binding to the extracellular domains induces dimerisation of the TLRs. The dimerisation of the TIR domains is required for the recruitment of

adaptor proteins. All TLRs recruit the MyD88 adaptor protein, apart from TLR3, which interacts with the TIR-domain-containing adaptor protein inducing interferon-β. Although MyD88 can bind directly to the TIR domains of the TLRs, in some cases of TLR4 and the TLR1/2 and TLR2/6 this interactions is facilitated by the TIR-domain containing adaptor protein (TIRAP or Mal) (Kenny et al., 2009). However, it should be noted that Mal was required only during stimulation of TLR2/6 and TLR2/1 at low ligand concentration (Kenny et al., 2009). Interestingly, Mal was found to negatively regulate TLR3-dependent production of IFN-β (Siednienko et al., 2010). In the context of other TLRs such as TLR9 the requirement for Mal seems to be cell specific (Gravina et al., 2016).

TLR4 utilises both TRIF and MyD88 pathways in response to LPS (Shen et al., 2008, Fitzgerald et al., 2003). TLR4 could have both surface expression and endosomal expression. Whereas TLR4 utilises MyD88 adaptor protein on the cell surface, endosomal TLR4 also recruits the TRIF-related adaptor molecule TRAM and TRIF (Kagan et al., 2008). Downstream of TLR4, TRIF was found to play a role in regulating expression of costimulatory molecules in LPS stimulated dendritic cells (Shen et al., 2008). TRIF adaptor protein interacts with TRAF3 and TRAF6. Upon ligand binding of TLR3, TRIF activates TRAF3 leading to activation of the TANK-binding kinase (TBK1) and the IKK-ε, which in turns regulate IRF3 and IRF7 and the induction of type I IFN (Hacker et al., 2006, Perry et al., 2004).

1.2.2. IL-1 receptor family

The IL-1 receptor family includes 11 members, which depending on the function can be classified into four groups: ligand binding receptors, IL-1R accessory proteins, inhibitory proteins and orphan receptors (Figure 1.2). These proteins form 4 major receptor signalling complexes the IL-1R, IL-33R, IL-36R and IL-18R (Garlanda et al., 2013). The IL-1 receptors share an intracellular signalling domain (TIR domain) with the TLRs and similarly require MyD88 as an adaptor protein (Garlanda et al., 2013). The IL-1R complex binds to IL-1α, IL-β and IL-38. IL-1α is present in epithelial cells and is released during necrosis and therefore is classified as an "alarmin" or danger signal (Suwara et al., 2013). IL-1α precursors are active and induce the production of the proinflammatory cytokines such as TNF-α and IL-6 in

human peripheral blood mononuclear cells (Kim et al., 2013). IL-1β is produced by hematopoietic cells, however unlike IL-1α, the IL-1β precursor is not active and requires activation. This is mediated by a multiprotein complex referred to as the inflammasome. Activation of inflammasomes leads to conversion of pro-caspase-1 into an active caspase-1, which cleaves pro-IL-1β into its mature form. Activation of IL-1β can also occur in the absence of caspase-1 and is mediated by the neutrophil proteinase-3 (Guma et al., 2009). IL-1β is a proinflammatory cytokine which is implicated in different immune mediated diseases including, arthritis, type 2 diabetes and others (Dinarello, 2011). The action of IL-1β can be blocked by another member of the IL-1 family, IL-1Ra, which competes with IL-1β for binding to the IL-1 receptor. Unlike IL-1, binding of IL-1Ra is unable to induce signalling downstream of the receptor (Dinarello, 2011). Mutations in the inflammasome that lead to increased IL-1β production or mutation in IL-1Ra are associated with the development of a number of auto-inflammatory diseases (Manthiram et al., 2017).

IL-18 is constitutively expressed in nearly all cells and, similar to IL-1β, activation of IL-18 requires cleavage by caspase-1. IL-18 is a proinflammatory cytokine and stimulation with IL-18 augments production of IFN-γ in NK cells and Th1 cells (Shigehara et al., 2001, Stegmann et al., 2015, Dinarello et al., 2013). IL-36 is another member of the IL-1 cytokine family and is found in different cells including immune and non-immune cells. IL-36 is also abundantly expressed in the skin and is involved in the promotion of IL-17 and IL-23 responses and thereby promotes the pathology of psoriasis (Lowes et al., 2013, Foster et al., 2014, Bridgewood et al., 2018). IL-38 is the least studied members of the IL-1 family. IL-38 binds to the IL-1R1 or IL-1Rp2 and competes with IL-1 and IL-36. It has been demonstrated that IL-38 has a protective effect in LPS-induced sepsis model in mice, as well as in experimental mouse model of arthritis (Xu et al., 2018) (Boutet and Najm, 2017). Overexpression of IL-38 in human THP-1 monocyte cell line led to a reduced production of inflammatory cytokines (Boutet and Najm, 2017). Addition of IL-38 to the culture medium also led to a partial reduction of IL-17 and IL-22 production in *Candida*-stimulated T cells *in vitro* (van de Veerdonk et al., 2012). IL-33 and the IL-33 receptor complex will be extensively discussed further in this chapter.

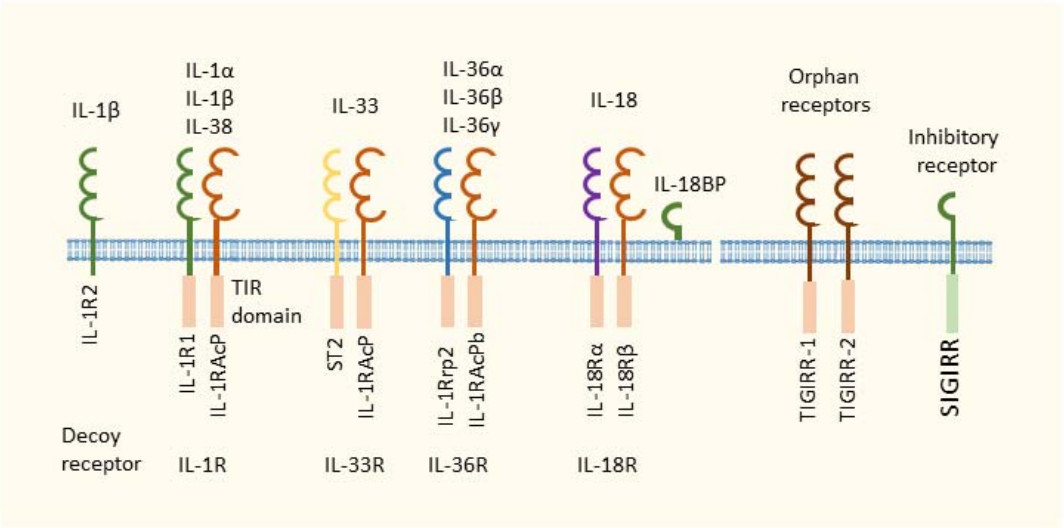

Figure 1.2 IL-1 Receptor family
IL-1R2 binds to IL-1β, however due to lack of the TIR domain this binding does not initiate signalling. IL-1R1 associates with the IL-1RAcP to form the IL-1R complex, which recognises IL-1α, IL-1β and IL-38. Similarly, ST2 also associates with the IL-1RAcP to form the IL-33R. The IL-36 receptor is made of IL-1Rrp2 which associates with IL-1RAcP and recognises the different isoforms of IL-36. The ligand binding receptor for IL-18 is made of IL-18Rα and IL-18Rβ. The soluble IL-18BP can bind IL-18 and acts as an inhibitory protein. The two orphan receptors TIGIRR-1 and TIGIRR-2 are not thought to use co-receptors. Homology studies suggest that these receptors can bind IL-18, however no activation has been demonstrated upon IL-18 stimulation. The SIGIRR has a single Ig extracellular domain and acts as a negative regulator of the IL-1R signalling.

1.3. IL-33/ST2 signalling pathway

1.3.1. ST2 receptor discovery

IL-33 is recognised by the ST2 receptor (encoded by the *IL1RL1*). ST2 (originally named T1, DER4 and Fit-1) was discovered in 1989, preceding the discovery of its ligand (Tominaga, 1989, Werenskiold et al., 1989). Despite the similarity between the IL-1 family receptors, ST2 binds IL-33 but not to any of the other IL-1 family cytokines (Kumar et al., 1995). At present there is no evidence for the existence of other ligands that are recognised by ST2. The *IL1RL1* gene is located on chromosome 2 in humans and chromosome 1 in mice together with other IL-1 receptor family members (Molofsky et al., 2015). There are two distinct promotors within the *IL1RL1* gene leading to expression of two forms of ST2: a soluble (sST2) and membrane bound form, with the membrane form more abundantly expressed (Bergers et al., 1994).

1.3.2. Soluble ST2

sST2 acts as a decoy receptor and sequesters free IL-33 resulting in no signalling. The presence of sST2 might have evolved as an extracellular mechanism to limit the activity of IL-33. sST2 is produced spontaneously by a variety of cells. sST2 is found in human serum from healthy people, but its levels are further induced during inflammatory and heart diseases (Dieplinger and Mueller, 2015). Higher levels of sST2 are associated with poor outcomes in patients with heart failure and mortality in patients with acute respiratory distress syndrome. Increased sST2 is detectable in patients with asthma, chronic obstructive pulmonary disease (COPD), systemic lupus erythematosus, rheumatoid arthritis, ulcerative colitis (Oshikawa et al., 2001, Li et al., 2015, Shi et al., 2018, Italiani et al., 2018, Diaz-Jimenez et al., 2017).

1.3.3. Expression of membrane bound ST2 on immune cells

T helper cells were one of the first subsets of immune cells that were discovered to express the ST2 receptor. ST2 was found to be preferentially expressed on Th2 differentiated cells, but not on Th1 (Lohning et al., 1998). The expression of ST2 on T cells is regulated by the transcription factor GATA3, which binds one of the two GATA consensus sites on the *IL1RL1* gene (Nawijn et al., 2001, Hayakawa et al., 2005). IL-33 is able to induce IL-5 production in T cells and *in vivo* administration of IL-33 led to an exacerbation in OVA asthma mouse model that was independent of IL-4 or STAT6 (Kurowska-Stolarska et al., 2008). A recent study indicates that IL-33 induces amphiregulin producing memory type Th2 cells which have a pathogenic role in airway lung fibrosis. Amphiregulin is a growth factor part of the EGF family which promotes regeneration of the epithelium. Dysregulation of amphiregulin production however has been associated with fibrosis (Zaiss et al., 2015). Moreover the T cell derived amphiregulin was also required for the activation and reprogramming of eosinophils, which in turn produce osteopontin and induce fibrosis (Morimoto et al., 2018).

Expression of ST2 is found also on regulatory T cells. Colonic Foxp3^{+ve} Treg cells, but not splenic Foxp3^{+ve} Treg cells were found to express ST2. IL-33 induces phosphorylation of GATA3 in inducible Treg (iTreg) cells. Once phosphorylated, GATA3 can bind to the *FOXP3* promotor and *IL1RL1* enhancer sites leading to their

induction (Schiering et al., 2014). $ST2^{+ve}$ Treg cells were also expanded in colonic tumours and in *APC* $^{Min/+ve}$ mice, which are used as a model of human familial adenomatous polyposis. This suggests that ST2 plays a negative role and promotes tumour development (He et al., 2017, Zhou et al., 2018a). $ST2^{+ve}$ Tregs are also present in adipose tissue. In these circumstances, *in vivo* administration of IL-33 led to an expansion of $ST2^{+ve}$ Tregs and reduced the obese phenotype in NZO mice, an inbred stain that develops severe obesity (Vasanthakumar et al., 2015).

Another major cell type involved in mediating IL-33 responses are the type 2 innate lymphoid cells (ILC2), which will be discussed later in this chapter. Because of their ability to produce cytokines in response to IL-33, ILC2 are involved in mediating a number of immune mediated diseases including helminth infections, respiratory viral infections, asthma, atopic dermatitis, allergic rhinitis, arthritis (Poposki et al., 2017, Mashiko et al., 2017, Newland et al., 2017, Klein Wolterink et al., 2012).

Human and murine mast cells express constitutively high levels of ST2 and produce a variety of cytokines including IL-5, IL-13, IL-6, TNF, GM-CSF, CXCL8 and CCL1 in response to IL-33 stimulation (Moritz et al., 1998, Schmitz et al., 2005a, Allakhverdi et al., 2007). The exacerbating effect of IL-33 in a mouse model of collagen induced arthritis was partially dependent on mast cell responses (Xu et al., 2008). Mast cells are also involved in the pathology of psoriasis induced by cutaneous injection of IL-33 (Hueber et al., 2011). In contrast, mast cell deficient $Kit^{W\text{-}sh/W\text{-}sh}$ mice exhibited exacerbated phenotype in experimental model of papain-induced lung inflammation; in this study the authors showed evidence that mast cell derived IL-2 promotes regulatory T cells which supress the IL-33 driven lung inflammation (Morita et al., 2015).

Eosinophils and basophils also express ST2. Transcriptomic analysis of IL-33 stimulated eosinophils revealed that IL-33 induced changes in more than 500 genes (Bouffi et al., 2013, Kroeger et al., 2009). Bone marrow can be induced to differentiate into eosinophils by culture in IL-5 containing media. Replacement of IL-5 by IL-33 for the final 6 days of culture resulted in eosinophils with a higher expression of the activation markers CD11b and CD69, increased granzyme B levels and a higher capacity for killing tumour cells (Lucarini et al., 2017).

NK and invariant NKT cells upregulate expression of ST2 when stimulated with IL-12. (Smithgall et al., 2008). Addition of IL-33 could also amplify the production of IFN-γ in IL-12 stimulated NK cells or after antigen stimulation of iNKT cells (Smithgall et al., 2008). iNKT cells express particular TCR rearrangement (Vα14Jα281 in mice and Vα24JαQ in humans) and recognise peptides loaded onto the MHC-I like CD1 molecule (Brutkiewicz and Sriram, 2002). iNKT cells had increased proliferation in response to *in vivo* stimulation with IL-7 and IL-33 compared to IL-7 alone (Bourgeois et al., 2009). Deficiency of ST2 in NK cells led to an impaired response to viral infection in mice (Nabekura et al., 2015). IL-33 was found to inhibit tumour growth *in vivo* by promoting expansion of NK cells and inducing higher IFN-γ production in CD8 T cells (Gao et al., 2015).

Dendritic cells also express ST2 and produce cytokines following stimulation with IL-33(Li et al., 2017, Göpfert et al., 2018). IL-33 induces activation of MAPK and NF-κB signalling pathways in bone marrow derived dendritic cells (Göpfert et al., 2018). The role of IL-33 mediated dendritic cell responses was highlighted by a study showing that conditional deletion of MyD88 in dendritic cells using a *CD11c-Vav Cre* leads to a reduction in the pathological inflammation during an experimental model of atopic dermatitis induced by the vitamin D3 analog MC903 (Li et al., 2017).

It has also been suggested in the literature that IL-33 is associated with an "alternative" or M2a -like activation of macrophages *in vivo* (Seo et al., 2017, Furukawa et al., 2017). "Alternative" activation of macrophages was originally described in response to the Th2 cytokine IL-4 and similar polarisation can also be driven via IL-13 (Stein et al., 1992, Doherty et al., 1993), suggesting that IL-33 might not directly affect macrophage function.

$CD11b^{+ve}$ peritoneal B1 B cells have been found to upregulate ST2 expression and expand *in vivo* in response to IL-33 intraperitoneal injection. IL-33 stimulation induced the production of IL-5, IL-13 and IgM in $CD19^{+ve}CD11b^{+ve}CD5^{+ve}$ and $CD19^{+ve}CD11b^{+ve}CD5^{-ve}$, but not in $CD19^{+ve}CD11b^{-ve}$ B cells, suggesting that only specific B cell subsets are IL-33 responsive (Komai-Koma et al., 2011).

1.3.4. IL-33/ST2 complex formation

Like the other members of the IL-1 receptor family, ST2 has an extracellular ligand binding domain made of 3 Immunoglobulin (Ig) like domains (D1, D2 and D3), a transmembrane domain and an intracellular portion containing the Toll-IL-1-intracellular domain (TIR domain) (Boraschi et al., 2018). The crystal structure of IL-33/ST2 complex has been solved, showing 1:1 stoichiometry. Similar to other IL-1 members, IL-33 has two binding regions, one which interacts with the D1 and D2 domains and the other interacts with the D3 domain of ST2 (Lingel et al., 2009).

Upon IL-33 binding to ST2, the IL-1 accessory protein (IL-1RAcP, also known as IL-1R3) is recruited, leading to formation of trimeric complex (Figure 1.3). IL-1RAcP is not able to bind IL-33 on its own, but has an essential role for downstream signalling. IL-1RAcP deficient mice did not respond to IL-33 stimulation *in vivo* and had reduced type two cytokine production and IgE levels in comparison to IL-33 stimulated WT mice (Chackerian et al., 2007).

The IL-33/ST2 signalling complex has been also shown to interact and cross activate the receptor tyrosine kinase c-Kit (CD117), known as a proto-oncogene since mutations in the Kit gene are linked to human cancers (Figure 1.3). c-Kit is activated by the stem cell factor SCF and the downstream signalling promotes cell survival, proliferation and migration (Foster and Zaidi, 2018). IL-33 stimulation of bone marrow derived mast cells (BMMC) leads to phosphorylation of Y721 in c-Kit independent of SCF (Drube et al., 2010). Stimulation of c-kit deficient BMMC with IL-33 failed to induce phosphorylation of ERK1/2 and led to a lower production of IL-6. Furthermore, SCF was found to enhance signalling and cytokine production in IL-33 stimulated BMMC. A co-immunoprecipitation experiment suggested that c-Kit binds to IL-1RAcP constitutively in mast cells, whereas association of c-Kit with ST2 receptor requires ligation of IL-33 and recruitment of the IL-1RAcP (Drube et al., 2010).

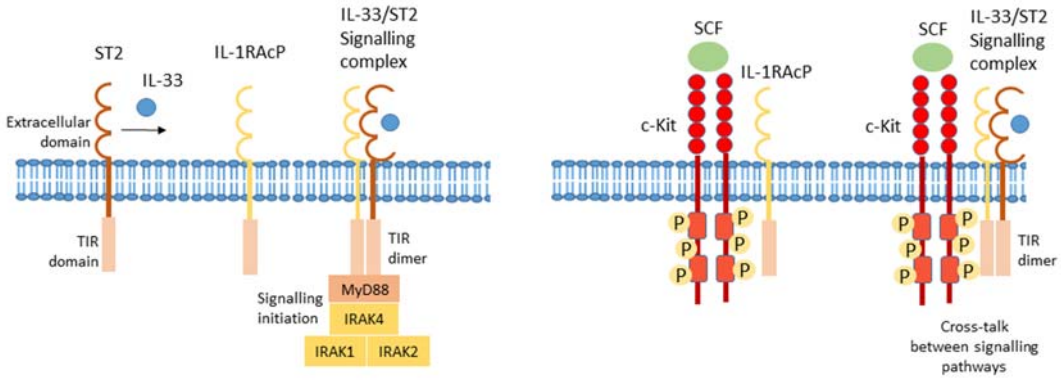

Figure 1.3 Activation of IL-33/ST2 receptor complex.
The extracellular domain of ST2 interacts with IL-33, followed by recruitment of the IL-1RAcP. The formation of trimeric complex facilitates dimersiation of the TIR domains of ST2 and IL-1RAcP and initiates signalling. In mast cells, the IL-1RAcP can also interact with the phosphorylated tyrosine receptor kinase c-Kit to further amplify the IL-33 signalling.

There are multiple mechanism of IL-33/ST2 complex formation (Figure 1.4). First, as described above the soluble ST2 can sequester free IL-33 preventing its binding to the receptor bound form and initiating signalling. Second, the IL-1 family member SIGIRR (TIR8 or IL-1R8) inhibits IL-33/ST2 signalling in Th2 cells. SIGIRR is highly expressed on polarised Th2 cells and forms a complex with IL-33 and ST2. SIGIRR deficiency leads to higher production of type two cytokines in TCR and IL-33 stimulated Th2 cells and enhanced response during OVA challenge (Bulek et al., 2009). The last known mechanism of regulating the formation of IL-33/ST2 complex involves the phosphorylation of ST2 on S446 by the glycogen synthase kinase 3β (GSK3β), which may be dependent on the focal adhesion kinase (FAK). This phosphorylation of ST2 leads to internalisation and degradation of the receptor and is limiting the IL-33 dependent cytokine production in Mouse lung epithelial (MLE-12) cells (Zhao et al., 2015). The GSK3β phosphorylation is required for the ubiquitination of the ST2 receptor by the E3 ligase FBXL19 and the consequent proteasomal degradation of ST2 (Zhao et al., 2012).

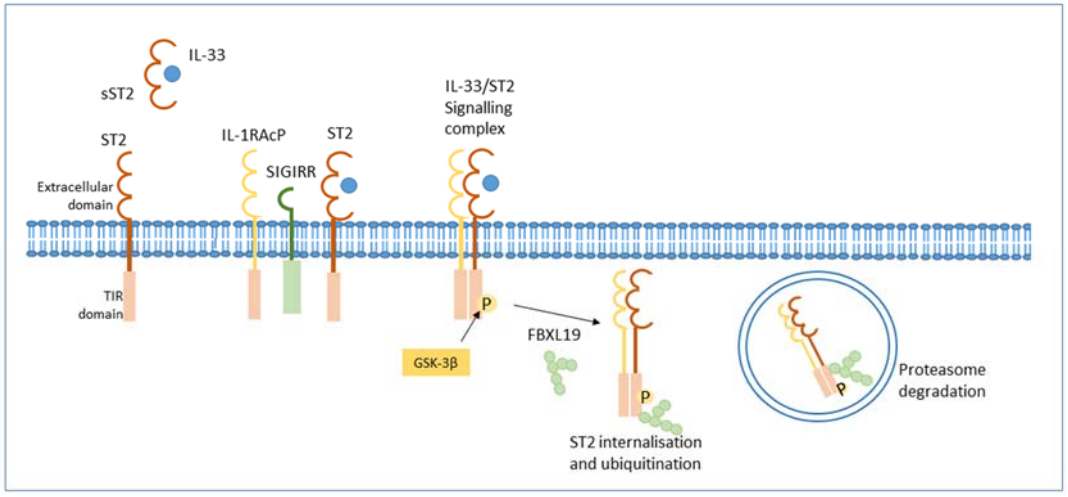

Figure 1.4 Inhibition of IL-33/ST2 receptor complex.
The soluble ST2 limits IL-33 signalling by acting as a decoy receptor and sequestering the free IL-33. The IL-1 family member SIGIRR prevents the formation of the IL-33/ST2/IL-RAcP trimeric complex and inhibit the inflammatory signaling. Phosphorylation of the TIR domain of ST2 by the GSK3β kinase leads to the internalization of the receptor, ubiquitination by the E3 ligase FBXL19 and proteasomal degradation.

1.3.5. IL-33/ST2 signalling pathway

1.3.5.1. Formation of the MyDDosome

The dimerisation of the TIR domains of ST2 and IL-1RAcP initiates the recruitment of MyD88, the interleukin-1 receptor associated kinases (Biragyn et al., 2002) and the E3 ligase TRAF6, which leads to MAPK signalling and NF-κB activation and production of inflammatory cytokines involved in type two immunity (Figure 1.5) (Schmitz et al., 2005).

MyD88 acts as an adaptor protein for most of the Toll-like receptors as well as the IL-1, IL-18 and IL-33 receptors (Cohen, 2014). While signalling downstream of the IL-33 receptor has not been studied in as much detail as IL-1 or TLR signalling, it is likely that it follows a canonical MyD88 dependent pathway. Where experimental evidence exists, this would support this view as discussed further below. The C-terminal domain of MyD88 binds to the TIR domain of the corresponding receptor, while the N-terminal death domain interacts with the IRAK kinases (Deguine and Barton, 2014). *In vivo* studies using MyD88 deficient mice highlighted its importance during IL-33 dependent type two inflammatory conditions such as lung inflammation, atopic dermatitis and gut inflammation (Yang et al., 2013, Denis et al., 2013, Li et al., 2017). Bone marrow derived basophils from MyD88$^{-/-}$ mice failed to secrete IL-4 and

IL-13 in response to IL-33 stimulation (Kroeger et al., 2009). MyD88 also plays a role in promoting eosinophil survival upon IL-33 stimulation and IL-5 withdraw (Willebrand and Voehringer, 2016, Li et al., 2018).

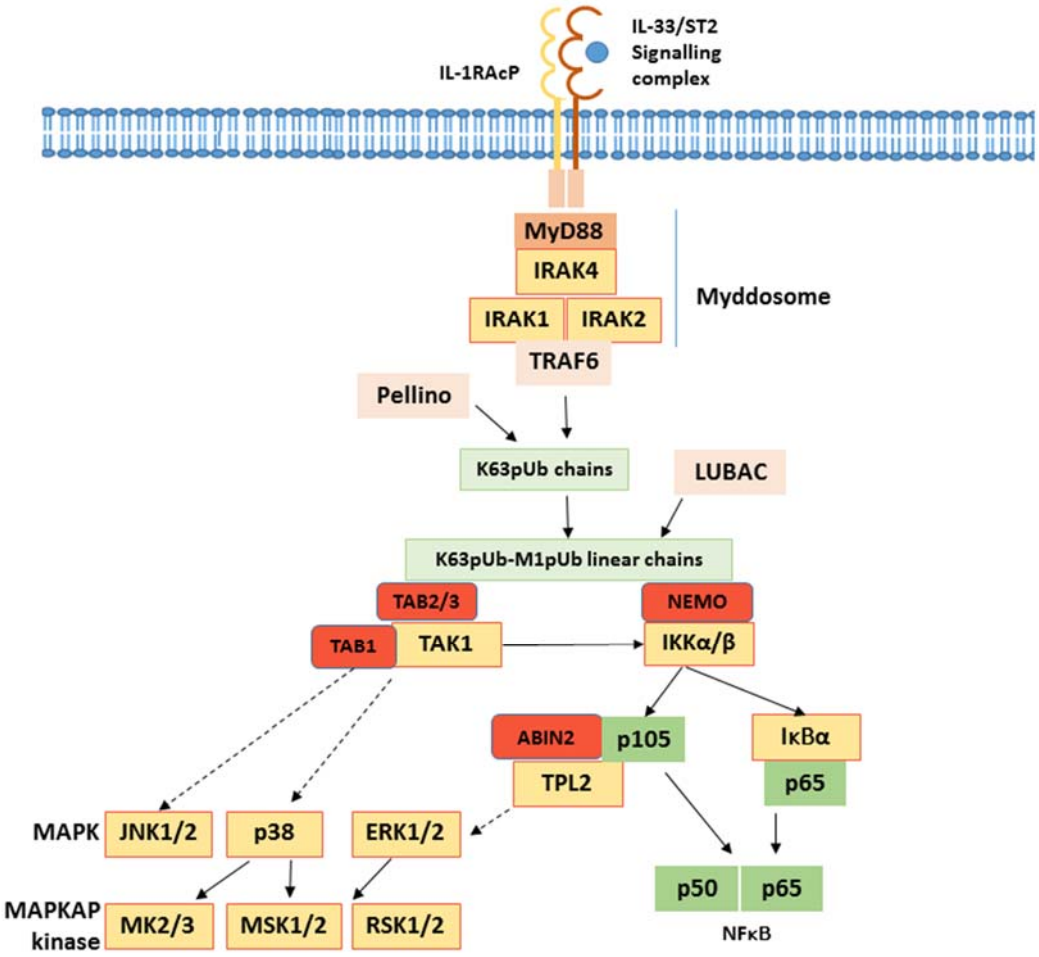

Figure 1.5 Model of IL-33 signalling pathway.
Ligation of IL-33 with the ST2 receptors leads to recruitment of the MyD88 adaptor protein. MyD88 interacts with the IL-1 receptor-associated kinase 4 (IRAK4). IRAK4 forms a complex with IRAK1 and IRAK2 and the E3 ligase TRAF6 (TNF receptor-associated factor 6). This then promotes the formation of K63 linked ubiquitin chains, most probably via TRAF6 and Pellino1/2. The linear ubiquitin assembly complex LUBAC generates the M1 linear ubiquitin chains which branch of the K63 chains leading to the formation of K63/M1 chains. TAB2/3 (TAK-1 binding protein 2 and 3) and NEMO bind to the K63 and M1 linear ubiquitin chains respectively so that the TAK1 (TGFβ activated protein kinase1) and IKK complexes co-localise, allowing TAK1 to activate IKKβ. TAK1 can activate the p38 and JNK MAPK pathways while IKKβ activates the canonical NF-κB pathway. IKK also activates TPL2, via the phosphorylation of p105. Tpl2 acts as the MAP3K for the ERK1/2 pathway in Myd88 dependent signaling. p38 and ERK1/2 activate further downstream kinases including MK2/3 (p38), MSK1/2 (ERK1/2 or p38) and RSK1/2/3 (ERK1/2).

The IRAK kinases are rapidly recruited to ST2 following stimulation of ST2-transfected 293 cells via MyD88 (Schmitz et al., 2005). There are four members of the

IRAK family: IRAK1, IRAK2, IRAK-M (also known as IRAK3) and IRAK4. While IRAK1 and IRAK4 are catalytically active, IRAK2 and IRAK-M are considered as pseudokinases since they lack kinase activity. IRAK4 phosphorylates IRAK1 and 2, these two then dissociate from the complex and activate the E3 ligase TRAF6. Interestingly, there seems to be a differential regulation of TLR and IL-33 signalling pathways by IRAK kinases (Rhyasen and Starczynowski, 2014). Mast cells lacking IRAK2 responded normally to LPS and PGN, but had impaired response to IL-33 stimulation and secreted lower levels of IL-6 (Sandig et al., 2013). In contrast, in BMMC cells deficient for IRAK1 the response to LPS or peptidoglycan (PGN) stimulation was dramatically inhibited, while *IRAK1*$^{-/-}$ deficient mast cells responded normally to IL-33 stimulation. Despite this, BMMCs from mice expressing a kinase dead IRAK1 knockin mutation showed reduced levels of IL-33 induced cytokine production (unpublished data). BMMCs from mice with a mutation that disrupts the interaction between IRAK2 and TRAF6 also showed reduced IL-33 induced cytokine production, while a combination of both IRAK1 and IRAK2 mutations had an even greater effect (unpublished data). This would suggest that both IRAK1 and IRAK2 are involved downstream of IL-33, but further work would be need to resolve these results with the earlier studies in IRAK knockouts. The importance of IRAK2 in mediating IL-33 responses was further highlighted using a small molecule which mimics the α-helical domain of IRAK2. This compound was found to compromise IRAK2-IRAK4 interaction, attenuated the downstream activation of NF-κB transcriptional activity and IL-5 and IL-13 cytokine production in IL-33 stimulated T cells. *In vivo* administration of this compound in mice led to an amelioration of the pro-inflammatory effects of OVA-induced asthma model (Li et al., 2018).

IRAK-M is a negative regulator of the TLR and IL-1R signalling (Kobayashi et al., 2002). A recent study suggest that IRAK-M controls IL-33 signalling through the prolyl-cis-trans isomerase PIN1. Upon IL-33/ST2 complex formation, the activated PIN1 recognises the phosphorylated form of IRAK-M and catalyses IRAK-M cis-trans isomerisation of a pS110-P motif, and this is required for the nuclear translocation of IRAK-M. Production of Th2 cytokines was dramatically reduced in PIN1 and IRAK-M knock out mice following intranasal treatment with IL-33 (Nechama et al., 2018).

The E3 ligase TRAF6 is also required for the IL-33 signalling pathway. TRAF6 deficiency in mouse embryonic fibroblasts (MEFs) was associated with loss of p38, JNK and NF-κB activation in response to IL-33. Production of IL-6, MCP-1 and MCP-3 in response to IL-33 was also decreased in *TRAF6*$^{-/-}$ MEFs (Funakoshi-Tago et al., 2008). Downstream of IL-1, TRAF6 and Pellino1/2 generate the K63 ubiquitin chains required for the TAK1 activation (Strickson et al., 2017). The E3 ligase LUBAC on the other hand generates M1 chains, which bind to the K63 chains to form linear ubiquitin chains facilitating the colocalisation of the TAK1 and the NEMO/IKK complexes (Emmerich et al., 2013). While the role of ubiquitination has not been extensively examined in IL-33 signalling, it is likely that it would follow a similar pattern to IL-1 signalling.

1.3.5.2. MAPK activation

14 MAPKs have been identified in mammalian cells that have been divided in to 4 main groups, the classical MAPKs ERK1 and 2, p38 MAPKs, JNKs and a group of less well understood atypical MAPKs. Activation of MAPKs requires phosphorylation of the MAPK TXY activation motif via a dual specificity MAPK Kinase (MAP2K), which is in turn activated by a MAPK Kinase Kinase (MAP3K) (Figure 1.6).

In the context of classical MyD88 dependent signalling, the TAK1 complex is required for the activation of the p38 and JNK MAPK pathways and indirectly for the activation of ERK1/2 via the IKK complex and TPL2 (Figure 1.5 and 1.6) (Arthur and Ley, 2013). p38 and ERK1/2 are the most studied MAPKs downstream of MyD88 and play key roles in MyD88 dependent cytokine production. The role of JNK is less clear, however it negatively regulates IFNβ production in BMDMs (McGuire et al., 2017).

ERK1/2 are also activated in response to IL-33 stimulation in ST2-transfected 293 cells (Schmitz et al., 2005a). ERK1/2 phosphorylation was detected in mouse MEFs upon IL-33 stimulation, surprisingly this was not dependent on TRAF6 in contrast to the phosphorylation of p38 and JNK, which was completely abolished in the *TRAF6* $^{-/-}$ MEFs (Funakoshi-Tago et al., 2008). Drube et al found that blocking c-Kit signalling attenuates ERK1/2 activation in HMC-1.1 cells and SCF stimulation

of BMMC cells amplifies ERK1/2 activation, highlighting the existence of differential regulation of ERK1/2 activation and a possible cross talk between the IL-33 and c-Kit signalling pathways (Drube et al., 2010). This highlights a potential difference between IL-33 and IL-1 or TLR signaling where ERK1/2 activation is dependent on TRAF6.

The role of JNKs is less studied in comparison to those of p38 and ERK1/2. JNK were found to regulate the production of IL-8 in IL-33 stimulated human umbilical vein endothelial cells (HUVECs) (Umebashi et al., 2018). A recent study demonstrates that IL-33 expression is increased in patients with renal cell carcinoma. Moreover, IL-33 was found to promote proliferation of renal carcinoma cells *in vitro* in a JNK-dependent manner, based on the use of SP600125. Further work would be required to confirm this due to the poor selectivity of SP600125 (Bain et al., 2003). Surprisingly, in this study IL-33 stimulation of the RCC did not induce activation of p38 and ERK1/2 (Wu et al., 2018). The IL-33 dependent proliferation of colon cancer cells and upregulation of cancer associated genes such as *Oct3/4* and *Notch3* were also dependent on JNK activation. (Fang et al., 2017).

p38 is possibly the most studied MAPK in MyD88 dependent signalling. p38 has 4 isoforms, α, β, γ and δ. Of these p38α is the most studied and is responsible for most of the effects of p38 inhibitors in immune cells; p38 γ and δ are not targeted by most p38 inhibitors while p38β does not seem to play a major role (Bain et al., 2007, Beardmore et al., 2005). Originally TAK1 was thought to be the MAP3K for the p38 pathway in TLR signalling. A recent study has however challenged this (Pattison et al., 2016). The authors showed that Tpl2 may phosphorylate MKK3 and MKK6 in addition to MKK1 and 2. Thus in some circumstances, such as TNF signalling, p38α activation may be dependent on Tpl2 (Pattison et al., 2016). In TLR4 signalling, MKK4 (normally considered as an MAP2K for JNK and a direct TAK1 target) is able to feed into the activation of p38, resulting in TLR4 stimulated p38 activation being independent of Tpl2. An important role for p38α in the IL-33 signalling pathway has been suggested by number of studies. p38α is phosphorylated upon IL-33 stimulation in different immune cells such as BMMC, ILC2 cells, Th2 cells (McCarthy et al., 2018, Tung et al., 2014, Furusawa et al., 2013, Endo et al., 2015, Gopfert and Andreas, 2018). In mast cells, p38 is critical for the IL-33 induced secretion of IL-13, IL-6, TNF and GM-CSF (McCarthy et al., 2018). The pharmacological inhibition of p38 using

the inhibitor SB203580 led to a significant reduction of IL-5 in human and murine Th2 cells, but did not affect the secretion of IL-4 and IL-13. The authors suggested a mechanism in which inhibition of p38 leads to reduction of the histone acetylation and methylation, inducing a chromatin remodelling at the *IL5* locus (Endo et al., 2015). In ILC2 cells stimulation with IL-33 induced activation and p38 dependent phosphorylation of GATA3. The authors found that phosphorylated GATA3 binds to the *IL5* and *IL13* promotor and could induce their transcription (Furusawa et al., 2013a).

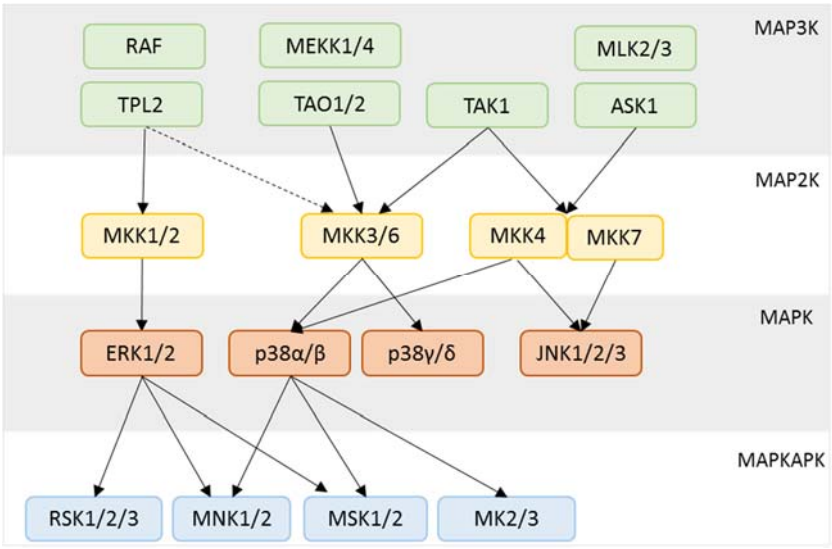

Figure 1.6 MAPK signalling cascade.
The MAP3K RAF and TPL2 phosphorylate and activate the MKK1/2, which then activate ERK1/2. TPL2 can also phosphorylate and activate MKK3/6 upon TLR and TNFR activation. MKK3/6 are activated by TAK1, MEKK1/4 or TAO1/2. MKK3/6 phosphorylate p38 MAPKs. TAK1 can also activate MKK4/7, which in turns phosphorylate and induce activation of the JNK1/2/3. MKK4, but not MKK7 also phosphorylate p38. The MAPKs have several substrates.. p38 and ERK1/2 can activate MSK1/2 and the MNKs. RSK1/2 are activated by ERK1/2, while MK2/3 phosphorylation is mediated by p38α

1.3.5.3.MAPKAPK 2/3 role in IL-33 signalling

ERK1/2 can phosphorylate and activate the downstream MAPKAP kinases RSKs (Ribosomal s6 kinase), MNK1/2 (Mitogen-Activated Protein Kinase Interacting Protein Kinase) and MSK1/2 (Mitogen- and stress-activated kinases). Similarly, p38 can activate MNKs, MSKs and the two MAPKAPKs (Mitogen-activated protein kinase-activated protein kinases) MK2 and MK3 (Figure 1.6) (Arthur and Ley, 2013).

The two isoforms MK2/3 are phosphorylated by p38α (Rouse et al., 1994). MK2/3 form a complex with p38α and stabilise p38α expression (Kotlyarov et al.,

2002) (Ronkina et al., 2007). MK2 deficient macrophages have a reduction in TNF production in response to LPS *in vitro* and are resistant to LPS-induced endotoxic shock (Kotlyarov et al., 1999). Although MK2 and 3 share functional similarities, loss of MK3 alone did not affect p38α expression or cytokine production in LPS-stimulated macrophages, however MK2/3 DKO mice displayed a further reduction in the ability to secrete TNF upon stimulation in comparison to MK2 KO cells. (Ronkina et al., 2007). In macrophages MK2 regulates TNF-α production at post-transcriptional level through a mechanism dependent on the AU-rich element-binding protein tristetraprolin (TTP) (Hitti et al., 2006). TTP binds mRNA AU-rich elements (ARE) in the 3'UTRs region and promotes their degradation by recruiting enzymes mediating mRNA deadenylation and or competing with the ARE-stabilising factor human antigen R (HuR) for binding to the 3'UTR (Marchese et al., 2010, Tiedje et al., 2012). MK2 phosphorylates S52 and S178 in tristetraprolin (TTP) (Chrestensen et al., 2004), which leads to the association of TTP with 14-3-3 protein and impairs the ability of TTP to recruit deadenylases (Clement et al., 2011). The importance of these phosphorylation events has been demonstrated using mice with mutation in the TTP encoding gene *ZFP36* in which S52 and S178 codons are replaced with alanine codons. Although the expression of TTP was lower in macrophages isolated from these mice, TTP levels were sufficient to mediate the degradation of cytokine mRNA such as *TNF*, *CXCL1* and *IL10* following stimulation with LPS. Moreover, $ZFP36^{aa/aa}$ displayed a protective phenotype upon i.p administration of LPS with significantly lower cytokine levels in the serum and hepatic damage in comparison to $ZFP36^{+/+}$ mice (Ross et al., 2015).

Work done in our lab demonstrated that MK2/3 regulate the production of multiple cytokines in IL-33 stimulated mast cells, including TNF-α, IL-6, IL-13 and GM-CSF (McCarthy et al., 2018). Whereas the production of TNF-α in response to LPS is regulated by the MK2/3 dependent phosphorylation of TTP, in mast cells TTP seems to be dispensable and MK2/3 might regulate the IL-33 cytokine production by phosphorylating the TTP related proteins Brf1 and/or Brf2 (McCarthy et al., 2018).

In addition to TTP, MK2 and/or 3 have a number of other substrates. MK2 can phosphorylate RSK in TLR stimulated dendritic cells, allowing RSK activation to bypass dependence on ERK1/2 (Zaru et al., 2007, Zaru et al., 2015). MK2 has also

recently been found to phosphorylate RIPK1 and protect cells from apoptosis (Menon et al., 2017).

1.3.5.4.NF-κB

The NF-κB family of transcription factors (Nuclear factor- κB) play an essential role in innate and adaptive immune function in addition to being involved in many other cellular processes. NF-κB regulates expression of inflammatory mediators such as genes encoding cytokines and chemokines, genes involved in promoting cell survival and inflammasome regulation. Therefore the activation of NF-κB is critical for mediating host defense, however dysregulation of NF-κB contributes to the development of inflammatory diseases and as a result must be tightly regulated (Liu et al., 2017). NF-κB transcription factors include five structurally related members: NF-κB1 (p105/p50), NF-κB2 (p100/p52), RelA (p65), RelB and c-Rel. NF-κB1 and NF-κB2 are post-translationally cleaved to p50 and p52, respectively (Liu et al., 2017). The NF-κB1 transcription factors act as homo- and heterodimers and can act both as transcriptional activators or repressors (Ryseck et al., 1992, Ruben et al., 1992). A number of different pathways has been shown to regulate NF-κB, however the canonical pathway is most relevant to MyD88 dependent signalling. In the canonical NF-κB pathway, NF-κB transcription factors are sequestered in the cytoplasm in resting cells by IκB proteins and this prevents their translocation to the nucleus (Yamamoto and Gaynor, 2004). The IκB family includes IκBα, IκBβ, IκBγ, IκBε, Bcl3 and IκBζ. All IκB family members are characterised by an Ankyrin repeats at the C-terminal region, which are required for the interaction with the NF-κB proteins. A key step of the canonical activation of NF-κB is the phosphorylation IκBα/β proteins by the IκB kinases (IKK). The activation of IKKβ relies on formation of the IKK complex containing NEMO, IKKα and IKKβ. IKKβ phosphorylates the IκB proteins at S32 and Ser36 in IκBα and S23 and S19 in IκBβ (Zandi et al., 1997). Once phosphorylated, the IκBα/β proteins are ubiquitinated by the E3 ligase β-TrCP SCF (Skip1/Cullin1 F box E3 ligase) (Cohen et al., 2004, Orian et al., 2000). This ubiquitination results in the addition of K48 linked polyubiquitin chains targeting the IκB protein for degradation by the proteasome (Sakurai et al., 1999, Zandi et al., 1997). The degradation of IκB proteins frees NF-κB and allows its translocate to the nucleus.

Similarly to other IL-1 members, IL-33 signalling leads to the activation of the NF-κB (Schmitz et al., 2005a). Upregulation of ICAM-1 and VCAM-1 in endothelial and mast cells in response to IL-33 is also dependent on the NF-κB activation (Choi et al., 2012, Numata et al., 2016). It has been also proposed that IL-33 can act as a transcription factor and modulate NF-κB. It has been demonstrated that IL-33 can bind the promotor of *p65* in endothelial cells and induce its expression (Choi et al., 2012). However, it has been also demonstrated that IL-33 can bind p65 via protein-protein interaction and limit the ability of p65 to associate with its target genes (Ali et al., 2011).

1.4. Interleukin-33

Interleukin-33 is a pleiotropic cytokine that plays a key role in regulating both innate and adaptive immunity. IL-33 was discovered in 2005 by Schmitz et al as a novel member of the IL-1 superfamily and most closely related to IL-18. IL-33 was shown to bind to the orphan IL-1 Receptor ST2 (the suppressor of tumorigenic 2) and trigger activation of both MAP kinases and NF-κB to promote type two immunity (Schmitz et al., 2005). IL-33 was later shown to be identical to a protein called nuclear factor from high endothelial venules (NF-HEV), which was found two years earlier in endothelial cells (Moussion et al., 2008).

1.4.1. Interleukin-33 expression

1.4.1.1. Endothelial cells

IL-33 is abundantly expressed in the nuclei of vascular endothelial cells in healthy human tissues. Due to the constitutive expression along the vascular system IL-33 is found in all human tissues (Moussion et al., 2008). During inflammation the expression of IL-33 in human endothelial cells can be further induced or downregulated depending on the circumstance. For example human endothelial cells were found to be the major source of IL-33 during inflammatory conditions such as rheumatoid arthritis and Crohn's disease (Moussion et al., 2008a), but its expression was downregulated in angiogenic wound healing (Kuchler et al., 2008).

In contrast to humans, where IL-33 is constitutively expressed in vascular endothelial cells, in mice the steady-state expression of IL-33 is observed only in few tissues including the vascular bed of adipose tissue and in liver sinusoidal endothelial cells (LSEC). However, IL-33 expression could be further induced in liver endothelial cells in response to viral or poly(I:C) hepatic injury, in colonic endothelial cells during inflammatory conditions like DSS-induced colitis and in the cardiac endothelial cells in response to myocardial pressure overload (Pichery et al., 2012, Arshad et al., 2015, Arshad et al., 2013, Chen et al., 2015).

1.4.1.2.Epithelial cells

Epithelial cells are the other major source of IL-33, particularly the epithelial cells in the respiratory system, gastrointestinal tract and skin. Increased IL-33 expression has been reported in sinonasal epithelial (SNEC) cells in patients with chronic rhinosinusitis with nasal polyps (Paris et al., 2014) (Lam et al., 2015). While in healthy controls IL-33 staining was observed only in the nuclei of the SNE cells, in patients with rhinosinusitis IL-33 was found also in the cytoplasm (Paris et al., 2014).

Studies with IL-33-LacZ gene trap reporter mice, in which βgeo insertion in the IL-33 gene was used to asses *il-33* promotor activity, showed that IL-33 is expressed in alveolar epithelial cells (Pichery et al., 2012). To study IL-33 expression *in vivo,* Hardman et al developed another IL-33 reporter mouse strain, in which the GFP-derived *Citrine* gene was inserted after the *il33* start codon. The expression of IL-33 in lungs was confirmed using this reporter strain. In fact, the citrine positive cells were found positive for the type-2 pneumocyte markers CD138 and the surfactant protein C (SPC) (Hardman et al., 2013). Expression of IL-33 was further induced in the type2 pneumocytes during challenge with ovalbumin and the fungal pathogens *Alternaria alternata* and *Cryptococcus neoformans* (Heyen et al., 2016, S. et al., 2013).

As mentioned above expression of IL-33 has been also reported in epithelial cells of the gastrointestinal tract and a number of studies have shown that IL-33 expression is increased in patients with inflammatory bowel disease (IBD) and in mouse models of IBD (Seidelin et al., 2010, Pastorelli et al., 2010, Gundersen et al., 2016). Skin keratinocytes are another source of IL-33(Anna et al., 2012, Balato et al.,

2014). Mouse keratinocytes express IL-33 constitutively, whereas in humans the expression of IL-33 is inducible (Sundnes et al., 2015, Pichery et al., 2012). Increased IL-33 expression in human keratinocytes has been found in patients with vitiligo, in the skin lesions of patients with atopic dermatitis and psoriasis (P. et al., 2015, Savinko et al., 2012, Balato et al., 2014).

1.4.1.3. IL-33 expression in other cell types

Using IL-33-LacZ gene trap reporter mice it was found that IL-33 is expressed in the nuclei of the fibroblastic reticular cells in mouse spleens and lymph nodes (Pichery et al., 2012). Mahapatro et al. showed that the pericryptal fibroblasts in the small intestine upregulate IL-33 in response to intraperitoneal injection of LPS (Mahapatro et al., 2016). Myofibroblast from colonic lesions of patients with ulcerative colitis, but not from Crohn's disease were also found to be positive for IL-33 (Sponheim et al., 2010). Induced expression of IL-33 was also found in mice cardiac fibroblasts and cardiomyocytes in response to injury (Sanada et al., 2007).

Immunohistochemistry analysis of tissues from healthy and asthmatic patients showed that along the epithelial and endothelial cells, the airway smooth muscle cells are also expressing IL-33. Stimulation of primary airway smooth muscle cells with TNF-α and IFN-γ led to an upregulation of IL-33 at mRNA and protein levels (Préfontaine et al., 2009).

A few reports suggest that IL-33 is also found in the nucleus of immune cells and more specifically in the monocytic cell line THP-1, in primary human monocytes and in M2 macrophages in the salivary glands from patients with Sjörgen's syndrome (Furukawa et al., 2017) (Nile et al., 2010). A small number of citrine positive immune cells (macrophages, DCs and neutrophils) were detected in the lungs of the IL-33 citrine reporter mice and the absolute numbers of IL-33 expressing cells was further increased in ovalbumin treated mice (Hardman et al., 2013). Interestingly, increased IL-33 expression was found in peritoneal macrophages from IL-10 deficient mice (Chen et al., 2017).

1.4.2. Interleukin-33 activity and release from the nucleus

1.4.2.1. IL-33 structure

IL-33 has a nuclear localisation sequence (NLS), a chromatin-binding motif, a central domain and a C-terminal IL-1-like cytokine domain (Figure 1.7). The presence of both chromatin binding motif and the cytokine domain suggests that IL-33 may have a dual function and could acts as a cytokine and regulator of gene transcription. IL-33 can bind the p65 subunit of NF-κB and inhibit NF-κB dependent gene expression following stimulation with IL-1β (Ali et al., 2011). The nuclear localisation of IL-33 is required for maintaining immune homeostasis since mice lacking the NLS succumbed to systemic inflammation due to inappropriate IL-33 release (Bessa et al., 2014). Lack of the NLS domain leads to release of IL-33 in the extracellular space, recruitment of eosinophils, inflammatory monocytes and consequently to lung inflammation, enlargement of the mesenteric lymph nodes (Bessa et al., 2014).

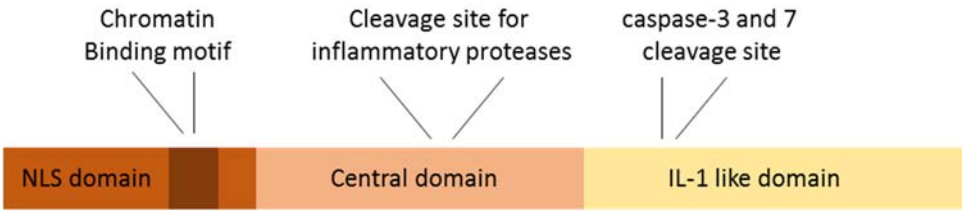

Figure 1.7 IL-33 structure.
IL-33 protein has three domains: nuclear localisation domain, a central domain and IL-1-like cytokine domain. The nuclear localisation domain is highly conserved among species and contains a chromatin binding motif. The central domain is linking the two other domains and contains cleavage sites for inflammatory proteases. The ST2 binding sites are located on the IL-1like domain, which also has cleavage sites for caspase-3 and caspase-7.

1.4.2.2. Caspase cleavage and inactivation of IL-33

IL-33 does not have a secretory sequence like other cytokines (Kakkar et al., 2012). Initially it was proposed that similar to the other members of the IL-1 family IL-1β and IL-18, IL-33 maturation requires cleavage in the IL-1 like domain by caspase-1 (Schmitz et al., 2005, Cayrol and Girard, 2009). However, it was later shown that the proteolytic cleavage of IL-33 is mediated by caspase-3 and 7, and not by caspase-1 (Luthi et al., 2009). Both murine and human IL-33 have a conserved cleavage motif "DGVD" located at Asp178 in humans and Asp175 in mice. Mutation in this motif results in completely impaired cleavage by caspase-3 and caspase-7.

Interestingly, in both studies of Luthi et al and Caryol et al it was found that caspase processing renders inactive IL-33 and mice stimulated with cleaved IL-33 had significantly decreased granulocyte infiltration in the peritoneum, blood and spleen and lower IL-5 and IL-4 production in comparison to mice treated with uncleaved IL-33 (Cayrol and Girard, 2009).

1.4.2.3. Secretion of active IL-33 form

IL-33 does not have a secretory sequence. In fact, IL-33 release is triggered during cell necrosis (such as induced by hydrogen peroxide or sodium azide treatment), endothelial cells undergoing mechanical injury, exposure to membrane damaging detergents or by freezing-thawing (Cayrol and Girard, 2009, Luthi et al., 2009). Therefore, IL-33 has been classed as an alarmin, which act as a danger signals following cellular damage resulting from tissue injury or inflammation (Cayrol and Girard, 2014). Increased levels of extracellular ATP have also been shown to induce IL-33 release from the airway epithelial cells challenged with the fungal pathogen *Alternaria alternata* through a mechanism relying on accumulation of Ca^{2+} in epithelial cells (Kouzaki et al., 2011).

Whereas cleavage of IL-33 by caspase-3 and caspase-7 leads to inactivation of the cytokine, a growing number of studies are showing that IL-33 can be cleaved by inflammatory proteases into active form (Figure 1.8). For example the neutrophil proteases elastase and cathepsin G can generate cleaved mature forms of IL-33, that have a higher biological activity than the full length IL-33 ($_{FL}$IL-33) (Cayrol and Girard, 2014). The mast cell derived serine proteases chymase, tryptase and granzyme B can also cleave IL-33 resulting in mature forms with more than 30-fold higher activity than the $_{FL}$IL-33 (Lefrancais et al., 2014). The cleavage sites for the inflammatory proteases were all located in the central domain of IL-33 (Cayrol and Girard, 2014, Lefrancais et al., 2014) .

More recent studies suggest that in the absence of immune cell derived inflammatory proteases, allergen derived proteases are also capable of cleaving and producing mature IL-33 (Snelgrove et al., 2014, Scott et al., 2018, Cayrol et al., 2018). Cayrol et al screened a variety of clinically relevant allergens causing asthma, rhinitis, and dermatitis and showed that the allergen derived proteases are able to cleave $_{FL}$IL-

33 into highly active shorter mature forms. Although FLIL-33 is still active, the authors suggested that the protease mediated processing of FLIL-33 is critical for increasing its biological activity, with the release and cleavage tightly coupled. Using a specific antibody against the central domain, which masks the protease cleavage sites but does not impair the activity of the IL-1 like cytokine domain, they demonstrated that airway eosinophilia, mucus and cytokine production are dependent on IL-33 protease processing (Cayrol et al., 2018). The cell endogenous Ca^{2+}-dependent proteases calpains can also cleave FLIL-33 *in vitro*. However, inhibition treatment with the calpeptin inhibitor did not prevent the IL-33 processing *in vivo* in *Alternaria* treated animals, most likely because the allergen derived proteases are sufficient to mediate the cleavage of IL-33 (Scott et al., 2018).

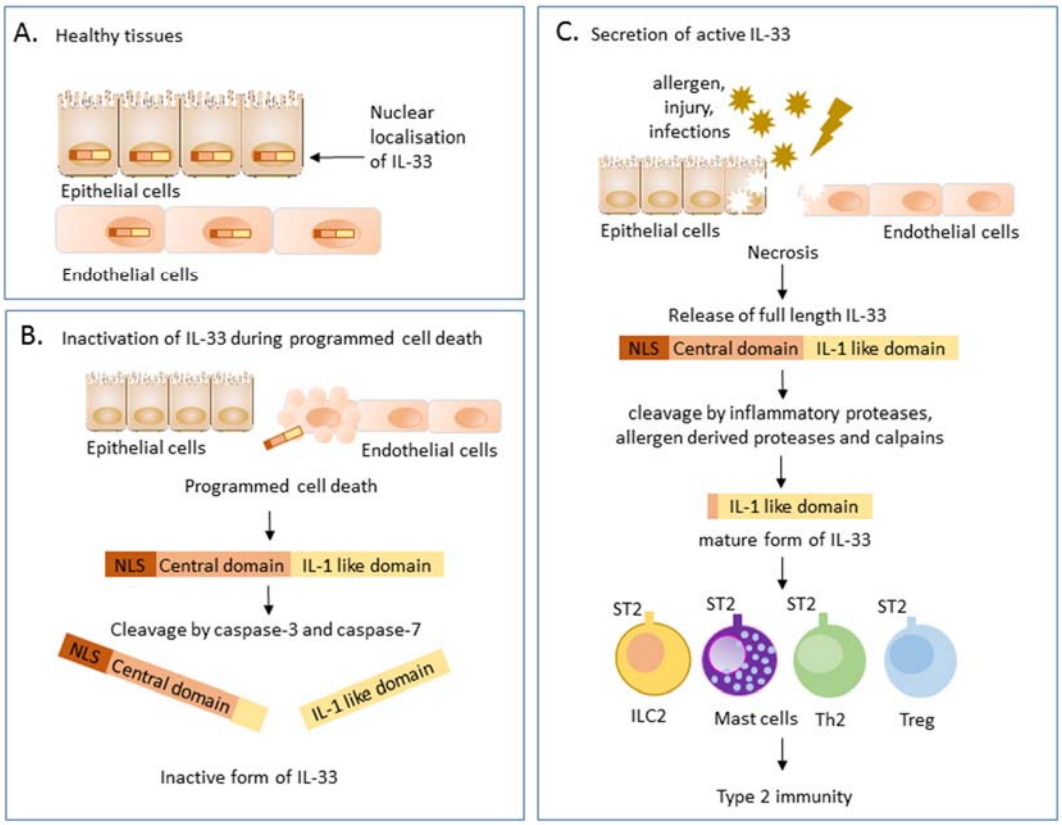

Figure 1.8 IL-33 release regulation.
A. In healthy tissues at steady state IL-33 is located in the nucleus. B. During apoptosis the full length IL-33 is cleaved by caspase-3 and caspase-7 and converted to inactive form. C IL-33 is released during necrosis caused by allergen challenge, mechanical injury or infection. The full length protein is then cleaved by immune cells or allergen derived proteases, which generate the mature short forms of IL-33. These are then recognized by the ST2 expressed on immune cells such as ILC2, mast cells, Th2 and Treg cells.

1.5. Type 2 innate lymphoid cells (ILC2s)

1.5.1. Innate lymphoid cells

Innate lymphoid cells are a recently identified group of lymphocytes within the innate immune system. ILCs lack antigen specific receptors, however in terms of the cytokines they produce they mimic various Th cell subsets. ILCs are found in both lymphoid and non-lymphoid tissues, particularly at the barrier sites including skin, respiratory and gastrointestinal systems (Spits et al., 2013). Based on their effector function, cell surface markers and the transcription factors required for their development, ILCs are subdivided into several distinct groups, summarised in Figure 1.9 (Spits et al., 2013). Group 1 includes NK cells and ILC1 cells, which are involved in protective immunity to viral infections and antimicrobial responses (Seillet et al., 2016). The second group includes type 2 innate lymphoid cells (ILC2s). ILC2 cells secrete type two cytokines in response to stimulation with the epithelial derived cytokines IL-25, IL-33 and TSLP and regulate immune responses during helminth infection, asthma and atopic diseases (Moro et al., 2010, Neill et al., 2010, Klein Wolterink et al., 2012). The third group includes lymphoid tissue inducer cells and ILC3s. LTi cells regulate the development of secondary lymphoid tissues (lymph nodes, spleen, tonsils, Peyer's patches and fat associated lymphoid clusters) (Mebius et al., 1997, Meier et al., 2007). ILC3 cells are involved in the maintenance of intestinal homeostasis, protection against extracellular bacteria and inflammatory bowel diseases (IBD) (Takatori et al., 2009). In 2017 a new group of ILCs with regulatory functions was discovered. ILCreg are found in human and mouse gut and limit the activity of ILC1s and ILC3s by secreting the anti-inflammatory cytokine IL-10. In contrast to regulatory T cells, the FoxP3 transcription factor was not required for their development, but they did require the cytokines TGF-β and IL-2 (Wang et al., 2017).

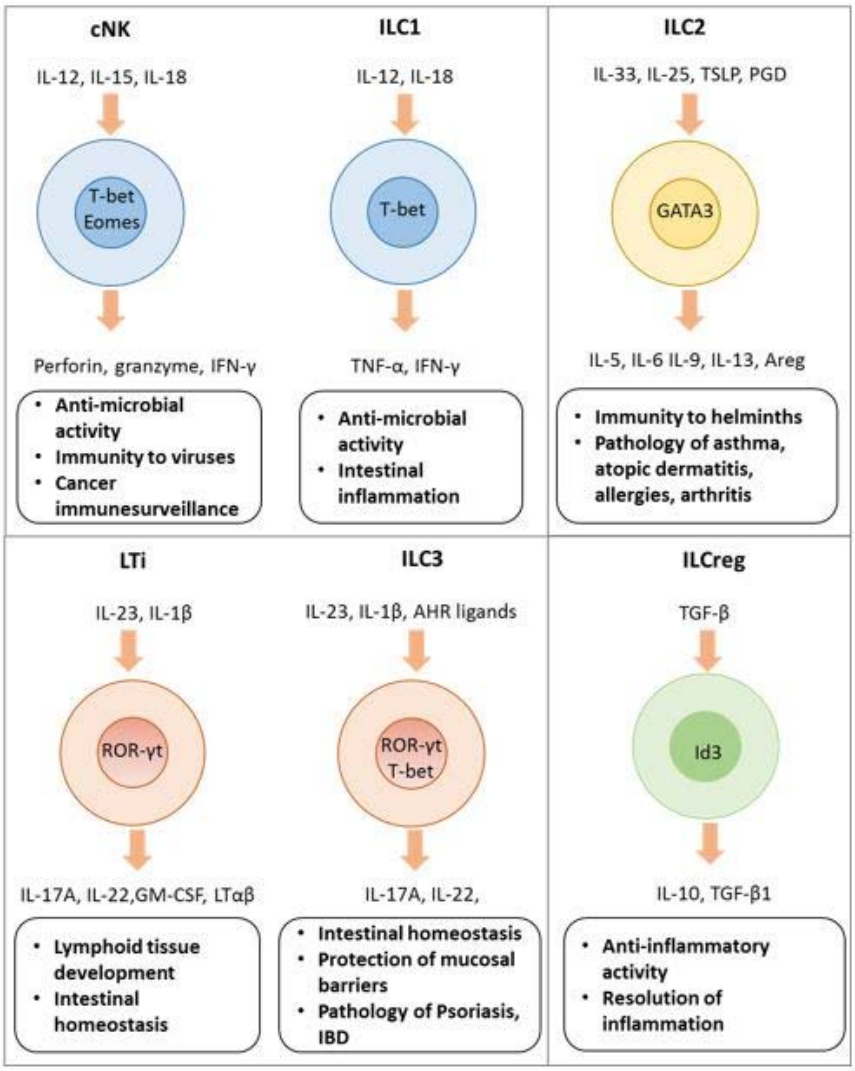

Figure 1.9 Innate lymphoid cells.
ILCs can be divided into 4 main groups, type 1, type 2 (yellow), type 3 (red) and ILCreg (green). The transcription factor required for their development along with the stimuli required for their activation and the main cytokines / inflammatory mediators they produce are indicated. The conventional NK cells are cytotoxic cells responding to IL-12, IL-15 and IL-18 stimulation and secreting perforin, granzymes and IFN. Similarly, ILC1s are also activated by IL-12 and IL-18 and produce IFN and TNF. ILC2s differentiation is dependent on GATA3. ILC2s respond to IL-25, IL-33 and TSLP and modulate type two immunity by secreting IL-5, IL-6, IL-9 and IL-13. Group 3 ILC is represented by LTi and ILC3s which require transcription factor ROR-γt and stimulation with IL-23, IL-1β for their effector functions. ILC3s express also the T-bet transcription factor and depending on the conditions they can adopt an ILC1s phenotype. ILCreg have regulatory functions. They respond to TGF-β stimulation and secrete IL-10 to limit over excessive inflammation in the gut.

1.5.2. Group 2 innate lymphoid cells discovery and characterisation

The first evidence for the existence of ILC2 cells was found in 2006 when Fallon et al. showed that during helminth infection with *Nippostrongylus brasilienis* a population of non-T and non-B cells secrete IL-4, IL-5 and IL-13 and promote

helminth expulsion (Fallon et al., 2006). However, it was not until 2010 that several labs reported the characterisation of ILC2s as a distinct population of cells, which were initially referred to as either neuocytes, innate helper 2 cells or natural helper cells (Moro et al., 2010, Neill et al., 2010, Price et al., 2010). ILC2s are found in lymphoid tissues such as spleen and mesenteric lymph nodes, as well as in some non-lymphoid organs including fat associated lymphoid clusters, lungs, skin and liver. In mice ILC2s are characterised by the lack of expression of markers of other immune cells (CD3, CD4, CD8, CD19, CD11b, CD11c, F4/80, FcεR,) and the expression of the IL-7R, IL-33 receptor (ST2), IL-25 receptor (IL-17RB), KLRG1, ICOS and c-kit. Human ILC2 are lineage negative and express IL-7R and the prostaglandin receptor CRTH2, CD161 and CCR6 (Trabanelli et al., 2018).

Similar to other ILCs, ILC2s originate from Common Lymphoid Progenitors (CLPs) in the bone marrow and their development requires multiple transcription factors. The transition of CLPs to the specific common helper innate lineage progenitor (CHILP) requires the transcription factor inhibitor Id2. Id2 regulates the activity of a group of E proteins and supresses the differentiation of T and B cells allowing divergence of the CLPs to the innate linage. Id2 is critical for the development of all innate lymphoid cells. (Yokota et al., 1999, Moro et al., 2009, Cherrier et al., 2012). Downstream of the CHILP, the development and maintenance of ILC2s depends on multiple transcription factors including ROR-α, Bcl11b, Gfi1 and GATA3 (Halim et al., 2012b, Walker et al., 2015, Spooner et al., 2013). Staggerer RORα$^{sg/sg}$ mice with a spontaneous deletion in the *Rora* gene resulting in truncated protein, have severely reduced ILC2s numbers (Halim et al., 2012). Given the importance of RORα in ILC2 development, an ILC2 deficient mouse model was made by specifically deleting RORα in IL-7R expressing cells (*Rora*$^{fl/sg}$*Il7r*^{Cre} mice), which resulted in a deletion in the lymphoid lineage. These mice have normal numbers of T cells and NK cells in the mesenteric lymph nodes, but no ILC2 cells. *Rora*$^{fl/sg}$*Il7r*^{Cre} mice had delayed worm expulsion during *N. brasiliensis* infection, reduced ILC2 expansion and T helper cellular responses. The authors suggested that ILC2 cells are required for the activation of Th2 cells through their MHC II expression (Oliphant et al., 2014).

Hoyler et al. demonstrated that the transcription factor GATA3 is expressed at high levels in ILC2 cells isolated from different tissues as well as in ILC bone marrow

progenitors, suggesting that GATA3 plays a role in the development and maintenance of ILC2 cells (Hoyler et al., 2012). Conditional deletion of GATA3 in Id2 positive cells resulted in complete loss of ILC2 populations (Hoyler et al., 2012). Blc11b is another transcription factor implicated in ILC2s development. Bcl11b is also a transcriptional regulator expressed in T cells, which plays a crucial role in defining T cell fate (Albu et al., 2011). Using Bcl11b reporter mice crossed to Id2 reporter mice it was shown that Bcl11b is expressed in mature ILC2s and ILC progenitors (Walker et al., 2015). In mature ILC2s Bcl11b was found to act upstream of GATA3 and RORα. Bcl11b deficient ILC2s have reduced expression of GATA3 and ROR-α and instead upregulate the ILC3s transcription factor ROR-γt and IL-23 receptor (Califano et al., 2015).

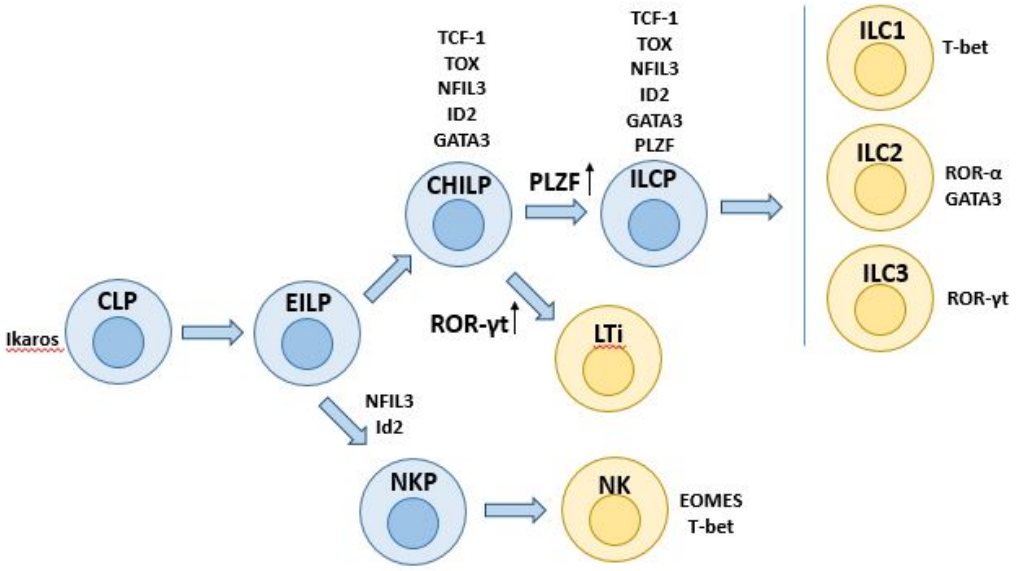

Figure 1.10 Innate lymphoid cells development.
ILCs develop from a common lymphoid progenitor (CLP) in the bone marrow. The transcription factor TCF-1 defines an early ILC progenitor EILP, which give rise to all innate lymphoid cells. Development of NK cells from the EILP is dependent on NFIL3. The EILP give rise to a specific common helper innate lineage progenitor (CHILP), from which helper like ILC develop. The transcription factor PLZF characterises committed $Id2^{+ve}GATA3^{+ve}$ ILC progenitor from which ILC1, ILC2 and ILC3 can develop. Development of LTi is independent of PLZF and results from upregulation of ROR-γt in the CHILP. Following of that the fate of the ILCs is determined by expression of T-bet for ILC1, GATA3 and RORα for ILC2 and ROR-γt for ILC3.

1.5.3. Activation and inhibition of ILC2 function

All innate lymphoid cells lack antigen specific receptors and are instead activated by cytokine stimulation. ILC2s responses are triggered by the cytokines IL-33, IL-25 or TSLP. In addition, lipid mediators such as prostaglandins and

leukotrienes or neuronal derived neuropeptides can also induce ILC2s activation (Figure 1.11) (Klose and Artis, 2016).

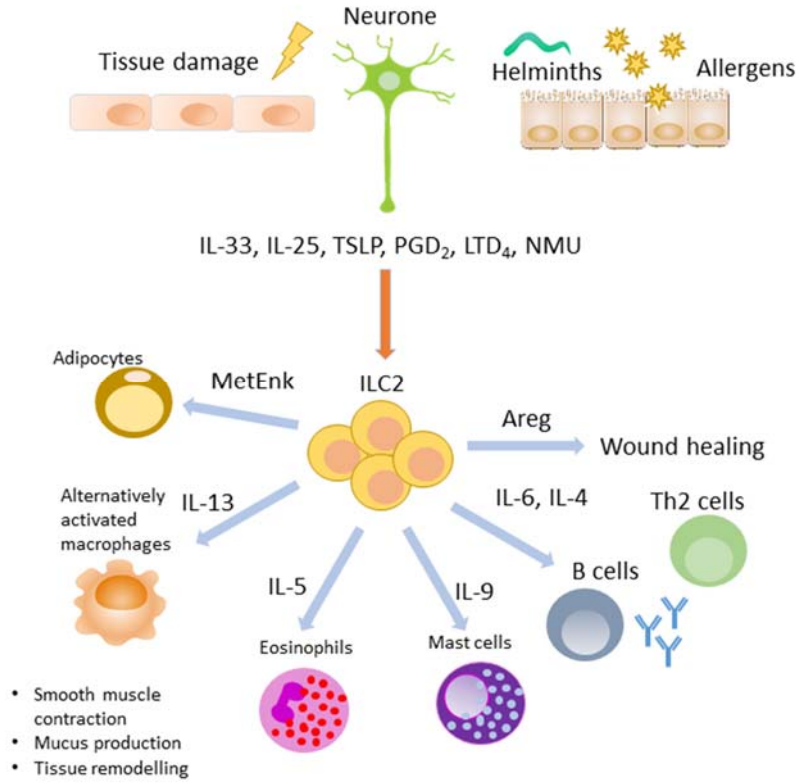

Figure 1.11 ILC2s activation.
ILC2s get activated by multiple signals including the epithelial derived cytokines IL-33, TSLP, and IL-25, lipid mediators such as Prostaglandin D2 or leukotriene D4 or neuron derived neuropeptides such as neuromedin U. Once activated ILC2s secrete effector molecules and mediate the function of other cells. By secreting Met-Enkephalin ILC2s stimulate the beiging of the white adipose tissue. Production of IL-13 leads to the activation of alternatively activated macrophages, IL-13 is also required for the goblet cell metaplasia and mucus production, smooth airway muscle cell contractions. Both IL-13 and IL-5 are promoting eosinophil survival and recruitment. ILC2s stimulate mast cell hyperplasia by secreting IL-9. IL-9 leads to increased expression of inflammatory proteases and cytokine production in mast cells. ILC2s can mediate adaptive immune cell function by secreting IL-6 and IL-4, which are promoting antibody production in B cells and differentiation of Th2 cells. The amphiregulin production by ILC2s promotes wound healing.

1.5.3.1. Activation of ILC2s by IL-33

IL-33 is a cytokine from the IL-1 family, which is released from cells undergoing necrosis or damage caused by inflammatory stimuli, allergens or mechanical injury (Cayrol and Girard, 2009). Murine ILC2s isolated from various

tissues including mesenteric fat, lungs, bone marrow and small intestine express the IL-33 receptor chain ST2 (Moro et al., 2015). ST2 is also expressed in ILC2 precursors (ILC2P) in the bone marrow (Hoyler et al., 2012). In fact stimulation with IL-33 and IL-7 is used as system to generate ILC2 from CLPs (Wong et al., 2012). *Il33*$^{-/-}$ and *St2*$^{-/-}$ mice have significant increase of ILC2s precursors in the bone marrow, but decreased mature ILC2s in the periphery (Stier et al., 2017). This suggests that loss of IL-33 signalling is required for the ILC2s egress from the bone marrow. Mechanistically, this was explained by the fact that stimulation with IL-33 leads to downregulation of the chemokine receptor CXCR4 which regulates the retention of developing leukocytes in the bone marrow (Stier et al., 2017, Brestoff et al., 2014). Human ILC2s isolated from skin or white adipose tissues also express ST2 (Salimi et al., 2013). Similar to mice, IL-33 was shown to have chemoattractant properties and induce migration of human ILC2s (Salimi et al., 2013).

IL-33 is considered as one of the most prominent activators of ILC2s function (Barlow et al., 2013). IL-33 induces production of type two cytokines both in human and murine ILC2s during *in vitro* stimulation (Salimi et al., 2013, Bartemes et al., 2014, Furusawa et al., 2013b). Upon *in vivo* administration of IL-33 in mice, ILC2s are a major subset producing IL-5 and IL-13 in the lungs of mice with house dust mite-induced or ovalbumin-induced allergic asthma (Klein Wolterink et al., 2012). ILC2 are also the predominant source of IL-13 during early stage of *N. brasiliensis* infection and loss of IL-33 led to a substantial reduction in the ILC2-derived IL-13 during *N. brasiliensis* without affecting Th2 responses (Neill et al., 2010, Hung et al., 2013). Because of their ability to mount a strong response to IL-33 stimulation, ILC2s play an important role in the pathology of asthma (Bartemes et al., 2012, Halim et al., 2012).

1.5.3.2. Activation of ILC2s by IL-25

IL-25 (IL-17E) is a cytokine which is part of the IL-17 family. Despite IL-25 sharing structural homology and some functional overlap with other members of the family, IL-25 has a distinct biological activities and induces type two like response. *In vivo* administration of IL-25 leads to splenomegaly, eosinophilia, increased production of IL-5 and IL-13 and increased IgE production (Fort et al., 2001). These *in vivo* effects of IL-25 were found to be mediated by a cell population that did not express T

and B cells markers or FcεR, but were positive for c-Kit (Fallon et al., 2006). Consequent studies suggested that IL-25 induces multipotent progenitor cells ($MMP^{type\ 2}$) which have the potential to differentiate into myeloid subsets and also type two innate lymphoid cells (Saenz et al., 2010, Huang et al., 2015, Saenz et al., 2013). Some groups suggest that IL-25 elicit specific type of inflammatory ILC2s, which upregulate KLRG1 expression and could adopt ILC3s phenotype due to expression of the RORγt transcription factor during lung inflammation (Huang et al., 2014).

In the gut IL-25 derived from tuft cells plays an important role in the maintenance of ILC2s. IL-25 knock out mice have reduced frequencies of ILC2s in the small intestine at steady state and following helminth infection. Tuft cell derived IL-25 was also found to stimulate IL-13 production by ILC2s, which was then required for tuft cell maintenance and IL-25 secretion, suggesting a homeostatic circle between the tuft cells and ILC2s (von Moltke et al., 2015).

1.5.3.3. Activation of ILC2s by TSLP

Thymic stromal lymphopoietin (TSLP) is secreted by epithelial, stromal and mast cells and its expression is highly induced in skin of patients with atopic dermatitis (Soumelis and Liu, 2004). Human and murine ILC2 cells express the TSLP receptor and its co-receptor CD127 (Mjösberg et al., 2012). When stimulated with TSLP, ILC2s from human blood and nasal polyps had a significant increase in the production of IL-13. Stimulation with both IL-33 and TSLP further amplified the ILC2s responses and led to an induction of other cytokines including IL-5, IL-9, GM-CSF and IL-4 (Mjösberg et al., 2012). In an experimental model of atopic dermatitis (AD) ILC2s were massively expanded in wild type mice, however genetic deletion of TSLP receptor resulted in impaired ILC2s expansion and reduced AD-like inflammation (Kim et al., 2013). Analysis of *in vitro* stimulated ILC2s isolated from human blood, showed that TSLP also promotes ILC2s survival (Camelo et al., 2017).

1.5.3.4. Activation of ILC2s by Lipid mediators

ILC2s function can be regulated not only by cytokine stimulation but also by lipid mediators like prostaglandins and leukotrienes (Konya and Mjösberg, 2016). These lipid mediators signal via specific G Protein Coupled Receptors (GPCRs). As

different GPCRs couple to various downstream signalling pathways via heterotrimeric G proteins with different G alpha subunit, different lipid mediators can have very different effects on the ILC2s. Inflammatory signals can induce the release of arachidonic acid from membrane lipids. Arachidonic acid is then converted to prostaglandins or leukotrienes. The COX enzymes catalyse the conversion of arachidonic acid to prostaglandin H2 (PGH_2), which is then converted further to either PGI_2, $PGF_{2\alpha}$, PGD_2 and PGE_2 (Harris et al., 2002). PGD_2 has strong association with asthma and allergic airway inflammation. During allergic response PGD_2 is released by mast cells or epithelial cells and promotes type two immunity (Arima and Fukuda, 2011). Human ILC2s are characterised by the expression of the prostaglandin PGD_2 receptor CRTH2 (Trabanelli et al., 2018, Mjosberg et al., 2011). PGD_2 has a chemoattractant effect on human ILC2s and can influence their migration to the inflamed tissues. PGD_2 stimulation also induces cytokine production in ILC2s (Xue et al., 2014). In contrast to human ILC2, PGD_2 did not activate murine ILC2s to produce cytokines, neither did it amplify the IL-33 dependent response. However, ILC2s accumulated in mouse lungs following *in vivo* intranasal administration of PGD_2. *Ptgdr2*$^{-/-}$ (also called Gpr44$^{-/-}$) mice which lack the prostaglandin PGD_2 receptor CRTH2 displayed less severe pathological changes following infection with *N. brasiliensis*. The authors suggested that this effect was mediated by lack of CRTH2 specifically in ILC2s, since *Ptgdr2*$^{-/-}$ mice which received adoptive transfer of WT ILC2 cells had significantly increased pathology in comparison to *Ptgdr2*$^{-/-}$ mice that were not reconstituted (Tait Wojno et al., 2015).

Prostaglandin E2 (PGE_2) has opposite role than PGD_2 and inhibits IL-33-dependent cytokine production in ILC2s. *In vivo* co-administration of IL-33 and PGE_2 resulted in lower ILC2s infiltration in the bronchoalveolar lavage fluid (BALF) in comparison to treatment with IL-33 alone (Zhou et al., 2018). Furthermore, PGE_2 was found to inhibit the IL-33-dependent increase of GATA3 and ST2 expression in ILC2s (Zhou et al., 2018). The same effect of PGE_2 on GATA3 expression was found also in human ILC2s (Maric et al., 2018).

Like the prostaglandins the leukotrienes are also synthesised from the arachidonic acid. The enzyme 5-lipoxygenase converts arachidonic acid to LTA_4. The last is converted to LTC_4. LTD_4 and LTE_4 are then synthesised from LTC_4.. LTC_4, LTD_4 and LTE_4 are referred as cysteinyl leukotrienes or cysLTs. The cysLTs are

synthesised by variety of immune cells including mast cells, eosinophils and basophils (Peters-Golden et al., 2006). cysLTs signalling results in Ca^{2+} influx in cells, decreased levels of cyclic AMP, activation of the PI3K-Akt pathway, as well as RAS-Raf-ERK pathway (Burke et al., 2016). Stimulation of ILC2s with LTD_4 induced production of IL-4, IL-5 and IL-13, this was accompanied by increased Ca^{2+} influx. *In vivo* administration of LTD_4 led to an increase in IL-5 positive ILC2s. Interestingly, increased levels of cysLTs were found in the BALF of mice stimulated with the fungal pathogen *Alternaria*. Furthermore, co-adminstration of *Alternaria* and cysLTs induced higher ILC2s expansion in comparison to treatment with *Alternaria* alone (Doherty et al., 2013). Double deletion of LTC_4 synthase and the LTB_4 receptor 1 in mice resulted in severely reduced ILC2s accumulation during chitin or *N. brasiliensis* induced lung inflammation (von Moltke et al., 2017). Taken together, these studies provide evidence that lipid mediators have an important role in ILC2 activation or inhibition and could be targeted to modulate ILC2 function.

1.5.3.5. Activation of ILC2 by neuropeptides and neurotransmitters

Recent studies identified a novel type of regulation of ILC2 cells by neuronal cells. Murine and human ILC2s express the G-protein-coupled receptor neuromedin U1 (Nmur), which recognises the neuropeptide neuromedin U (Endo et al., Eder et al., Cardoso et al., 2017, Klose et al., 2017, Wallrapp et al., 2017). NUM is preferentially found in the gut and the genitourinary system, but is also found in the spinal cord and brain (Raddatz et al., 2000). NUM alone was able to induce IL-5 and IL-13 production in ILC2 isolated from either gut or lungs. NMU induced calcium influx and ERK1/2 activation in ILC2s. Inhibition of ERK1/2 or calcineurin in NMU stimulated ILC2s led to a decrease in IL-5 production (Cardoso et al., 2017). The authors showed that neurons secrete NMU in response to stimulation with IL-33 or *N. brasiliensis* and this process was dependent on MyD88 (Cardoso et al., 2017). Furthermore conditional deletion of MyD88 in neurons resulted in impaired cytokine production by ILC2s during *N. brasiliensis* infection (Cardoso et al., 2017). The link between ILC2s and neurons was suggested by another group showing that in the small intestine ILC2s co-localise with NMU positive neurons. Similarly, they showed that NMU induces cytokine production by ILC2s and *in vivo* administration of NMU triggers ILC2-dependent lung inflammation (Klose et al., 2017). Interestingly, ILC2s could also

sense neuronal signals which limit their response. Expression of β2-adrenergic receptor (β2AR) was found on ILC2s isolated from mouse gut. Treatment with β2AR agonist resulted in impaired cytokine production in ILC2 and impaired worm clearance *in vivo* (Moriyama et al., 2018).

1.5.3.6. E-cadherin-KLRG1 interaction

KLRG1 (killer-cell lectin like receptor) is a C-type lectin expressed on NK cells, T cells and ILC2s (Hoyler et al., 2012, Jonjic, 2010, Corral et al., 2000). KLRG1 is an inhibitory receptor with an intracellular immunoreceptor tyrosine based inhibitory motif (ITIM). KLRG1 binding tomembers of the cadherin family leads to inhibition of NK and T cell function (Jonjic, 2010). Upregulated KLRG1 expression is commonly associated with activation in ILC2s (Wallrapp et al., 2017). However, treatment of PMA or IL-33 stimulated human ILC2 cells with E-Cadherin led to a reduced levels of *GATA3, IL13,* and *IL5* mRNA levels relative to PMA or IL-33 stimulation alone. The authors suggested that the interaction of E-cadherin and KLRG1 could have an important role in the pathology of atopic dermatitis, a condition in which the expression of E-cadherin in keratinocytes is reduced and ILC2 numbers and type two cytokines are increased (Salimi et al., 2013, Trautmann et al., 2001).

1.5.3.7. ICOS-ICOSL interaction in ILC2s

ILC2s express inducible T-cell co-stimulator (ICOS) (Paclik et al., 2015). In T cells the ICOS signalling plays an important role in survival and regulates cytokine production (Coyle et al., 2000). ILC2 numbers are significantly reduced in ICOS and ICOS ligand deficient mice (Paclik et al., 2015). The response of ICOSL and ICOS deficient mice was also impaired during IL-33 induced airway inflammation (Paclik et al., 2015, Maazi et al., 2015). ICOS ligand expression was also detected on mouse and human ILC2s, suggesting that ICOS-ICOSL interaction among ILC2s could influence their homeostasis (Paclik et al., 2015, Maazi et al., 2015). Furthermore, it was found that ICOSL on ILC2s binds to ICOS expressed on inducible regulatory T cells and this binding has an inhibitory effect on ILC2 function both *in vitro* and *in*

1.6. Aims

IL-33 dependent responses in ILC2s have been implicated in a number of pathological conditions such as asthma, atopic dermatitis and helminth infections. Therefore, the first aim of this study was to investigate the role of IL-33 signalling pathway in type two innate lymphoid cells (ILC2s). Due to the implication of MAPKAPKs MK2/3 in regulating IL-33 dependent cytokine production in mast cells, another aim was to characterise ILC2s in mice deficient of these kinases and to understand if they are important for regulation of the cytokine production in ILC2s.

In addition, initial data indicated that IL-33 induces major changes in size and proliferation of ILC2s. Consequently, the IL-33 mediated metabolic changes were investigated, including upregulation of nutrient transports, mTOR and c-Myc activation and amino acid uptake. The role of the amino acid transporter Slc7a5 was also studied using *Slc7a5*$^{fl/fl}$*Vav-iCre*$^{+/-}$ mice.

As part of this work, ABIN1[D485N] knockin mice, which spontaneously develop a Lupus-like autoimmune condition, were examined to see if they had normal numbers of ILC2s. This revealed the presence of a greatly expanded population of patrolling monocytes in the tissues of these mice, and this became focus of study during my PhD.

II. Materials and methods

2.1. Animals

MK2/3 (*Mapkapk2*^{tm1mgl} / *Mapkapk3*^{tm1mgl}) knock out mice were obtained from Prof. Matthias Gaestel (Hannover Medical School) (Kotlyarov et al., 1999b, Zaru et al., 2007). To generate a conditional MK2 mice, *Mapkapk2*$^{tm1a(EUCOMM)Hmgu}$ were purchased from the International Mouse Phenotyping Consortium. *Mapkapk2*$^{tm1a(EUCOMM)Hmgu}$ were crossed to Flpe transgenic mice (TaconicArtemis) to remove the LacZ and marker cassette. The conditional MK2 allele was then crossed away from the Flpe transgene and further crossed to *Vav-iCre* mice (de Boer et al., 2003), to selectively delete MK2 in immune cells. ABIN1[D485N] (*Tnip1*^{tm1Pcoh}) (Nanda et al., 2011), IRAK1[D359A] (*IRAK1*^{tm1Pcoh}) (Goh et al., 2012), IRAK4[D329A] (*IRAK4*^{tm1Pcoh}) (Nanda et al., 2016) and IRAK2[E525A] (*IRAK2*^{tm1Pcoh}) (Pauls et al., 2013a) knock in mice were obtained from Professor Philip Cohen (University of Dundee). *Slc7a5*$^{fl/fl}$ (*Slc7a5*^{tm1Daca}) bred to *Vav-iCre*$^{+/-}$ mice were obtained from Professor Doreen Cantrell (University of Dundee) (Poncet et al., 2014). TLR7 (B6.129S1-*Tlr7*^{tm1Flv}/J,) and IL-6 (B6;129S2-*IL6*^{tm1Kopf}/J) knock out mice were purchased from Jackson Laboratory (Lund et al., 2004, Kopf et al., 1994). MyD88 (*Myd88*^{tm1Aki}) knock out mice were provided by S. Akira (Adachi et al., 1998). All mice were bred on a C57Bl/6J background and wild type mice for backcrossing obtained from Charles River Laboratories UK. Animals were maintained in specific pathogen-free conditions according with EU and UK regulations. Non breeding mice were housed in same-sex groups, in individually ventilated sterile cages and were given standard diet R&M1 or R&M3 (SDS, Special Diets Services). Animals were maintained in rooms with controlled 12h/12h light/dark cycle (lights on at 7:00 AM), 21°C temperature, and relative humidity of 45%–65%. All the work was performed under a UK Home Office project license and subject to local ethical review.

Colony maintenance, PCR genotyping and breeding of MK2/3 KO and conditional MAPKAPK2 (Vav-cre) was done by Tsvetana Petrova and Simon Arthur. Colony mainatince for the ABIN1 crosses was carried out by Sambit Nanda (MRC PPU) and genotyping carried out by the Genotyping Service in the MRC PPU. Routine welfare

checks and cage changing was carried out by Biological Services, University of Dundee.

2.2. Genotyping

Mice were genotyped from ear biopsy. DNA was extracted by digestion in buffer containing 10 mg/ml Proteinase K in 28 mM NaCl, 55 mM Tris HCl, pH 8.0, 0.1% SDS. Samples were incubated at 55ºC for 6h, 96ºC for 10 min (to kill the Proteinase K) and then stored at -20ºC until use. PCR reaction mix is shown in Table 2.1, primers used for the genotyping are listed in Table 2.2 and the PCR program in Table 2.3. Samples were run on 2% Agarose gels made in TAE buffer and bands visualized using Syberafe DNA dye (Invitrogen).

Table 2.1. PCR reaction mix

Reagent	**Stock concentration**	**Final concentration**	**Volume**
Taq Buffer (Promega)	5x	1x	5
dNTP	2 mM	0.2 mM	2.5
Fwd primer	10 µM	0.2 µM	0.5
Rev Primer	10 µM	0.2 µM	0.5
Go-Taq (Promega)			0.1 µl
H_20			14.4 µl
DNA			2 µl

Table 2.2. Primer sequences for genotyping

Mouse line	Target sequence	Primer sense
MK2 Vav Cre	Loxp forward	5' TGTCATCATGTATATTTTGTAAGTGGGCTG 3'
MK2 Vav Cre	Loxp reverse	5' GGCTAGCCCATTAGCTAGTTTCTAC 3'
MK2 Vav Cre	5' Arm forward	5' GTCCAGCTTGACTTCATGCTCCTG 3'
MK2 Vav Cre	CSD-Neomycin cassete forward	5' GGGATCTCATGCTGGAGTTCTTCG 3'
MK2 Vav Cre	Floxed region reverse	5' CAACTCTCATTCCATCAGCTAAGAGC 3'
MK2 Vav Cre	Cre forward	5' AAA TGG TTT CCC GCA GAA CC 3'
MK2 Vav Cre	Cre reverse	5' TAG CTG GCT GGT GGC AGA TG 3'
MK2/3 double knock out	Mapkap2 (for)	5' CGTGGGGGTGGGGTGACATGCTGGTTGAC 3'
MK2/3 double knock out	Mapkap2 (rev WT)	5' GGTGTCACCTTGACATCCCGGTGAG 3'
MK2/3 double knock out	Mapkap2 (rev NEO)	5' TGCTCGCTCGATGCGATGTTTCGC 3'
MK2/3 double knock out	Mapkap3 (for WT)	5' TTAGTTGTTTGGCCATGACCTCCAGCTTTC 3'
MK2/3 double knock out	Mapkap3 (for NEO)	5' TGCTTTACGGTATCGCCGCTCCCGATTC 3'
MK2/3 double knock out	Mapkap3 (rev)	5' ATAGCTGGTCCTCGAATGGGCCAGCCTG 3'

Table 2.3. PCR program for genotyping

Step	Temperature	Time
1	95°C	2 min
2	95°C	30s
3	60°C	30s
4	72°C	30s
5 Go to step 2, repeat 36 times		
6	72°C	5 min
7	10°	Forever

2.3. Media and Buffers

Table 2.4. Media and Buffers

Solution	Recipe
Complete RPMI	RPMI-1640 medium with 10% heat-inactivated FBS, 50 U/ml penicillin-streptomycin, 5mM L-glutamine, 10mM HEPES buffer, 1mM sodium pyruvate, 50 µM 2-mercaptoethanol
R20F Eosinophil media	RPMI containing 20% FCS, 100 IU/ml penicillin, 10 mg/ml streptomycin, 5mM L-glutamine, 1x non-essential amino acids, 1 mM sodium pyruvate and 50µM 2-mercaptoethanol
BMDM media	DMEM containing 10% FBS, 5mM L-Glutamine, 50 U/mL Penicillin, 100 mg/mL Streptomycin , 0.25 mg/mL amphoceterin (Life Technologies) and 5 ng/mL M-CSF (R&D Systems)
MACS buffer	PBS with 0.5% BSA and 2mM EDTA
FACS buffer	PBS with 1% BSA
Blood collection buffer	10% FBS, 10% RBC lysing buffer (Sigma) and 2mM EDTA in RPMI
ELISA Coating buffer	0.1M NaHCO3, pH 8.2 in MilliQ H2O
ELISA Coat Wash buffer	1M KPO4 and 0.05% Tween 20 in MilliQ H2O
ELISA Assay wash buffer	NaCl, 1M NaPO4, 2.7M KCl and 0.05% Tween 20 in MilliQ H_2O
EAR digestion buffer	28mM NaCl, 55mM Tris HCl, ph 8.0, 0.1% SDS, MilliQ H_2O
TAE buffer 10x	40 mM Tris-acetate, 1mMof EDTA, disodium salt.

2.4. Isolation of cells from spleen and mesenteric lymph nodes

Single cell suspensions from spleens were obtained by gently mashing the spleen through 40 µm nylon cell strainer (VWR) in 5 ml of complete RPMI media. Suspensions were centrifuged at 450g for 5 minutes at room temperature (RT), supernatant was removed and red blood cells were lysed by resuspending the pellet in 1 ml of RBC lysing Buffer (Sigma) for 2 min at RT. Cells were washed by adding 10

mL ice cold PBS, pelleted by centrifugation at 450g for 5 minutes and resuspended in 10 ml complete RPMI media. Cell suspensions were filtered through 40 µm nylon cell strainer to remove any clumps.

2.5. Isolation of cells from lungs, mesenteric fat and eWAT

Lung and mesenteric fat digestion was performed as previously described (Moro et al., 2015a). Briefly, lungs were placed into a 40 µm cell strainer (VWR) in a 58 mm cell culture dish (Nunclon, Thermo Scientific) and cut into small segments. 7 ml of RPMI containing 50 µg/ml Liberase TM (Sigma Aldrich) and 10 µg/ml DNaseI (Roche/Sigma Alderich) were added to the lung segments and they were incubated for 45 min at 37°C. Lung segments were mashed through 40 µm cell strainers and washed with 13 ml of 5% FBS in HBSS. Cell suspensions were centrifuged (450g for 5 minutes at RT) and red blood cells were lysed as described above. Cell pellets were resuspended in 5ml complete RPMI media and filtered through a 40 µm cell strainer.

Single cell suspensions from mesenteric fat or epididymal white adipose tissue were obtained by dissecting and placing the tissue into a 15ml falcon tube containing 7 ml of 4% BSA in DMEM. For isolation of cells from multiple mice, mesenteric fat from up to 6 mice was placed into a 50 ml falcon tube containing 25 ml of 4% BSA in DMEM. The fat tissue was cut into small segments, Liberase^{TM} (50 µg/ml) and DNaseI (10 µg/ml) were added to the tubes and they were incubated for 1 hour at 37°C in water bath. Tubes were vigorously shaken every 15 minutes. Following the incubation red blood cells were lysed as described above. Cells were resuspended in RPMI media and filtered through 40 µm cell strainer.

2.6. Isolation of blood leukocytes

For phenotyping blood, mouse tail was cut superficially and 4-5 drops of blood were collected in 1mL ice cold blood collection buffer. Collection of blood was carried out by staff in Biological Services, University of Dundee or Dr Sambit Nanda. Alternatively, blood was collected from the heart via cardiac puncture and placed in heparin coated tubes. 50 µl from the blood were added to 1mL ice cold blood collection buffer. Tubes were centrifuged at 450g for 5 minutes at 4°C, pellets were

resuspended in 1ml of RBC lysis buffer and incubated for 5 minutes at room temperature. Cells were centrifuged as above, supernatant was aspirated and cells were resuspended in 1 mL FACS buffer and kept on ice before flow cytometry analysis.

2.7. Isolation of bone marrow

Femurs and tibias were dissected under sterile conditions. The epiphyses were cut, the bone marrow was flushed with sterile 20 mL of PBS and the suspension was passed through a 100 μm cell strainer (VWR). Cells were centrifuged at 450g for 5mins at RT, red blood cells were lysed as previously described and cell pellets were resuspended in PBS.

2.8. Cell culture and stimulation

2.8.1. Purification and cell culture of type two innate lymphoid cells

ILC2 cells were purified from mesenteric fat cell suspensions using magnetic sorting. Cells were counted on haemocytometer and up to $1x10^7$ cells were incubated in 100 μl of CD16/CD32 Fc block (1:50 in MACS buffer) (BD Biosciences) for 20 minutes at 4°C. To deplete other immune cells, a cocktail of biotinylated anti-CD3, anti-CD11b, anti-CD11c, anti-Ly6C/Ly6G, anti-F4/80, anti-CD19, anti-B220, anti-NK1.1 and anti-TER119 antibodies (antibody dilutions are listed in Table 2.5) was added to the mesenteric cells and they were incubated for further 20 minutes at 4°C. Unbound antibodies were removed by adding 10 ml of MACS buffer and the cell suspension was centrifuged at 450g for 5 mins. Supernatant was aspirated away and cells were incubated with streptavidin conjugated magnetic microbeads (Miltenyi Biotec) for 10 minutes at 4°C according to manufacturer's instruction. After incubation cells were washed with MACS buffer and centrifuged (450g for 5 minutes). The cell pellet was then resuspended in 1 ml of MACS buffer and passed through a LD depletion column (Miltenyi Biotec) that had been pre-wetted in MACS buffer and placed on a magnetic separator. The column was washed two times by adding 1 ml of MACS buffer. The flow through and washes were collected in a 15 ml falcon, cells were centrifuged (450g for 5 minutes), resuspended in 100 μl of biotinylated anti-CD45 antibody diluted 1:200 in MACS buffer and incubated for 20 minutes at 4°C.

Cells were washed with MACS buffer and incubated with streptavidin microbeads for 10 minutes at 4°C. After the incubation, the cells were washed in MACS buffer, resuspended in 1 ml of MACS buffer and passed through a pre-wetted MS column (Miltenyi). The column was washed twice with 1ml of MACS buffer. The flow through was discarded, the column was removed from the magnetic separator and placed into a new 15 ml falcon tube. The cells bound to the column were eluted by adding 2 ml of MACS buffer and using the column plunger. Cells were counted on haemocytometer and cultured at 0.5-1x10^5 density in 200 µl of complete RPMI media supplemented with IL-2 (20 ng/ml) and IL-7 (10 ng/ml) in 96-well plate for 5 days at 37°C and 5% CO_2. On day 3 half of the media was replaced with fresh media containing IL-2 (20 ng/ml) and IL-7 (10 ng/ml).

Table 2.5. Biotinylated antibodies for depletion of Lineage positive cells

Antigen	Clone	Concentration		Company
CD3ε	145-2C11	0.5 µl for 1x10^6 cells	Biotin	BioLegend
CD11b	M1/70	0.5 µl for 1x10^6 cells	Biotin	BioLegend
Ly-6G/Ly-6C (Gr-1)	RB6-8C5	0.5 µl for 1x10^6 cells	Biotin	BioLegend
TER-119	Ter-119	0.5 µl for 1x10^6 cells	Biotin	BioLegend
CD45R/B220	RA3-6B2	0.5 µl for 1x10^6 cells	Biotin	BioLegend
NK 1.1	PK136	0.5 µl for 1x10^6 cells	Biotin	BioLegend
CD19	6D5	0.5 µl for 1x10^6 cells	Biotin	BioLegend
CD11c	N418	0.5 µl for 1x10^6 cells	Biotin	BioLegend
F4/80	BM8	0.5 µl for 1x10^6 cells	Biotin	BioLegend
CD45	30-F11	1:200	Biotin	BioLegend

2.8.2. Stimulation of ILC2 cells

Cultured ILC2 cells were plated in 96 well plates at a density of 2500-5000 cells in 100 µl of complete RPMI media for stimulation (without IL-2 and IL-7). ILC2 cells were pre-incubated with inhibitors (listed in Table 2.6) for 1 hour before stimulation. The agonists used are listed in Table 2.7. Following the stimulation, 50 µl from the culture media was carefully collected at the times indicated in the figure legends without disturbing the cells to measure cytokine production. At the end of the

stimulation, cells were stained by adding 150 µl of PBS with DAPI (0.5 µg/mL) in each well. Plates were analysed on BD FACSVerse to determine absolute counts of live DAPI negative cells. For time course stimulations of ILC2, cells were plated in 100 µl of media and stimulated with 100 ng/mL IL-33. 50 µl of the culture media were collected on day 1 and day 3 and replaced with fresh 50 µl media with the corresponding stimuli and inhibitors. On day 5 the media was collected and cells were counted as described above.

Table 2.6. Small molecule inhibitors

Name	Target	Concentration	Reference
VX-745	p38α/β	1 µM	(Tsai et al., 2013)
PD-184352	MKK1/2	2 µM	(Mayes et al., 2013)
JNK-in8	JNK1/2	3 µM	(Zhang et al., 2012)
PF-3644022	MK2/3	5 µM	(Mourey et al., 2010)
Akti-1/2	Akt	1 µM	(Logie et al., 2007)
Dasatinib	c-kit/Bcr-Abl	10 nM	(Kitagawa et al., 2013)
Cmp2s	MK2/3	5 µM	(Xiao et al., 2013)
Rapamycin	mTORC1	20 nM	(Bain et al., 2007)

Table 2.7. Agonists

Name	Target	Concentration	Source
IL-33	ST2	100 ng/mL	Peprotech
IL-2	CD25	20 ng/mL	Peprotech
IL-25	IL-17RB	10 ng/mL	Peprotech
R837	TLR7	1 µg/mL	Invivogen
LPS	TLR4	100 ng/mL	Sigma
PMA	multiple targets including activation of PKC and ERK1/2	50 ng/mL	Merck Millipore
Ionomycin	Elicits Ca^{2+} influx	1 µg/mL	Merck Millipore

2.9. Flow cytometry

2.9.1. Cell counting

Cell suspensions obtained from bone marrow, lungs, spleens, lymph nodes were diluted 1:10 or 1:20 in total volume of 1 ml of PBS with 0.5 µg/ ml of DAPI (BioLegend) and analysed on BD FACSVerse. Absolute numbers were calculated using FlowJo software (Tree Star). Alternatively, cells were counted using Precision Count Beads (BioLegend) according to manufacturer's instruction. Briefly, cells were diluted 1:10 in PBS with 0.5 µg/ ml of DAPI to a total volume of 950 µl. 50 µl count beads were added to the cell suspension and cells were acquired on a BD FACSCanto. Data were analysed using FlowJo software to obtain event numbers in the beads and live cell gates. Beads were gated based on autofluorescence in the FITC and APC/Cy7 channels and the absolute number of DAPI negative live cells was calculated using the formula:

$$\text{Absoluite cell count}\left(\frac{\text{cells}}{\mu\text{l}}\right) = \frac{live\ cells\ count\ x\ beads\ volume}{beads\ count\ x\ cell\ volume}\ x\ beads\ concentration$$

2.9.2. Extracellular staining

Staining for flow cytometry analysis was performed using standard techniques. Briefly, cells were blocked with 50 µl rat anti-mouse CD16/CD32 Fc block (BD Pharmigen) (1:50 in FACS buffer) and incubated for 20 minutes at 4°C. For detection of surface antigens cells were stained with the appropriate fluorophore conjugated antibodies (listed in Table 2.8) for 20 minutes at 4°C. Cells were then washed by adding 1 ml of FACS buffer and centrifuged at 450g for 5 minutes at 4°C. Pellets were resuspended in 400 µl of FACS buffer. For dead cell exclusion 0.5 µg/ ml of DAPI (Biolegend) or 0.25 µg of 7-AAD (eBioscience) were added to the tubes before acquiring. Samples were analysed using FACSCanto or BD LSRII Fortessa (BD Bioscience) and results were further analysed by FlowJo software (Tree Star).

2.9.3. Intracellular staining

To measure TNF-α and IL-6 production by flow cytometry, $1x10^6$ cells isolated from spleen and lungs were stimulated in 1 ml of complete RPMI media in the

presence of 5 µg/ml Brefeldin and/or 2µM Monensin (BioLegend). Media was washed and cells were resuspended in 100 µl of FACS buffer. To measure IL-13 production in ILC2 cells, 20 000 cells were stimulated in 200 µl of RPMI media for 28 hours, in the last 4 hours of the stimulation 2µM Monensin were added to the cells. Following the stimulation, cells were fixed by adding 100 µl of IC Fixation Buffer (eBioscience) and 20 minutes incubation at 4°C. Cells were washed and supernatants were discarded. 300 µl of 1x Permeabilisation buffer (eBioscience) were added into the tubes and the cells were incubated for 20 min at 4°C. Cells were then blocked and stained as described above.m

Table 2.8. Flow cytometry antibodies

Target	Fluorophore	Clone	Dilution	Stock conc	Source
Lieange	PE	mixed	1:50		BioLegend
CD45	APC-eFluor 780	30-F11	1:200	0.2 mg/ml	ThermoFisher
CD3ε	FITC	17A2	1:200	0.5 mg/ml	BioLegend
CD19	FITC	6D5	1:200	0.5 mg/ml	BioLegend
CD8	FITC	53-6.7	1:200	0.5 mg/ml	BioLegend
F4/80	FITC	BM4	1:200	0.2 mg/ml	BioLegend
CD11b	FITC	M1/70	1:200	0.5 mg/ml	BioLegend
CD11c	FITC	N418	1:200	0.5 mg/ml	BioLegend
NK1.1	FITC	PK136	1:200	0.5 mg/ml	BioLegend
c-Kit	PE/Cy7	2B8	1:200	0.2 mg/ml	BioLegend
KLRG1	APC	2F1	1:200	0.2 mg/ml	BD Biosciences
Sca1	APC/Cy7	D7	1:200	0.5 mg/ml	BD Biosciences
ST2	PerCP-eFluor710	RMST2-2	1:200	0.2 mg/ml	ThermoFisher
ST2	BV421	DIH9	1:200	0.2 mg/ml	BioLegend
CD45.1	BV510	A20	1:200	0.2 mg/ml	BioLegend
CD45.2	PerCp/Cy5.5	104	1:200	0.2 mg/ml	BioLegend
CD45	BV510	30-F11	1:200	0.2 mg/ml	BioLegend
NK1.1	APC/Cy7	PK136	1:200	0.5 mg/ml	BioLegend
CD11c	PE/Dazzle594	N418	1:200	0.2 mg/ml	BioLegend
CD11b	PE/Cy7	M1/70	1:600	0.2 mg/ml	BioLegend
Ly-6G/Ly-6C (Gr-1)	PerCp/Cy5.5	RB6-8C5	1:400	0.2 mg/ml	BioLegend
Ly-6G/Ly-6C (Gr-1)	FITC	RB6-8C5	1:400	0.2 mg/ml	BioLegend

Ly-6C	FITC	HK1.4	1:400	0.5 mg/ml	BioLegend
Ly-6C	BV421	HK1.4	1:400	0.5 mg/ml	BioLegend
CX3CR1	PE	SA011F11	1:200	0.2 mg/ml	BioLegend
CD115	APC	AFS98	1:200	0.2 mg/ml	BioLegend
I-A/I-E (MHC II)	AlexaFluor700	M5/114.15.2	1:200	0.5 mg/ml	BioLegend
CD45R (B220)	APC	RA3-6B2	1:200	0.2 mg/ml	ThermoFisher
CD95 (Fas)	PE	SA367H8	1:400	0.2 mg/ml	BioLegend
Gl7	FITC	GL7	1:400	0.5 mg/ml	BioLegend
TCR-β	FITC	H57-597	1:50	0.5 mg/ml	BioLegend
CD4	PerCp/Cy5.5	GK1.5	1:200	0.2 mg/ml	BioLegend
CXCR5	APC	L138D7	1:100	0.2 mg/ml	BioLegend
PD-1	BV421	29F.1A12	1:100	0.2 mg/ml	BioLegend
TNF-alpha	APC	MP6-XT22	1:400	0.2 mg/ml	BioLegend
IL-6	PE	MP5-20F3	1:100	0.2 mg/ml	ThermoFisher
IL-13	PE	eBio13A	1:200	0.2 mg/ml	ThermoFisher
IL-5	APC	TRFK5	1:100	0.2 mg/ml	BioLegend
IL-4	PE/Cy7	11B11	1:100	0.5 mg/ml	BioLegend
TLR7	PE	58557	1:100	0.2 mg/ml	BDPharmigen
Phospho-p38 (Thr180/Tyr182)	Alexaflour647	3D7	1:100		Cell Signalling
Phospho-S6 (Ser235/236)	Alexaflour647	D57.2.2E	1:100		Cell Signalling
Phospho ERK1/2 (Thr202/Tyr204) Antibody	BV421	6B8B69	1:100		BioLegend

2.9.4. Detection of protein phosphorylation

ILC2 cells were seeded in 500 µl complete RPMI media in sterile 4 ml polystyrene round-bottom flow cytometry tubes. Cells were rested for 3 hours in complete RPMI media before pre-incubation for 1 hour with inhibitors listed in Table 2.6. Cells were stimulated with 100 ng/ml IL-33 for the indicated time. After the stimulation, ILC2 cells were fixed by adding 500 µl of ice cold 4% PFA and 20 mins incubation on ice. Tubes were centrifuged (450g for 5 minutes) and supernatant was removed. Cells were permeabilised by adding 1 ml of ice cold 90% methanol while vortexing. Tubes were incubated overnight in the freezer at -20 °C. On the next day tubes were left for

30 mins on the bench. Cells were then washed with 2 ml of FACS buffer and stained as described above in 2.9.3.

2.9.5. Kynurenine uptake assay

ILC2 cells were left untreated or stimulated for 24 hours with 100 ng/ml of IL-33. Following the stimulation the cells were centrifuged at 450g for 5 min, supernatant was discarded and cells were resuspended in 0.5 ml of HBSS (37°C). Data were collected on BD FACS canto with the violet laser. To determine the baseline uptake of kynurenine, each sample was acquired initially for 2 minutes before adding the kynurenine to a final concentration of 200 µM. The samples were then collected for further 5 min. Data were analysed in FlowJo by plotting the fluorescence in the V450 channel against time.

2.10. Cell sorting

2.10.1. Sorting of ILC2 cells

Lineage negative cells were depleted as described above in 2.8.1 from mesenteric cell suspensions. Cells were then stained with anti-Lineage (PE), anti-CD45 (APCeFlour780), anti-Sca1 (FITC), anti-KLRG1 (APC) and anti-ST2 (PerCP-eFluor710) diluted in MACS buffer. ILC2 cells were defined as $DAPI^{-ve}Lineage^{-ve}CD45^{+}KLRG1^{+}Sca1^{+}ST2^{+}$ and sorted on BD Influx™ cell sorter.

2.10.2. Sorting of neutrophils, $Ly6C^{+ve}$ and $Ly6C^{-ve}$ monocytes

Neutrophils, $Ly6C^{+ve}$ and $Ly6C^{-ve}$ monocytes were sorted from spleens of WT and ABIN1 knock in mice. Splenocytes were resuspended in 500 µl CD16/32 Fc block (1:50 in MACS buffer) and incubated on ice for 20 mins. Cells were incubated for another 20 mins at 4°C with biotinylated antibodies against TER119, CD3, CD19 and NK.1.1 (0.5 µl per $1x10^6$ cells from each antibody) to deplete red blood cells, T, B and NK cells. Unbound antibodies were removed by adding 10 ml of MACS buffer and centrifuging the tubes at 450g for 5 minutes. Pellets were resuspended in Streptavidin Microbeads (Miltenyi) diluted in MACS buffer according to manufacturer's

instructions and passed through LD columns. The cells in the flow through were collected and stained with antibodies against CD45 (BV510), NK1.1(APCCy7), CD11b(PeCy7), Ly6C(FITC), CX_3CR1(PE) and CD115 (APC). Neutrophils ($DAPI^{-ve}CD45^{+ve}NK1.1^{-ve}CD11b^{+ve}Ly6C^{mid}Gr1^{high}$), Ly6C^{+ve} inflammatory ($DAPI^{-ve}CD45^{+ve}NK1.1^{-ve}CD11b^{+ve}Ly6C^{high}CX_3CR1^{+ve}CD115^{+ve}$) and Ly6C^{-ve} patrolling monocytes ($DAPI^{-ve}CD45^{+ve}NK1.1^{-ve}CD11b^{+ve}Ly6C^{-ve}CX_3CR1^{+ve}CD115^{+ve}$) were sorted on BD Influx™ cell sorter.

2.11. RNA extraction

Lung tissues were ground to a fine powder in the presence of liquid N_2 using cellcrusher (Stratech). 20-30 mg of the powder were lysed in 350 µl of LBP lysis buffer (Macherey-Nagel) and RNA was extracted using NucleoSpin® RNA Plus kit according to manufacturer instruction (Macherey-Nagel). RNA concentration was determined using a Nanodrop 1000 spectrophotometer. RNA samples were stored at -80°C. cDNA was synthesised from 200 ng of RNA in a 20 µl reaction volume containing 4 µl iScript Reaction buffer and 1 µl iScript reverse transcriptase (Bio-Rad). Samples were incubated in a thermal cycler, at 25°C for 5 minutes, 42°C for 30 minutes and 85°C for 5 minutes. cDNA samples were diluted 1:10 in nuclease-free water and stored at -20°C.

2.12. Real-time quantitative PCR

Quantitative PCR was performed in 384 well plate (Bio-rad) using Syber®Premix Ex Taq™ II (Takara) and CFX 384 thermal cycler (Bio-Rad). Reaction mix is shown in Table 2.9 and primers are listed in Table 2.10.

Table 2.9. Quantitative PCR reaction mix

Reagent	Amount	Final concentration
Syber®Premix Ex Taq™ II (2x)	7 µl	1x
Forward Primer (10 µM)	0.28 µl	0.4 µM
Reverse Primer (10 µM)	0.28 µl	0.4 µM
cDNA	4 µl	
H_2O (nuclease-free water)	2.44 µl	

Table 2.10. Quantitative PCR primers

Gene	Forward primer	Reverse primer
18S	GTAACCCGTTGAACCCCATT	CCATCCAATCGGTAGTAGCG
GAPDH	ACAGTTCTTATGTGGTGACCC	TGCACCACCAACTGCTTAG
IL4	AATGCCGATGATCTCTC	CTTGATAAACTTAATTGTCTCTC
IL5	AGGCTTCCTGTCCCTACTCA	CCCCCACGGACAGTTTGATT
IL6	TTCCATCCAGTTGCCTTCTTG	AGGTCTGTTGGGAGTGGTATC
IL13	GCAGCAGCTTGAGCACATTT	GCAGACAGGAGTGTTGCTCT
IL33	CAATGACCAATCTGTTAGT	CATAGTAGGGTAGTAGCA
Arg1	CTCCAAGCCAAAGTCCTTAGAG	AGGAGCTGTCATTAGGGACATC
Eotaxin	GCAGAGCTCCACAGCGCTTCTATTCCT	GTTTTTGGTCCAGGTGCTTTGTGGCATCC
Ym1	GGCAATTCTTCTGAACGTACAGCTGGG	GAAGTCATCCATGTCCAGGGGCCAG

PCR conditions were as follows: Initial denaturation was done at 95ºC for 30 seconds, followed by 60 cycles of 95ºC for 1 second and 60ºC for 25 seconds. The melting curve analysis of the PCR products was done at 95ºC for 1 minute, 65ºC for 1 minute, followed by an increase in 0.5ºC increments every 5 seconds.18S and GAPDH mRNA were used as housekeeping genes for normalisation of the input. The mRNA levels were calculated using the following equation:

$$relative\ mRNA\ level = \frac{E_i^{(Ct_{ic} - Ct_{is})}}{E_h^{(Ct_{hc} - Ct_{hs})}}$$

where E is the efficiency of the PCR primer pair, Ct is the threshold cycle, i is the mRNA of interest, h is the housekeeping gene, s is the sample and c is the unstimulated control.

2.13. Histology

2.13.1. Fixation and paraffin embedding of lung tissues

Freshly dissected lungs were fixed in 4% PFA for 48 hours at room temperature. Samples were then transferred in embedding cassettes (Simport- M490-2) in 70% ethanol for 3-4 hours. Immediately prior to embedding, the cassettes were rinsed in PBS for 5 minutes. The cassettes were placed in Citadel Tissue processor (Thermo Shandon) and run on the program shown in Table 2.11. Tissues were then embedded into paraffin blocks.

Table 2.11. Citadel program

Solution	Time
50% Ethanol	1 hours
70% Ethanol	2 hours
80% Ethanol	2 hours
90% Ethanol	2 hours
100% Ethanol	2 hours
100% Ethanol	2 hours
100% Ethanol	2 hours
Xylene	1 hours
Xylene	2 hours
Xylene	2 hours
Paraffin wax	3 hours
Paraffin wax	3 hours

2.13.2. Slide preparations and staining

5 μM sections were cut using microtome and mounted on slides. Slides were left to air dry for 1 hour at room temperature and then further dried in a 60°C oven overnight. Slides were deparaffinised and dehydrated and stained with haematoxylin and eosin using standard technics as shown in Table 2.12.

Table 2.12. Deparaffinised and dehydrated and H&E staining.

Deparaffinised and Dehydrated		Haematoxylin and Eosin	
Xylene	5 min	Haematoxylin	1 min
Xylene	5 min	Running tap water	10 min
100% Ethanol	2 min	80% EtOH	2 min
100% Ethanol	2 min	Eosin	10s
95% Ethanol	2 min	95% EtOH	2 min
95% Ethanol	2 min	95% EtOH	2 min
75% Ethanol	2 min	100% EtOH	2 min
50% Ethanol	2 min	100% EtOH	2 min
dH_2O	2 min	Xylene	2 min
		Xylene	2 min

2.14. Enzyme-linked immunosorbent assay

2.14.1. Preparation of mouse serum

Mouse blood was obtained by superficial tail cut or by cardiac puncture. Blood was collected in eppendorf tubes, left at 4°C for 30 minutes to allow blood clotting and centrifuged at 6797g for 5 minutes at 4°C. Serum was carefully collected and transferred into a new tube. Samples were stored at -20°C before analysis.

2.14.2. Detection of anti-dsDNA and anti-nuclear antibodies (ANA)

Autoantibodies to dsDNA and antinuclear antibodies (total Ig; Alpha Diagnostics International) were measured according to manufacturer's instruction. Serum samples were diluted 50x times in the corresponding buffers provided in the kit.

2.15. Multiplex assay for cytokines and chemokines detection

Supernatants from cell cultures were collected and stored at -80°C prior to analysis. Cytokines in supernatants were measured using a Luminex-based Bio-Plex assay (Bio-Rad Laboratories) using manufacturer's instructions. Standards were reconstituted in the cell culture medium and used to determine cytokine

concentrations. Plates were read using a Luminex 100/200 machine and Bio-Rad's Bio-Plex manager software.

2.16. *In vivo* experiments

2.16.1. *Alternaria Alternata* asthma model

WT mice (10-12 weeks old) were treated intranasally with 10 or 20 μg of a sterile extract of *Alternaria alternata* (Stallergenes Greer) diluted in 25ul of PBS or PBS alone 3 times a week for 5 weeks. The mice received one final dose at week 6 and were culled 24 hours after the last treatment. Bronchoalveolar lavage fluid (BALF), lung tissue and blood samples were collected post mortem to investigate immune cell infiltration within the tissues, cytokine production and levels of serum IgE. Half of the lungs were fixed and analysed for tissue remodelling and mucus production. Administration of the *Alternaria alternata* was done by Dr Sarah Thomson.

2.16.2. Bone marrow chimera experiment

CD45.1 WT (120 days old) mice were lethally irradiated with two doses of 4.5 Gy and 5 Gy given 3 hours apart. Mice were irradiated one at a time, in the middle compartment of the irradiator. The recipient mice were split into two groups and each mouse was injected with $2.5x10^6$ bone marrow cells in 200μl PBS through the tail vein. i.v. injection was carried out by staff in Biological Services, University of Dundee. The two groups were reconstituted with either CD45.2 WT or CD45.1 WT and CD45.2 ABIN1 KI bone marrow cells mixed in 1:1 ratio. The antibiotic Levofloxacin (0.67g/L) was added to the drinking water during the first two weeks after the irradiation to reduce the risk of infection. Wet mash, jelly and baby food were given to the mice as supportive measure. Mouse weight was monitored during the length of the study. Mice were culled 4 months after the irradiation by a schedule 1 procedure. Spleen, lungs, and kidneys were harvested for FACS analysis and histology analysis. Serum obtained from the blood was tested for presence of autoantibodies. Intravenous injection into the tail vein was done by Dr Sarah Thomson. Tail bleeds were done by Dr Sambit Nanda.

2.16.3. *In vivo* stimulation with imiquimod (TLR7 agonist)

WT mice (10-13 weeks old) were treated with 60 mg experimental cream containing 5% of the TLR7 agonist imiquimod (Aldara). The cream was applied topically, once per day on both ears. Mice were split into 5 groups, each with different duration of treatment: 0, 2, 3, 4 and 5 days. Mice were culled 4 hours after the last administration and blood, spleen and lungs were harvested for flow cytometry analysis. Application of the cream was done by Dr Manuel Van Gijsel Bonnello.

2.16.4. *In vivo* administration of IRAK4 inhibitor

ABIN1[D485N] (6 weeks old) mice were split in control and experimental groups. The control mice were fed with normal R&M3 diet and the experimental group was fed with R&M3 containing 1000 mg per kg of the IRAK4 inhibitor PF-06426779 (Pfizer). An additional control group of age matched WT animals was included in the study. WT mice were given normal R&M3. Blood samples were collected from the tail vein at the start of the study and at week 5. Mice were culled after 10 weeks and tissues were analysed. Welfare monitoring and tail bleeds were done by Dr Sambit Nanda.

2.17. Statistical analysis

Statistical significance was determined using two-tailed, unpaired Student t-test or ANOVA with post hoc Tukey HSD testing was carried out in RStudio. Plots with the indicated mean values ± standard deviation (SE) were made in RStudio using ggplot2, ggpubr, ggpubsci packages.

III. Investigating the role of MAPKs and MAPKAPKs in IL-33-dependent ILC2 responses

3.1. Flow cytometry characterisation of ILC2 cells and *in vitro* culture system

ILC2s do not express lineage-defining surface markers (CD3e, CD8, CD19, CD11b, CD11c, F4/80, Gr-1 and NK1.1), however they do express KLRG1 and Sca-1 and the cytokine receptors CD25, CD127 (IL-7 receptor) and ST2 (IL-33 receptor) (Halim, 2015). ILC2 cells are tissue resident cells found in the fat-associated lymphoid clusters (FALC), mesentery, spleen, liver, small intestine and lungs. To identify ILC2s, cell suspensions from lungs, mesenteric lymph nodes, mesenteric fat and white adipose tissues were stained for expression of Lineage markers, CD45, KLRG1, Sca1, ST2 and c-Kit and gating strategies are illustrated in Figure 3.1. Briefly, ILC2s were defined as the Sca1 and KLRG1 double positive cells in the $CD45^{+ve}Lineage^{-ve}$ gate. While most of the ILC2s in the mesenteric fat and white adipose tissue were positive for the IL-33 receptor ST2, ILC2s from the lungs and mLN expressed very low levels of ST2. Expression of c-Kit was low in all stained tissues. Similar observations were made in other studies, showing that ST2 and c-kit expression in ILC2 cells varies in different tissues (Bartemes et al., 2012, Moro et al., 2015).

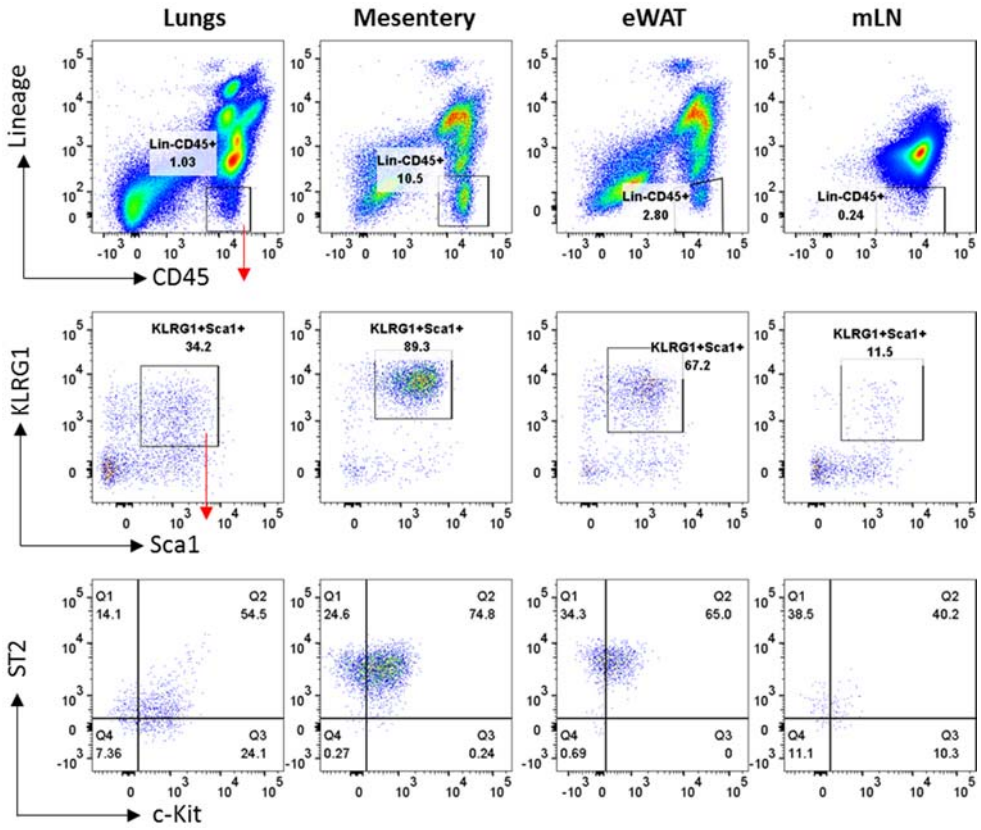

Figure 3.1 Gating strategy for identifying ILC2s.
Single cell suspensions from lungs, mesenteric fat, mesenteric lymph nodes (mLN) and epididymal white adipose tissue (eWAT) were stained with antibodies against CD45 (BV510), Lineage markers (CD3e, CD8, CD19, CD11b, CD11c, F4/80, Gr-1 and NK1.1, all conjugated to FITC), KLRG1 (APC), Sca-1 (APC/Cy7), c-kit (PE/Cy7) and ST2 (PerCP-eFluor710) and analysed by flow cytometry. Doublets and were excluded using FSC-A and FSC-W and live cells were gated as DAPI negative. ILC2 cells were characterised as $Lineage^{-ve}CD45^{+ve}KLRG1^{+ve}Sca1^{+ve}$. The $Lineage^{-ve}CD45^{+ve}KLRG1^{+ve}Sca1^{+ve}$ population was further analysed for expression of ST2 and c-kit.

Studying ILC2s function *in vitro* has been challenging due to their low abundance and most of the investigators use flow cytometry based cell sorting to isolate pure populations. This can be time consuming, costly and there is a considerable cell loss during the staining procedure and sorting. Although, there are commercially available kits for enrichment of the ILC2 cells using magnetic sorting, these kits do not provide completely purified ILC2s populations. In the mesenteric fat ILC2s are the major population of innate lymphoid cells consisting of around 90% of the lineage negative immune cells. In addition, mesenteric ILC2s have high expression of the IL-33 receptor (Figure 3.1). As the primary aim of this work was to examine IL-33 signalling in ILC2s, for these reasons the mesenteric fat was selected as a source of ILC2s. To study ILC2s *in vitro*, I first optimised a protocol for depletion of other

immune cell using a cocktail of biotinylated antibodies recognising CD3ε, B220, CD19, Ly-6G/Ly-6C (Gr-1), CD11b, TER-119, NK1.1 and F4/80 and streptavidin-conjugated magnetic beads. Flow cytometry analysis of the depleted mesenteric cells, showed that most of the other immune cells were effectively depleted and the majority of the $CD45^{+ve}$ cells were lineage negative (Figure 3.2). Furthermore, around 90% of the $Lineage^{-ve}CD45^{+ve}$ population expressed the ILC2s markers KLRG1 and Sca1. Although most of the cells after the depletion were $CD45^{-ve}$ cells, these non-haematopoietic cells did not express high levels of the ST2 chain of the IL-33 receptor, in contrast to the ILC2s which did express high levels of ST2 (Figure 3.3).

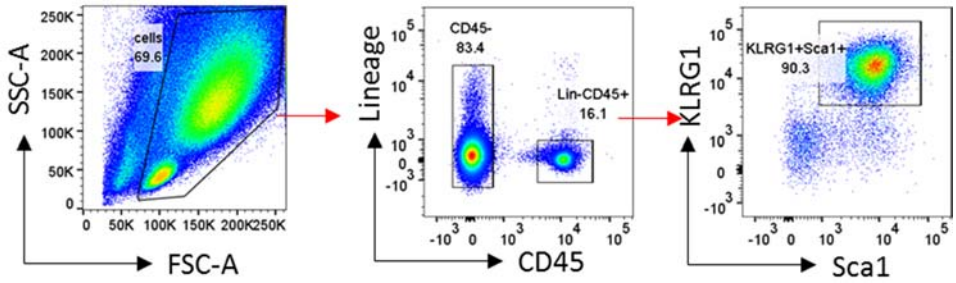

Figure 3.2 Depletion of lineage positive immune cells from mesenteric fat.
CD3ε, B220, CD19, Ly-6G/Ly-6C (Gr-1), CD11b, TER-119, NK1.1 and F4/80 positive immune cells were depleted from mesenteric fat cell suspension by magnetic sorting. Cells were stained with antibodies against CD45 (APC-eFluor780), Lineage (PE), KLRG1 (APC) and Sca1 (FITC) and ST2 (PerCP-eFluor710) and analysed on BD FACSCanto. The representative FACS plots show the purity of the cultures after the magnetic sorting.

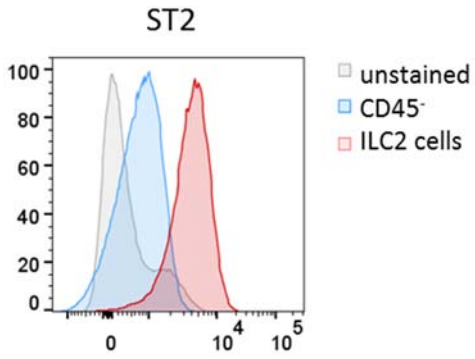

Figure 3.3 Expression of ST2 in $CD45^{-}$ and ILC2 cells.
CD3ε, B220, CD19, Ly-6G/Ly-6C (Gr-1), CD11b, TER-119, NK1.1 and F4/80 positive immune cells were depleted from mesenteric fat cell suspension by magnetic sorting. Cells were stained as in Figure 3.2. The histogram represents expression of ST2 in $CD45^{-ve}$ cells and in ILC2 cells.

ILC2s respond to the epithelial derived cytokines IL-33, IL-25 and TSLP. IL-33 has been shown to drive production of IL-5, IL-9 and IL-13 (Furusawa et al., 2013). Therefore, I stimulated cells obtained after lineage depletion with IL-33 to measure cytokine production. IL-33 induced secretion of IL-9, IL-13, GM-CSF and IL-10 in a time dependent manner (Figure 3.4). Production of IL-5 was also increased following the stimulation, however appreciable levels of IL-5 were also produced by unstimulated cells. On day 1, similar levels of IL-6 were detected in the media of both unstimulated and IL-33 stimulated cells. In the IL-33 stimulated cultures IL-6 levels did not change dramatically between day 1 and 5, however the levels did decrease over time in the unstimulated cultures (Figure 3.4).

To understand better what is the source of the IL-33 independent IL-5 and IL-6 production, lineage positive cells were depleted from mesenteric cell suspension, the cells were then stained with fluorescent conjugated antibodies and ILC2 cells ($DAPI^{-ve}CD45^{+ve}Lin^{-ve}KLRG1^{+ve}Sca1^{+ve}$) were sorted using fluorescent activated cell sorting. The FACS sorted ILC2s produced IL-9, IL-13 and GM-CSF similar to the lineage depleted mesenteric cells, but the high levels of IL-5 and IL-6 were not observed in unstimulated cells and production of IL-5 and IL-6 were detected only in the supernatants from cells stimulated with IL-33 (Figure 3.5). In addition, IL-6 production was increased over time, which was not observed in the mixed cultures. Taken together, these data indicated that although the CD45 negative cells are not expressing high levels of the IL-33 receptor, their presence can influence the cytokine production measured in the cultures. Moreover, comparing responses between mice from different genotypes using the mixed cultures would not be reliable as it would not be possible to determine if an effect of genotype was intrinsic to the ILC2s or due to a phenotype in the $CD45^{-ve}$ cells.

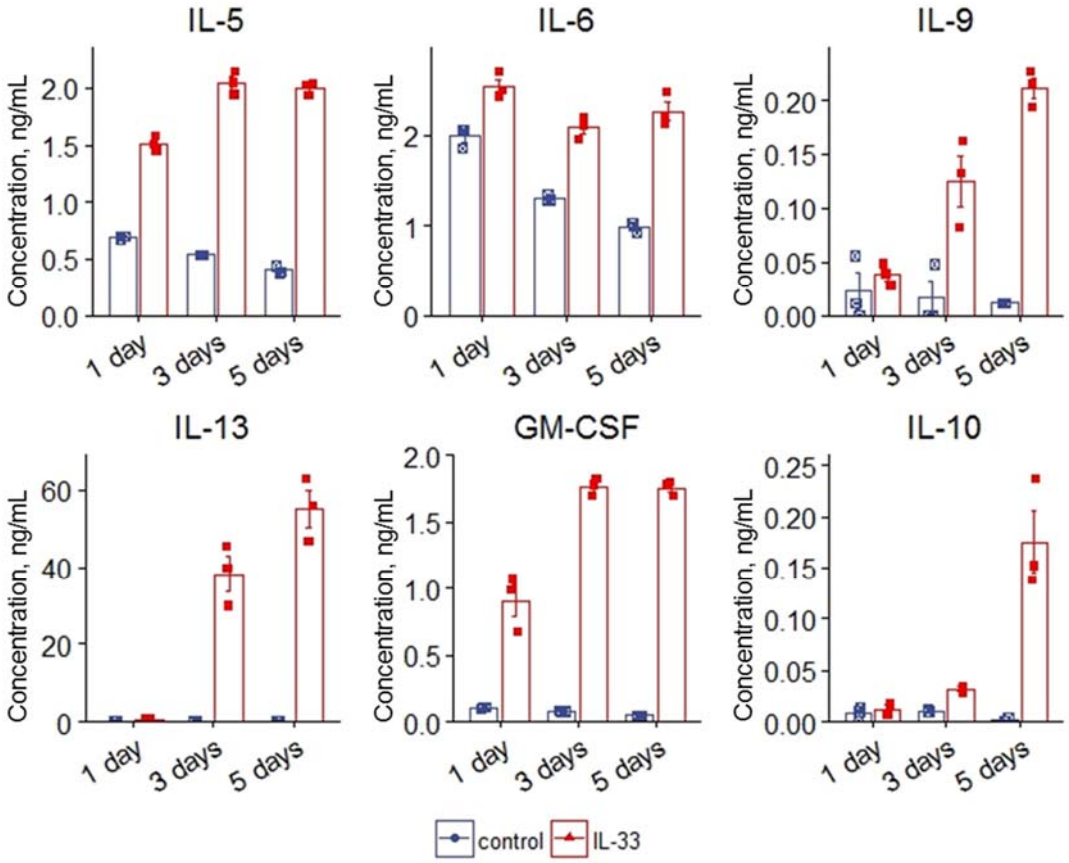

Figure 3.4 IL-33 dependent cytokine production in lineage depleted ILC2 cells
CD3ε, B220, CD19, Ly-6G/Ly-6C (Gr-1), CD11b, TER-119, NK1.1 and F4/80 positive immune cells were depleted from mesenteric fat by magnetic sorting. $5x10^3$ cells per well were cultured with or without IL-33 (100 ng/ml). Supernatants were collected 1, 2 and 5 days after the stimulation and analysed by multiplex cytokine assay. The stimulation was done in triplicate and error bars show the average value ± standard error of the mean. Symbols represent individual measurements. Results are representative from 2 experiments.

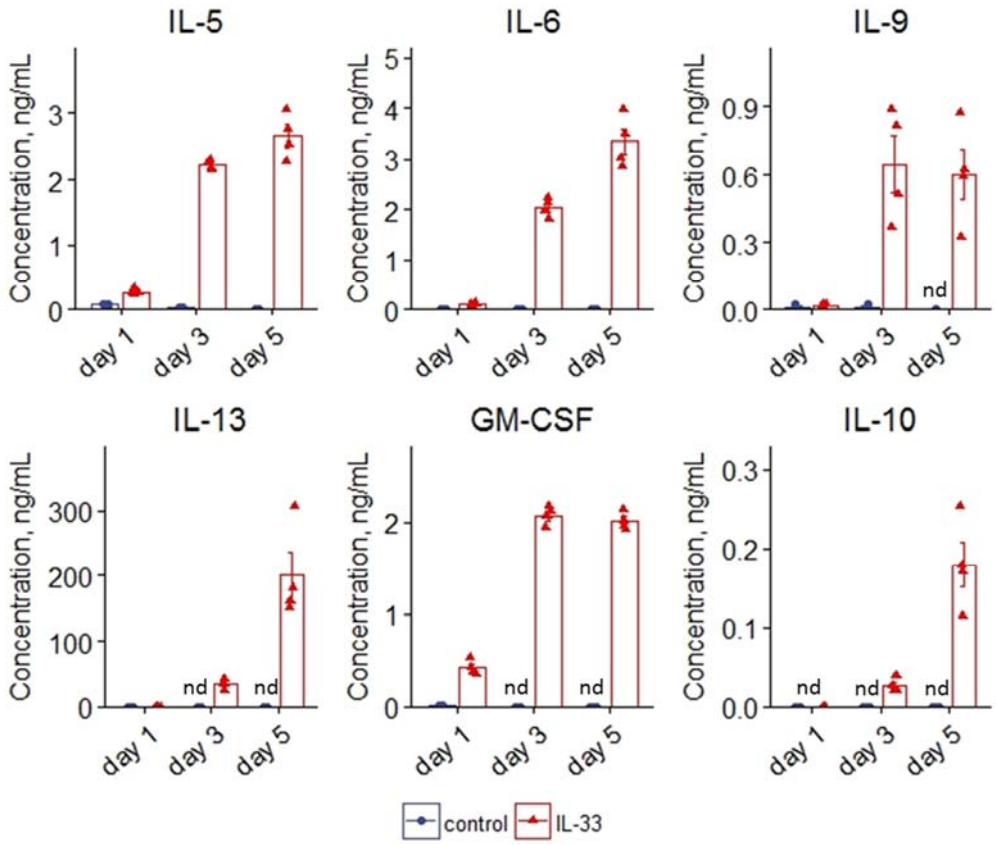

Figure 3.5 IL-33 dependent responses in FACS sorted ILC2s.
Lineage^{-ve}CD45^{+ve}KLRG1^{+ve}Sca1^{+ve} cells were sorted by FACS from mesenteric fat cell suspensions (pulled from 11 WT mice) and 5x10^3 cells per well were cultured with or without IL-33 (100 ng/ml). Supernatants were collected 1, 2 and 5 days after the stimulation and analysed by multiplex cytokine assay. The stimulation was done in quadruplicate and error bars show the average value ± standard error of the mean. Symbols represent individual measurements. Results are representative from 2 experiments.

To further optimise the ILC2s *in vitro* cultures, following the depletion of lineage positive cells, the ILC2 were further purified by another round of magnetic sorting consisting of positive selection of CD45^{+ve} cells. The cells were then cultured in IL-2 and IL-7 for 5-7 days. Culturing of ILC2s in IL-2 or IL-7 has been used to maintain or grow ILC2s at a gradual rate, whereas combination of IL-25 and IL-7 or IL-2 and IL-33 leads to rapid growth and activation (Moro et al., 2015, Huang et al., 2014). Although there is a considerable enrichment after the 2 rounds of magnetic sorting, not all of the CD45 negative cells are removed by these steps and the ILC2s represent around 50-60% of all live cells (not shown). The culture conditions with IL-2 and IL-7 are favorable for the ILC2s, but not for the non-immune cells, resulting in more than 95% purity of the ILC2s cultures and yield of 10 000 - 20 000 cells per

mouse depending on the age of the mice. The purity of the cultures is shown in Figure 3.6.

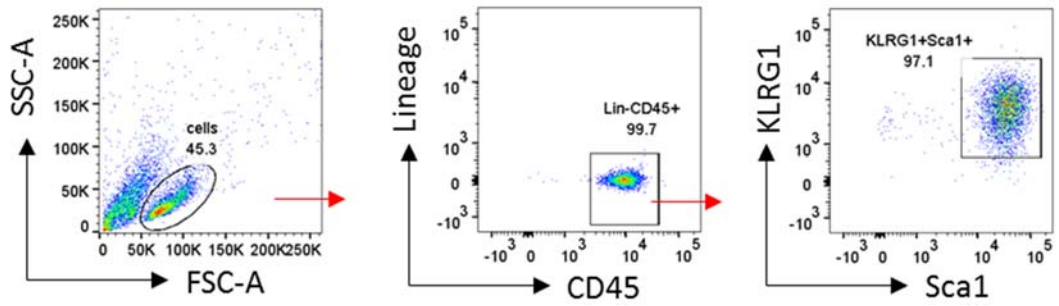

Figure 3.6 Purification of ILC2 cells from mesenteric fat.
ILC2 cells were purified from mesenteric fat by magnetic depletion of Lineage positive cells and positive selection of $CD45^{+ve}$ cells. Cells were cultured in IL-7 (10ng/mL) and IL-2 (20ng/mL) for 5 days and stained with antibodies against CD45(BV510), Lineage markers (CD3e, CD8, CD19, CD11b, CD11c, F4/80, Gr-1 and NK1.1 all conjugated to FITC), KLRG1 (APC) and Sca1(PE/Cy7) and analysed on BD FACSCanto. Flow cytometry plots show the purity.

Administration of IL-33 or IL-25 leads to expansion of ILC2 cells in mice (Barlow et al., 2013, Huang et al., 2015, Klein Wolterink et al., 2012). Whereas IL-33 drives cytokine production in ILC2s, stimulation of ILC2s with IL-25 alone is not able to induce cytokine release in ILC2s (Klein Wolterink et al., 2012, Camelo et al., 2017, Salimi et al., 2013). Similarly, IL-2 does not induce cytokine in ILC2s, but augments IL-33 dependent cytokine production (Roediger et al., 2015). To confirm these findings, ILC2s cultured using the above described method were stimulated with IL-25, IL-33 or IL-33 in combination with IL-2 or IL-25. Stimulation of ILC2s with IL-33 led to a significant increase in the production of IL-5, IL-6, IL-9, IL-13 and GM-CSF. In contrast, IL-25 did not induce responses in ILC2s, neither did it amplify IL-33 dependent responses. Addition of IL-2 only affected IL-33 dependent IL-13 secretion, but not the production of other cytokines (Figure 3.7). These data were in line with previous reports in the literature and confirmed that IL-33 is a potent activator of ILC2s. Interestingly, the amounts of cytokines produced from the *in vitro* grown ILC2s following 24 hours stimulation with IL-33 were higher in comparison to the cytokines production from FACS sorted ILC2s after 24 hours, suggesting that priming the cells in IL-2 and IL-7 is driving a faster ILC2s response.

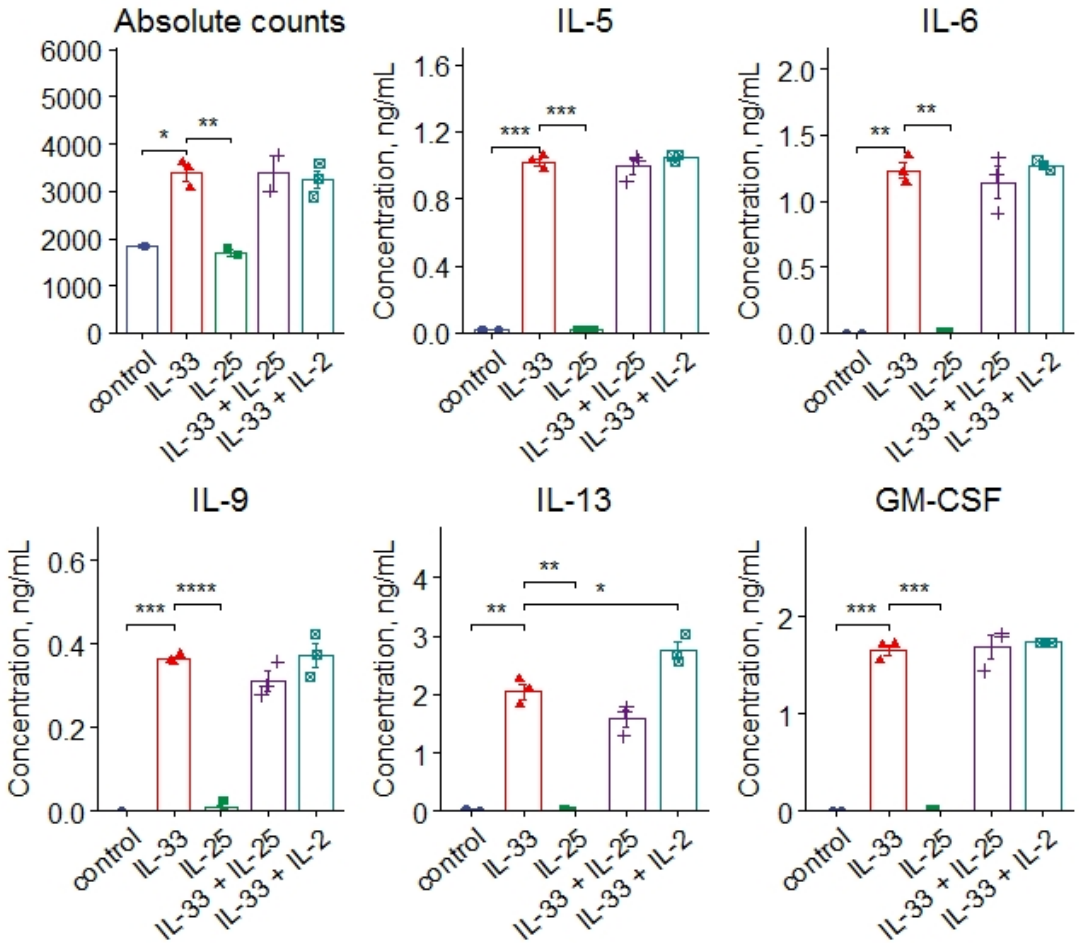

Figure 3.7 IL-33 activates mesenteric ILC2s.
Cultured ILC2 cells were plated at $5x10^3$ per well and stimulated with the indicated combinations of IL-25 (10ng/mL), IL-33 (100ng/ml) and IL-2 (20ng/ml) for 24h. Cells were stained with DAPI (0.5 µg/mL) and analysed on BD FACSVERSE to determine absolute numbers of live cells Supernatants were analysed for IL-5, IL-6, IL-9, IL-13 and GM-CSF by multiplex cytokine assay. The stimulation was done in triplicate and error bars show the average value ±SEM. Significance was calculated relative to IL-33 stimulated by two-tailed unpaired Student's t-test; * denotes $p<0.05$, ** denotes $p<0.01$ and **** denotes $p<0.0001$.

3.2. Investigating the role of c-Kit in IL-33 dependent ILC2 response.

The production of IL-13 by ILC2 cells was strongly dependent on the duration of the stimulation with IL-33, with more than 100 fold difference between day 1 and day 5 (Figure 3.5), suggesting that there is a feedback mechanism leading to the amplified cytokine production. Interestingly, in mast cells c-Kit has been suggested to interact with the IL-1RAcP constitutively from the IL33-ST2 receptor complex leading to enhanced signalling and IL-6 production (Drube et al., 2010). Although mesenteric ILC2s express very low levels of c-Kit (Figure 3.8A), stimulation with IL-

33 led to an increase in c-Kit expression (Figure 3.8A). Moreover, ILC2s stimulated with IL-33 in the presence of dasatinib, which inhibits a number of tyrosine kinases including c-kit, led to a significant reduction in the secretion of IL-13 (Figure 3.8B). However, dasatinib has several targets including Abl and Src family tyrosine kinases. Hence, there is a possibility that it blocks IL-13 production in ILC2s independent of c-kit. Since most of the available c-kit inhibitors also have other targets, it would be interesting to confirm these finding using ILC2s isolated from c-Kit deficient mice (Furusawa et al., 2013).

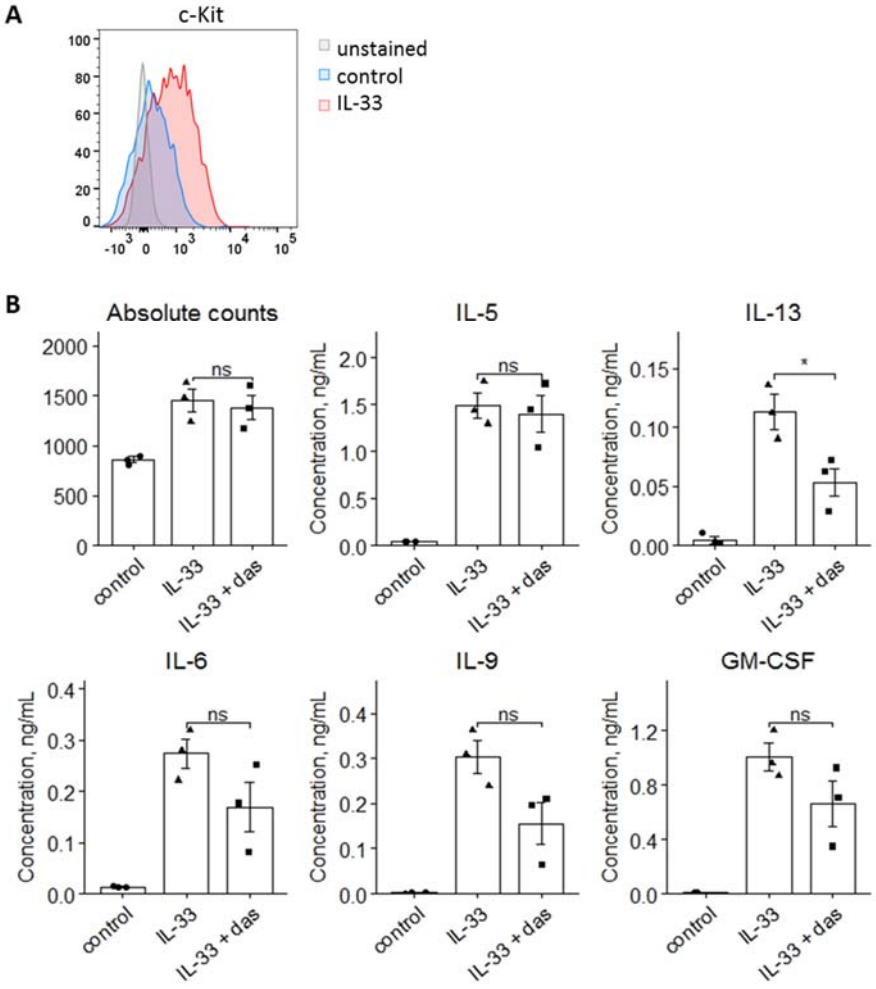

Figure 3.8 c-Kit is involved in regulating IL-33 dependent responses in ILC2s.
A. Cultured ILC2s were stimulated with or without IL-33 for 24 hours. Following the stimulation, cells were analysed on BD FACSCanto to determine expression of c-Kit. The representative histogram plot shows c-Kit expression in control and IL-33 stimulated ILC2. B. Purified ILC2 cells were cultured at $2.5x10^3$ per well and stimulated with DMSO, IL-33 (100ng/ml) alone or IL-33 with in the presence of c-kit inhibitor dasatinib (10nM). Cells were stained with DAPI (0.5 µg/mL) and analysed on BD FACSVERSE to determine absolute numbers of live cells. Culture media was analysed for IL-5, IL-6, IL-9, IL-13 and GM-CSF by multiplex cytokine assay. The stimulation was done in triplicate and error bars show the average value ±SEM. Significance between the stimulated samoles ± dasatinib (10nM) was calculated by two-tailed unpaired Student's t-test; * denotes $p<0.05$, ns denotes not significant.

3.3. Importance of p38/MK2/3 axis in IL-33 signalling pathway in ILC2

IL-33 signal transduction leads to activation and phosphorylation of the MAPK kinases p38 and ERK1/2 in different immune cells such as Th2 cells, mast cells, eosinophils. (Schmitz et al., 2005, Park et al., 2016, Drube and Kraft, 2016, Chow et al., 2010, McCarthy et al., 2018). To confirm if these pathways were activated in ILC2s, intracellular staining and flow cytometry was used to examine ERK1/2 and p38 phosphorylation. Stimulation with IL-33 induced rapid phosphorylation of both p38 and ERK1/2 in ILC2 cells, suggesting that these kinases are involved in the regulation of IL-33 induced responses in ILC2 cells.

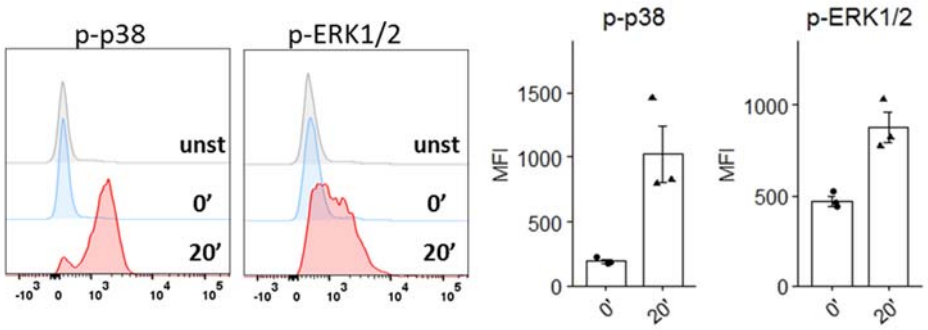

Figure 3.9 IL-33 induces activation of p38 and ERK1/2 in ILC2s.
Cultured ILC2 cells were rested for 2 hours before stimulation with 100ng/ml of IL-33 for the indicated time points. Cells were fixed, permeabilised and acquired on BD FACSCanto. Representative histograms of p-p38 and p-ERK at 0 and 20 are shown. Unst shows unstained cells. Bar plots show average of the median fluorescence intensity (MFI) of p-p38 and p-ERK1/2 from 3 biological replicates. Error bars show standard error of the mean.

The p38 MAP kinase has been previously found to regulate production of IL-5 and IL-13 in ILC2s, however the role of downstream of p38 kinases MK2/3 has not been studied in the context of ILC2s (Furusawa et al., 2013). Our lab and others have shown that MK2/3 play important role in regulation of mast cell responses to IL-33. (Drube et al., 2016, Gopfert and Andreas, 2018, McCarthy et al., 2018). Therefore, to further elucidate the role of MAPKs in regulating ILC2s function, ILC2s were stimulated with IL-33 in the presence of p38, ERK1/2 and two different MK2/3 inhibitors. Following stimulation, the cells were counted on day 5 to assess viability. The samples only cultured with DMSO and no IL-33 had very low numbers of live cells, suggesting that the presence of either IL-33 or IL-2 and IL-7 is required for the

maintenance of the ILC2s (Figure 3.10). The cell numbers in the samples stimulated with IL-33 were around 2-3 fold higher than the initially plated cells, whereas the cell counts with inhibitors were similar to the counts at the start of the stimulation. This suggested that the presence of inhibitors is either blocking proliferation or having a cytotoxic effect.

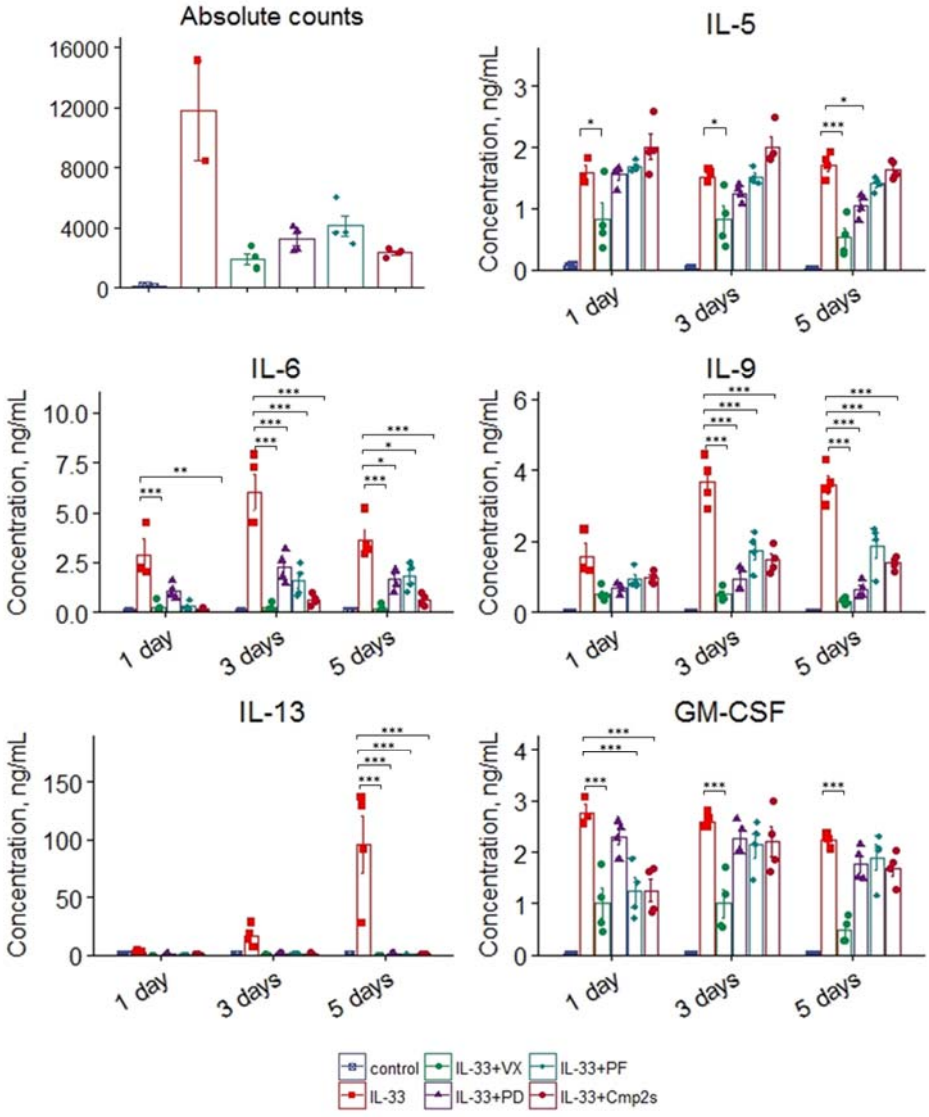

Figure 3.10 Regulation of cytokine production in ILC2 by p38, ERK1/2 and MK2/3. ILC2 cells were cultured at $5x10^3$ cells per with IL-33 (100ng/ml) in the presence of either DMSO, p38 inhibitor VX745 (1µM), MEK1/2 inhibitor PD184352 (5 µM), or the MK2/3 inhibitors Cmp2s (5µM) and PF3644022 (5µM). Control cells were incubated in DMSO but no IL-33. Culture media was sampled at 1, 3 and 5 days after the stimulation and cell numbers were determined at day 5. Bar plots represent the average value of 4 biological replicates (each biological replicate was made by pulling cells from 4 mice). Error bars represent the standard error of the mean. Statistical significance was determined by two way ANOVA with Tukey's test for posthoc analysis. Comparisons of IL-33 vs IL-33 with inhibitors are shown. $p < 0.05$ is indicated by *, $p < 0.01$ by ** and $p < 0.001$ by ***

Secretion of IL-6, IL-9 and IL-13 was blocked in the presence of all inhibitors. IL-5 was partly reduced in the presence of the p38 inhibitor VX475, but not by the other inhibitors. Production of GM-CSF was also blocked by inhibition of p38 and significantly reduced in the presence of MK2/3 inhibitors at the early time point only. In contrast to the FACS sorted ILC2s, where there was an increase in the production of IL-10 after 5 days stimulation, the magnetically sorted and cultured ILC2s did not secrete measurable amounts of IL-10 (not shown).

The above data could be explained by either a direct role of ERK1/2 and p38 in cytokine production or an indirect role in controlling cell survival/proliferation. To examine this, ILC2s were stimulated with IL-33 in the presence of p38, ERK1/2 and JNK inhibitors for 24 hours. After the stimulation the cells were counted to assess viability (Figure 3.11). The presence of the inhibitors did not have cytotoxic effect and the ILC2s numbers were similar to the numbers in the cultures stimulated with IL-33 alone. Consistent with Figure 3.10, the p38 inhibitor VX745 had the most prominent effect on the cytokine production in ILC2s and supressed production of all measured cytokines (Figure 3.11). Hence, p38 regulates cytokine production not only by supressing IL-33 dependent ILC2s proliferation, but also has a direct effect either on the production or the secretion of cytokines. Inhibition of ERK1/2 also had an effect on the production of IL-9 and IL-13 and led to a modest decrease in GM-CSF. In contrast JNK do not seem to play a major role in regulating IL-33 responses in ILC2s as JNK inhibition only led to a partial reduction of IL-6.

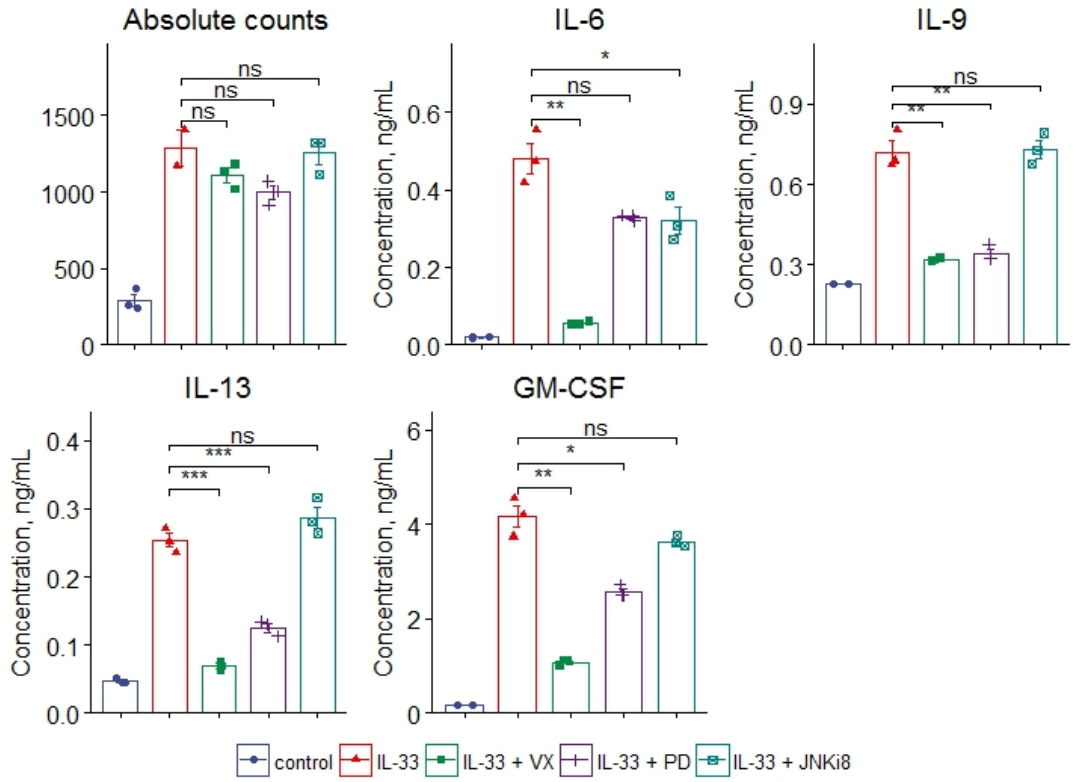

Figure 3.11 Regulation of cytokine production in ILC2s by MAPKs.
Cultured ILC2 cells were stimulated with DMSO, IL-33 (100ng/mL) or IL-33 and p38 inhibitor VX-745 (1µM), MEK1/2 inhibitor PD184352 (5 µM) and JNK1/2/3 inhibitor JNK-IN-8 (3 µM). Following the stimulation cells were stained with DAPI (0.5 µg/mL) and analysed on BD FACSVERSE to determine absolute numbers of live cells. Supernatants from the cell cultures were analysed for IL-5, IL-6, IL-13 and GM-CSF by multiplex cytokine assay. The stimulation was done in triplicate and error bars show the average value ± standard error of the mean. Significance between IL-33 alone and inhibitor treated samples was calculated by two-tailed unpaired Student's t-test; * denotes ($p<0.05$), ** denotes ($p<0.01$), ns denotes not significant.

MK2/3 are directly activated by p38 and are known to mediate some of the effects of p38 on cytokines production in macrophages and mast cells (McCarthy et al., 2018). 24 hours stimulation of ILC2s in the presence of the MK2/3 inhibitor Cmp2s did not influence the cell viability, but led to a significant reduction in the production of IL-13 (Figure 3.12).

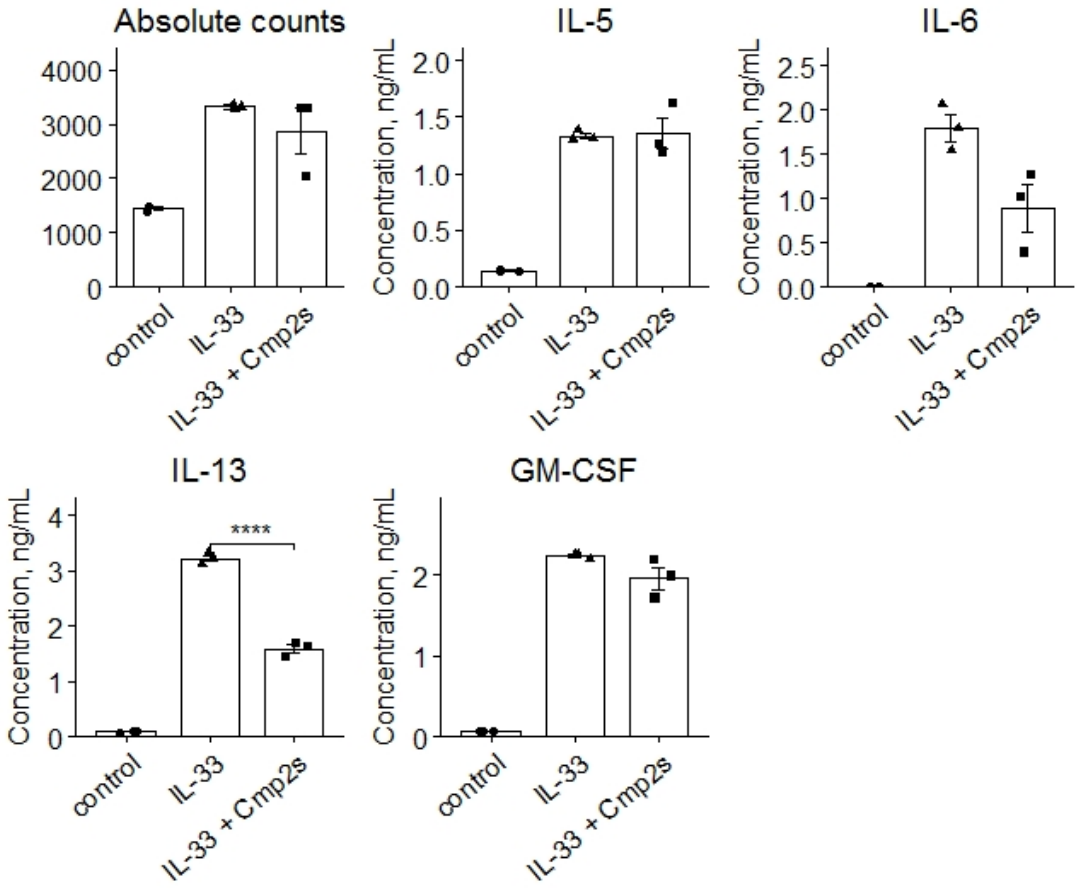

Figure 3.12 Regulation of cytokine production in ILC2s by MK2/3.
Cultured ILC2 cells were stimulated with DMSO, IL-33 (100ng/mL) or IL-33 and MK2/3 inhibitor 1 Cmp2s (5µM). Following the stimulation cells were stained with DAPI (0.5 µg/mL) and analysed on BD FACSVERSE to determine absolute numbers of live cells. Supernatants from the cell cultures were analysed for IL-5, IL-6, IL-13 and GM-CSF by multiplex cytokine assay. The stimulation was done in triplicate and error bars show the average value +/- standard error of the mean. Significance between IL-33 alone and inhibitor treated samples was calculated by two-tailed unpaired Student's t-test; **** denotes ($p<0.0001$), ns denotes not significant.

To address the question if loss of MK2/3 results in regulating the IL-33 induced IL-13 production by blocking its secretion from the cells, ILC2 cells were stimulated with IL-33 in the presence of the Golgi complex inhibitor Monensin. Similarly, IL-33 induced production of IL-13 in ILC2s following stimulation, which was reduced by both MK2/3 inhibitors Cmp2s (5µM) and PF3644022 (5µM) (Figure 3.13). These data suggested that inhibition of MK2/3 is not regulating IL-13 production by blocking its secretion, but most likely is involved in IL-13 regulation at transcriptional or post-transcriptional level.

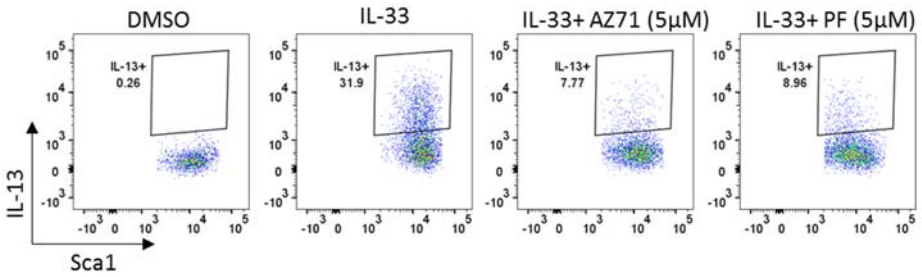

Figure 3.13 IL-33 activates mesenteric ILC2s.
Purified ILC2 cells were cultured in the presence of DMSO, IL-33 (100ng/ml), or IL-33 with either of the MK2/3 inhibitors AZ71 (5µM) and PF3644022 (5µM). 24 hours after the stimulation monensin (2nM) was added to the cell cultures and the cells were incubated for another 4 hours. Cells were fixed and permeabilised and analysed on BD FACSCanto for expression of Lineage markers (FITIC), KLRG1 (APC), Sca1 (PE/Cy7) and IL-13(PE). Plots shows Sca1 and IL-13 expression in Lineage^{-ve} KLRG1^{+ve} cells.

3.4. Characterisation of ILC2s in MK2/3 double knock out mice.

The *in vitro* data in Figure 3.10 suggested that MK2/3 have a role in ILC2s proliferation, as well as in the production of IL-13. Therefore, next I characterised the ILC2s populations in the lungs, mesenteric lymph nodes, mesenteric fat and epididymal white adipose tissue (eWAT) of MK2/3 double knock out mice. Although, there was an increase of the Lineage negative CD45^{+ve} immune cells in the lungs, mesentery and eWAT in the knock out mice, the percentages of KLRG1^{+ve}Sca1^{+ve} cells was lower and ILC2s total cell numbers were not different from those in the WT mice (Figure 3.14). ILC2s in the mLN of the MK2/3 mice were significantly reduced. Interestingly, the expression of KLRG1 was lower in the eWAT of MK2/3 knock out ILC2s (Figure 3.15). Although KLRG1is an inhibitory ITIM motif containing receptor, the upregulation of KLRG1^{+ve} expression has been associated with the activation of ILC2s (Wallrapp et al., 2017). Hence, MK2/3 deficient ILC2s in the eWAT might have a less activated phenotype than WT ILC2s.

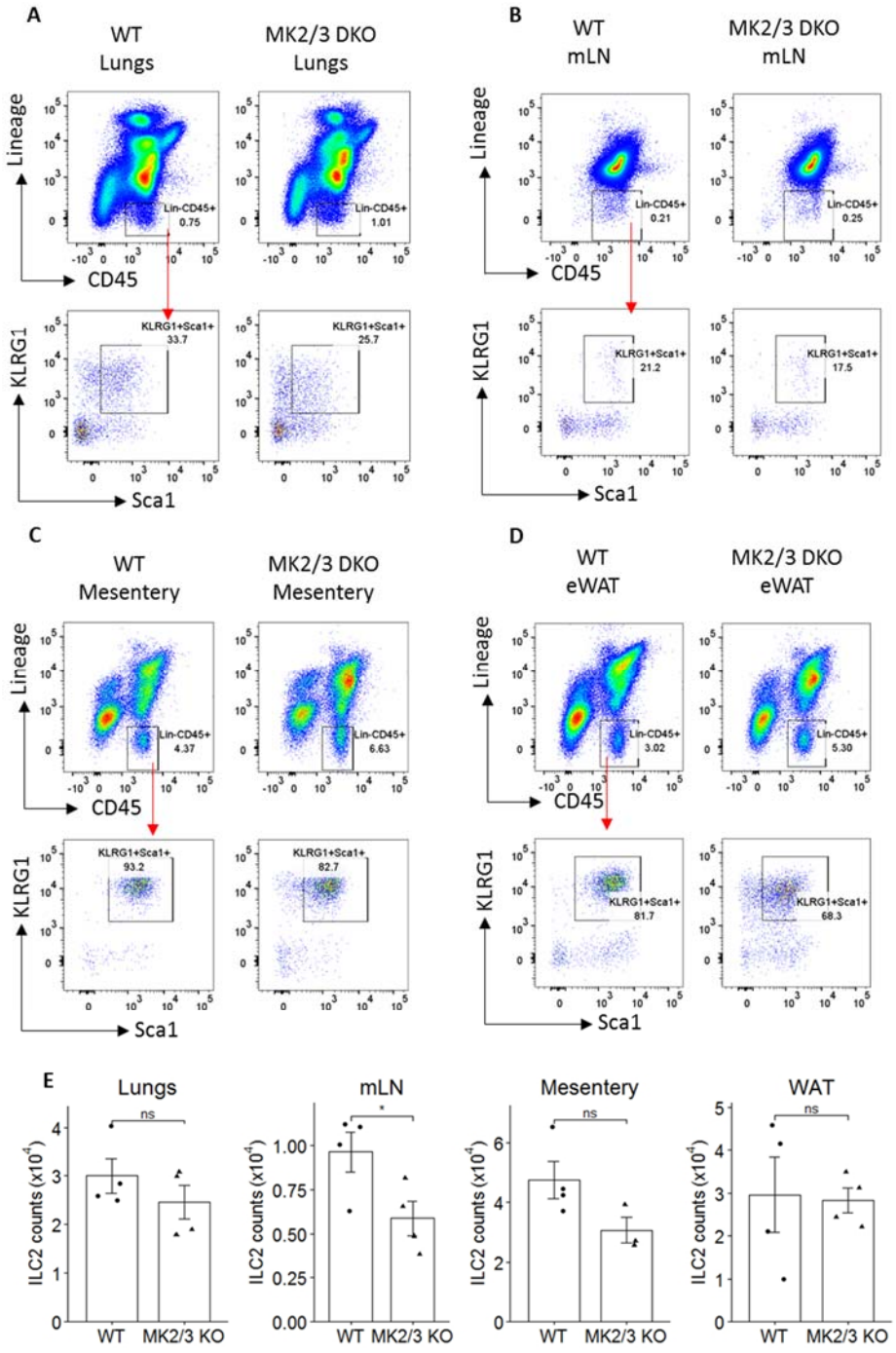

Figure 3.14 ILC2s in MK2/3 knock out mice.
Cells obtained from lungs, mesenteric lymph nodes, mesenteric fat and epididymal white adipose tissue (eWAT) from WT (n=4) and MK2/3 DKO (n=4) were analysed for expression of Lineage markers (FITC), CD45 (BV510), KLRG1 (APC) and Sca1(Pe/Cy7) and DAPI and analysed on BD LSRFortessa. Representative plots are showing percentage of Lineage^{-ve} CD45^{+ve} cells from all live single cells and percentage of KLRG1^{+ve} Sca1^{+ve} ILC2 cells within the Lineage^{-ve}CD45^{+ve} population in lungs (A) mLN (B), mesentery (C) and eWAT (D). Bar plots represent absolute numbers of ILC2 cells in the lungs, mLN, mesentery and eWAT. Symbols represent individual biological replicates. (E). Error bars represent the standard error of the mean. Significance between WT and MK2/3 knock out samples was calculated by two-tailed unpaired Student's t-test; * denotes ($p<0.05$), ** denotes ($p<0.01$), ns denotes not significant.

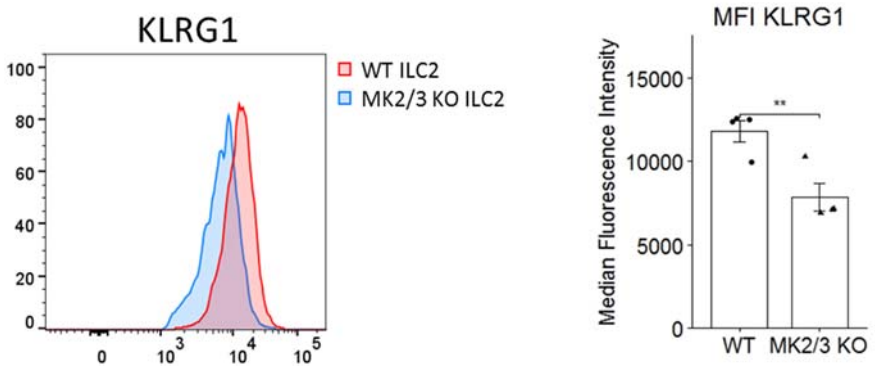

Figure 3.15 KLRG1 expression is decreased in ILC2s from the eWAT.
Samples were stained and analysed as in figure 3.14. Representative plots are showing the expression of KLRG1 in WT and MK2/3 KO ILC2s isolated from eWAT. Bar plots represent the median fluorescence intensity of KLRG1. Symbols represent individual biological replicates and error bars represent the standard error of the mean. Significance between WT and MK2/3 knock out samples was calculated by two-tailed unpaired Student's t-test; ** denotes ($p<0.01$).

To confirm the data obtained using MK2/3 inhibitors showing a role of MK2/3 in regulating IL-33 dependent cytokine production in ILC2s, *in vitro* cultured ILC2s isolated from mesenteric fat of WT and MK2/3 mice were stimulated with IL-33 for 24 hours. Live cells were counted and cytokine production was normalised for 1000 cells. Similar to the data obtained with the MK2/3 inhibitors, the MK2/3 knock out ILC2 cells produced significantly less IL-13 in response to IL-33 (Figure 3.16). In addition IL-6 production was also significantly reduced in the knock out cells. IL-5, IL-9 and GM-CSF production in response to IL-33 was not affected by MK2/3 knockout. Both IL-6 and IL-13 are implicated in diseases such as asthma and atopic dermatitis (Eder et al., 2011, Rincon and Irvin, 2012, Neveu et al., 2010). IL-13 activity leads to increased bronchial hyperresponsiveness and promotes the switching of B cells antibody production from IgM to IgE (Corren, 2013). IL-6 is a pleotropic cytokine, which in the context of allergic airway inflammation has been found to regulate mucus production (Neveu et al., 2009). Therefore, targeting MK2/3 could be potentially used for developing therapies for treating allergic airway inflammatory diseases.

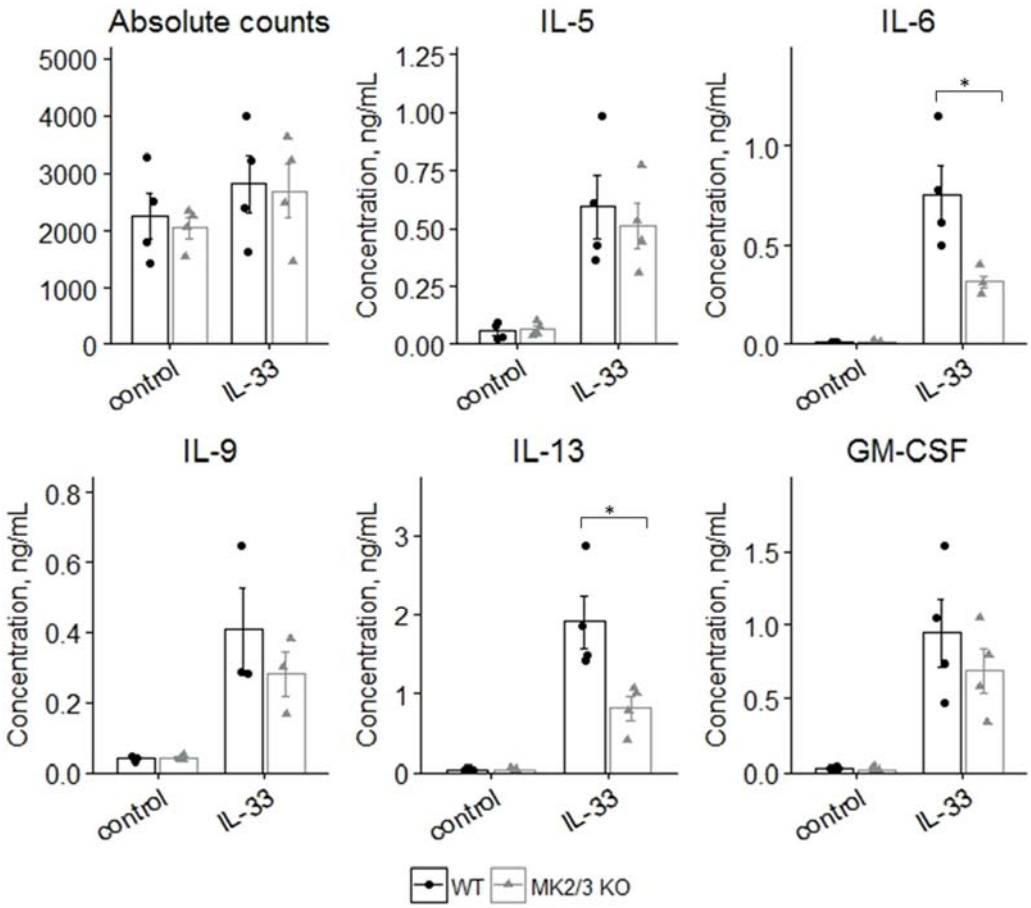

Figure 3.16 Regulation of cytokine production ILC2s by MK2/3.
Cultured ILC2 cells from WT and MK2/3 KO mice were cultured with or without IL-33 (100ng/ml) for 24 hours. Supernatants were analysed for IL-5, IL-6, IL-9, IL-13 and GM-CSF by multiplex cytokine assay. Following the stimulation cells were stained with DAPI (0.5µg/mL) and absolute counts were obtained by BD FACSVerse. Supernatants were analysed by multiplex cytokine assay. Values were normalised for 1000 cells. Bar plots represent the average value of 4 biological replicates (each biological replicate was made by pulling cells from 4 mice). Error bars represent the standard error of the mean. Significance between IL-33 stimulated WT and MK2/3 knock out samples was calculated by two-tailed unpaired Student's t-test; ** denotes ($p<0.05$).

3.5. *Alternaria alternata* induced airway inflammation mouse model

The *in vitro* data from this study supported the hypothesis that MK2/3 are important for regulating the production of IL-13 and IL-6 in ILC2 cells in response to IL-33. In addition our lab has shown that inhibition or loss of MK2/3 in mast cells leads to complete blockade of cytokine induction in response to IL-33. Loss of MK2 has been previously reported to have a protective phenotype during OVA-induced airway inflammation (Gorska et al., 2007). OVA treated MK2 knock out mice had

significantly reduced airway remodelling, immune cell infiltration and type two cytokine induction, which the authors suggested is due to loss of MK2/3 in non-immune cells. (Gorska et al., 2007).

To expand these findings and study the effect of MK2 deletion specifically in immune cells, we set up another model of allergic lung inflammation induced by treatment with *Alternaria alternata* spores. *Alternaria alternata* is a fungal aeroallergen which has a long history of association with respiratory allergy (Denning et al., 2006). Infection of mice with *Alternaria* leads to increased production of IgE, airway inflammation, airway hyperactivity and it is used as an asthma model in mice (Havaux et al., 2005). *Alternaria* induces release of IL-33 and TSLP that promotes the production of IL-13 and IL-5 by ILC2s and Th2 cells (Snelgrove et al., 2014, Löser et al., 2017). Studies with ST2 deficient mice showed that the response to *Alternaria* is strongly dependent on IL-33 signalling, since ST2 knock out mice are rescued from *Alternaria* induced inflammation (Snelgrove et al., 2014). Immune cell infiltration occurs rapidly after the administration of *Alternaria,* however tissue remodelling of the respiratory system requires longer time. To set up the model we stimulated mice with two different concentrations of *Alternaria* intranasal. The mice received a total of 16 doses and were culled 24 hours after the last administration to analyse airway inflammation (Figure 3.17). Treatment with both doses induced airway remodelling, thickening of the bronchial bed and immune cell infiltration (Figure 3.17).

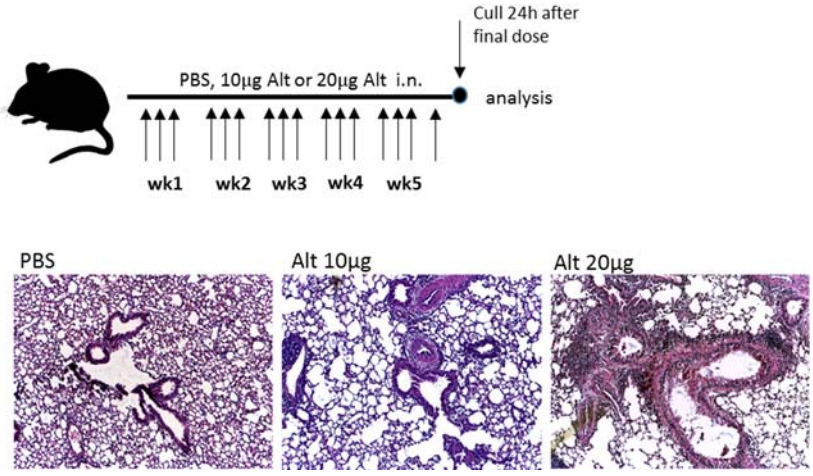

Figure 3.17 *Alternaria* induced allergic asthma model.
10-12 weeks old mice were treated intranasal with PBS, 10 µg or 20µg purified *Alternaria alternata* extract 3 days a week for 5 weeks and one final dose on week six. The mice were culled and lungs were harvested for analysis. The representative microscopy images show *Alternaria*-induced pulmonary inflammation in lungs tissue sections (H&E staining).

The *Alternaria* treatment induced a significant increase in eosinophil numbers both in the lungs and the bronchoalveolar lavage fluid (BAL) and this was independent of the *Alternaria* concentration used (Figure 3.18). ILC2 cells were also significantly increased. In the lungs this increase was dependent on the dose of *Alternaria* (Figure 3.19).

A.

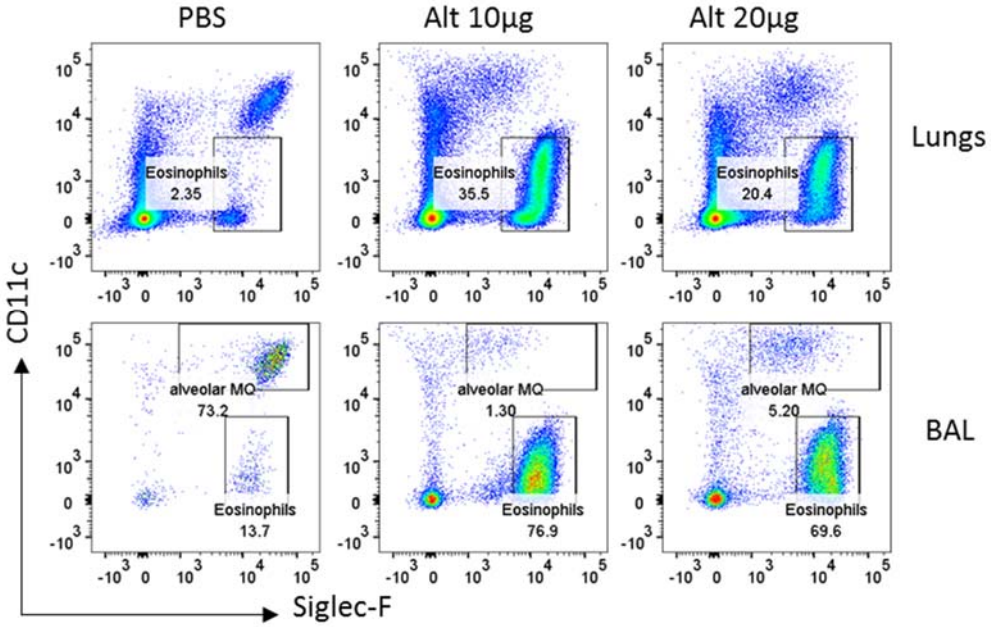

B.

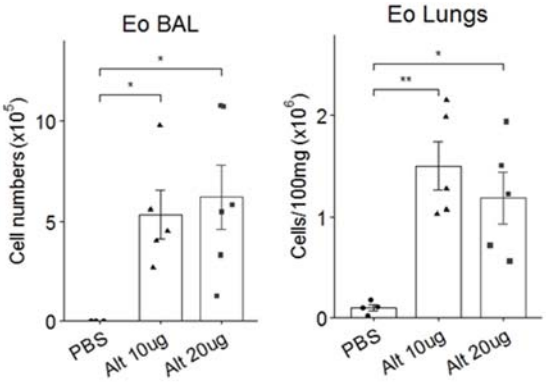

Figure 3.18 *Alternaria* induces eosinophilia in the lungs and bronchoalveolar lavage. 10-12 week old mice were treated intranasally with PBS, 10 µg or 20µg purified *Alternaria alternata* extract 3 days a week for 5 weeks. The mice received one final dose on week six and were culled 24 hours after the last administration. Lungs and bronchoalveolar lavage fluid were harvested for analysis. Single cell suspensions were stained with DAPI, anti-CD11c and anti-SiglecF to characterise eosinophils and alveolar macrophages and analysed on BD LSRFortessa. A. Representative FACS plots showing percentage of Eosinophils (Siglec-$F^{+ve}CD11c^{-ve}$) in lungs and BAL from DAPI negative single cells. B. Total eosinophil numbers in BAL and lungs. Symbols represent individual mice. Bar plots show average and standard error of the mean. Significance relative to PBS was calculated by two-tailed unpaired Student's t-test; * denotes ($p<0.05$), ** denotes ($p<0.01$).

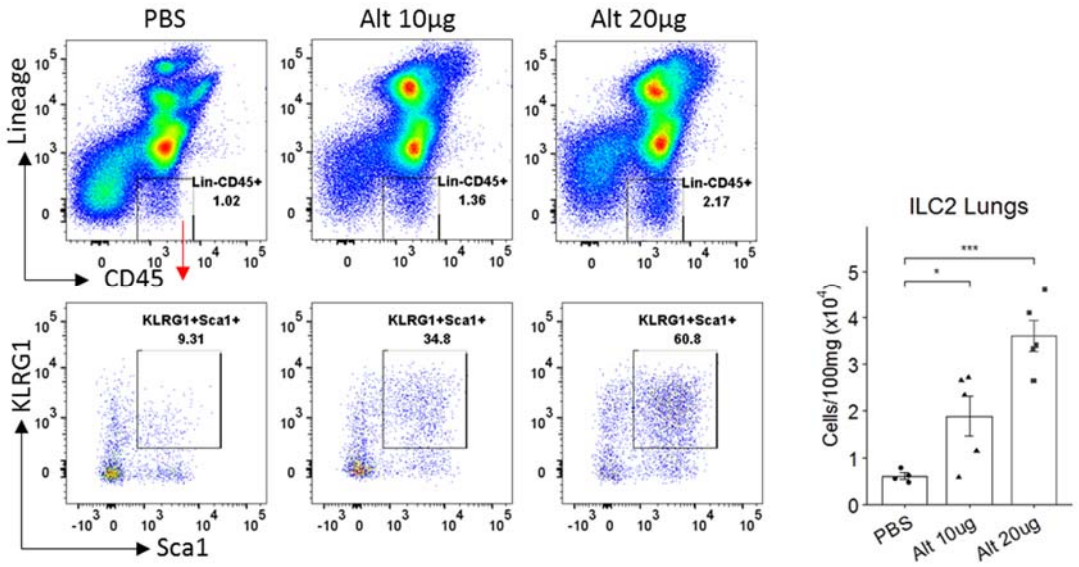

Figure 3.19 *Alternaria* induces increase in the ILC2 numbers in the lungs in a dose dependent manner.
Mice were treated as described in Figure 3.17. Single cell suspensions from the lungs were analysed for expression of Lineage markers (FITC), CD45 (BV510), KLRG1 (APC) and Sca1 (APC/Cy7) and DAPI and analysed on BD LSRFortessa. Representative plots are showing percentage of Lineage^{-ve} and CD45^{+ve} cells from all live single cells and percentage of KLRG1^{+ve} Sca1^{+ve}ILC2 cells within the Lineage^{-ve}CD45^{+ve} population in lungs. The bar graph shows absolute numbers of ILC2s in the lungs. Significance between PBS and *Alternaria* treated mice was calculated by two-tailed unpaired Student's t-test; * denotes ($p<0.05$), ** denotes ($p<0.01$).

The *Alternaria* treatment led to an increased mRNA levels of the type 2 cytokines *IL4, IL5* and *IL13* (Figure 3.20). Significant induction for most of the cytokines was observed only in the lungs of animals treated with the higher dose, with the low dose giving intermediate values. Induction of *IL6* and *IL33* mRNA was also observed. The eosinophil chemoattractant Eotaxin (CCL11) mRNA was also strongly induced in the treated animals, which was in line with the observed eosinophilia in the lungs and the BAL (Figure 3.20). Interestingly, *IL-33* mRNA levels were only increased following treatment with 20 µg of *Alternaria*. In addition to the cytokine induction, induction of *Arg1* and *Ym1* mRNA was also observed (Figure 3.20). Arginase-1 and YM1 are markers for alternatively activated murine macrophages or M2 macrophages (Raes et al., 2005, Raes et al., 2002). The M2 macrophages are important regulators of the pathology of asthma, contributing to the eosinophilia and collagen deposition around the airways (Draijer et al., 2018). Taken together, the treatment with 20µg Alt extract provides more reliable read outs for studying *Alternaria* dependent lung inflammation in mice.

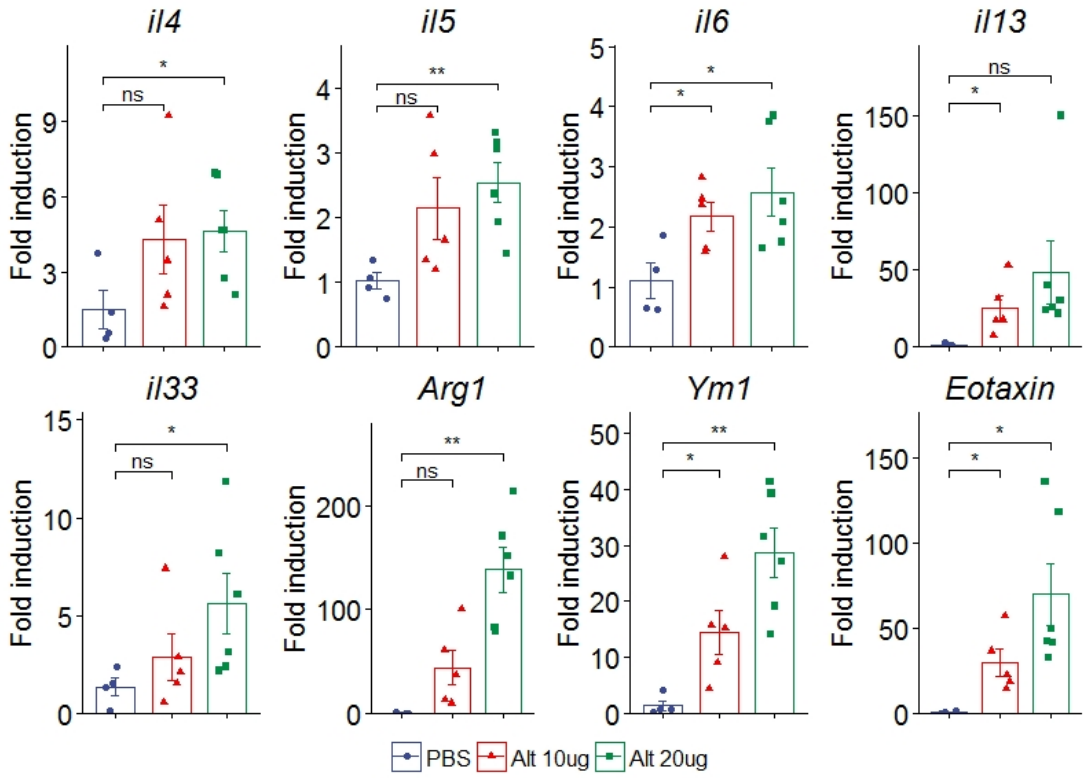

Figure 3.20 Increased expression of genes regulating type two immunity following *Alternaria in vivo* administration.

10-12 weeks old mice were treated intranasally with PBS, 10 µg or 20µg purified *Alternaria alternata* extract 3 days a week for 5 weeks and one final dose on week six. The mice were culled 24 hours after the last administration. Lung tissues were lysed in RLT buffer and total RNA was purified (Takara RNA isolation kit). Total RNA was reverse-transcribed using iScript (Bio-Rad) and qPCR was carried out using SYBR green based methods. 18S and GAPDH were used as a normalisation control and fold induction was calculated for IL-4, IL-5, IL-6, IL-13, IL-33, Arg1, Eotaxin and Ym1. Symbols represent individual mice, bars show average and standard error of the mean values. Significance between PBS and *Alternaria* treated mice was calculated by two-tailed unpaired Student's t-test; ns denotes ($p>0.5$)* denotes ($p<0.05$), ** denotes ($p<0.01$).

3.6. Discussion

An increasing number of studies indicate the importance of innate lymphoid cells in regulating inflammatory diseases (Poposki et al., 2017, Nechama et al., 2018, Miller et al., 2010a). ILC2s cells are strategically located at the barrier site, where they can communicate with epithelial and endothelial cells to respond to environmental stimuli. ILC2s have very low abundance, but they are potent producers of cytokines and can modulate the function and recruitment of other immune cells during inflammation. To study ILC2s function *in vitro*, first I have optimised a method for enrichment of the ILC2s population by depleting other immune cells. This resulted in generation of mixed cultures, with ILC2s and $CD45^{-ve}$ non-immune cells (Figure 3.2). Although the $CD45^{-ve}$ cells were not expressing the IL-33 receptor, high levels of IL-5 and IL-6 were detected in the supernatant of control unstimulated samples, which were not detected in supernatants from FACS sorted ILC2s (Figure 3.4 and 3.5). This could be explained by the fact that adipocytes and adipose tissue have been shown to be a source of IL-6 both in humans and mice (Antunes et al., 2006, Harkins et al., 2004). The effect of IL-6 on ILC2s has not been studied, however IL-6 has been found to modulate function of lineage negative cells in the gut and promote IL17A and IL-22 production (Powell et al., 2015). These data implicate that cross talk between the ILC2s and adipocytes could influence responses in both cell types, therefore the purity of the cultures plays an important role in studying ILC2s.

Consequently, I have further optimised the magnetic purification by doing an additional step of positive selection with anti-CD45 antibody and culturing the cells in IL-2 and IL-7, which greatly improved the purity of the ILC2s cultures (Figure 3.6). Moreover, ILC2s sorted using this method responded in a very similar way to FACS sorted cells, secreting IL-5, IL-6, IL-9, IL-13 and GM-CSF, but with slightly different kinetics. Whereas the FACS sorted ILC2s had very low response following a 24 hours stimulation with IL-33 and cytokines were detected after 3 and 5 days of stimulation, the magnetically sorted ILC2s secreted higher levels of the type two cytokines even at 24 hours (Figure 3.6 and 3.10). This effect is most likely a result from the priming of the cells in IL-2. *In vivo* stimulation of mice with IL-2 leads to expansion of ILC2 cells (Roediger et al., 2015). IL-2 has been shown to induce IL-9 production in ILC2s isolated from papain-treated mice independent of stimulation with IL-33 (Wilhelm et

al., 2011). In contrast, here IL-2 did not have any effect on IL-9 production in IL-33 stimulated ILC2 cells, but led to an increase production of IL-33 dependent IL-13 (Figure 3.7). This may be due to the culture in IL-2 and IL-7 downregulating their ability to respond to IL-2 in the acute stimulation or that the primary effect of IL-2 is already maximal.

Surprisingly, IL-10 production was only detected in FACS sorted ILC2s after 5 days of stimulation, but not in the supernatants of the magnetically sorted and cultured ILC2s in IL-2 and IL-7 (data not shown). This was not expected as IL-2 is known to induce IL-10 production in regulatory T cells in a STAT5 dependent manner and IL-2 is required for the immune suppressive function of Tregs (Tsuji-Takayama et al., 2008) (Cheng et al., 2013). IL-2 was also found to induce IL-10 production in IL-33 and IL-7 expanded ILC2 and the addition of retinoic acid further amplified the induction of IL-10 (Seehus et al., 2017). These findings suggest that the culture conditions could influence cytokine production in ILC2 and they can adopt different phenotype depending on the environment.

ILC2 express low levels of c-Kit, however IL-33 stimulation led to an increased expression of c-Kit. The receptor tyrosine kinase c-Kit has been shown to co-immunoprecipitate with the IL-33-ST2 receptor complex (Drube et al., 2010). SCF ligation with c-Kit triggers receptor dimerisation and autophosphorylation of the receptor leading to recruitment of proteins containing Src homology 2 (SH2 domains) including Shc, the growth factor receptor-bound protein 2 (Grb2) and the Ras guanylnucleotide exchanging factor Sos (son of sevenless). Sos mediates the exchange of GDP for GTP on Ras, Ras then interacts with Raf1 leading to the activation of cascade of multiple protein kinases, including MEK1 and ERK1/2 (Moodie et al., 1993) (Taylor and Metcalfe, 2000). Addition of SCF to BMMC culture media leads to a hyper responsive mast cell phenotype (Ito et al., 2012). Here, I demonstrated that the tyrosine kinase inhibitor dasatinib significantly downregulates production of IL-13 (Figure 3.8). Similar effect was also observed using the MEK1/2 inhibitor which blocks ERK1/2 phosphorylation. Therefore it will be interesting to understand if SCF leads to ERK1/2 activation in ILC2. One study suggests that ILC2 isolated from $KitW^{-sh}$, carrying a mutation in regulatory elements upstream of the *c-kit* gene, have normal cytokine production and SCF is not amplifying IL-33 dependent production of IL-5, IL-6 and IL-13 in ILC2s (Furusawa et al., 2013a). However, there are not any

other reports in the literature looking at c-Kit role in ILC2 cells and more research is needed to understand the role of c-Kit in modulating ILC2s responses.

The role for c-Kit in regulating airway inflammation and type two immunity has been shown in an OVA experimental model of allergic asthma, where administration of the tyrosine kinase inhibitor dasatinib led to a significant reduction in the airway hyperresponsivness, leukocyte infiltration in the lungs and BAL and decreased production of IL-13 and an increase in the anti-inflammatory cytokine IL-10 (Silva et al., 2016). The authors did not look at the effect on dasatinib on ILC2s expansion, however it will be interesting to understand if the effect of dasatinib was due to supressing ILC2s function. Another tyrosine kinase inhibitor bosutinib was also found to have a protective role during experimental model of lung fibrosis induced by silica particles (Carneiro et al., 2017). These inhibitors are not specific for c-Kit only, but also for other tyrosine kinases. Therefore it is possible that their effect is mediated through another mechanism independent of c-Kit. However studies using the $Kit^{W\text{-}sh}$ mice, showed that these mice exhibit decreased eosinophilia and IgE production in house dust mite induced lung inflammation, but did not rescue lung pathology and mucus production. Hence, c-Kit signalling has a potential role in regulating allergic asthma (de Boer et al., 2014).

Male SJL-$Kit^{W\text{-}sh}$ mice have been shown to have an exacerbated phenotype in experimental autoimmune encephalitis, however female mice SJL-$Kit^{W\text{-}sh}$ mice were protected. Interestingly the phenotype observed in the male SJL-W/W^{v} mice was linked to decreased frequency of mature ILC2s and ILC2s precursors, reduction in the type two cytokines and a shift to Th17 type of response mediating the diseases exacerbation. (Russi et al., 2015).

The inhibition of the MAPKs ERK1/2 using MEK1/2 inhibitors led to a reduction in production of IL-13, IL-9 and IL-6. ERK1/2 have been shown to regulate IL-5 and IL-13 production in bone marrow derived ILC2s (Suzuki et al., 2015). However, my results did not indicate any effect of ERK1/2 on IL-5 production (Figure 3.10). This could be potentially explained by the different methodology of ILC2s extraction and cultures. Deficiency of Spred1, which is known to negatively regulate ERK1/2 activation by supressing Raf1 phosphorylation, leads to exacerbation in OVA and papain induced airway inflammation. $Spred1^{-/-}$ mice have higher ILC2s increases in the papain-induced asthma model and significant increase in the production of type

two cytokines (Suzuki et al., 2015, Inoue et al., 2005). Interestingly, ERK1/2 regulates cytokine production in ILC2s in response to the neurone derived peptide neuromedin U (Cardoso et al., 2017). Taken together, our and others data support the importance of ERK1/2 in mediating ILC2s function and the potential of targeting these kinases for drug development. It will be also interesting to study the effect of the kinases downstream of ERK1/2 such as MSKs and RSKs in ILC2 cells.

It has been demonstrated previously that upon stimulation with IL-33, p38 and GATA3 are phosphorylated in ILC2 cells. Using the p38 inhibitor SB203580 Furusawa and his colleagues showed that inhibition of p38 leads to reduced phosphorylation of GATA3, which also resulted in blockade in the production of IL-5, IL-13 and IL-6 (Furusawa et al., 2013). GATA3 can bind directly to the GATA3 response element (CGRE), which is upstream of the *il13* gene and upregulate *il13* expression in Th2 cells and ILC2 cells (Furusawa et al., 2013, Yamashita et al. 2002). Here, I showed that the p38 inhibitor VX745 blocks not only IL-5, IL-6 and IL-13 production, but it has also an effect on GM-CSF, and IL-9 responses (Figure 3.10 and 3.11). The presence of p38 inhibitor also led to a reduction in the proliferation of ILC2, suggesting that p38 has a critical role in ILC2 function (Figure 3.10). While a number of p38 inhibitors failed to proceed in clinical trials, recently two p38 inhibitors BCT-197 and AZD7624 have been developed for treatment of COPD and corticosteroid-resistant asthma. One of the compounds, BCT-197, shows promising results in Phase II clinical trials, whereas the compound AZD7624 did not show any beneficial effect in patients with COPD (Patel et al., 2018). However AZD7624 is currently in a clinical trials for treatment of patients with corticosteroid resistant asthma (ClinicalTrials.gov, 2016).

Here, I showed that MK2/3 knock out mice have relatively normal ILC2 numbers. Despite this, when stimulated with IL-33 MK2/3 deficient ILC2 had lower production of IL-6 and IL-13 (Figure 3.16). Previous studies have found that knockout of MK2 and 3 can lead to a decrease in p38a levels (Ronkina et al., 2007). Importantly, similar results for IL-33 induced IL-13 and IL-6 production were obtained with a selective MK2/3 inhibitor (Figure 3.11 and 3.12), which does not affect p38 expression levels (Ronkina et al., 2007b, McCarthy et al., 2018). Data from our lab showed that loss of MK2/3 in mast cells leads to inhibition of TNF-alpha and GM-CSF, whereas I did not observe any major difference in the production of GM-CSF in MK2/3 deficient ILC2

cells, suggesting that although the signalling pathways are very similar between the immune cells, there are some differences in how the production of individual cytokines is regulated. The mechanism of how MK2/3 regulate IL-13 and IL-6 production in ILC2s is still not clear, however the intracellular staining for IL-13 suggest that MK2/3 is not blocking the secretion of the cytokine. In macrophages and mast cells MK2/3 is regulating cytokine production at the post-transcriptional level via TTP and possibly the related proteins Brf1 and Brf2 (Hitti et al., 2006, McCarthy et al., 2018). Therefore, it is possible that the same mechanism applies to ILC2s. Future studies will be required to confirm this hypothesis. In addition, in the next chapter I have demonstrated that Akt or mTORC1 inhibition leads to a similar reduction of IL-6 and IL-13. We have previously showed that in MK2/3 deficient macrophages and T cells have reduced phosphorylation of the ribosomal S6 protein and Akt, suggesting that the effect of MK2/3 in ILC2s could be also due to reduced activation in the mTOR pathway (Hayakawa et al., 2017, McGuire et al., 2013).

MK2 has been shown to play a role in the OVA-induced asthma model. The authors proposed that the protective mechanism was due to decreased vascular permeability in the MK2 mice. Since adoptive transfer of activated MK2 sufficient T cells did not reconstitute the inflammation observed in the WT mice, they suggested that the rescue in lung inflammation does not rely on the immune system (Gorska et al., 2007). It should be considered however that in this study the mice were analysed after up to 96 hours after the OVA challenge. Recent reports have shown that ILC2 rather than Th2 cells mediated early responses during papain and OVA induced inflammation, whereas Th2 are required for the latter responses. (Klein Wolterink et al., 2012, Halim et al., 2014). Considering the role of MK2/3 in regulation of type two cytokine production *in vitro*, the impact of the immune cells should not be excluded.

IL-13 is one of the main cytokines involved in the pathology of asthma (Corren, 2013). However the anti-IL13 antibody therapy lebrikuzimab recently failed in Phase 3 clinical trials and asthmatic patients did not have an improvement of the lung function upon anti-IL13 treatment (Korenblat et al., 2018). Hence, targeting MK2/3 might provide an alternative approach for development of asthma treatment. In addition to IL-13, MK2/3 regulate production of other cytokines such as IL-6, TNF-alpha and GM-CSF in mast cells. It will be also interesting to investigate the role of

MK2/3 in modulating Th2 cellular responses, which are a key population in regulating the pathology of asthma. We have previously shown that loss of p38 and MK2/3 leads to enhanced Treg frequencies, which may have another positive impact in limiting the pro-inflammatory type two response (Hayakawa et al., 2017). Therefore, it is critical to first establish the role of MK2/3 in the experimental model of asthma. To study the role of MK2 in regulating development of asthma, we have set up an *Alternari*a induced lung inflammation model, which will be carried initially in *MK2-Vav-iCre* mice, which have specific deletion of MK2 only in the immune cell compartment.

IV. Singalling pathways regulating ILC2 metabolism

4.1. Introduction

4.1.1. Immunometabolism

In recent years the field of immunometabolism has emerged as a major new field in immunological research. Immunometabolism can be subdivided into two main areas of research, the first area focuses on understanding the role of the immune system in regulating host metabolism, while the second area explores the cell-intrinsic metabolic changes within the immune cells and how these are shaping the immune responses (Pearce and Pearce, 2013). Inflammatory stimuli trigger a variety of processes in immune cells including proliferation, migration to the sites of inflammation, upregulation or downregulation of certain genes and production of inflammatory mediators, which all require energy and are accompanied with major metabolic changes within the cells. For example, naïve T cells supply ATP through oxidative phosphorylation. Similarly, regulatory T cells and tissue resident memory T cells are also dependent on exogenous free fatty acids and their oxidative phosphorylation as a source of energy (Michalek et al., 2011, Pan et al., 2017). In contrast, when T cells encounter antigens they undergo clonal expansion and effectively "switch" their metabolism to use glycolysis as an energy source (Greiner et al., 1994). This fact is interesting as glycolysis is a much less efficient then oxidative phosphorylation in terms of generation of ATP. One reason for this phenomenon could be explained by the switch away from oxidative phosphorylation would mean amino acids and fatty acids would be less likely to be used for generating ATP, and hence more available to be used as cellular building blocks (Pearce, 2010). Furthermore, many of the glycolysis intermediates could feed into other pathways such as the pentose phosphate pathway leading to the synthesis of nucleotides (O'Neill et al., 2016).

Metabolic changes during activation are also characteristic for the innate immune cell populations. Cytokine stimulated NK cells upregulate both glycolysis and

oxidative phosphorylation, with a preferential increase in glycolysis (Gardiner and Finlay, 2017). Both metabolic pathways were found to be dependent on the activity of the transcription factor Srebp, which promotes fatty acid and cholesterol synthesis (Assmann et al., 2017). During activation with PMA, neutrophils use glycolysis as a source of energy. Moreover, it was found that the release of neutrophil extracellular traps (NETs) is dependent on glucose (Rodríguez-Espinosa et al., 2015). Similarly, dendritic cells activated by TLR stimulation also upregulate the glucose transporter Glut1 and switch their metabolism to glycolysis (Everts et al., 2012). Interestingly, availability of glucose was found to modulate DC responses and their ability to interact with T cells. Replacing glucose with galactose in the media of LPS stimulated DCs led to a prolonged expression of the co-stimulatory molecules CD80 and CD86 and increased *IL12* mRNA levels (Lawless et al., 2017). CD8 T cells co-cultured with glucose deprived DCs had higher proliferative capacity and higher production of IFN-γ. The authors suggested that in an inflammatory environment T cells are competing with DC for nutrients and limiting the availability of glucose to DCs leading to enhanced proinflammatory DC responses, which in turn promote T cells (Lawless et al., 2017).

Macrophages use two distinct metabolic pathways to supply energy depending on their phenotype. “Classical” macrophages are activated by bacterial derived antigens such as LPS or IFN-γ, have a highly inflammatory phenotype and rely on glycolysis to mount their response. In contrast, “M2a” macrophages, which are activated by IL-4 or IL-13, regulate responses during parasite infections and promote tissue repair, use oxidative phosphorylation of fatty acids (Vats et al., 2006). IL-4 promotes induction of PPARγ-coactivator-1β (PGC-1β), which is a transcriptional coactivator of genes involved in promoting mitochondrial biogenesis, fatty acid oxidation and oxidative phosphorylation (Lin et al., 2005). Another distinct feature of LPS and IL-4 activated macrophages is in the way they metabolise arginine. In M1 macrophages arginine is converted to nitric oxide by inducible nitric synthase (Lefrancais et al.), which is required for the killing capacity of the macrophages (Rath et al., 2014). In IL-4 activated macrophages arginine is converted to ornithine and urea by the enzyme arginase (Rath et al., 2014). These evidences support the hypothesis that cell intrinsic metabolism plays an important role in determining the fate of the immune cells.

4.1.2. Activation and regulation of mTOR signalling

One of the kinases involved in the regulation of cell growth and metabolism of both adaptive and innate immune cells, is the mammalian target of rapamycin or mTOR. mTOR is a serine/threonine kinase from the PI3K-related kinase family, which can be activated by variety of stimuli such as grow factors, hormones, cytokines and antigen receptor ligation. mTOR can also sense changes in nutrients such as amino acids or the energy levels through the activation of AMPK. (Jones and Pearce, 2017). mTOR exists as a catalytic subunit in two distinct complexes mTORC1 and mTORC2 (Saxton and Sabatini, 2017). In mTORC1, mTOR makes a complex with Raptor (regulatory protein associated with mTOR) and mLST8. Raptor is involved in substrate recruitment, while mLST8 stabilises the catalytic domain. In the mTORC2 complex, mTOR is associated with Rictor (rapamycin insensitive companion of mTOR), mLST8, and mSin1 (Saxton and Sabatini, 2017). The DEP-domain containing mTOR-interacting protein (DEPTOR) can bind to both of the complexes and inhibit their kinase activity (Peterson et al., 2009).

The complexity of mTOR signalling is highlighted by the fact that the pathway is regulated at multiple levels (Figure 4.1). The canonical pathway of mTOR regulation requires PI3K (Phosphoinositide 3-kinase) and Akt (also known as protein kinase B) activation. PI3K activation leads to the generation of phosphatidylinositol-3,4,5-triphosphate (PI(3,4,5,)P_3), which is required for the activation of Akt by PDK1 (PI(3,4,5)P_3-dependent protein kinase). PDK1 phosphorylates Akt on T308 and facilitates its activation. (Alessi et al., 1997). The mTORC2 complex is required for the phosphorylation of Akt at S473, which then primes the phosphorylation of Akt at T308 (Sarbassov et al., 2005). Once activated, Akt phosphorylates and inhibits the activity of Tuberous Sclerosis Complex 2 (Heyen et al., Inoki et al., 2002). TSC2 is a GTPase-activating protein which supresses the activity of mTOR pathway by binding the GTPase Rheb and promoting the conversion of GTP to GDP (Inoki et al., 2003). The active GTP-bound form of Rheb is required for the activation of mTORC1 (Laplante and Sabatini, 2009). mTOR activation can also occur independent of Akt. The Ras/Raf1/ERK pathway has been shown to inhibit the TSC2 suppressive effect in mTOR signalling pathway though an ERK2 dependent phosphorylation of TSC2 at S664 (Ma et al., 2005). MK2 can also phosphorylate TSC2 at S1210, this phosphorylation leads to the binding of 14-3-3 and TSC2, which leads to the inhibition

of the TSC1-TSC2 complex (Li et al., 2003). In TLR stimulated macrophages MK2 can also promote Akt phosphorylation and potentially mTOR activation, via increasing the levels of PIP3 in the membrane, although the substrate of MK2 in this process is not clear (McGuire et al., 2013).

Amino acid availability is also known to activate mTORC1 through the Rag GTPases RagA, RagB, RagC and RagD. The Rag GTPases act as a heterodimers, in which either of RagA or RagB interacts with RagC or RagD (Powis and De Virgilio, 2016). Increased concentrations of amino acids stimulates the binding of guanosine triphosphate (GTP) to RagA and RagB, whereas RagC and RagD are loaded with GDP, a process mediated by a group of proteins referred to as the Ragulator complex. The Ragulator complex is a pentameric complex made of p18 (Lamtor1), p14 (Lamptor2), MP1 (Lamptor3) and two additional proteins Lamtor 4 and 5 encoded by *Lamtor1, Lamtor2, Lamtor3*, *C7orf59* and *HBXIP* respectively (Sancak et al., 2010, Bar-Peled et al., 2012). Moreover the Ragulator complex facilitates the localisation of the mTORC1 complex to the lysosomal membrane in a Rag-dependent manner, where it can interact with Rheb (Bar-Peled et al., 2012). Once activated, mTORC1 can phosphorylate the ribosomal protein S6 kinase p70 S6K and the eIF4E-binding protein (4E-BP1) leading to the activation of multiple factors involved in mRNA translation. mTORC1 also regulates PPARγ and the transcription factor sterol regulatory element-binding protein 1c (SREBP1c) to promote lipid metabolism (Zoncu et al., 2010).

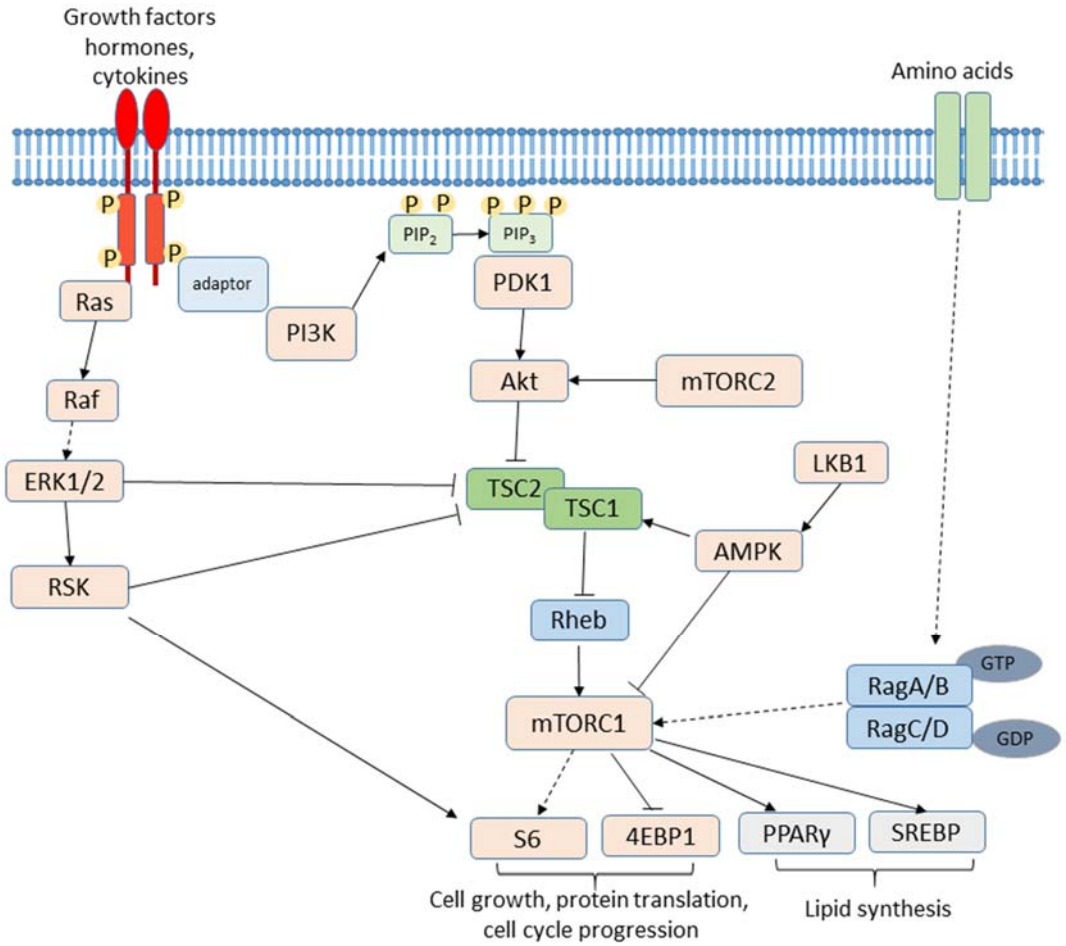

Figure 4.1 Activation of mTOR signalling pathway.
Ligation of the receptor tyrosine kinases leads to the activation of PI3K and the generation of PIP3 from PIP2. PIP3 is required for the activation of PDK1 kinase, which phosphorylates T308 and activates Akt. The mTORC2 complex also phosphorylates Ak on S437. Akt phosphorylates TSC2 and inhibits TSC2 suppressive function, leading to the activation of mTORC1 complex. Other kinases such as ERK1/2 and RSK1/2 also phosphorylate and inhibit TSC2. In contrast TSC2 phosphorylation by AMPK has opposite effect and leads to the inhibition of mTORC1 activity. Availability of amino acids leads to the GTP loading on the RagA/B dimer, which facilitate the co-localisation of Rheb and mTORC1 and the activation of the mTORC1 complex. The mTOR signalling regulates variety of processes such as cell cycle progression, growth, proliferation and lipid synthesis.

The mTOR pathway is negatively regulated by the AMP-activated protein kinase (AMPK). AMPK senses changes in the ATP/ADP and ATP/AMP ratios. AMPK is phosphorylated at T172 and activated by the LKB1-STRAD-MO25 complex or the Calmodulin-activated protein kinase kinase CaMKKβ. This phosphorylation increases the affinity of AMPK to AMP (Hawley et al., 2003, Hawley et al., 2005). During energy stress leading to decrease in ATP and increase in AMP, AMPK is activated to switch on catabolism and the generation of ATP (Hardie et al., 2012). AMPK also switches off anabolism by inactivating mTORC1. AMPK phosphorylates TSC2 on T1227 and S1345 (Inoki et al., 2003). In contrast to the Akt phosphorylation which supresses TSC2, AMPK dependent phosphorylation has the opposite effect and stimulates TSC2 to supress mTORC1 activation (Inoki et al., 2003). Moreover AMPK can inhibit mTORC1 complex directly, by phosphorylating Raptor leading to inactivation of Raptor through 14-3-3 binding (Gwinn et al., 2008).

4.1.3. Metabolic pathways shaping ILC2s responses

Little is known how ILC2s metabolism is regulated during homeostasis and during activation. A limited number of studies suggest a role of arginine and fatty acid metabolism in the regulation of ILC2s. As mentioned above differences in arginine metabolism determine the effector functions in macrophages. The enzyme arginase 1 (Arg1) which metabolises arginine into urea and ornithine, is highly expressed in murine ILC2s precursors in the bone marrow and also in mature ILC2s from the peripheral tissues (Monticelli et al., 2016). Arginase specific deletion in IL-7 receptor expressing cells (*Arg1*$^{flox/flox}$ *Il7r-Cre*$^{+}$*)* had a protective effect in murine mode of papain-induced lung inflammation. In this model, the *Arg1*$^{flox/flox}$*Il7rCre*$^{+}$ had significantly lower number of ILC2s and eosinophils, decreased production of IL-5 and IL-13 and reduced airway remodelling relative to wild type mice (Monticelli et al., 2016). The authors suggested that this is due to lack of Arginase in ILC2s, and not in the other IL-7R expressing cells T and B cells, since Arg1 expression was not detected on T and B cells in naïve and papain stimulated WT animals. *In vitro* inhibition of Arg1 with N$^{\omega}$-hydroxy-nor-arginine (nor-NOHA) leads to reduction in the IL-33 dependent ILC2s proliferation, suggesting the critical role in the arginine metabolism for the ILC2s function. Interestingly, the authors demonstrated that nor-

NOHA blocks the glycolytic pathway in IL-33 stimulated ILC2s, but not oxidative phosphorylation (Monticelli et al., 2016). In contrast, another study showed that Arg1 is not required for ILC2s mediated responses in an infection model with the helminth *Nippostrongylus brasiliensis* (Bando et al., 2013). This could be explained by the fact that ILC2s function depends on the inflammatory context. Another explanation could be that, in Monticelli et al. study the authors suggested that Arg1 is required for the glycolytic pathway which might be important during papain-induced asthma, whereas it has been shown that in another model of helminth infection ILC2s relay on fatty acid oxidation (Wilhelm et al., 2016). Treatment with the fatty acid oxidation inhibitor etomoxir led to an impaired *T. muris* immune response. Mice treated with etoximir had increased worm burden, decrease in the ILC2s numbers and the production of IL-5 and IL-13. In contrast, blocking glycolysis with 2-deoxy-d-glucose [2-DG] had no effect on the type 2 immune responses (Wilhelm et al., 2016). In support to these findings, transcriptional analysis of the different innate lymphoid cells revield that ILC2s express a number of genes involved in lipid metabolism, such as *RXR, Pparγ, Dgat2,* and *Alox5* (Robinette et al., 2015). The RXR retinoid X receptor and peroxisome proliferator-activated receptor PPARγ complex recognise fatty acids and their metabolites and induce transcription of genes involved in the lipid and glucose metabolism. Dgat2 is a diacyglycerol acyltransferase which catalyses the final step in triglyceride synthesis. The arachidonate 5-lipoxygenase Alox5 is involved in the production of leukotrienes and reactive oxygen species from arachidonic acid (Robinette et al., 2015).

4.1.4. Regulation of host metabolism by ILC2 and IL-33 signalling

Another aspect of immune metabolism is the understanding of how the immune system regulates the host metabolism. The immune system plays an important role in mediating the homeostasis of adipose tissue. Increased chronic production of pro-inflammatory cytokines, such as TNF-α, IL-6 and IFN-γ, has been associated with obesity. In contrast, type two immune responses are associated with the lean adipose tissue and limit obesity by regulating the browning of the white adipose tissue and by supressing pro-inflammatory type 1 responses (Cautivo and Molofsky, 2016). An increasing number of studies suggest that both ILC2 and IL-33 are involved in the regulation of obesity, type two diabetes and atherosclerosis (Han et al., 2015, Miller

et al., 2010a, Hams et al., 2013b, Newland et al., 2017). Administration of recombinant IL-33 reduces obesity in genetically obese ob/ob mice by enhancing type two immunity (Miller et al., 2010). IL-33 also increases the frequencies of ILC2s and eosinophils in mice on high fat diet. Furthermore, ILC2s produce methionine-enkephalin and promote the upregulation of Ucp1 and the browning of the adipose tissue (Brestoff et al., 2014). Similarly IL-25 also promotes the regulatory effects of ILC2 and NKT cells during high fat diet induced obesity and adoptive transfer of ILC2 and NKT cells in obese mice leads to transient weight loss in obese animals (Hams et al., 2013a).

4.2. Aims

Considering the importance of IL-33 in ILC2s responses and the limited information about the metabolic changes that occur in activated ILC2s, the aim for this part of my project was to investigate IL-33 dependent metabolic changes in ILC2 cells. I also looked at the role of mTOR signalling in ILC2s effector function.

4.3. Results

IL-33 stimulation in ILC2 cells led to a substantial increase in the size and granularity of the cells (Figure 4.2). The increase in size was detectable after 24 hours of IL-33 stimulation, however it was much greater following 72 hours stimulation (Figure 4.2). The longer stimulation also led to around 3-4 fold increase in cell number in comparison to the initially plated cells (Figure 4.2). Taken together, these results suggest that IL-33 induces changes in the growth and proliferation of the cells.

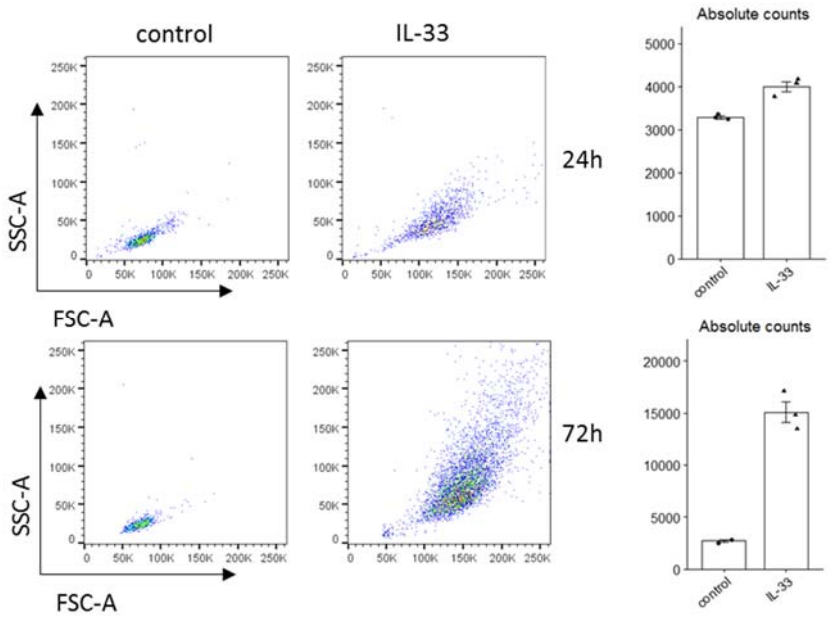

Figure 4.2 IL-33 induces proliferation and an increase in size in ILC2 cells.
Cultured ILC2 cells were plated +/- 100ng/ml of IL-33 for 24 or 72 hours. Cells were stained with DAPI (0.5 µg/mL) and analysed on BD FACSVerse to determine absolute numbers of live cells. Plots represent FSC-A and SSC-A of DAPI negative live cells. Bar plots represent the average value of 3 technical replicates. Error bars represent the standard error of the mean.

mTOR signalling plays a critical role in the regulation of cell growth and proliferation by activating anabolic pathways. ILC2s cultured in IL-2 and IL-7 had constitutive phosphorylation of the ribosomal S6 protein, therefore to address the question if mTOR is activated in ILC2 cells in response to IL-33, I rested the cells in complete RPMI media with no IL-2 or IL-7, before stimulation with IL-33 alone or IL-33 and the mTORC1 inhibitor rapamycin or the RSK1/2 inhibitor LJI308 and measured the phosphorylation of S6 on S235/236. IL-33 stimulation of ILC2s led to a phosphorylation of the ribosomal protein S6. This phosphorylation was completely blocked in the presence of rapamycin and only partially reduced in the presence of

RSKs inhibitor, suggesting that mTORC1 complex has a major role in the regulation of S6 phosphorylation in ILC2s (Figure 4.3). In addition flow cytometry analysis of the changes in the FSC-A and SSC-A showed that rapamycin reduced the increase in cell size in IL-33 stimulated ILC2 cells, but not their granularity (Figure 4.4).

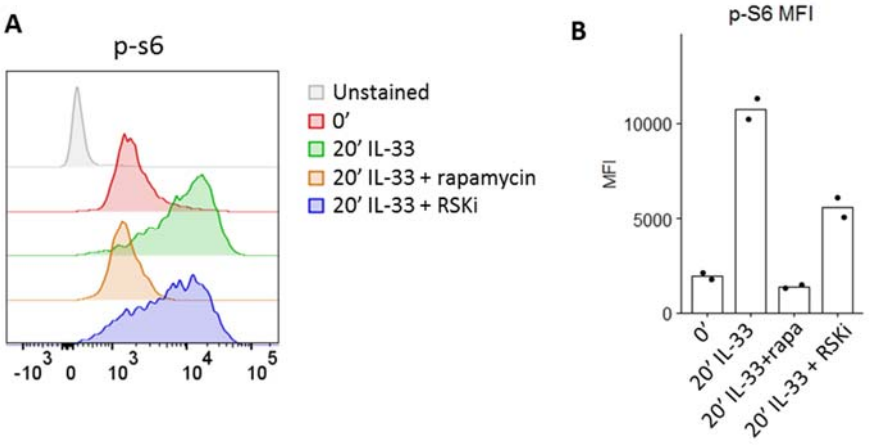

Figure 4.3 S6 activation in ILC2s.
Cultured ILC2s were rested for 3 hours in ILC2 media lacking IL-2 and IL-7 and pre-incubated for a further 1 hour with rapamycin (20nM) or RSK inhibitor LJI308 (10 µM) or DMSO before stimulation with 100ng/ml of IL-33 for 0 or 20 minutes. Phosphorylation of S6 ribosomal protein was measured by flow cytometry. A. Live cells were gated based on FSC-A and SSC-A and the overlaid histograms show p-S6. B. Bar plots show average of the median fluorescence intensity (MFI) of p-S6 from one biological replicate done in duplicate.

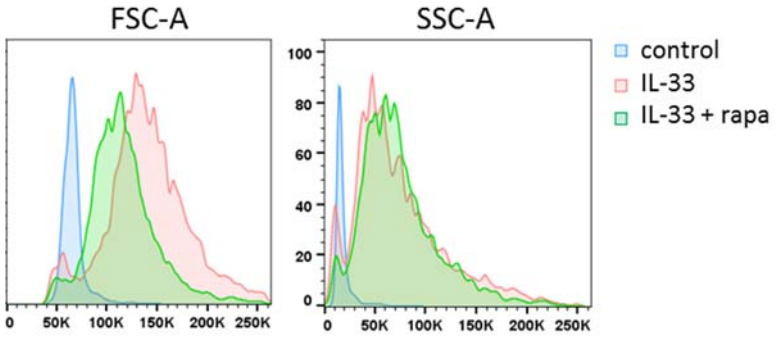

Figure 4.4 mTORC1 controls ILC2 cell size.
Cultured ILC2 cells were stimulated with DMSO, IL-33 (100ng/mL) or IL-33 and rapamycin (20nM) for 72 hours and analysed by flow cytometry BD LSRFortessa. The overlaid histogram show changes in FSC-A and SSC-A

The of role mTORC1 in the regulation of IL-33 dependent cytokine production in ILC2s is largely unexplored, with only one study suggesting that mTORC1 activation is required for the IL-5 and IL-13 production in ILC2s *in vitro* and rapamycin ameliorates IL-33 induced lung inflammation *in vivo* (Salmond et al.,

2012). To confirm these findings and understand the effect of mTORC1 in the production of other cytokines, I stimulated ILC2 cells with IL-33 in the presence of the mTORC1 inhibitor, rapamycin. Inhibition of mTORC1 led to a significant reduction in IL-6 and IL-13 production, but did not affect any of the other cytokines tested including IL-5 (Figure 4.5).

The canonical activation of mTORC1 is mediated by the PI3K/Akt pathway. To further dissect the pathway and understand the role of Akt in regulating ILC2s responses, ILC2s were stimulated with IL-33 in the presence of Akt inhibitor Akti-1/2. Inhibition of Akt did not affect the viability of the cells, however, similar to rapamycin, it led to a significant reduction in IL-6 and IL-13 production (Figure 4.6).

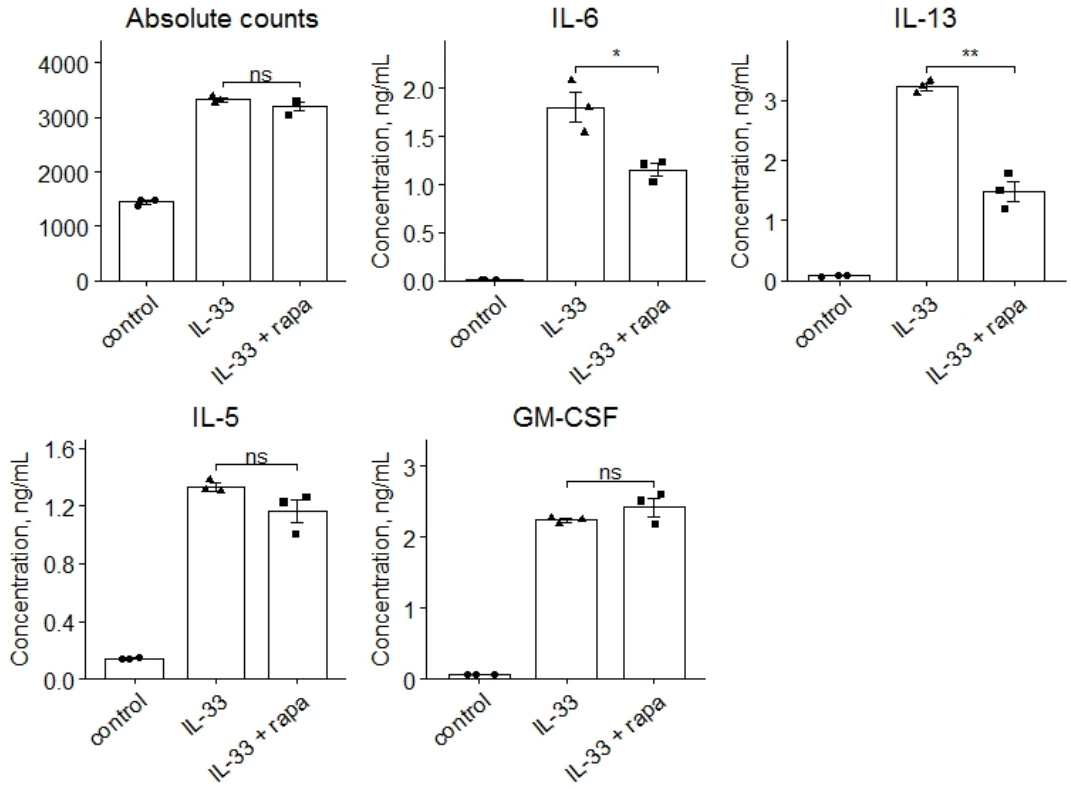

Figure 4.5 mTORC1 activation in ILC2s.
Cultured ILC2 cells were pre-incubated with DMSO or rapamycin (20nM) and then stimulated with IL-33 (100ng/mL) for 24 hours. Control cells received DMSO but not IL-33. Following the stimulation cells were stained with DAPI (0.5 µg/mL) and analysed on BD FACSVERSE to determine absolute numbers of live cells. Supernatants from the cell cultures were analysed for IL-5, IL-6, IL-13 and GM-CSF by multiplex cytokine assay. Bar plots represent the average value of stimulations done in triplicate. Error bars represent the standard error of the mean. Significance between IL-33 alone and inhibitor treated samples was calculated by two-tailed unpaired Student's t-test ; * denotes ($p<0.05$), ** denotes ($p<0.01$).

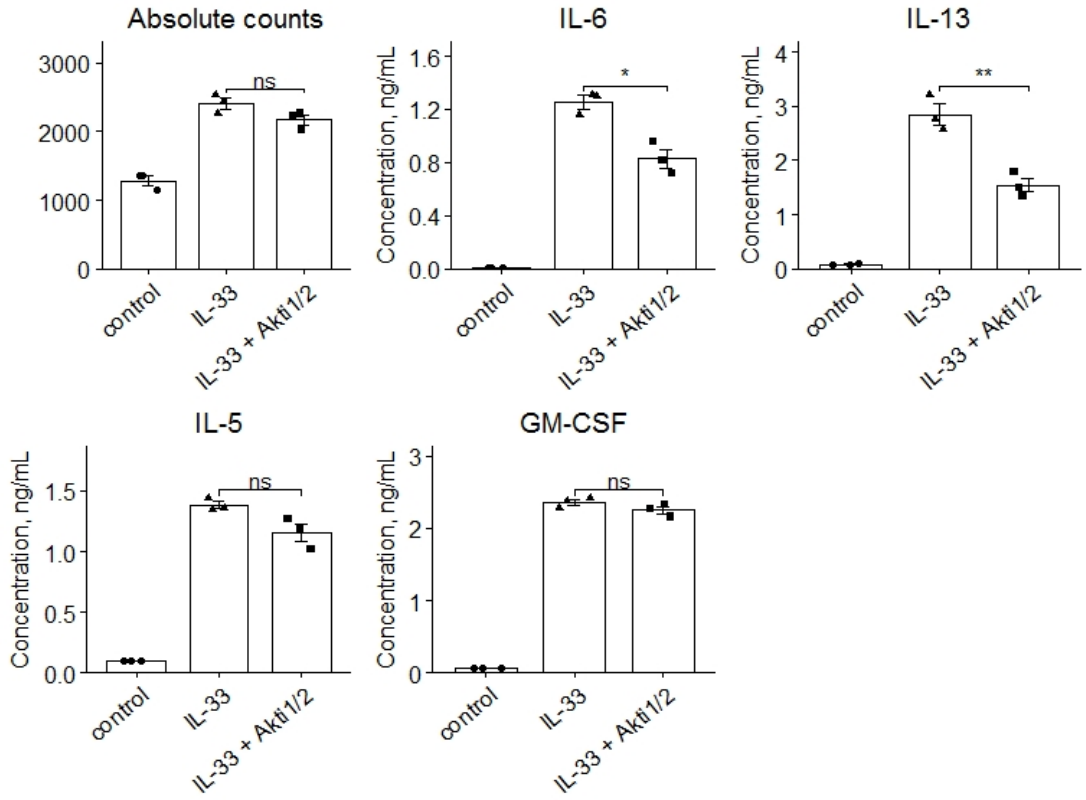

Figure 4.6 Regulation of cytokine production by Akt and PI3K.
Cultured ILC2s cells were pre-incubated with DMSO or the Akt inhibitor Akti-1/2 (1μM) and then stimulated with IL-33 (100ng/mL) for 24 hours. Control cells received DMSO but not IL-33. Following stimulation, cells were stained with DAPI (0.5 μg/mL) and analysed on BD FACSVERSE to determine absolute numbers of live cells. Supernatants from the cell cultures were analysed for IL-5, IL-6, IL-13 and GM-CSF by multiplex cytokine assay. Stimulation was done in triplicate and bar graphs show the average values +/- SEM. Significance between IL-33 alone and inhibitor treated samples was calculated by two-tailed unpaired Student's t-test; * denotes ($p<0.05$), ** denotes ($p<0.01$).

The proto-oncogene Myc plays a central role in the regulation of cellular metabolism leading to cellular proliferation and differentiation. The MYC family includes c-Myc, N-Myc and L-Myc (Chen et al., 2018). Dysregulation of Myc members is involved in more than 50% of cancers, which is not surprising considering that Myc are master transcription factors and regulate expression of around 15% of all genes (Dang et al., 2006). The transcriptional activity of c-Myc is required for the regulation of genes involved in the cell cycle, protein synthesis, ribosomal biogenesis, mitochondrial function and signal transduction (Dang et al., 2006). Using a tamoxifen-inducible Cre system to delete c-Myc in T cells, it was shown that c-Myc was required both for growth and proliferation in activated CD8 T cells (Wang et al., 2011b, Preston et al., 2015). c-Myc was also required for upregulation of genesinvolved in glycolysis

and glutaminolysis. In addition, loss of c-Myc led to a reduction in the amino acid transporter CD98 (Wang et al., 2011b).

Given the critical role of c-Myc in modulating T cell growth, next I examined the expression of c-Myc in ILC2 cells using mice which express c-Myc GFP fusion protein, previously described by Huang et al. (Huang et al., 2008). Stimulation with IL-33 led to an increase of c-Myc expression in ILC2s (Figure 4.7). To ensure that the change in the fluorescence was not due to increased autofluorescence caused by the increase in the size and the granularity of the ILC2s, c-Myc WT ILC2s were also analysed at the same time. Only a minor shift was observed in the GFP channel of the IL-33 stimulated WT ILC2s. Together these results suggest that IL-33 is indeed driving expression of c-Myc.

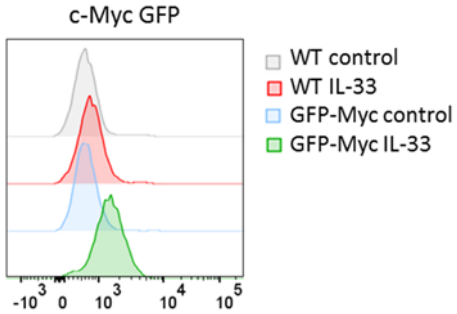

Figure 4.7 IL-33 induces c-Myc in ILC2s. |
ILC2s were prepared from wild type and GFP-Myc mice and cultured with or without IL-33 (100 ng/mL) for 24 hours. Cells were then analysed by flow cytometry. The representative plot is gated on live cells based of forward and side scatter and shows expression of c-Myc in cultured ILC2 cells from WT and GFP-Myc mice.

As mentioned above c-Myc was found to regulate the amino acid transporter CD98 in activated CD8 T cells (Wang et al., 2011b). CD98 is a heterodimer made of heavy and light chains (Nakamura et al., 1999). The heavy chain, which is encoded by *Slc3a2,* contains transmembrane and cytosolic domains, which are required for integrin signalling (Cantor and Ginsberg, 2012). There are several different light chains that can bind to the CD98 heavy chain through a disulfide bond such as Slc7a5 (LAT1), Slc7a8 (LAT2), Slc7a7 (γ-LAT1) and Slc7a6 (γ-LAT2) (Cantor and Ginsberg, 2012). LAT1 and LAT2 are the two major transporters for large neutral amino acids such as leucine, isoleucine, tyrosine, methionine and tryptophan. The availability of amino acids such as leucine has been shown to activate mTORC1 activity (Wolfson et al., 2016, Nicklin et al., 2009). In addition to the amino acid, the

supply for iron is also needed for enhanced cell metabolism and growth. Iron transport is mediated via the CD71 transferrin receptor, which expression has been shown to be increased on the surface of activated T cells (Motamedi et al., 2016). Moreover CD71 expression was found to be dependent on c-Myc in TCR-stimulated CD8 T cells (Preston et al., 2015). Expression of both CD98 and CD71 were increased in ILC2s stimulated with IL-33, suggesting that the cells might have higher uptake of amino acids and iron. Whereas expression of CD98 was detected even in the unstimulated ILC2s, CD71 was only detected in ILC2s upon IL-33 stimulation. Interestingly, treatment with rapamycin led to a partial reduction in CD71 expression, but blocked the IL-33-induced increase in CD98.

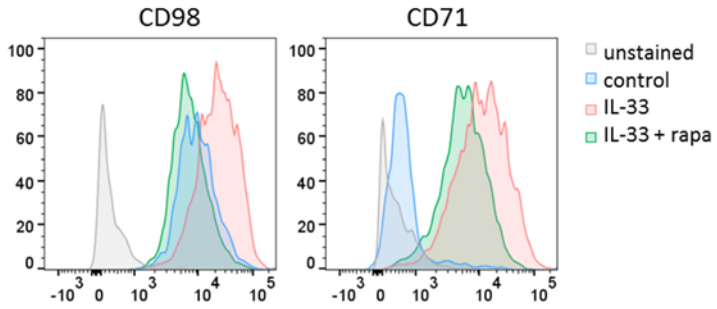

Figure 4.8 CD98 and CD71 expression in ILC2s.
Cultured ILC2 cells were preincunated with DMSO or rapamycin (20nM) and then stimulated with IL-33 (100ng/mL) for 72 hours. Control cells received DMSO but not IL-33. Cells were then analysed by flow cytometry on a BD LSRII (Fortessa). Live cells were gated based on FSC-A and SSC-A. Plots show expression of CD98 (left) and CD71 (right).

Recently the Cantrell lab developed a single cell assay for monitoring System L amino acid transporters using the L-tryptophan metabolite kynurenine (Kyn) (Sinclair et al., 2018). Kynurenine emits fluorescence with an excitation wavelength of 380 nm and an emission spectrum of 480 nm, which can be detected by flow cytometry using the violet laser (Sinclair et al., 2018). Control or IL-33 stimulated ILC2s were first acquired for 2 minutes to measure basal fluorescence in the violet channel, then Kyn was added to the samples and they were further acquired for another 5 minutes to measure changes in fluorescence. IL-33 stimulated ILC2s had a higher uptake of kynurenine in comparison to the unstimulated cells (Figure 4.9). To ensure that Kyn was not binding unspecifically to the cell membrane, but is indeed transported in to the cell, BCH (2-aminobicyclo-(2,2,1)-heptane-2carboxylic acid), an inhibitor of System L amino acid transporter, was used (Kim et al., 2008). The presence of

inhibitor led to a substantial reduction in the fluorescent signal, confirming that the cells are taking up Kyn.

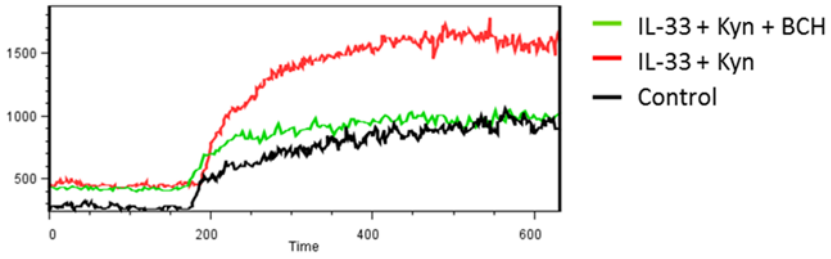

Figure 4.9 Kyn uptake in ILC2 cells.
Cultured ILC2 cells were stimulated with or without IL-33 (100ng/mL) for 24 hours. After stimulation cells were analysed by flow cytometer using 405 nm excitation (violet laser) and band pass filter 450 ± 50 on BD FACSCanto Unstimulated and stimulated samples were acquired for 2 mins to determine baseline florescence before addition of Kyn (200uM). Where indicated the system L amino acid transporter inhibitor BCH (10mM) was added prior to acquisition. Plots show fluorescence (450nm) of ILC2 cells over time.

Slc7a5 expression is critical for CD8 differentiation, metabolic reprogramming and clonal expansion (Sinclair et al., 2013). More recently it has been demonstrated that Slc7a5 may also be regulating responses in human monocytes. Slc7a5 was induced in monocytes upon LPS stimulation. In addition, pharmacological inhibition of Slc7a5 with either BCH or the LAT1 inhibitor JPH203 supressed the production of IL-1β in LPS stimulated monocytes (Yoon et al., 2018). Given the importance of Slc7a5 in immune function, next I investigated the role of Slc7a5 in ILC2s using *Slc7a5*$^{fl/fl}$ mice crossed to *Vav-iCre* mice, resulting in a conditional deletion of *Slc7a5* in immune cell populations. Interestingly, the *Slc7a5*$^{fl/fl}$*Vav-iCre*$^{+/-}$ mice had significant reduction in body weight, as well as in epididymal white adipose tissue weight (Figure 4.10). ILC2 cells were decreased in the eWAT, but not in the lungs (Figure 4.11). Macrophages were also reduced in the eWAT, in contrast to the eosinophils which were not changed in the knock out mice (Figure 4.12).

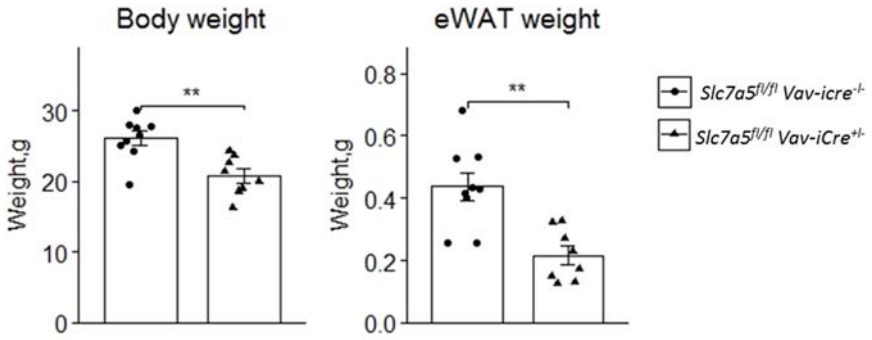

Figure 4.10 Loss of Slc7a5 in the immune cells leads to weight loss and body fat.
Bar plots show total body weight and eWAT weight of 4 month old *Slc7a5*$^{fl/fl}$*Vav-iCre*$^{-/-}$and *Slc7a5*$^{fl/fl}$*Vav-iCre*$^{+/-}$. Each symbol represents individual biological replicate. Error bars represent standard error of the mean. Significance was calculated by two-tailed unpaired Student's t-test; * denotes ($p<0.05$), ** denotes ($p<0.01$).

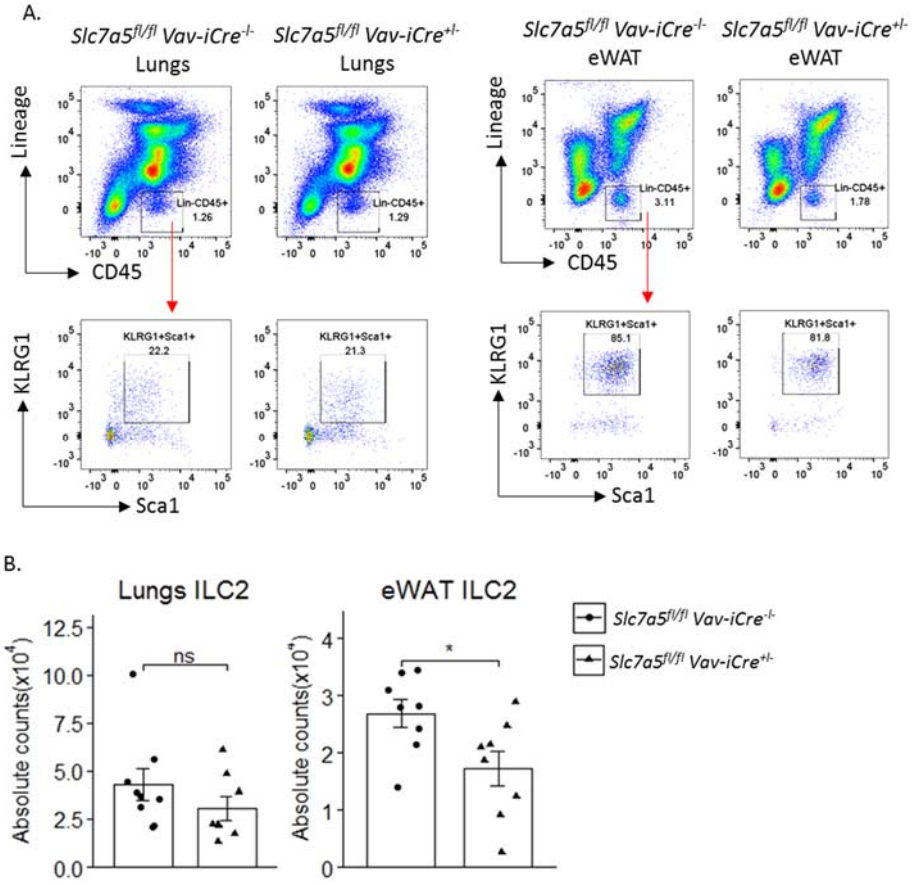

Figure 4.11 *Slc7a5*$^{fl/fl}$*Vav-iCre*$^{+/-}$ mice have reduced ILC2s in the eWAT.
Lungs and epididymal white adipose tissue (eWAT) from *Slc7a5*$^{fl/fl}$*Vav-iCre*$^{-/-}$and *Slc7a5*$^{fl/fl}$*Vav-iCre*$^{+/-}$ (4 months old) were digested to obtain single cell suspension. Cells were stained for expression of Lineage markers (FITC), CD45 (PerCP/Cy5.5), KLRG1(APC) and Sca1(APC/Cy7) and DAPI and analysed on BD LRSII Fortessa. (A) Representative plots are showing percentage of Lineage- and CD45^{+ve} cells from all live single cells and percentage of KLRG1^{+ve}Sca1^{+ve} ILC2 cells within the Lineage-CD45^{+ve} population in lungs and the eWAT. (B) Bar plots represent summary of absolute numbers of Lineage^{-}veCD45^{+ve}KLRG1^{+ve}Sca1^{+ve} ILC2 cells in the lungs and eWAT (D) and body weight. Each symbol represents individual biological replicate. Error bars represent the standard error of the mean. Significance was calculated by two-tailed unpaired Student's t-test; * denotes ($p<0.05$), ** denotes ($p<0.01$).

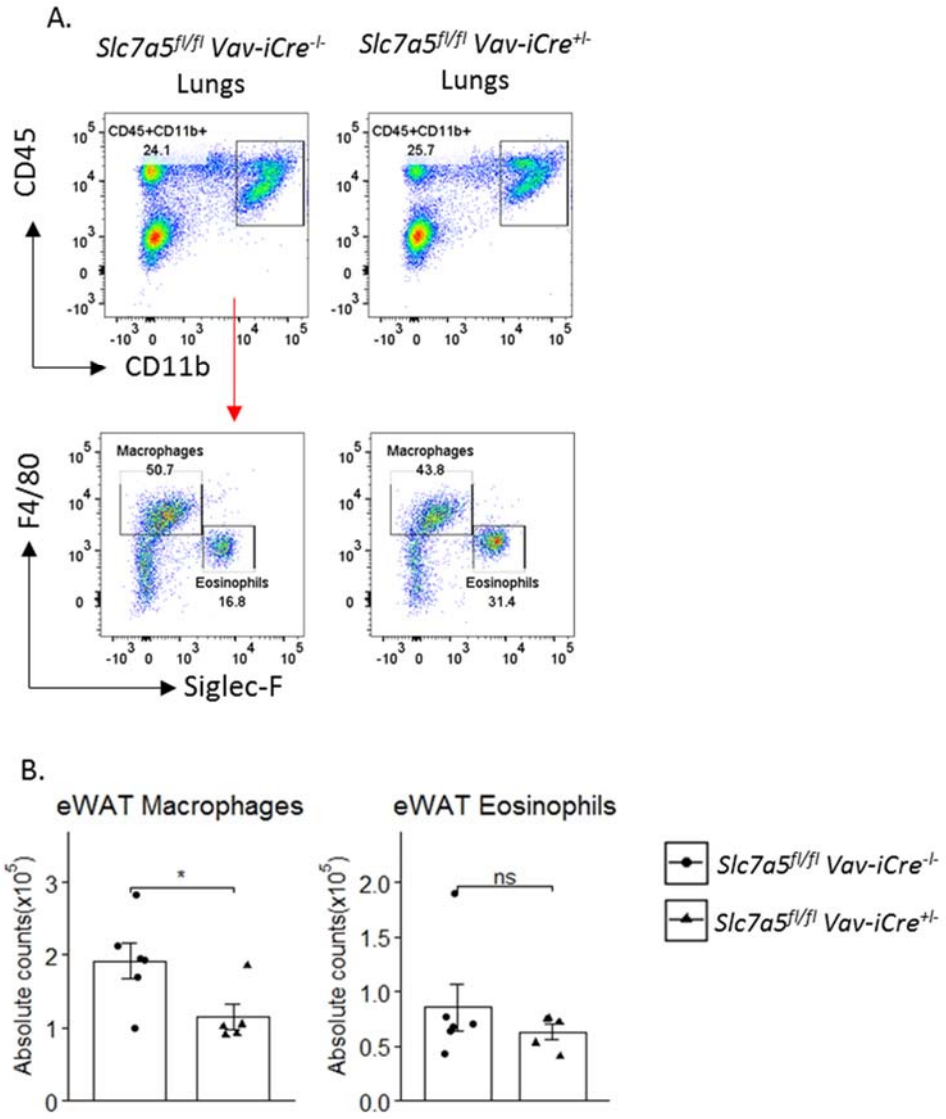

Figure 4.12 *Slc7a5*$^{fl/fl}$*Vav-iCre*$^{+/-}$ mice have reduced Macrophages.
Epididymal white adipose tissue (eWAT) from *Slc7a5*$^{fl/fl}$*Vav-iCre*$^{-}$and *Slc7a5*$^{fl/fl}$*Vav-iCre*$^{+/-}$ (4 months old) were digested to obtain single cell suspension. Cells were analysed for expression of CD45 (BV510), CD11b (PE/Cy7), F4/80 (FITC) and Siglec-F (PE) on BD LRSII Fortessa. (A) Representative plots are showing percentage of CD45^{+ve}CD1b^{+ve} and percentage of F4/80^{+ve}Siglec-F^{-ve} Macrophages and F4/80^{low}Siglec-F^{+ve} eosinophils. (B) Bar plots represent summary of absolute numbers of the macrophages and eosinophils in the eWAT (D) and body weight. Each symbol represents individual biological replicate. Error bars represent the standard error of the mean. Significance was calculated by two-tailed unpaired Student's t-test; * denotes ($p<0.05$), ** denotes ($p<0.01$).

Next, I wanted to understand if Slc7a5 is required for ILC2s cell growth during IL-33 stimulation. Cultured ILC2s from the mesenteric fat of *Slc7a5*$^{fl/fl}$*Vav-ICre*$^{-/-}$ and *Slc7a5*$^{fl/fl}$*Vav-iCre*$^{+/-}$ mice were stimulated with IL-33 and analysed by flow cytometry. ILC2 cells isolated from *Slc7a5*$^{fl/fl}$*Vav-iCre*$^{+/-}$ failed to enlarge in response to IL-33 suggested by FSC-A and SSC-A analysis (Figure 4.13). The size of

unstimulated Slc7a5 knockout ILC2s was also smaller in comparison those of WT ILC2s. In addition, Slc7a5 knockout ILC2s failed to uptake Kyn. Taken together these data indicated that Slc7a5 plays a critical role in sustaining ILC2s in the adipose tissue and is also required for IL-33 dependent cell growth and amino acid uptake.

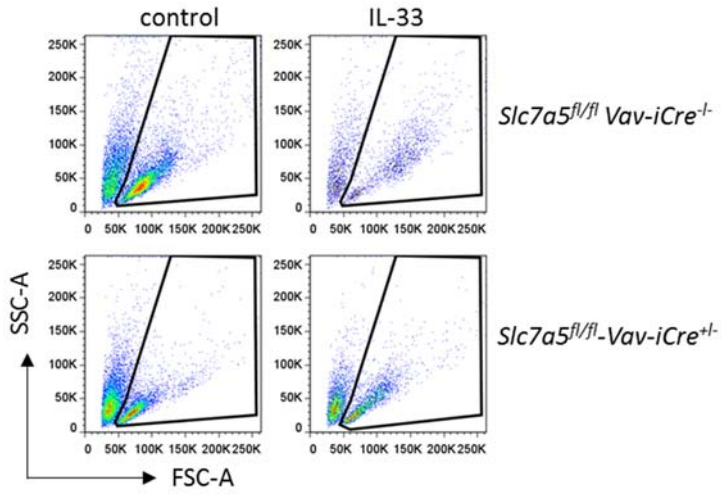

Figure 4.13 Slc7a5 is required for ILC2s cell growth.
ILC2 cells isolated from *Slc7a5*$^{fl/fl}$*Vav-iCre*$^{-}$and *Slc7a5*$^{fl/fl}$*Vav-iCre*$^{+/-}$ were cultured +/- 100ng/ml of IL-33(100 ng/ml) for 24. Cells were analysed on BD FACACanto and plots represent FSC-A and SSC-A of ILC2s.

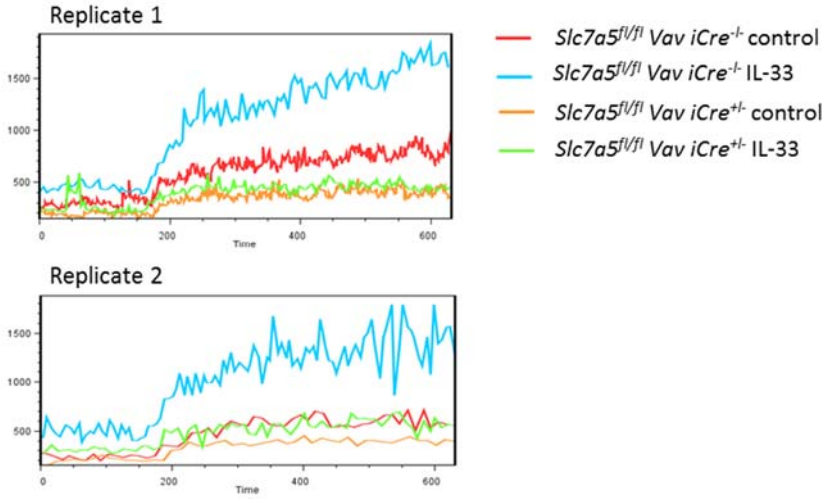

Figure 4.14 Slc7a5 transports Kyn in ILC2s.
Purified ILC2 cells from *Slc7a5*$^{fl/fl}$*Vav-iCre*$^{-}$and *Slc7a5*$^{fl/fl}$*Vav-iCre*$^{+/-}$ mice were stimulated with IL-33 (100ng/mL) and analysed by flow cytometer using 405 nm excitation (violet laser) and band pass filter 450 ± 50 on BD FACSCanto. Unstimulated and stimulated samples were acquired for 2 mins to determine baseline florescence. Kynurenine (200uM) was added to the cells and samples were acquired for another 5 minutes. Plots show fluorescence (450nm) of ILC2 cells over time. Results are representative for two biological replicates.

4.4. Discussion

Activation of immune cells is accompanied by major metabolic changes. Here I showed that IL-33 induces cell growth and proliferation in ILC2s and activation of mTOR signalling pathway, as indicated by the phosphorylation of S6. Although RSK1/2 are shown under some circumstances to phosphorylate ribosomal protein S6 on S235/236 independent of the mTOR-pathway (Roux et al., 2007), inhibition of RSK1/2/3 had only a partial effect on the S6 phosphorylation in ILC2s. In contrast, rapamycin completely blocked the phosphorylation of S6 suggesting that mTORC1, but not RSK1/2 are mediating S6 phosphorylation in IL-33 stimulated ILC2s (Figure 4.3). Inhibition of mTOR by rapamycin led also to a reduction of IL-6 and IL-13 (Figure 4.5). Interestingly, it has been found that rapamycin blocks IL-5 and IL-13 production by ILC2s (Salmond et al., 2012), whereas I did not observe any effect of rapamycin on IL-5 production (Figure 4.5). This could be explained by the different methodology of isolating the cells since, they have used ILC2 isolated from lungs of mice treated with recombinant IL-33. Moreover in this study rapamycin was used at 5 times higher concentration and it is possible that the reduction of IL-5 is due to an off target effect (Salmond et al., 2012).

The exact mechanism of how IL-33 is inducing mTOR signalling activation is not clear. Both ERK and the downstream activated 90 kD ribosomal S6 kinases RSKs have been shown to phosphorylate TSC2 and activate the mTORC1 complex in HEK293 cells (Ma et al., 2005; Roux et al., 2004; Roux et al., 2007). In addition, ERK1/2 phosphorylates and activates Raptor to promote mTORC1 activity (Carriere et al., 2011). However, the finding that RSK inhibition does not block S6 phosphorylation would argue against this as the primary mechanism regulating mTOR activation. Here, I demonstrated for first time that inhibition of Akt also blocks IL-6 and IL-13 similar to rapamycin, which would be consistent with mTORC1 activation downstream of the PI3 kinase – Akt pathway (Figure 4.6). However, based on these data is difficult to predict if Akt activation is directly dependent on IL-33 stimulation or is a secondary response. In mast cells stimulation with IL-33 induces phosphorylation of Akt that is sensitive to PI3 kinase inhibitors, although the molecular mechanism linking IL-33 to PI3 kinase signalling is unclear (Drube et al., 2016)(McCarthy et al., 2018). Interestingly, it has been shown that in macrophages pharmacological inhibition or loss of MK2/3 leads to reduction of phosphorylation of

Akt on both S437 and T308 upon TLR stimulation by mediating the availability of PIP3 in the phospholipid membrane (McGuire et al., 2013). Another possible way in which IL-33 could activate PI3 kinase – Akt signalling would be via c-Kit. As discussed in the previous chapter c-Kit could synergise with the IL-33 receptor complex in mast cells (Drube et al., 2010). Upon ligation of c-Kit with SCF, the SH2 domain of the receptor interacts with the p85 subunit of PI3K leading to allosteric activation of the PI3K catalytic subunit (Roskoski, 2005). Activation of PI3K and PDK1 would allow the phosphorylation of Akt on T308 (Alessi et al., 1997).

mTOR inhibition led to a partial reduction of the IL-33 dependent size increase in ILC2s, suggesting that another pathway might be involved in driving the robust changes in ILC2s (Figure 4.4). I have shown that expression of c-Myc was also upregulated in ILC2 stimulated with IL-33 (Figure 4.7). Comprehensive transcriptomics analysis has highlighted the critical role of Myc in regulating T and B cells responses following antigen receptor activation (Murn et al., 2009, Wang et al., 2011b, Sabò et al., 2014). Deletion of Myc in T cells severely impaired the proliferation and growth by controlling genes essential for the cell cycle progression such as cyclins and CDKs. Myc was also found to be critical for the downstream events in the mTOR signalling, suggested by the fact that Myc deficient T cells had lower levels of S6 phosphorylation (Wang et al., 2011b). The authors attributed that to a reduction of *Slc3a2* (encoding CD98 heavy chain) and *Slc7a5* amino acid (Wang et al., 2011b, Nicklin et al., 2009). Interestingly, Slc7a5 was required for c-Myc expression in CD8 T cells. Upon TCR activation both WT and Slc7a5 knock out T cells upregulated c-Myc levels mRNA levels, however Slc7a5 T cells did not upregulate c-Myc at the protein level, suggesting that there is a bidirectional regulation of Slc7a5 and c-Myc (Sinclair et al., 2013a). Similar findings were observed also in NK cells deficient of Slc7a5, which did not upregulate c-Myc at protein level upon IL-2/IL-12 stimulation (Loftus et al., 2018).

In agreement with the enhanced expression of Myc in ILC2s following IL-33 stimulation, CD98 and CD71 expression was also upregulated (Figure 4.8). Unstimulated ILC2s also expressed measurable levels of CD98, this is in line with RNAseq data in the Immgen database showing that among the innate lymphoid cells ILC2 isolated from small intestine have the highest expression of *Slc3a2* amongst the innate lymphoid cell populations analysed (Figure 4.13). In line with the increased

expression of CD98, I found that ILC2s stimulated with IL-33 showed an enhanced ability to take up the L-tryptophan metabolite kynurenine (Figure 4.9). Among the light chains that can bind to the CD98 heavy chain and mediate transport of amino acids, Slc7a5 has been found to play a critical role in many cell types, including T cells, NK cells and human monocytes (Loftus et al., 2018, Sinclair et al., 2013a, Yoon et al., 2018). Here I demonstrated that Slc7a5 is also regulating ILC2s responses following activation. Slc7a5 deficient ILC2s had impaired cell growth upon activation with IL-33 and complete abrogation of Kyn uptake (Figure 4.13 and Figure 4.14). Moreover, ILC2s numbers were also significantly reduced in the white adipose tissue, but not in the lungs. These data suggested that there might be a differential mechanism of regulation of tissue ILC2s and a specific role of Slc7a5 in the adipose ILC2s. Another interesting observation is that according to Immgen database *Slc7a8* (LAT2) has a much higher expression than *Slc7a5* (LAT1) on ILC2s isolated from the small intestine (Figure 4.15). It is possible that resting ILC2 cells rely on Slc7a8, while in activated state when cells are rapidly growing they require Slc7a5. In addition, the prerequisite for either LAT1 or LAT2 function may depend on the tissues in which the ILC2s are found. This would explain why ILC2s numbers in the lungs were not affected in the Slc7a5$^{fl/fl}$ Vav cre mice while those in the eWAT ILC2s were reduced.

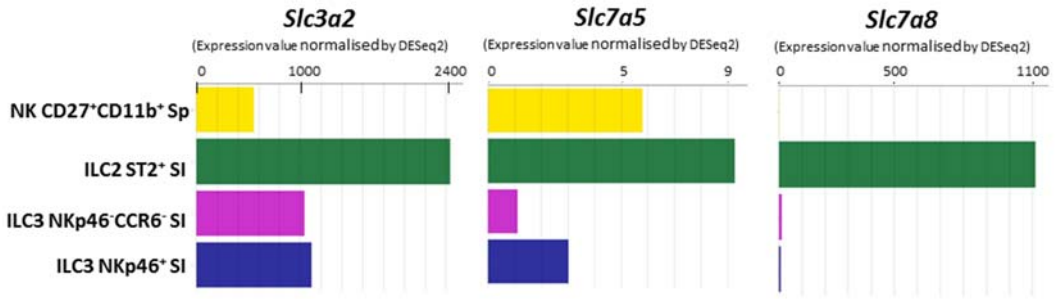

Figure 4.15 *Slc3a2, Slc7a5* and *Slc7a8* expression in innate lymphoid cells populations. Bar graphs were generated using the Immgen RNASeq data base and show the expression of *Slc3a2, Slc7a5* and *Slc7a8* in CD27^{+ve}CD11b^{+ve} NK cells, ST2^{+ve} ILC2s and NKp46^{+ve}CCR6^{-ve} and NKP46^{+ve} ILC3 isolated from the small intestine

Finally, we have observed a decreased body weight in the *Slc7a5*$^{fl/fl}$*Vav-iCre*$^{+/-}$ in comparison to *Slc7a5*$^{fl/fl}$*Vav-iCre*$^{-/-}$ mice, suggesting that the weight loss is a result of a defect in the immune cell compartment (Figure 4.10). Although ILC2s have been found to mediate the beiging of the white adipose tissue by secreting Met-Enkephalin in response to IL-33 (Brestoff et al., 2014), it is unlikely that ILC2s would be

responsible for the observed weight loss in the *Slc7a5*$^{fl/fl}$*Vav-iCre*$^{+/-}$ mice. Considering that Slc7a5 deficient ILC2s have impaired cell growth in response to IL-33, it is likely that their ability to produce effector molecules such as IL-13, IL-4, IL-5 and Met-Enkephalin will also be impaired. The numbers of white adipose macrophages were also reduced in the *Slc7a5*$^{fl/fl}$*Vav-iCre*$^{+/-}$ knock out mice (Figure 4.12). At present it is not clear if this effect is intrinsic to the macrophages or as a result in a defect in ILC2s or another Slc7a5 dependent immune cell type affecting macrophage numbers. White adipose tissue macrophages are important mediators of adipose tissue homeostasis (Boutens and Stienstra, 2016). It has been shown that macrophages in lean and obese adipose tissue have different metabolic properties (Serbulea et al., 2018). For example the macrophages in obese adipose tissue are highly energetic and exhibit high oxidative phosphorylation rate as well as increased aerobic glycolysis (measured by the extracellular acidification rate ECAR), whereas macrophages obtained from lean mice had both low oxygen consumption rate (OCR) and low ECAR (Serbulea et al., 2018). In human monocytes stimulated with LPS, inhibition of Slc7a5 with either BCH or JPH203 led to a significant reduction in ECAR. The authors showed that the leucine influx plays an important role in activation of mTOR and the glycolytic pathway (Yoon et al., 2018). Amino acid transport was also required for optimal TNF-α and IL-β production. Therefore, it is possible that the body weight loss in the *Slc7a5*$^{fl/fl}$*Vav-icre*$^{+/-}$ mice is due to the loss of Slc7a5 in macrophages, their impaired glycolytic metabolism and inability to produce pro-inflammatory cytokines (Tzanavari et al., 2010).

4.5. Conclusions and future prospective

IL-33 induces activation of two major metabolic regulators in ILC2s, the mTOR pathway and transcription factor c-Myc. Inhibition of mTOR and Akt led to a significant reduction in the production of IL-6 and IL-13. Further research would be needed to understand the exact mechanism of how IL-33 is activating mTOR signalling in ILC2s and the molecular mechanism by which is regulated IL-6 and IL-13 production. Inhibition of PI3K leads to reduction in the cytokine production in IL-33 stimulated mast cells (McCarthy et al., 2018). Therefore, it will be also interesting to investigate the role of PI3K in the ILC2s cytokine production. The massive increase

in the ILC2s size upon IL-33 stimulation suggest a major changes in the metabolic pathways, therefore it will be critical to establish if in this context ILC2s rely on glycolysis similarly to activated T cells or oxidative phosphorylation, which is a typical metabolic pathway for IL-4 stimulated macrophages (Pearce and Pearce, 2013). A recent study suggests that blocking glycolysis promotes ILC2s development *in vitro*, whereas blocking oxidative phosphorylation has a negative impact (Li et al., 2018b). The authors demonstrated that mice with conditional deletion of the E3 ligase VHL have a substantial decrease in the ILC2s numbers in the periphery due to enhanced HIF1α expression (Li et al., 2018b). VHL is an E3 ligase that ubiquitinates and targets HIF1α for proteasomal degradation (Haase, 2009). HIF1α transcription factor is regulating the expression of a number of genes involved in the glycolysis pathway including key enzymes such as hexokinase 1 and 2, 6-phosphofructokinase (Marin-Hernandez et al., 2009). Therefore it will be interesting to study the role of HIF1α in ILC2s cells development and function.

We found that the Slc7a5 amino acid transporter regulates cell growth and Kyn uptake in ILC2s. The role of Slc7a5 in mediating the effector function of ILC2s is still unknown, however it is possible that similar to T and NK cells, Slc7a5 is required for the expression of Myc in IL-33 stimulated ILC2s (Sinclair et al., 2013a, Loftus et al., 2018). Future work will be required to understand the role of Slc7a5 in both the cytokine production and proliferative capacity of ILC2s and activation of the mTOR pathway. More work will be also required to understand, how the loss of Slc7a5 in the immune cell compartment is regulating the body weight in mice. As discussed above the macrophages might play an important role in this process, therefore it will be interesting to study the metabolic properties and the cytokine production in Slc7a5 knock out macrophages.

V. Investigating the role of ABIN1 in the development of autoimmunity

5.1. Introduction

5.1.1. Regulation of MyD88 signalling by the ubiquitin system

The TLRs play a critical role in mediating innate immune responses and pathogen clearance. TLR ligation leads to activation of the MAPK signalling as well as NF-κB resulting in the production of multiple inflammatory mediators such as cytokines and chemokines. However, if not controlled, these inflammatory mediators could disturb immune haemostasis and cause autoimmunity or inflammatory diseases (Kondo et al., 2012). Posttranslational modifications including ubiquitination are key regulators of innate immune signalling (Aksentijevich and Zhou, 2017). Ubiquitination is a process in which a monomeric or polymeric ubiquitin molecule is attached to a protein. Ubiquitination is a three step process. The first step is mediated by Ub-activating enzymes E1 and consists of transferring of free ubiquitin (Ub) to the active site cysteine residue on E1, a process which requires energy from ATP. The second step is catalysed by the E2 ubiquitin conjugating enzyme and leads to the transfer of Ub from E1 to an active site cysteine residue on E2. In the final step an E3 ligase catalyses the transfer of the Ub to a lysine residue of the target protein. This process results in a covalent bond being formed between the C-terminus of Ub and the amino group in the lysine side chain. Ub contains 7 lysine residues all of which can potentially be ubiquitinated allowing the formation of poly Ub chains. In addition, Ub can be also linked to an N-terminal methionine (Met) residue of another Ub molecule leading to formation of linear ubiquitin chains. The structure of a poly Ub chain depends on the amino group in the Ub molecule that is used, and different chain types have different properties and functions. For example, addition of ubiquitin chains linked via Lys11 and Lys48 targets protein for degradation by the proteasome system, while Lys63 or Met1 linked chains facilitate protein interactions and are involved in

regulating a number of cellular processes including innate immune signalling and DNA damage pathways (Aksentijevich and Zhou, 2017).

Activation of the TLR and IL-1 family members leads to the recruitment of MyD88, IRAK4, IRAK1 kinases and IRAK2 pseudokinase leading to formation of the Myddosome. Interaction of TRAF6 with the C-terminal regions of IRAK1 and IRAK2 is required for the activation of TRAF6 and the downstream signalling (Ye et al., 2002). IRAK1 and IRAK4 also phosphorylate and enhance the E3 ligase activity of Pellino isoforms (Ordureau et al., 2008). It has been demonstrated that in HEK293 cells stably expressing IL-1R both TRAF6 and Pellinos are required for the generation of the K63 Ub chain downstream of the IL-1 receptor, suggested by the fact that K63-Ub chains formation was completely abolished in TRAF6/Pellino1/Pellino2 triple CRISPR/Cas9 knock out cells, but not in TRAF6 or Pellino1/2 knock out cells (Strickson et al., 2017). In addition, the E3 ligase LUBAC (linear ubiquitin assembly complex) catalyses the attachment of M1 linked linear ubiquitin chains to the K63 chains. The NF-κB essential modulator (NEMO), which is the regulatory subunit of the IKK complex and the TAK1-binding proteins (TAB2 and TAB3) that is part of TAK1 complex, bind to M1 and K63 ubiquitin chains, respectively. This leads to co-recruitment of the TAK1 and IKK complexes and the TAK1 dependent activation of the IKK complex and activation of NF-κB and downstream signalling events (Emmerich et al., 2013b, Cohen and Strickson, 2017). Ubiquitination is a reversible process and is controlled by deubiquitinases (DUBs). In the context of innate immune signalling DUBs such as cylindromatosis (CYLD), OTULIN and A20 have a key role in the negative regulation of NF-κB signalling (Lork et al., 2017) (Figure 5.1). CYLD catalyses the removal of several polyubiquitin linkages including K63 chains. CYLD removes ubiquitin chains on several components of the MyD88 signalling pathway including TRAF6, TAK1 and NEMO (Kovalenko et al., 2003, Sun, 2009) (Figure 5.1A). OTULIN specifically cleaves Met1-Ub and overexpression of OTULIN attenuated NF-κB activation and delayed JNK phosphorylation (Keusekotten et al., 2013, Fiil et al., 2013) (Figure 5.1B). In humans, loss of function mutations in *Otulin* lead to an early onset auto-inflammatory condition, characterised with neutrophilic dermatitis, inflammation, diarrhoea and failure to thrive (Zhou et al., 2016). Mutation of the active site cysteine to alanine (C129A) in OTULIN leads to embryonic lethality in mice. The embryonic lethality is delayed when the mice are crossed to RIPK1$^{-/-}$

mice. Using a tamoxifen inducible Cre system it has been demonstrated that inactivation of OTULIN in adult animals leads to rapid weight loss, increased inflammation, cell death and organ damage (Heger et al., 2018). This phenotype was ameliorated when blocking necroptosis and apoptosis by crossing the mice to caspase-8 and RIPK3 mutant mice, suggesting that the phenotype was dependent on inflammation caused by increased cell death (Heger et al., 2018).

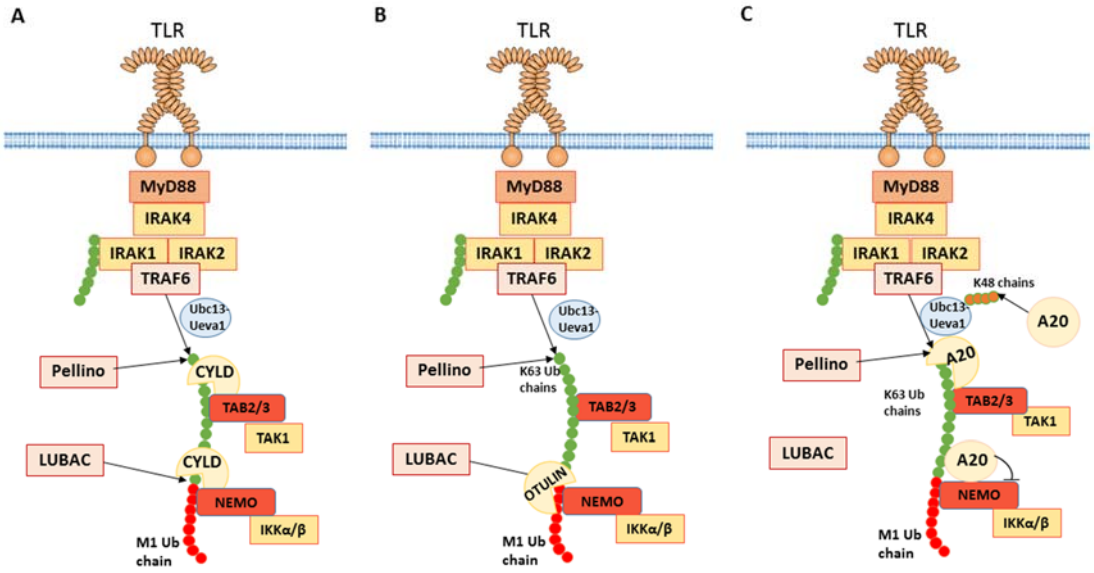

Figure 5.1 Regulation of TLR signaling by ubiquitin chains.
TLR ligation leads to recruitment of MyD88 and the kinases IRAK4, IRAK1 and IRAK2 and the subsequent recruitment of the E3 ligase TRAF6. TRAF6 together with Pellino 1/2 and the E2 conjugating complex Ubc13-Ueva1are required for the generation of K63 ubiquitin chains. LUBAC is another E3 ligase which catalyses the attachment of M1 ubiquitin chains to the K63 chains leading to formation of linear polyubiquitin chains. The last are required for co-recruitment of TAK1 and IKK complexes. A. CYLD is a deubiquitinase which removes K63 ubiquitin chains from TAB2/3 and NEMO, preventing the co-recruitment of the TAK1 and IKK complexes. B. OTULIN specifically cleaves M1 ubiquitin chains and similarly to CYLD regulates the activation of IKK complex. C. A20 is an ubiquitin editing enzyme which have dual activity, it can cleave K63 linked ubiquitin chains, but it can also add K48 ubiquitin to the E2 ligase Ubc13, leading to Ubc13 degradation. In this way the interaction between TRAF6 and Ubc13 is disrupted leading to inhibition of NF-κB signalling. In addition A20 can be bind the K63/M1 polyubiquitin chains through a non-covalent binding. This facilitates an interaction between the ZnF7 domain of A20 and NEMO and blocks the activation of the IKK complex.

The ubiquitin editing protein A20 (TNF-α induced protein 3 (TNFAIP3)) was discovered in 1990 as primary response gene in TNF-α stimulated endothelial cells (Dixit et al., 1990, Opipari et al., 1990). Genomic studies have linked polymorphisms in the *A20* gene to multiple human autoimmune diseases including, rheumatoid arthritis, systemic lupus erythematosus, psoriasis, Crohn's disease and type I diabetes

(Fan et al., 2011, Tejasvi et al., 2012, Wang et al., 2010, Bank et al., 2014). A20 knockout (*TNFAIP3*$^{-/-}$) mice show signs of a spontaneous inflammatory response characterised by increased numbers of lymphocytes, granulocytes and myeloid cells as well as severe tissue damage in multiple organs, cachexia and premature death. The *TNFAIP3*$^{-/-}$ mice displayed also aberrant differentiation of the skin, with an increase of the thickness of the epidermal and dermal layers (Lee et al., 2000). A20 is thought to regulate the MyD88 signalling via several mechanisms. The catalytic activity of the N-terminal OTU (ovarian tumor) domain of A20 is required for the hydrolysis of K63 ubiquitin chains, while the C-terminal zing finger ZnF4 domain catalyses the addition of K48 ubiquitin to proteins targeting them for proteasomal degradation (Verstrepen et al., 2010; Wertz et al., 2015)(Shembade et al., 2010) (Figure 5.1C). Interestingly, mice with mutation in the OTU DUB domain of A20 (*TNFAIP*^{C103A}) or with a mutation in the E3 ligase domain ZnF4 (*TNFAIP*$^{ZNF4/ZNF4}$) are born normal, do not develop autoimmunity and have normal lymphocyte numbers, suggesting that the DUB and the E3 ligase activity of A20 alone are not sufficient for limiting NF-κB signalling (De et al., 2014, Lu et al., 2013). In addition, it has been demonstrated that A20 can supress IKK complex activation by a non-catalytic mechanism. This inhibition was mediated by the ZnF7 domain of A20 which is required for binding of polyubiquitin chains. The last were found to mediate A20-NEMO interaction, which was required for preventing the phosphorylation of IKK by TAK1 (Skaug et al., 2011) (Figure 5C).

5.1.2. Regulation of innate immune signalling by ABIN1

The ABIN1 protein was discovered in 1999 as an A20 binding protein using yeast two-hybrid screening (Heyninck et al., 1999). Overexpression of ABIN1 was found to have a similar effect as A20, suggesting that the inhibitory effect of A20 in the NF-κB signalling is mediated by its interaction with ABIN1 (Heyninck et al., 1999). ABIN1 is part of a family of 5 proteins, including NEMO, ABIN2, ABIN3 and optineurin (OPTN). As discussed above NEMO plays a critical role in the co-recruitment of IKK and TAK1 complexes and the activation of IKK by the TAK1 complex (Emmerich et al., 2013). ABIN2 is part of the TPL2 kinase complex, which is made of ABIN2, p105 and TPL2 and regulates ERK1/2 activation in response to LPS or TNF stimulation (Papoutsopoulou et al., 2006). ABIN2 is important for the stabilisation of TPL2 kinase and in *Tnip2*$^{-/-}$ macrophages the expression of TPL2 is

lost (Papoutsopoulou et al., 2006). Enforced expression of ABIN3 (encoded by *TNIP3*) was found to play a negative role in the regulation of NF-κB in response to TLR, IL-1 or TNF stimulation in THP-1 cells. However, macrophages isolated from *TNIP3*$^{-/-}$ deficient mice had no differences in TLR signalling activation in comparison to WT mice. This was due to the fact that in mice, ABIN3 does not have a complete homology with the human ABIN3 and lacks the ubiquitin-binding domain (Weaver et al., 2007). OPTN binds to the TANK-binding kinase TBK1 and is phosphorylated by TBK1 at S177 (Morton et al., 2008, Gleason et al., 2011). Mutation of D477 to N (*OPTN*$^{D477N/D477N}$) which renders OPTN (*OPTN*$^{D477N/D477N}$) unable to bind ubiquitin chains, results in reduced IFNβ production in LPS or Poly(I:C) stimulated BMDMs (Gleason et al., 2011). In contrast, NF-κB activation was increased in the *OPTN*$^{D477N/D477N}$ BMDMs in response to RANKL stimulation (Obaid et al., 2015). More recent studies have shown that OPTN binds to IRAK1 and regulates NF-κB activation recruiting the deubiquitinating enzyme CYLD and preventing TRAF6 polyubiquitination. (Tanishima et al., 2017).

The ABIN1 protein is encoded by the *TNIP1* gene (Tumor necrosis factor-induced protein 3-interacting protein 1) located on chromosome 5q32–33.1 in humans and chromosome 11 in mice (Verstrepen et al., 2009). The importance of ABIN1 function has been highlighted by a number of genetic studies showing that in humans polymorphism in *TNIP1* gene is associated with psoriasis, psoriatic arthritis, SLE and systemic sclerosis (Nair et al., 2009, G'Sell et al., 2015, Gateva et al., 2009, He et al., 2010, Indhumathi et al., 2015, Zuo et al., 2015, Bossini-Castillo et al., 2013, Caster et al., 2013).Reduced expression of *TNIP1* mRNA has been found also in SLE and psoriatic patients (Adrianto et al., 2012, Chen et al., 2015b).

ABIN1is expressed in several tissues including peripheral blood skeletal muscle, liver, but the level of expression of ABIN1 is quite high in immune organs such as thymus and spleen (Verstrepen et al., 2009) (Gleason et al., 2011). ABIN1 has four ABIN homology domains (AHD). The AHD-1 domain is required for the interaction with A20. The AHD-2 domain has an ubiquitin binding function and shares sequence homology with ubiquitin binding domains of ABIN2, ABIN3, NEMO and OPTN. Therefore, the AHD-2 domain has been also known as UBAN domain (ubiquitin binding domain of ABIN and NEMO) (G'Sell et al., 2015). The mechanism by which ABIN1 regulates NF-κB signalling is still not fully understood. Mutation in

ABIN1, which impaired the ability of ABIN1 to bind either NEMO or A20 were not sufficient to supress NF-κB activation, however when both of the regions required for binding of A20 and NEMO in the ABIN1 protein were mutated, NF-κB activation was blocked (Mauro et al., 2006). Therefore, the authors proposed that ABIN1 interacts with NEMO and recruits A20 to the NEMO/IKK (Figure 5.2A). In contrast, in another study it has been demonstrated that deletion of the UBAN domain in ABIN1 alone is sufficient to inhibit NF-κB activation in HEK293T cells, suggesting that ABIN1 might mediate NF-κB signalling independent of its interaction with A20 (Heyninck et al., 2003). Considering that both ABIN1 and NEMO bind preferentially M1-linked ubiquitin chains it is possible that ABIN1 inhibits NF-κB by competing with NEMO for binding ubiquitin chains and therefore disrupting the activation of the IKK complex (Clark et al., 2013) (Figure 5.2B).

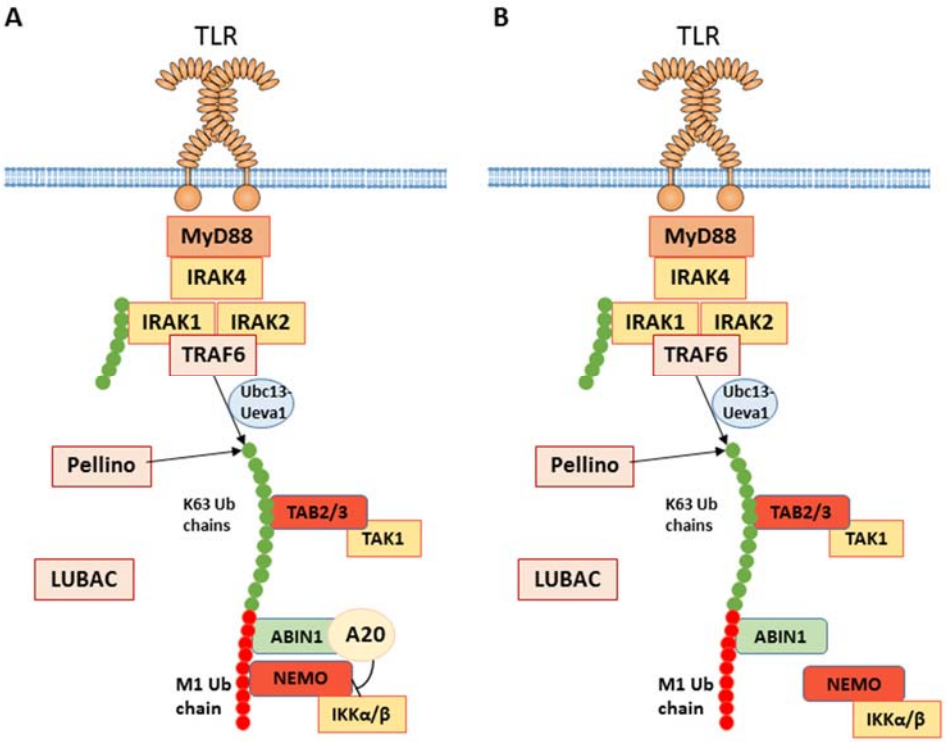

Figure 5.2 A model of ABIN1 dependent regulation of TLR signalling.
A. ABIN1 could interact with NEMO, A20 and polyubiquitin chains and potentially recruit A20 to the NEMO/IKK complex leading to inhibition of downstream signalling. B. Another possible mechanism by which ABIN1 restricts the activation of the pathway is by direct competition with NEMO for binding K63/M1 polyubiquitin chains.

In addition to restricting NF-κB activation, ABIN1 also has a critical role in regulating TNF-α-induced cell death (Oshima et al., 2009). Upon TNF stimulation the

TNF receptor (TNFR) associates with the TRADD adaptor protein (TNFR-associated death domain protein) and the Fas associated protein with death domain (FADD). This process is required for the recruitment of pro-caspase-8, which is then proteolytically cleaved to its active form. Cleaved caspase-8 mediates the activation of other caspases including caspase-3. Activated caspase-3 then triggers DNA fragmentation and degradation of cytoskeletal proteins (Sedger and McDermott, 2014). TNF-α stimulation induced increased cell death in *TNIP1*$^{-/-}$ deficient MEFs, Jurkat T cells, HepG2 hepatoma cells and HT1080 fibrosarcoma cells (Oshima et al., 2009). Oshima and his colleagues demonstrated that ABIN1 inhibits the association of FADD and caspase-8 and that ABIN1 deficient cells have enhanced association between caspase-8 and FADD. Restoring WT ABIN1 into *TNIP1*$^{-/-}$ 3T3 cells led to a protection from TNF-induced cell death. In contrast, restoring the *TNIP1*$^{-/-}$ 3T3 cells with ubiquitin binding domain mutant of ABIN1 did not rescue the susceptibility of *TNIP1*$^{-/-}$ 3T3 cells to TNF-induced cell death, suggesting ABIN1 restricts cell death through its ubiquitin binding function. (Oshima et al., 2009). *TNIP1*$^{-/-}$ mice were born below Mendelian ratio due to enhanced TNF-α induced apoptosis in the liver. The mice that survived after birth developed lupus like autoimmunity, neutrophilia, immune cell infiltration in the tissues and glomerulonephritis, cachexia and died prematurely within 4 months of age (Zhou et al., 2011). Whereas crossing the *TNIP1*$^{-/-}$ mice to TNFR1 knock out mice rescued the TNF-induced apoptosis in the liver, the inflammatory phenotype was not affected in the double knock mice (Zhou et al., 2011).

Mutation of Asp 485 to Asn in murine ABIN1 or Asp 472 to Asn in human, which is in the UBAN domain of ABIN1, impairs the ability of ABIN1 to bind ubiquitin chains. Mice homozygous for the knock-in mutation of Asp 485 to Asn (ABIN1[D485N]) are born at normal Mendelian ratios, but develop a lupus-like inflammatory condition with splenomegaly, increased formation of germinal centres, production of anti-nuclear antibodies and deposition of immunocomplexes in the kidney leading to glomerulonephritis (Nanda et al., 2011). B cells and bone marrow derived dendritic cells isolated from ABIN1[D485N] mice have enhanced NF-κB and MAPK activation and cytokine production in response to TLR stimulation in comparison to cells isolated from WT mice (Nanda et al., 2011). To examine the pathways that drive autoimmunity in these mice, the ABIN1[D485N] mice have been

crossed onto a number of other different knockouts. While cross to RIP2 or IFNAR1 knockout mice did not supress the inflammatory phenotype in the ABIN1[D485N] mice, crossing to MyD88 deficient mice or mice with catalytically inactive IRAK4 and IRAK1 kinases led to a rescue of the lupus like autoimmunity (Nanda et al., 2011, Nanda et al., 2016).

5.1.3. Immunopathogenesis in systemic lupus erythematosus

Systemic lupus erythematosus is an autoimmune diseases, characterised by the presence of autoreactive antibodies against nucleic acids or nuclear proteins and formation of immune complexes which can be detected in various organs. The manifestation of SLE are diverse and can range from mild cutaneous inflammation to severe kidney pathology and cardiovascular problems with life-threatening prognosis (Tsokos et al., 2016). SLE is a relatively rare disease and affects more women than men (Carter et al., 2016). In the UK the disease incidence during 1999-2012 were 4.91/100 000 people and overall prevalence of 97.04/100 000 in 2012 with a highest incidence and prevalence within the Black Caribbean ethnicity (Rees et al., 2016). Similar number of incidence of 5.5 and 5.6 per 100 000 were reported also in two independent studies in the US (Somers et al., 2014, Lim et al., 2014). The current biological therapies for SLE treatment are very limited and although a substantial progress has been made in the understanding of SLE pathogenesis, there is only one targeted drug that has been approved in the last 50 years for treatment of lupus: belimumab or benlysta. Belimumab is a human monoclonal recombinant antibody which recognises and binds to the B cell-activating factor BAFF, leading to the decreased B cell survival and reduction of the antibody production (Dubey et al., 2011). In addition, the anti-CD20 chimeric monoclonal antibody rituximab is also used as an “off-label” drug (Felten et al., 2018). Standard therapies include non-corticosteroid anti-inflammatory drugs and immunosuppressants such as corticosteroids, methotrexate, azathioprine, cyclophosphamide, and mycophenolate mofetil (Dubey et al., 2011). However, broad spectrum immunosuppression, increases the risk of infections in the patients, therefore more specific therapies are required for treatment of the disease.

One of the key mechanisms for breaking immune tolerance in SLE is proposed to be the impaired clearance of apoptotic cells. This notion has been supported by studies showing that monocyte derived macrophages from SLE patients have impaired phagocytosis of apoptotic cells (Tas et al., 2006, Munoz et al., 2009). Increased apoptotic cell number has been also found in the skin of patients with SLE (Kuhn et al., 2006). The link between apoptosis and SLE has been also demonstrated in mice. MRL/*lpr* mice, which are one of the most commonly used models for SLE, have a mutation in the death receptor Fas (Watanabe-Fukunaga et al., 1992). In another lupus prone mouse strain, (NZB x NZW) F_1 mice, the levels of DNase I mRNA, which is involved in the fragmentation of DNA during apoptosis were reduced and as a result chromatin particles were deposited in the kidneys of (NZB x NZW)F_1 (Zykova et al., 2008). Other cell death pathways such as necrosis are also considered as contributing factors for lupus development (Fan et al., 2014). In contrast to apoptosis, where dying cells are phagocytosed and cleared, during necrosis the membrane integrity of the cells is lost and cellular components are released including factors such as nucleic acids and ribonucleoproteins, mitochondrial components and ATP that can act as damage associated molecular patterns (DAMPs) and stimulate the innate immune system (Vanden Berghe et al., 2010).

Another potential source of nuclear antigens are the neutrophil extracellular traps (NETs), which contain DNA, histones, elastase, myeloperoxidase and other granular proteins. In response to microbial stimuli the neutrophils release decondensed DNA and granular proteins. Although NET formation is important for microbial clearance, the insufficient clearance or overproduction of NETs can promote tissue damage and development of lupus (Villanueva et al., 2011, Mistry and Kaplan, 2017, Apel et al., 2018). A specific type of neutrophils called low density gradient (Nair et al.) neutrophils has been identified in blood samples from lupus patients (Villanueva et al., 2011, Kaplan, Lood et al., 2016). LDG neutrophils have enhanced capacity to produce NETs and higher cytokine production in response to GM-CSF stimulation than autologous “normal” neutrophils (Denny et al., 2010, Villanueva et al., 2011).

5.1.4. TLRs in systemic lupus erythematosus

The nucleic acid sensing TLRs TLR3/7/8 and 9 have been implicated in the pathology of lupus, with a most prominent role of TLR7. These TLRs are important in the recognition of pathogen derived nucleic acids. They can however also recognise some host nucleic acids; as this would stimulate inflammation, mechanisms have evolved to prevent this happening. Key amongst these is the endosomal and ER restricted location of TLR3/7/8 and 9; this protects from recognition of the host nucleic acid present in the cytoplasm or released into the extracellular space during cell death. However, internalisation of nuclear immune complexes through the FcγR could lead to the activation of nucleic acid sensing TLRs (Santiago-Raber et al., 2009). The critical role of TLR7 in the development of SLE has been highlighted by a number of studies in mice. BXSB mice develop lupus like autoimmunity, which is greatly accelerated in the BXSB.*Yaa* males, in which translocation of portion of the X chromosome to the Y chromosome leads to duplication of 17 genes including *TLR7* (Pisitkun et al., 2006). Transgenic mice expressing more copies of *TLR7* also developed lupus like autoimmunity (Deane et al., 2007). Loss of TLR7 in MRL/*lpr* attenuates disease progression, autoantibody production and immune cell activation (Christensen et al., 2006). TLR7 is also required for the spontaneous formation of germinal centre B cells, which are involved in the auto-antibody production in lupus (Soni et al., 2014). Increased expression of TLR9 has been reported in patients with SLE (Rao et al., 2015). Cross of MRL/*lpr* mice to *TLR9*$^{-/-}$ mice led to a reduction in anti-dsDNA antibodies, however it did not reduce the infiltration of activated lymphocytes or the kidney pathology (Christensen et al., 2005). In addition, TLR9 deficiency has been shown to exacerbate disease severity in MRL/*lpr* mice rather than having protective effect (Christensen et al., 2006). Later it was demonstrated that *TLR7*$^{-/-}$ cross rescues the exacerbated phenotype in the TLR*9*$^{-/-}$/MRL/*lpr*. Therefore, the authors suggested that TLR9 limits the activity of TLR7 and loss of TLR9 results in enhanced TLR7 signalling and disease exacerbation (Nickerson et al., 2010).

Plasmocytoid dendritic cells (pDCs) are a specialised subset of dendritic cells which express TLR7 and TLR9 and can sense nucleic acids (Buechler et al., 2013). Moreover, they are considered as the most potent producers of IFNγ and thereby mediating immunity in viral infections (Siegal et al., 1999). Whereas pDCs are decreased in the blood of patients with lupus, their numbers seem to be increased in

the skin and kidneys, suggesting that pDC might migrate from the blood into the tissues (Cella et al., 1999, Fiore et al., 2008, Vermi et al., 2009). In lupus patients pDC have been shown to internalise nucleic acid containing immune complexes trough the FcγRIIa, leading to the recognition of these IC by the TLR9 and TLR7 receptors and production of IFN-α (Means et al., 2005). A number of studies have shown that peripheral blood mononuclear cells isolated from lupus patients are characterised by upregulation of IFN induced genes (Bennett et al., 2003, Crow and Wohlgemuth, 2003, Baechler et al., 2003). As a result, one of the main current strategies for the development of therapies for lupus is focused on targeting the IFN pathway (Felten et al., 2018).

5.1.5. Aims

Considering the role of ABIN1 in the development of SLE both in human and mice, the aim of the project was to characterise the changes in innate immune cells in ABIN1[D485N] mice and to further investigate the mechanism underlying the pathology in these mice. While in the beginning we wanted to look at ILCs, the initial experiments indicated that there was a massive increase in monocytes in the ABIN1[D485N] mice. Changes in the monocytes were also investigated in ABIN1[D485N] mice crossed to MyD88 KO or IRAK4 and IRAK1 knock in mice, in which the lupus phenotype is prevented. I also characterise the potential of pharmacological inhibition of IRAK4 to prevent and/or treat lupus like autoimmunity observed in ABIN1[D485N] mice. Last, the importance of TLR7 in mediating inflammatory responses in ABIN1[D485N] was studied by crossing ABIN1[D485N] mice to TLR7 KO mice. The role of TLR7 in mediating monocyte responses *in vitro* and *in vivo* was also addressed.

5.2. Results

5.2.1. Characterisation of innate immune populations in ABIN1[D485N] mice

ABIN1[D485N] mice are characterised by splenomegaly with an increase in the total number of splenic B cells, $Gr1^{+ve}CD11b^{+ve}$ cells and also aberrant T cells with an activated phenotype (Nanda et al., 2011). However, the changes in the innate immune compartment in lymphoid and non-lymphoid tissues of ABIN1[D485N] mice have not been extensively investigated. Analysis of the innate lymphoid populations, revealed that there is a slight increase in the lineage negative ILC2 populations in the lungs of ABIN1[D485N] mice (not shown), however a much bigger change was observed in the lineage positive cells. Further characterisation of the lungs showed that the ABIN1[D485N] increase in the lineage positive gate was due to a massive increase in a population of cells expressing high levels of CD11b and intermediate levels of CD11c (Figure 5.3).

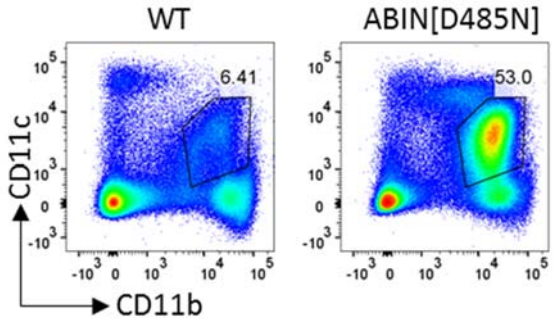

Figure 5.3 Expansion of $CD11b^{high}CD11c^{inter}$ cells in the lungs of ABIN1[D485N] mice. Lungs cells from WT and ABIN1 mice were stained with anti-mouse CD11b (PE/Cy7) and anti-mouse CD11c (APC) antibodies and DAPI and acquired on BD FACSCanto. Leukocytes were gated based on FSC-A and SSC-A. Doublets were gated out using FSC-W and FSC-A and live cells were gated as DAPI negative. The representative plots show percentage of $CD11b^{high}CD11c^{inter}$ from live single cells.

CD11b and CD11c are expressed in many immune cells including monocytes, macrophages, and dendritic cells (Yu et al., 2016). In addition, CD11b expression is also found in NK cells and granulocytes such as neutrophils and eosinophils (Misharin et al., 2013, Yu et al., 2016, Fu et al., 2011). In mice there are two distinct population of monocytes: $Ly6C^{+ve}$ inflammatory (also referred as classical) monocytes and $Ly6C^{-ve}$ patrolling (non-classical) monocytes, which express CD11b, the M-CSF receptor CD115, the fractalkine chemokine receptor CX_3CR1 and CD64 (Geissmann et al., 2003, Jakubzick et al., 2017). Monocytes develop in the bone marrow and

migrate through the blood into the tissues where they can differentiate into tissue macrophages or dendritic cells (Jakubzick et al., 2017, Yona et al., 2013). Moreover it has been demonstrated Ly6C^{+ve} inflammatory monocytes act as an intermediate precursor from which the Ly6C^{-ve} patrolling monocytes develop (Yona et al., 2013). Since patrolling monocytes haven been characterised by expression of both CD11b and CD11c, next we wanted to address the question if the increased population of cells in the ABIN1[D485N] mice express other markers characteristic for the patrolling monocytes. Therefore, a 10-color staining panel was optimised and cells isolated from blood, lungs, spleen and kidneys were analysed by flow cytometry. Details of the antibodies used in the stain are listed in Table 5.1.

Table 5.1 Flow cytometry panel for characterisation of innate immune cell populations in ABIN1[D485N] mice.

Target	Fluorophore	Clone	Dilution	Stock conc	Source
CD45	BV510	30-F11	1:200	0.2 mg/ml	BioLegend
NK1.1	APC/Cy7	PK136	1:200	0.5 mg/ml	BioLegend
CD11c	PE/Dazzle594	N418	1:200	0.2 mg/ml	BioLegend
CD11b	PE/Cy7	M1/70	1:600	0.2 mg/ml	BioLegend
Ly-6G/Ly-6C (Gr-1)	PerCp/Cy5.5	RB6-8C5	1:400	0.2 mg/ml	BioLegend
Ly-6C	FITC	HK1.4	1:400	0.5 mg/ml	BioLegend
CX3CR1	PE	SA011F11	1:200	0.2 mg/ml	BioLegend
CD115	APC	AFS98	1:200	0.2 mg/ml	BioLegend
I-A/I-E (MHC II)	AlexaFluor700	M5/114.15.2	1:200	0.5 mg/ml	BioLegend

The gating strategy for identifying blood monocytes is represented in Figure 5.4. Doublets and dead cells were excluded from the analysis. The blood monocytes were characterised as CD115 and CD11b double positive cells and were subdivided into Ly6C^{+ve}CX$_3$CR1^{+ve} and Ly6C^{-ve}CX$_3$CR1^{+ve} populations. Both of these populations were further analysed for expression of CD11c and MHCII. Blood inflammatory monocytes were defined as CD11b^{+ve}CD115^{+ve}Ly6C^{+ve}CX$_3$CR1^{+ve} and patrolling monocytes as CD11b^{+ve}CD115^{+ve}Ly6C^{-ve}CX$_3$CR1^{+ve}MHCII^{-ve}. While the patrolling monocytes expressed low to intermediate levels of CD11c, the Ly6C^{+ve}

monocytes were negative for both CD11c and MHCII. The $CD115^{-ve}CD11b^{+ve}$ population was predominantly made of $Gr1^{high}$ neutrophils (PMN) and $NK1.1^{+ve}$ cells.

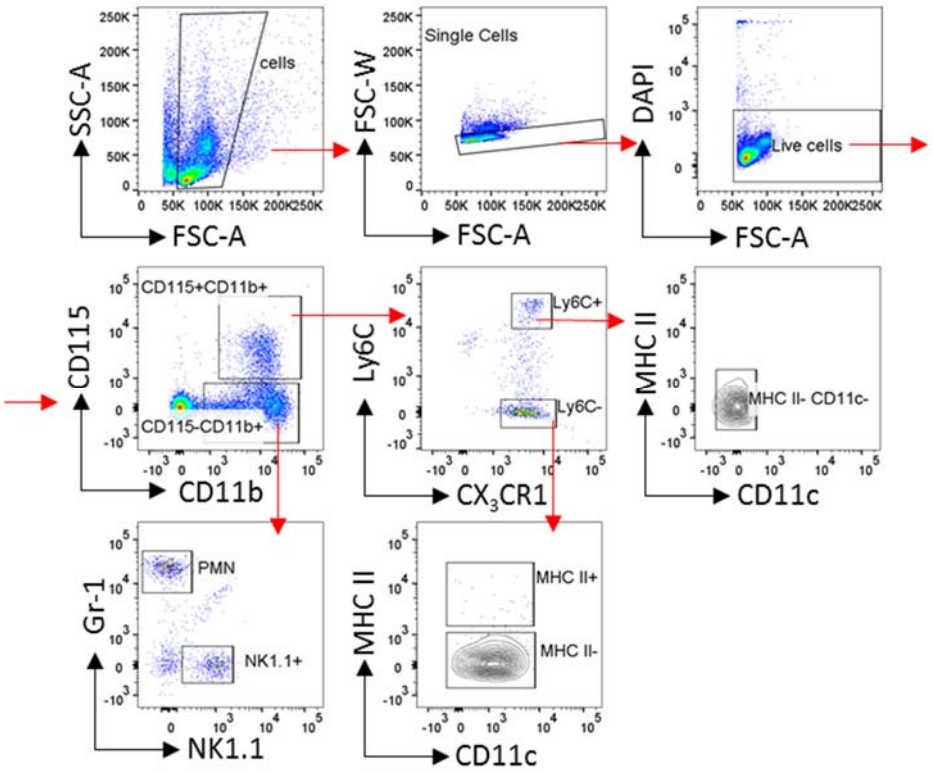

Figure 5.4 Gating strategy for identifying monocytes in murine blood.
Blood leukocytes isolated from WT mice were stained with DAPI, and with fluorophore conjugated antibodies against CD45 (BV510), CD115 (APC), CD11b (Pe/Cy7), Ly6C (FITC), CX_3CR1 (PE), MHCII (AlexaFluor700), CD11c (PE-Dazzle 594), Gr1 (PerCp/Cy5.5) and NK1.1 (APC/Cy7) and analysed on BD LSR Fortessa II. Leukocytes were gated based on FSC-A and SSC-A, doublets were gated out using FSC-W and FSC-A and live cells were identified as DAPI negative cells. Live cells were than analysed for expression of CD115 and CD11b. $CD115^{+ve}CD11b^{+ve}$ positive cells were split into two populations based on expression of $Ly6C^{+ve}$ and CX_3CR1^{+ve}: $Ly6C^{+ve}$ CX_3CR1^{+ve} and $Ly6C^{-ve}$ CX_3CR1^{+ve} cells. The last were further analysed for expression of MHCII and CD11c. Patrolling monocytes were defined as $Ly6C^{-ve}CX_3CR1^{+ve}MHCII^{-ve}$ and the inflammatory monocytes as $Ly6C^{-ve}CX_3CR1^{+ve}MHCII^{-ve}CD11c^{-ve}$. $Gr\text{-}1^{+ve}$ cells within the $CD115^{-ve}CD11b^{+ve}$ were defines as neutrophils (PMN) and $NK1.1^{+ve}$ as NK cells.

The expression of CD115 defines monocytes both in human and mouse blood, however it has been demonstrated that CD115 stability depends on multiple factors and could be downregulated if blood samples are not refrigerated (Breslin et al., 2013). Isolation of cells from non-lymphoid tissues such as lungs and kidneys requires digestion at 37°C or both digestion and density gradient centrifugation, which can impair the stability of CD115. Therefore, an alternative gating strategy was applied to characterise monocytes in the spleen and lung tissues (Figure 5.5 A and B). Doublets and dead cells were excluded and proportion of $CD45^{+ve}$ immune cells, which were

negative for NK1.1 were gated for further characterisation. NK1.1 positive cells were excluded from the analysis as some NK cells subsets express CD11b and CX_3CR1 (Hamann et al., 2011, Fu et al., 2011). The $Gr1^{high}$ cells were defined as neutrophils (PMN) and remaining CD11b positive cells were analysed for expression of CX_3CR1 and Ly6C. Although eosinophils also express CD11b and Ly6C, they do not express CX_3CR1 and therefore $CD45^{+ve}NK1.1^{-ve}CD11b^{+ve}Ly6C^{+ve}CX_3CR1^{+ve}$ cells were characterised as inflammatory $Ly6C^{+ve}$ monocytes (Jung et al., 2000). The patrolling $Ly6C^{-ve}$ monocytes were defined as $CD45^{+ve}NK1.1^{-ve}CD11b^{+ve}Ly6C^{-ve}CX_3CR1^{+ve}MHCII^{-ve}$. In contrast to the blood, where in the $Ly6C^{-ve}CX_3CR1^{+ve}$ gate majority of the cells were $MHCII^{-ve}$ patrolling monocytes, splenic and lungs $Ly6C^{-ve}CX_3CR1^{+ve}$ cells contained population of a $MHCII^{+ve}CD11c^{+ve}$ cells (potentially representing $CD11b^{+ve}$ monocyte derived dendritic cells) and $MHCII^{+ve}CD11c^{-}$ cells (Figure 5.5 A and B). The monocyte derived dendritic cells are characterised as $CD11b^{+ve}CD11c^{+ve}MHCII^{+ve}CD24^{+ve}$. In addition, in some tissues such as the skin and gut it has been demonstrated that they express SIRP-α and CX_3CR1 (Ginhoux et al., 2009, Ko and Chang, 2015).

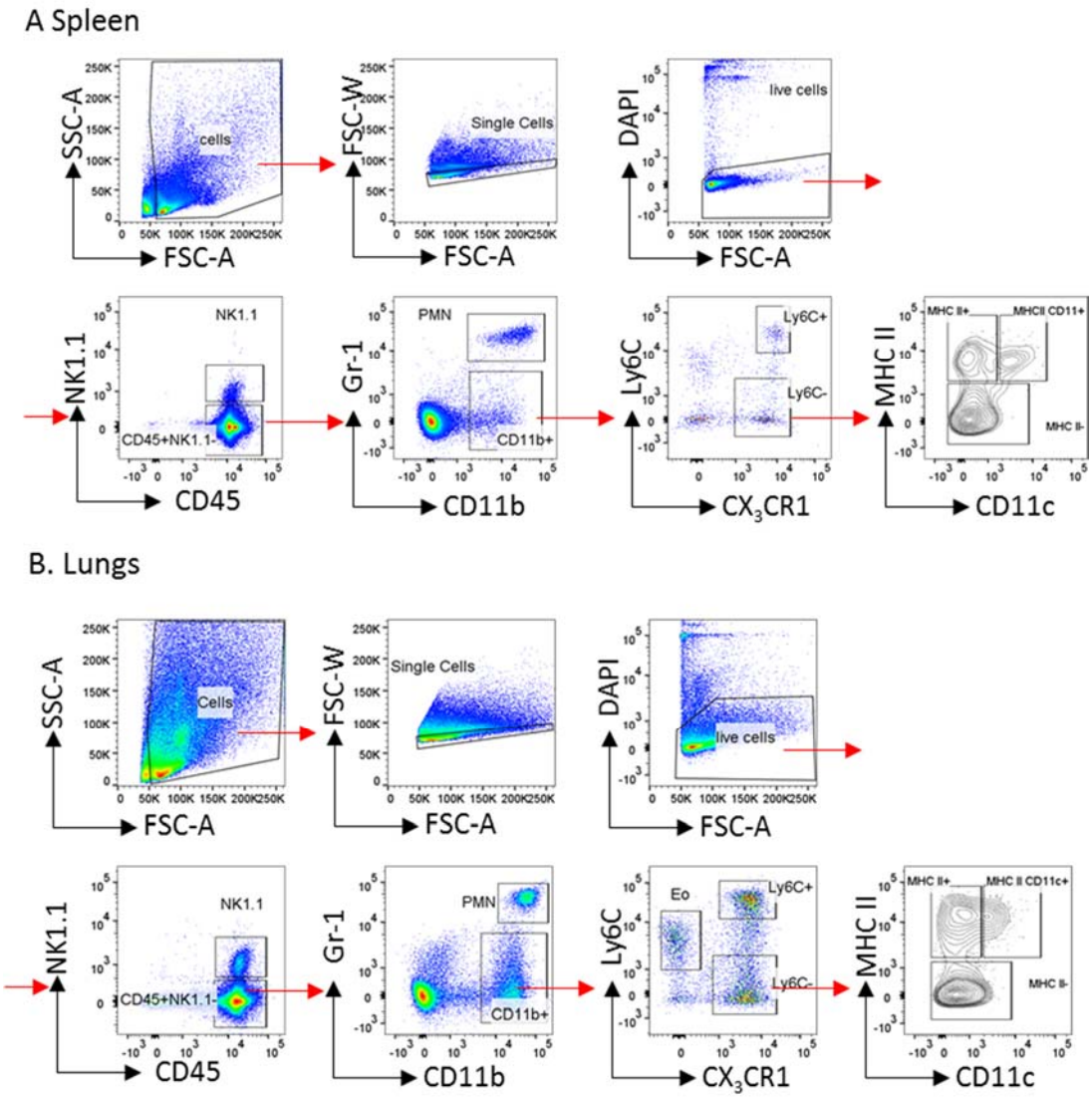

Figure 5.5 Gating strategy for identifying monocytes in murine lungs and spleen.
Single cell suspensions from the lungs and spleen were isolated as described in the Materials and Methods and red blood cells removed by RBC lysis. Cells were stained and acquired as in Figure 5.2. The representative plots show gating strategy for identifying monocytes in the spleen (A) and lungs (B). Leukocytes were gated based on FSC-A and SSC-A, doublets were gated out using FSC-W and FSC-A and live cells were identified as DAPI negative cells. Live cells were than analysed for expression of CD45 and NK1.1. $CD45^{+ve}NK1.1^{-ve}$ were gated and further analysed for Gr-1 and CD11b expression. PMN neutrophils were identified as $Gr1^{high}CD11b^{high}$. The remaining $CD11b^{+ve}$ cells were subsequently analysed to identify $Ly6C^{+ve}CX3CR1^{+ve}$ and $Ly6C^{-ve}CX3CR1^{+ve}$ cells. MHC II^{-ve}, MHC $II^{+ve}CD11c^{-ve}$ and MHC $II^{+ve}CD11c^{+ve}$ populations were identified within the $Ly6C^{-ve}CX3CR1^{+ve}$ cells.

ABIN1[D485N] mice develop splenomegaly and autoantibodies when they are 3-4 months old (Nanda et al., 2011). To characterise the monocyte populations and how the change in their numbers correlates with disease progression and spleen enlargement, WT and ABIN1[D485N] mice were analysed at 4, 8, 16 and 22 weeks of age using the above described staining panel. While there was no difference in

spleen size in the 4 and 8 week old WT and ABIN1[D485N] mice, 16 and 22 week old ABIN1[D485N] mice had more than 3 fold bigger spleens in comparison to WT mice (Figure 5.6).

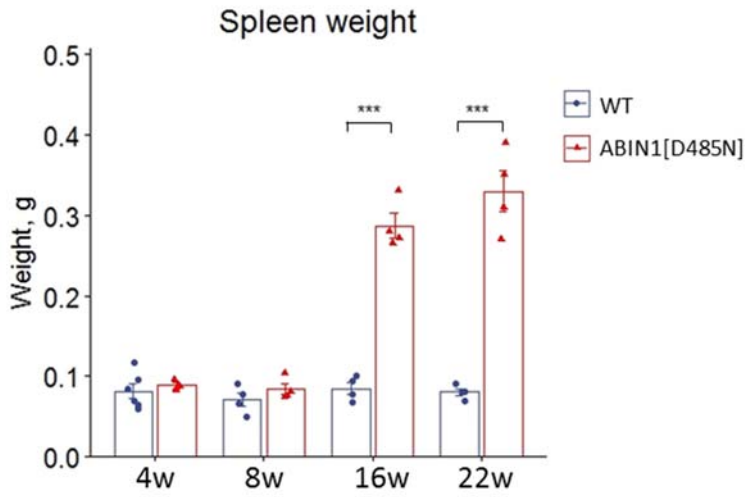

Figure 5.6 Increased spleen size in ABIN1[D485N] mice.
The plot represents spleen weights of 4, 8, 16 and 22 week old WT and ABIN1[D485N] mice. Symbols indicate individual mice. Significance between the two genotypes was calculated by two-way ANOVA and Tukey HSD as posthoc test; *** denotes $p<0.001$. Error bars represent ± standard error of the mean.

Analysis of the blood of WT and ABIN1[D485N] mice showed a massive increase in $CD115^{+ve}CD11b^{+ve}$ monocytes in ABIN1[D485N] mice by 22 weeks of age (Figure 5.7). A more detailed analysis showed that difference between the inflammatory $Ly6C^{+ve}$ monocytes in WT and ABIN1[D485N] was observed only in the 22 week old animals (Figure 5.7B). In contrast, a higher percentage of $CD115^{+ve}CD11b^{+ve}Ly6C^{-ve}CX_3CR1^{+ve}MHCII^{-ve}$ patrolling monocytes was found even in the 4 week old ABIN1 knock in mice. Moreover, in the 16 and 22 week old ABIN1[D485N] mice the patrolling monocytes were representing more than 30% of all blood leukocytes, whereas in WT animals patrolling monocytes were only around 3%.

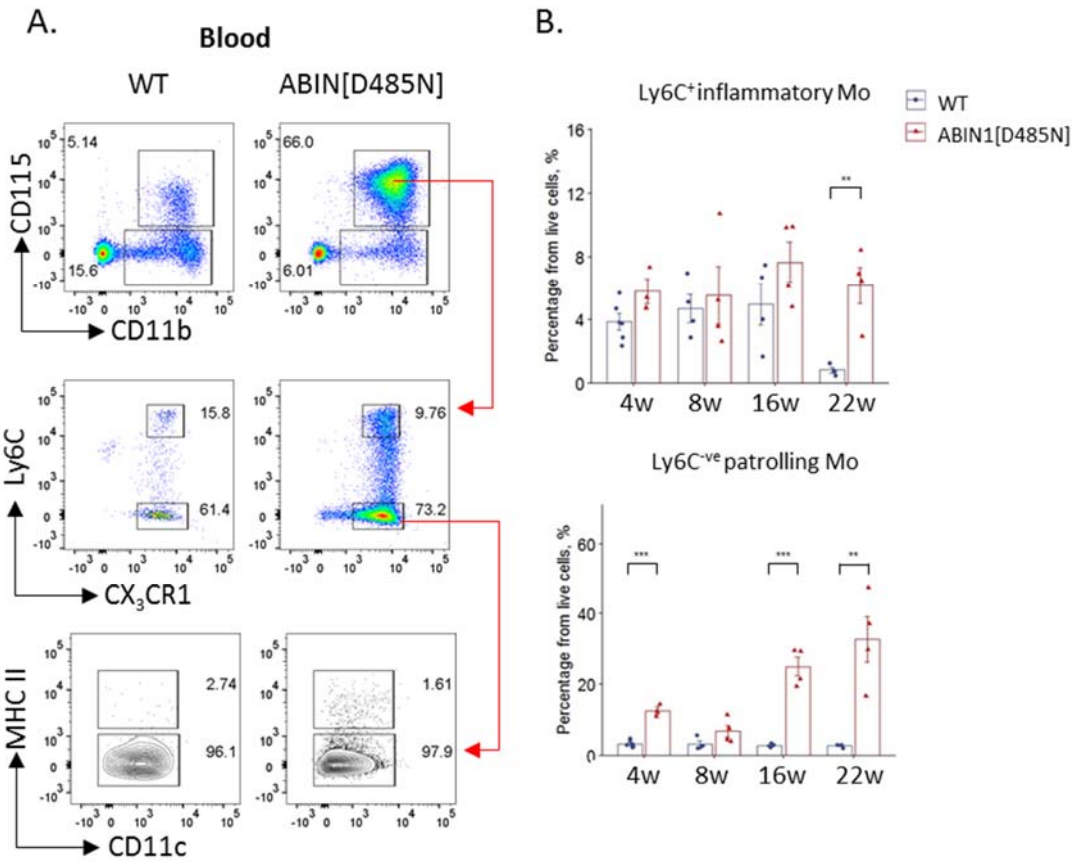

Figure 5.7 Increase in patrolling monocytes in the blood of ABIN1[D485N] mice.
Blood leukocytes were isolated from 4, 8, 16 and 22 week old WT and ABIN1[D485] mice and stained with DAPI and with fluorophore conjugated antibodies against CD45 (BV510), CD115 (APC), CD11b (Pe/Cy7), Ly6C (FITC), CX_3CR1 (PE), MHC II (AlexaFluor700), CD11c (PE-Dazzle 594), Gr1 (PerCp/Cy5.5) and NK1.1 (APC/Cy7) and analysed on BD LSR Fortessa II. A. The representative FACS plots show monocytes in blood of 22 week old WT and ABIN1 mice. The first plots show the percentages of $CD115^{+ve}CD11b^{+ve}$ and $CD115^{-ve}CD11b^{+ve}$ populations from all live (DAPI negative) single cells. $CD115^{+ve}CD11b^{+ve}$ cells were further gated and analysed for expression of Ly6C and CX_3CR1. The final gates show the percentages of MHC II^{+ve} and MHC II^{-ve} cells within the $Ly6C^{-ve}CX3CR1^{+ve}$ population. B. Bar graphs show the percentages (relative to the total number of of $Ly6C^{+ve}$ inflammatory monocytes ($Ly6C^{+ve}CX3CR1^{+ve}$), $Ly6C^{-ve}$ patrolling monocytes ($Ly6C^{-ve}CX3CR1^{+ve}MHC\ II^{-ve}$) and $Ly6C^{-ve}CX3CR1^{+ve}MHC\ II^{+ve}$. Error bars show the average values ± SEM. Significance between genotypes was determined by two-way ANOVA and Tukey HSD as posthoc test; * denotes $p<0.05$, ** denotes $p<0.01$, and *** denotes $p<0.001$.

Major changes in the innate immune populations were also observed in the spleens of ABIN1 mice (Figure 5.8A and B). Both the inflammatory $Ly6C^{+ve}$ and the patrolling monocytes $Ly6C^{-ve}$ monocytes were increased in the 16 and 22 week old knock in animals. Similar to the blood, differences in the numbers of patrolling monocytes were apparent even in the 4 week old mice. The absolute numbers of both $CD45^{+}NK1.1^{-ve}CD11b^{+ve}Ly6C^{-ve}CX3CR1^{+ve}MHCII^{+ve}CD11c^{-ve}$ and the

$CD45^{+}NK1.1^{-ve}CD11b^{+ve}Ly6C^{-ve}CX3CR1^{+ve}$ $MHCII^{+ve}CD11c^{+ve}$ monocyte derived dendritic cells were also increased (Figure 5.8B). As previously reported (Nanda et al., 2011), the neutrophil population was also expanded in the spleens of ABIN1[D485N] mice (Figure 5.8B). Interestingly, ABIN1[D485N] neutrophils had lower expression of Gr-1 and SSC-A, suggesting that they have lower granularity and might represent low density gradient neutrophils, similar to those described in lupus patients (Figure 5.8C) (Villanueva et al., 2011).

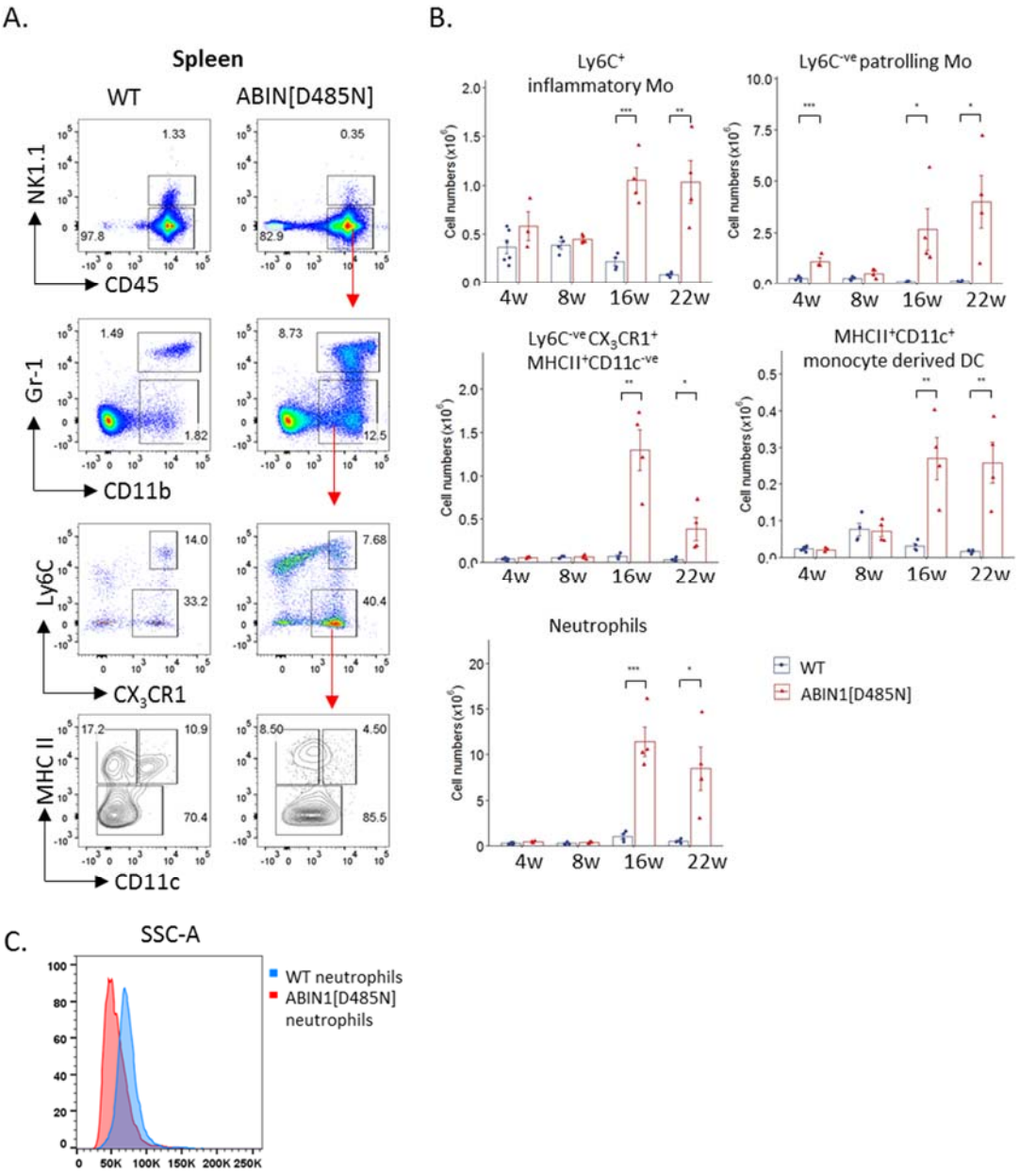

Figure 5.8 Characterisation of splenocytes in ABIN1[D485N] mice.
Splenocytes were isolated from 4, 8, 16 and 22 week old WT and ABIN1[D485] mice. Samples were stained and analysed as in Figure 5.5. A. Representative FACS plots showing the gating strategies for identifying immune cell populations in 22 week old WT and ABIN1 mice. B. Bar graphs show the absolute numbers of $Ly6C^{+ve}$ inflammatory ($CD45^{+}NK1.1^{-ve}CD11b^{+ve}Ly6C^{+ve}CX3CR1^{+ve}$), $Ly6C^{-ve}$ patrolling monocytes ($CD45^{+}NK1.1^{-ve}CD11b^{+ve}Ly6C^{-ve}CX3CR1^{+ve}MHCII^{-veve}CD11c^{-ve}$), $CD45^{+}NK1.1^{-ve}CD11b^{+ve}Ly6C^{-ve}CX3CR1^{+ve}MHCII^{+ve}CD11c^{-ve}$ and $CD45^{+}NK1.1^{-ve}CD11b^{+ve}Ly6C^{-ve}CX3CR1^{+ve}MHCII^{+ve}$ $CD11c^{+ve}$ populations C. Absolute numbers of neutrophils ($CD45^{+}NK1.1^{-ve}CD11b^{+ve}Gr1^{+ve}$ cells) in the spleens of WT and ABIN1[D485] mice. Error bars show the average values ± SEM. Symbols represent data from individual mice. Significance between genotypes was determined by two-way ANOVA and Tukey HSD as posthoc test; *denotes $p<0.05$, ** $p<0.01$, and *** denotes $p<0.001$. E. Representative histogram showing SSC-A in WT and ABIN1 [D485N] neutrophil gate ($CD45^{+ve}NK1.1^{-}CD11b^{+ve}Gr\text{-}1^{high}$).

In the lungs, no difference in the inflammatory monocytes between WT and ABIN1[D485N] mice was observed by 22 weeks of age, however the patrolling monocytes were significantly increased in the 16 and 22 week old ABIN1[D485N] mice (Figure 5.9B). The 16 week old knock in mice had also higher numbers of $CD45^{+}NK1.1^{-ve}CD11b^{+ve}Ly6C^{-ve}CX3CR1^{+ve}MHCII^{+ve}CD11c^{-ve}$ cells and $CD45^{+}NK1.1^{-ve}CD11b^{+ve}Ly6C^{-ve}CX3CR1^{+ve}MHCII^{+ve}CD11c^{+ve}$ monocyte derived dendritic cells. In contrast to spleen, the neutrophils in the lungs of ABIN1[D485N] had normal Gr1 expression, normal SSC-A (data not shown) and no significant difference in neutrophil numbers were found when compared to WT (Figure 5.9B).

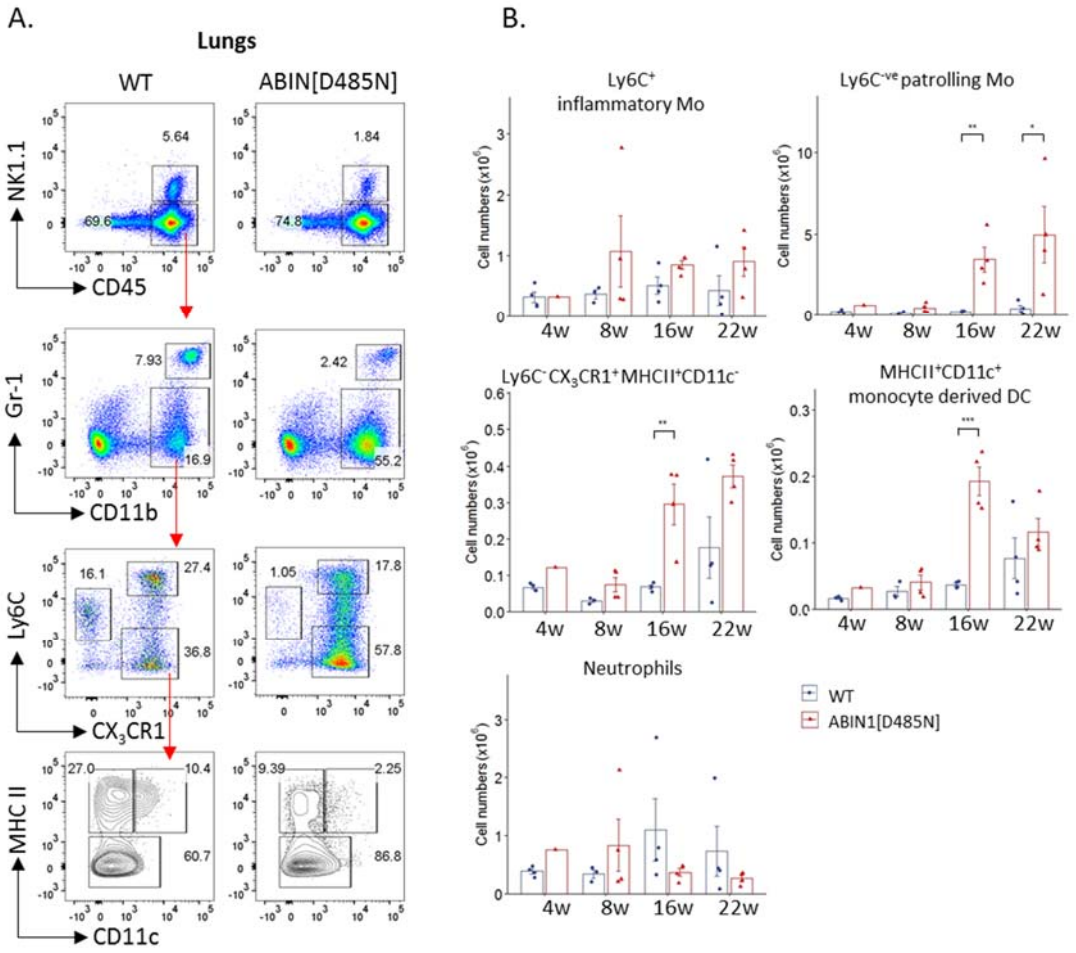

Figure 5.9 Characterisation of lung cells in ABIN1[D485N] mice.
Cells were isolated from lungs of 4, 8, 16 and 22 week old WT and ABIN1[D485] mice were stained and analysed as in Figure 5.5B. A. Representative FACS plots showing the gating strategies for identifying immune cell populations in the lungs of 22 weeks old WT and ABIN1 mice. B. Bar graphs show the absolute numbers of $Ly6C^{+ve}$ inflammatory and $Ly6C^{-ve}$ patrolling monocytes, $CD45^{+}NK1.1^{-ve}CD11b^{+ve}Ly6C^{-ve}CX3CR1^{+ve}MHCII^{+ve}CD11c^{-ve}$ cells and the monocyte derived dendritic cells. Error bars show the average values ± SEM. Significance between genotypes was determined by two-way ANOVA and Tukey HSD as posthoc test;* denotes $p<0.05$, ** denotes $p<0.01$, and *** denotes $p<0.001$.

Substantial changes in the immune cells were also found in the kidneys of 22-week old ABIN1[D485N] mice (Figure 5.10). Interestingly, staining for $CD11b^{+ve}$ cells showed that in the kidneys of WT mice there is a population of $CD11b^{+ve}$ intermediate expressing cells. This population was almost absent in the knock in mice, where most of the CD11b positive cells appeared to express high levels of CD11b (Figure 5.10A). Further characterisation of the $CD11b^{+ve}$ cells revealed that the $CD11b^{inter}$ cells in the WT mice were mostly $Ly6C^{-ve}CX_3CR1^{+ve}MHCII^{+ve}CD11c^{+ve}$ monocyte derived dendritic cells (moDC). The percentages of the moDC in the ABIN[D485N] mice were reduced (Figure 5.10A) in contrast to the patrolling

monocytes, which were more than 10 times higher than those in the WT mice (Figure 5.10B).

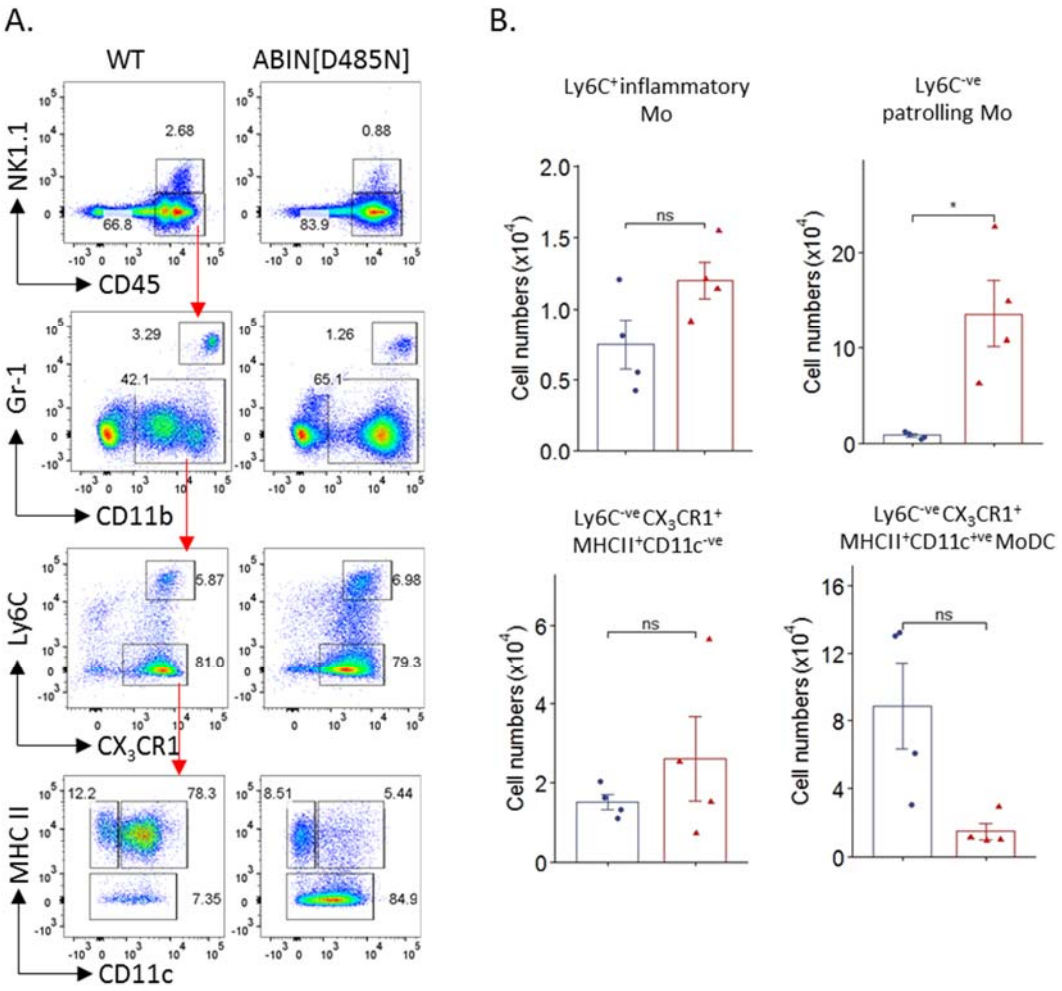

Figure 5.10 Characterisation of kidney cells in ABIN1[D485N] mice.
Cells isolated from the kidneys of 22 week old WT and ABIN1[D485] mice were stained described above. A. The representative FACS plots are showing the gating strategies used for identifying immune cell populations in the kidneys. B. Bar graphs show the absolute numbers of $Ly6C^{+ve}$ inflammatory and $Ly6C^{-ve}$ patrolling monocytes, $CD45^{+ve}NK1.1^{-ve}CD11b^{+ve}Ly6C^{-ve}CX3CR1^{+ve}MHCII^{+ve}CD11c^{-ve}$ cells and monocyte-derived dendritic cells. Error bars show the average values ± SEM. Significance between genotypes was calculated by unpaired Student's t-test; * denotes $p<0.05$

.

5.2.2. The autoimmunity in ABIN1[D485N] mice is a result of defect in the hematopoietic cells.

ABIN1[D485N] knock in mice display aberrant phenotype in multiple immune cell populations, with a more than 10-fold increase in patrolling monocytes. However, it has not been demonstrated if the autoimmune pathology in the ABIN1[D485N] mice is a result from a primary defect in immune cells or non-immune cells. To address this question, we carried out a bone marrow chimera experiment. CD45.1 WT host mice were lethally irradiated and split into control group engrafted with CD45.2 WT bone marrow cells (BM) and experimental group that received CD45.2 ABIN1[D485N] and CD45.1 WT bone marrow cells mixed in a 1:1 ratio. Mice were sacrificed 4 months after the adoptive transfer and tissues were analysed (Figure 5.11). Initially experiments were carried out by reconstituting WT host animals only with ABIN1 BM cells, however reconstitution with ABIN1 cells in combination with the irradiation was not well tolerated and the mice developed skin inflammation similar to psoriasis before appearance of the lupus phenotype (data not shown).

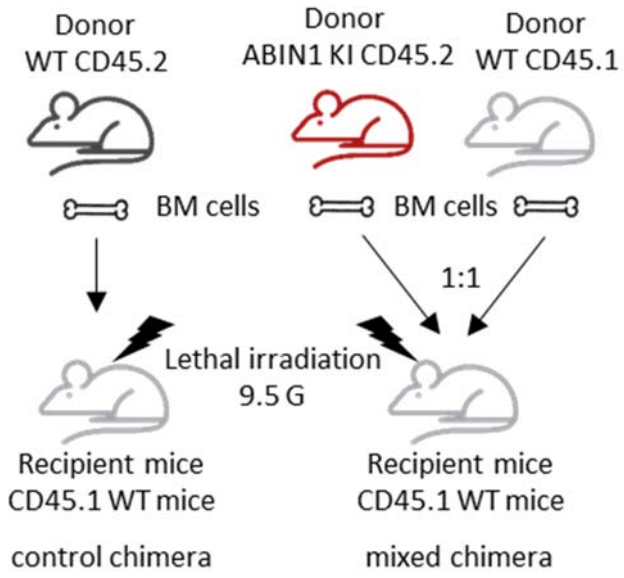

Figure 5.11 Bone marrow chimera experimental design.
Female and male CD45.1 WT (120 days old) mice were lethally irradiated with 9.5 Gy and reconstituted 24 hours after the irradiation with $2.5x10^6$ bone marrow cells from either CD45.2 WT mice (control chimera) or cells isolated from CD45.1 WT mice and CD45.2 ABIN1[D485N] mixed in 1:1 ratio (mixed chimera). Donor and recipients were gender matched. The mice were culled 4 month after the irradiation.

The mice that received the mixed ABIN1[D485N] and WT bone marrow had multiple autoimmunity hallmarks observed in the ABIN1[D485N] knock in mice including splenomegaly, increased anti-nuclear antibodies (ANA) and germinal centre B cells (Figure 5.12). The monocyte populations were also significantly increased in comparison to the control group (Figure 5.13). Taken together, these data indicated that the autoimmunity in the ABIN1[D485N] mice is a result of mutation in ABIN1 in hematopoietic cells and not in non-immune cells. To address the question if the increase in the monocytes is a result of a cell intrinsic defect, the $Ly6C^{+ve}$ inflammatory and $Ly6C^{-ve}$ patrolling monocytes were analysed for expression of CD45.1 (WT cells) and CD45.2 (ABIN1[D485N] cells). In 5 out of 7 mice that received mixed CD45.2 ABIN1[D485N] and CD45.1 WT bone marrow cells, the proportion of CD45.2 cells was higher in both types of monocytes. However, in two of the mice the monocytes were predominantly $CD45.1^{+ve}$ from WT origin, suggesting the environment could also influence the increase of monocytes and is not completely restricted to the lack of ABIN1 ubiquitin binding function in the monocytes.

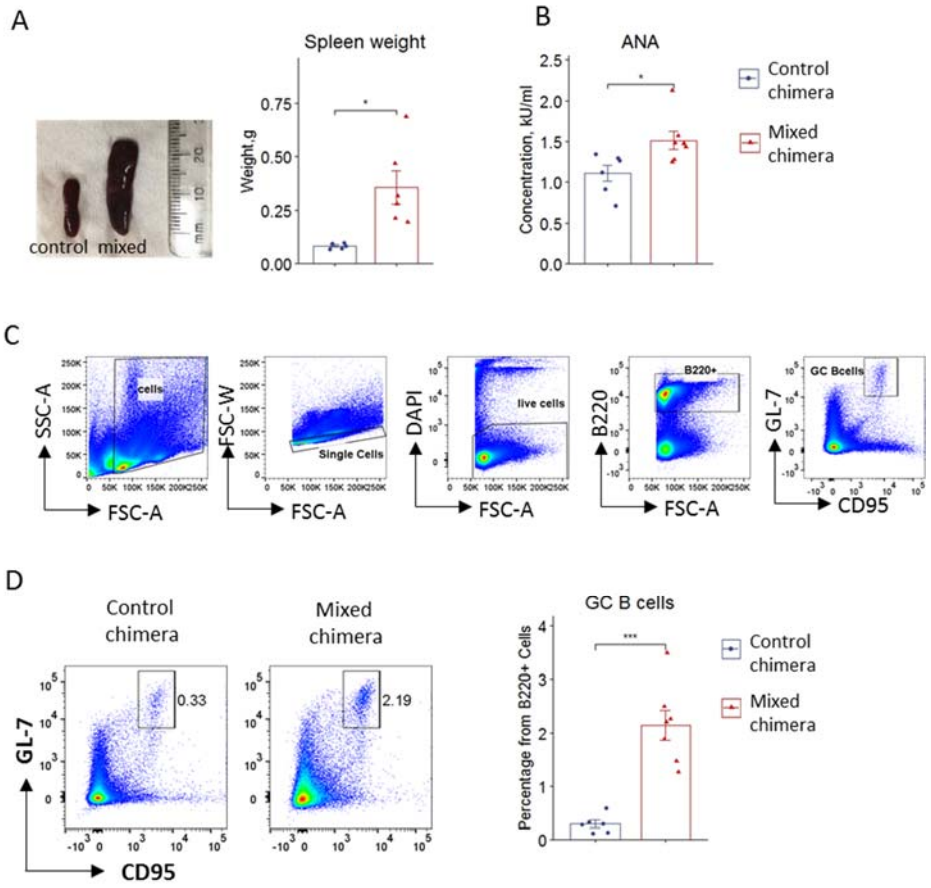

Figure 5.12 Autoimmunity in ABIN1[D485N] mice is due to a defect in immune cells. Mice were treated as described in Figure 5.11 A. Representative image showing spleen size. The bar graph shows average values of the spleen weights. B. Total antinuclear antibodies (ANA) in the serum were measured by ELISA and plots show average values ±SEM. C. Splenocytes were stained with DAPI, anti-B220(APC), anti-CD95(PE) and anti-GL-7(FITC) antibodies and analysed on BD FACSCanto. Doublets and dead cells were gated out. The FACS plots represent the gating strategy used for identifying germinal centre B cells. D. The representative plots show percentage of $CD95^{+ve}GL\text{-}7^{+ve}$ germinal centre B cells from the $B220^{+ve}$ population. The bar graph show average values of GCB cell percentages. Error bars reperesent standard error of the mean. Significance between the two groups was calculated using unpaired Student's t-test. * denotes $p<0.05$ and *** denotes $p<0.001$.

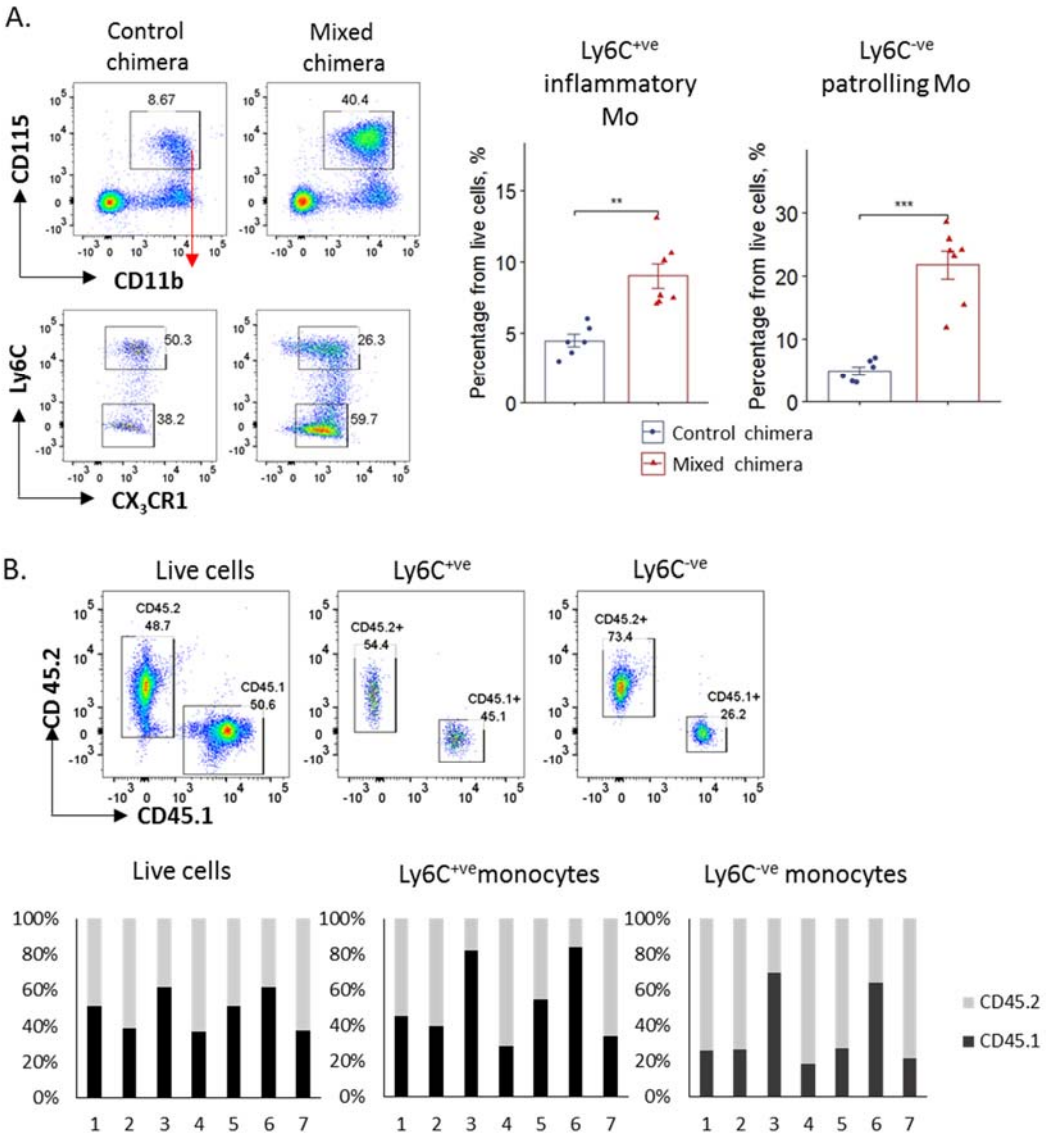

Figure 5.13 Adoptive transfer of ABIN1[D485N] bone marrow cells into WT mice leads to increase in the monocytes.

Mice were treated as described in Figure 5.11. A. Representative flow cytometry plots show the percentage of $CD115^{+ve}CD11b^{+ve}$ cells from DAPI negative single cells and the percentages of $Ly6C^{+ve}CX_3CR1^{+ve}$ and $Ly6C^{-ve}CX_3CR1^{+ve}$ from the $CD115^{+ve}CD11b^{+ve}$ gate. The bar graphs show the average of the percentages of $Ly6C^{+ve}CX_3CR1^{+ve}$ and $Ly6C^{-ve}CX_3CR1^{+ve}$ from all live cells. Symbols represent individual biological replicates Significance between the two groups was calculated using unpaired student's t-test. * denotes $p<0.05$ and *** denotes $p<0.001$. B. The representative plots show the proportion of CD45.1 and CD45.2 positive cells in the $DAPI^{-ve}$ live cell, $Ly6C^{+ve}CX_3CR1^{+ve}$ and $Ly6C^{-ve}CX_3CR1^{+ve}$ gates. The bar graphs show the percentages of CD45.1 and CD45.2 positive for each individual mouse engrafted with mixed CD45.1 WT and CD45.2 ABIN[D485N] bone marrow cells.

5.2.3. Loss of MyD88 or IRAK1 and IRAK4 kinase activity rescues the increase of the monocytes in ABIN1[D485N] mice

The ABIN1 ubiquitin binding function is required to limit responses downstream of TLRs in B cells and in myeloid cells. B cells and BMDCs isolated from ABIN1[D485N] mice have increased MAPK and NF-κB activation and higher cytokine production in response to either LPS (a ligand for TLR4) or R848 (a ligand for TLR7/8), suggesting that these pathways could contribute to the lupus-like phenotype (Nanda et al., 2011). Moreover, loss of components of the TLR signalling pathway such as the adaptor protein MyD88 or the IRAK1 and IRAK4 kinase activity leads to complete rescue of the splenomegaly, autoantibody production and kidney pathology in the ABIN1[D485N] mice (Nanda et al., 2011, Nanda et al., 2016). To understand if enhanced MyD88 signalling in the ABIN[D485N] mice is driving the massive increase in the monocytes, next I characterised the monocyte populations in ABIN1[D485N] x MyD88 KO, ABIN1[D485N] x IRAK1[D359A] and ABIN1[D485N] x IRAK4[D329A] KI mice. The increase in $Ly6C^{-ve}$ patrolling monocytes in blood, lungs and spleen was rescued in all three double mutant mice (Figure 5.14). Similarly, the increase in $Ly6C^{+ve}$ inflammatory monocytes in the blood was prevented. The $Ly6C^{+ve}$ inflammatory monocytes in the ABIN1[D485N] x IRAK4[D329A] mice were also significantly reduced in the lungs and spleens. Reduction in the $Ly6C^{+ve}$ monocytes in the spleen and lungs was observed also in the other two double mutants, however more replicates will be needed to determine the significance. In addition to the changes in the monocytes populations, the neutrophil numbers in the spleens of the ABIN1[D485N]xMyD88 KO, ABIN1[D485N]xIRAK1[D359A] and ABIN1[D485N]xIRAK4[D329A] KI mice were also significantly decreased in comparison to the ABIN1[D485N] mice. These data suggested that MyD88 signalling is important for the expansion of the monocytes populations in the ABIN1[D485N] mice and targeting this pathway could be beneficial in terms of developing therapies for SLE treatment.

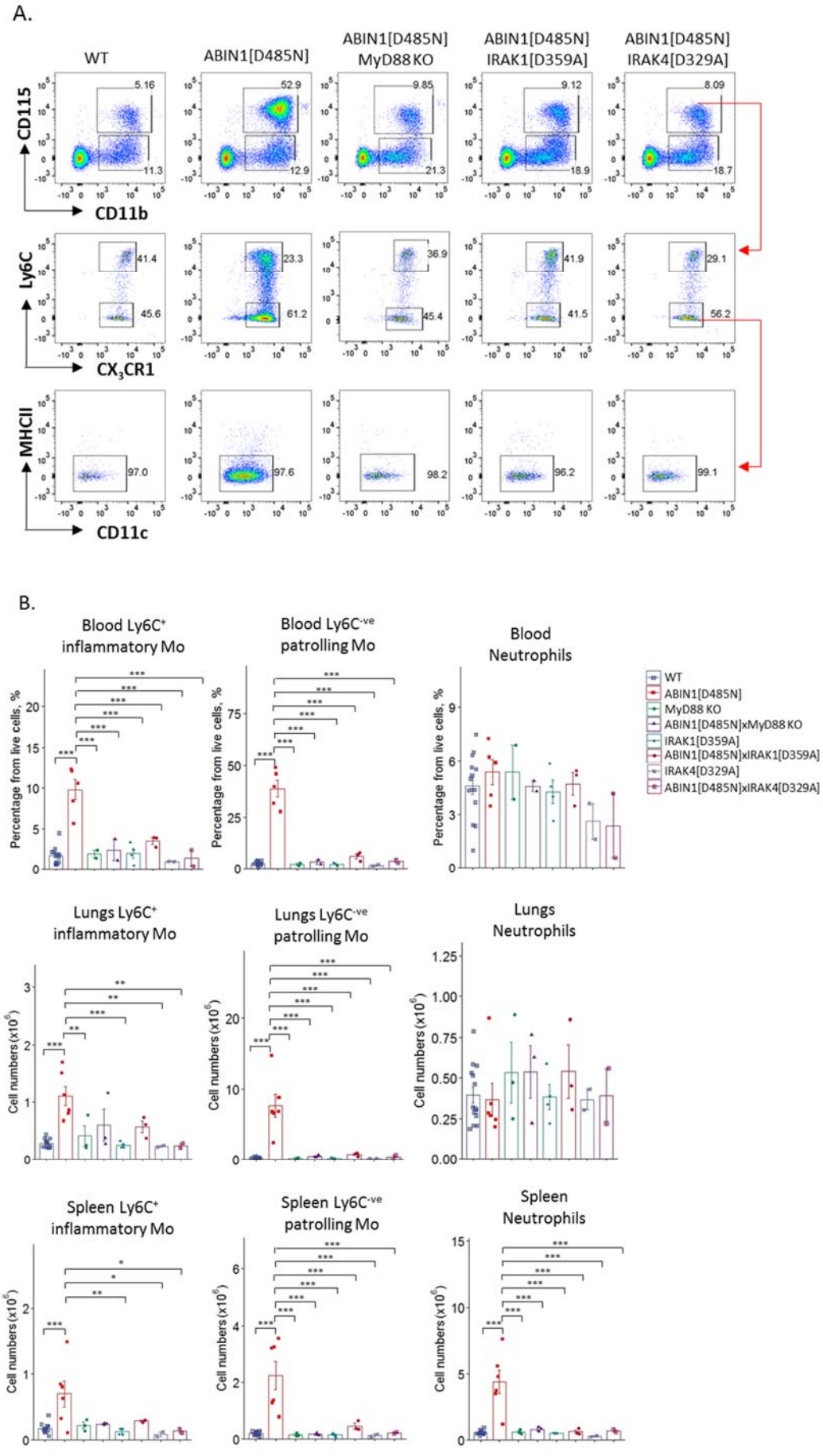
A.
WT
ABIN1[D485N]
ABIN1[D485N] MyD88 KO
ABIN1[D485N] IRAK1[D359A]
ABIN1[D485N] IRAK4[D329A]
CD115
CD11b
Ly6C
CX3CR1
MHCII
CD11c
5.16
11.3
52.9
12.9
9.85
21.3
9.12
18.9
8.09
18.7
41.4
45.6
23.3
61.2
36.9
45.4
41.9
41.5
29.1
56.2
97.0
97.6
98.2
96.2
99.1
B.
Blood Ly6C+ inflammatory Mo
Blood Ly6C-ve patrolling Mo
Blood Neutrophils
Lungs Ly6C+ inflammatory Mo
Lungs Ly6C-ve patrolling Mo
Lungs Neutrophils
Spleen Ly6C+ inflammatory Mo
Spleen Ly6C-ve patrolling Mo
Spleen Neutrophils
Percentage from live cells, %
Cell numbers (x10^6)
WT
ABIN1[D485N]
MyD88 KO
ABIN1[D485N]xMyD88 KO
IRAK1[D359A]
ABIN1[D485N]xIRAK1[D359A]
IRAK4[D329A]
ABIN1[D485N]xIRAK4[D329A]

Figure 5.14 Increase in the monocytes is prevented in ABIN1[D485N] crossed to MyD88 knock out mice or kinase-inactive mutants of IRAK1 and IRAK4.
Blood leukocytes and single cell suspensions from the lungs and spleens of 4 month old WT, ABIN1[D485N], MyD88 KO, ABIN1[D485N]xMyD88 KO, IRAK1[D359A], IRAK4[D329A] ABIN1[D485N]xIRAK1[D359A] and ABIN1[D485N]xIRAK4[D329A] mice were stained as described in Figure 5.4 and 5.5 and analysed on BD LSR Fortessa II. A. The representative plots are showing percentages $CD115^{+ve}CD11b^{+ve}$ and $CD115^{-ve}CD11b^{+ve}$ populations from live (DAPI negative) single cells. $CD115^{+ve}CD11b^{+ve}$ cells were further gated and analysed for expression of Ly6C and CX_3CR1. Inflammatory monocytes were defined as $CD115^{+ve}CD11b^{+ve}Ly6C^{+ve}CX_3CR1^{+ve}$. The $CD115^{+ve}CD11b^{+ve}Ly6C^{-ve}CX_3CR1^{+ve}$ were further analysed for expression of MHC II. Patrolling monocytes were defined as $CD115^{+ve}CD11b^{+ve}Ly6C^{-ve}CX_3CR1^{+ve}MHCII^{-}$. B. Bar graphs show the average value (±SEM) of percentages of $Ly6C^{+ve}$ inflammatory monocytes, $Ly6C^{-ve}$ patrolling monocytes and the neutrophils ($CD115^{-ve}CD11b^{+ve}Gr\text{-}1^{high}$) from the live cell gate in the blood and total numbers of $Ly6C^{+ve}$ inflammatory monocytes, $Ly6C^{-ve}$ patrolling monocytesand neutrophils in the lungs and spleen. Symbols represent individual biological replicates. Statistical significance between genotypes was calculated using one-way ANOVA and Tukey HSD. * $p<0.05$, ** $p<0.01$ and *** denotes $p<0.001$.

To further elucidate the therapeutic potential of inhibition of IRAK4, next we fed 6 week old ABIN1[D485N] mice with chow diet containing the IRAK4 inhibitor PF-06426779. The inhibition of IRAK4 led to a rescue of the splenomegaly in the ABIN1[D485N] mice (Figure 5.15A). The percentage of germinal centre B cells in the spleen also appeared to be reduced, although not significant with the numbers of animals analysed (Figure 5.15B). Blood samples were collected at the beginning of the study, at 5 weeks and in the end of the study (10 weeks) to monitor changes in the monocyte populations. Flow cytometry analysis showed that an increase in the patrolling monocytes was detected in the ABIN[D485N] animals even at the start of the study when the mice were 6 weeks old (Figure 5.16A). Whereas the patrolling monocytes continue to increase in the ABIN1[D485N] on normal chow diet, the ABIN1[D485N] mice fed with IRAK4 inhibitor containing diet had a significantly lower percentage of monocytes at the end of the study. Moreover, IRAK4 inhibition prevented the increase in the patrolling monocytes also in the lungs and spleen (Figure 5.16B). Taken together, we have demonstrated that IRAK4 inhibition reduces the lupus like autoimmunity in ABIN1[D485N] mice.

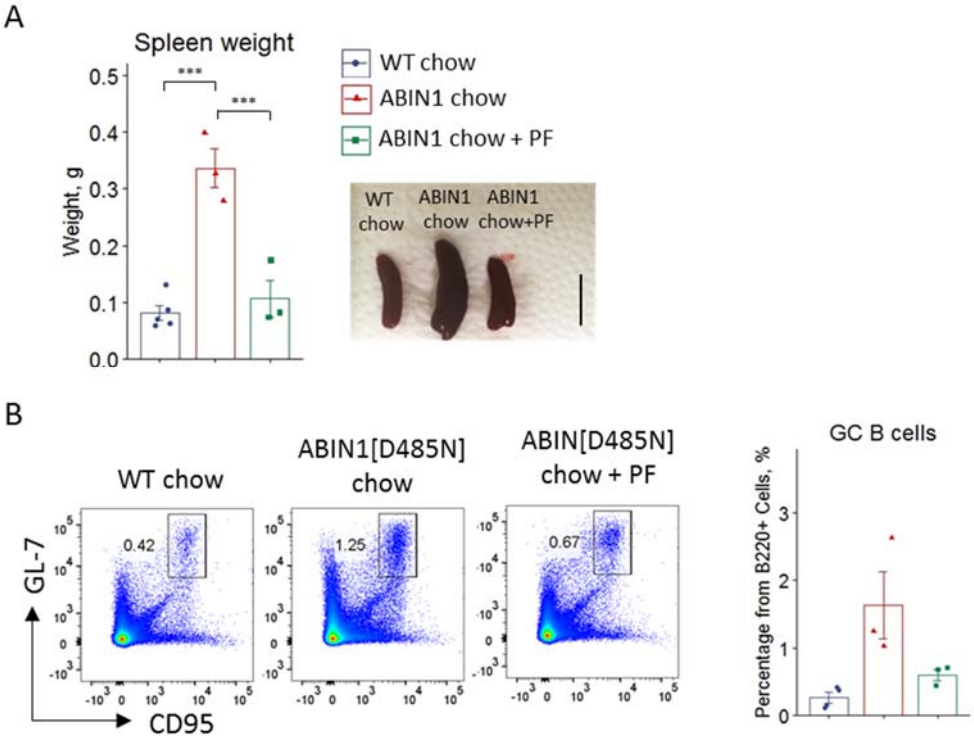

Figure 5.15 Pharmacological inhibition of IRAK4 prevents autoimmunity development in ABIN1[D485N] mice.
6 week old ABIN[D485N] mice were given either normal chow or chow containing 1000mpk PF-06426779 (IRAK4 inhibitor). Mice were culled 10 weeks after the start of the study. A. The bar graph show average values of the spleen weights ±SEM and the right image shows spleen enlargement, bar equals 1 cm. B. The representative plots show the percentage of splenic $CD95^{+ve}GL\text{-}7^{+ve}$ germinal centre B cells from the $B220^{+ve}$ population. Statistical significance between groups was calculated using one-way ANOVA and Tukey HSD. *** denotes $p<0.001$.

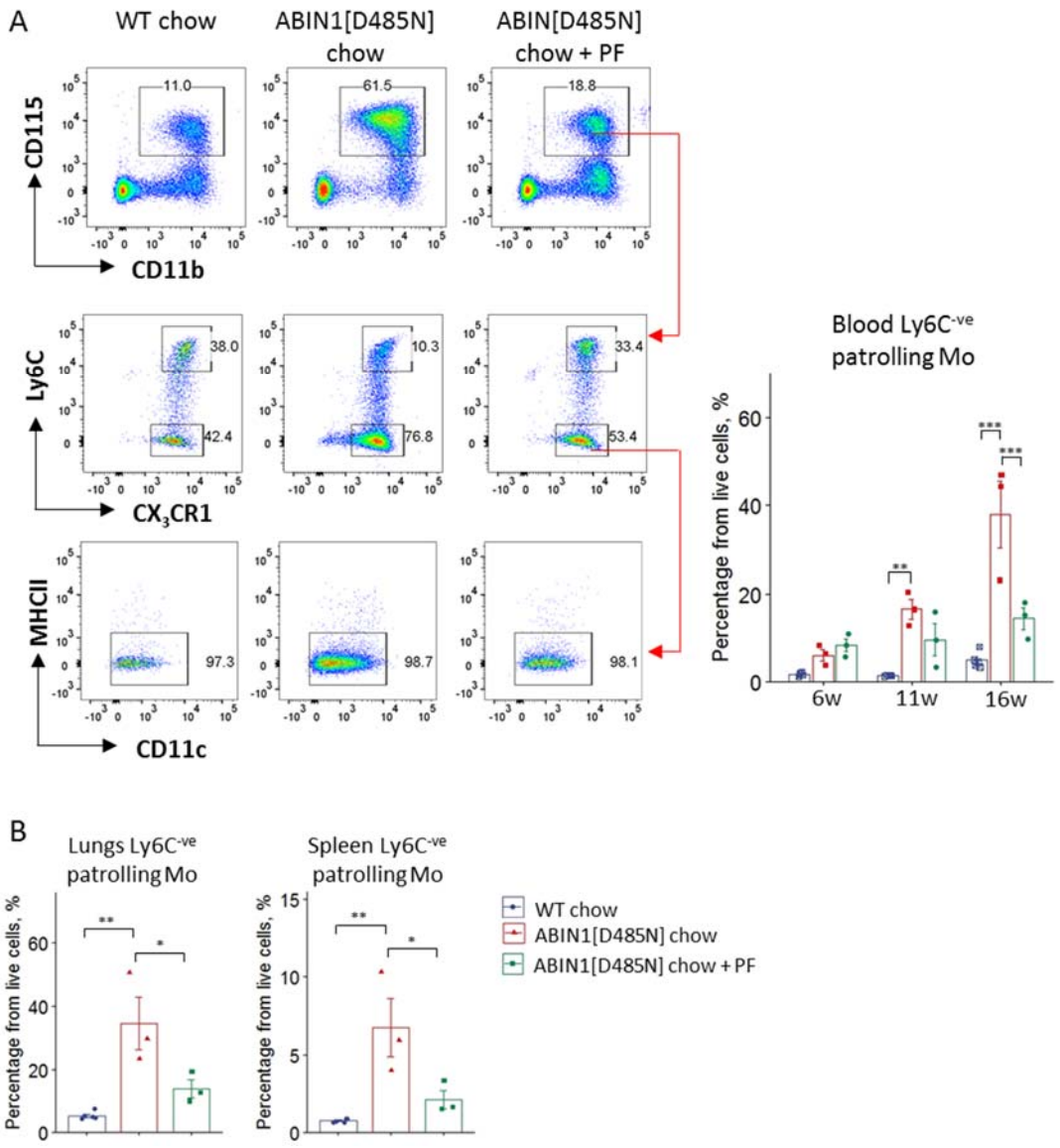

Figure 5.16 Pharmacological inhibition of IRAK4 rescues increase in the monocytes in ABIN1[D485N] mice.

Mice were treated as in previous figure. Blood samples were collected at 6, 11 and 16 week via tail vein or cardiac puncture and analysed for changes in the monocyte populations. Flow cytometry analysis was done as described above (Figure 5.4 and 5.5). A. Representative flow cytometry plots show changes in the $CD115^{+ve}CD11b^{+ve}$, $CD115^{+ve}CD11b^{+ve}Ly6C^{+ve}CX_3CR1^{+ve}$ and $CD115^{+ve}CD11b^{+ve}Ly6C^{-ve}CX_3CR1^{+ve}$ populations in 16 week old animals. The bar graph represents average values of the $Ly6C^{-ve}$ patrolling monocytes percentages from the live cells gate in 6, 11 and 16 weeks old animals. Significance was calculated by two-way ANOVA followed by Tukey HSD. B. Bar graphs show changes in the $Ly6C^{-ve}$ patrolling monocytes in the lungs and spleen. Significance was calculated by one-way ANOVA followed by Tukey HSD. Error bars represent ±SEM. * $p<0.05$, ** $p<0.01$ and *** denotes $p<0.001$. Tail bleeds and welfare monitoring was done by Dr. Sambit Nanda.

5.2.4. Investigating the role of TLR7 in the SLE development in ABIN1[D485N] mice.

All TLR receptors except TLR3 require MyD88 adaptor protein for mediating downstream signalling (Kawai and Akira, 2011). Among the TLR receptors, the nucleic acid sensing TLR7 and 9 have been linked to human SLE (Celhar and Fairhurst, 2014). Enhanced expression of TLR7 has been found in a Mexican population with SLE (Garcia-Ortiz et al., 2010). TLR7 overexpression in mice also leads to lupus like autoimmunity development (Deane et al., 2007). Analysis of the inflammatory and the patrolling monocytes in blood, lungs and spleens of ABIN1[D485N] x TLR7 KO mice showed significant reduction when compared to ABIN1[D485N] mice, suggesting that TLR7 signalling has a critical role in driving the autoimmune responses in the knock in mice (Figure 5.17). In addition, crossing of the ABIN1[D485N] mice to TLR7 KO mice led to a significant reduction in the splenomegaly, as well as reduction of in the numbers of germinal centre B cells. The expansion of germinal centre B cells requires help from a specialised Th subset referred to as T follicular helper (T_{fh}) cells. Numbers of T_{fh} cells were increased in the spleens of ABIN1[D485] and this was rescued in TLR7 KO crosses (Figure 5.18).

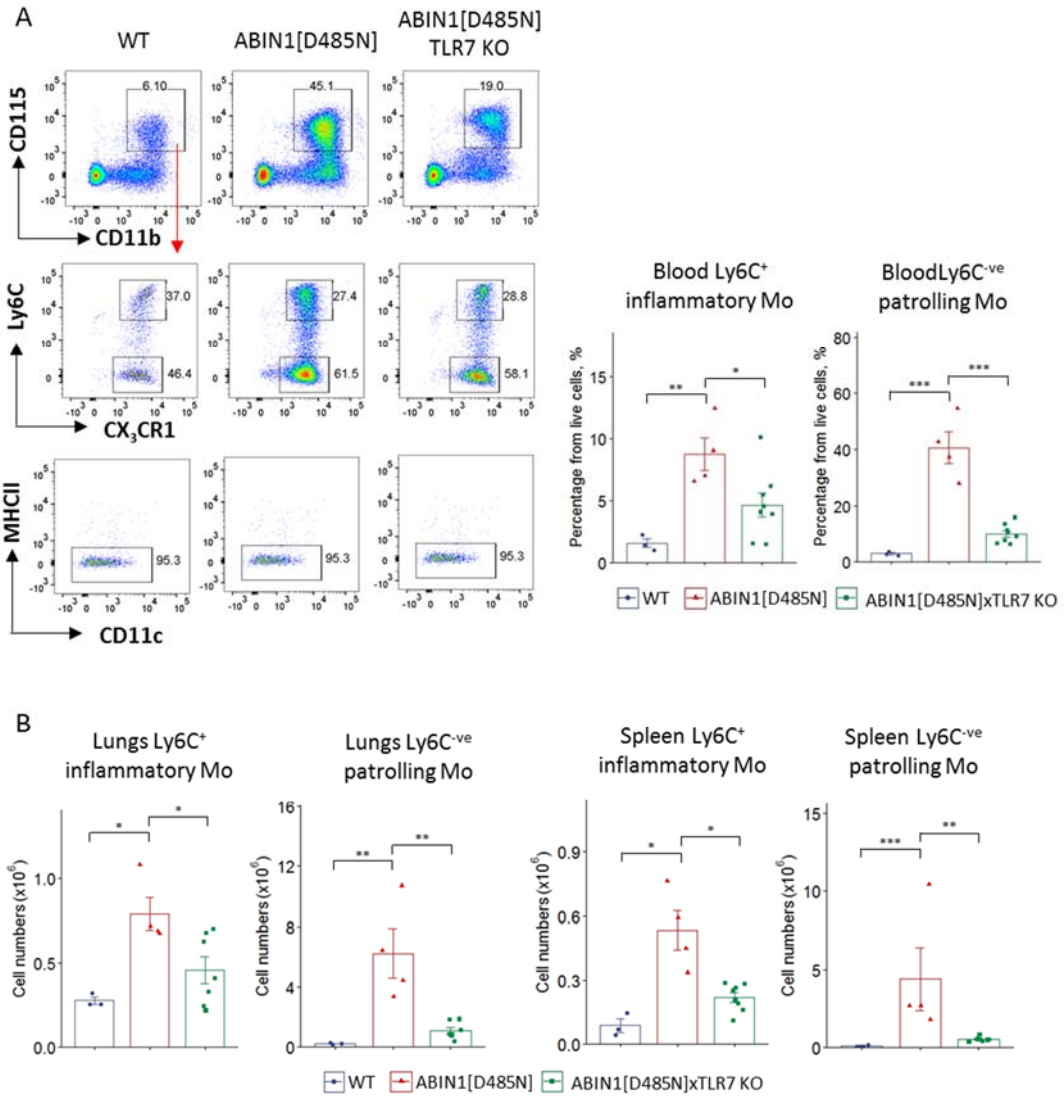

Figure 5.17 Characterisation of monocyte populations in ABIN1[D485N]xTLR7 KO mice.

Blood, lungs and spleens of 4 month old WT, ABIN1[D485N] and ABIN[D485N]xTLR7 KO mice were analysed for changes in the monocytes. A. The flow cytometry plots show changes in the $CD115^{+ve}CD11b^{+ve}$, $CD115^{+ve}CD11b^{+ve}Ly6C^{+ve}CX_3CR1^{+ve}$ and $CD115^{+ve}CD11b^{+ve}Ly6C^{-ve}CX_3CR1^{+ve}$ populations in the blood. The bar graph represents average values of the percentage of $Ly6C^{+ve}$ inflammatory and $Ly6C^{-ve}$ patrolling monocytes from all live cells. B. Same as A, except bar graphs show total numbers of $Ly6C^{+ve}$ inflammatory monocytes and $Ly6C^{-ve}$ patrolling in lungs and spleen. Symbols represent individual biological replicates. Statistical significance between genotypes was calculated using one-way ANOVA followed by Tukey HSD. * $p<0.05$, **$p<0.01$ and *** $p<0.001$.

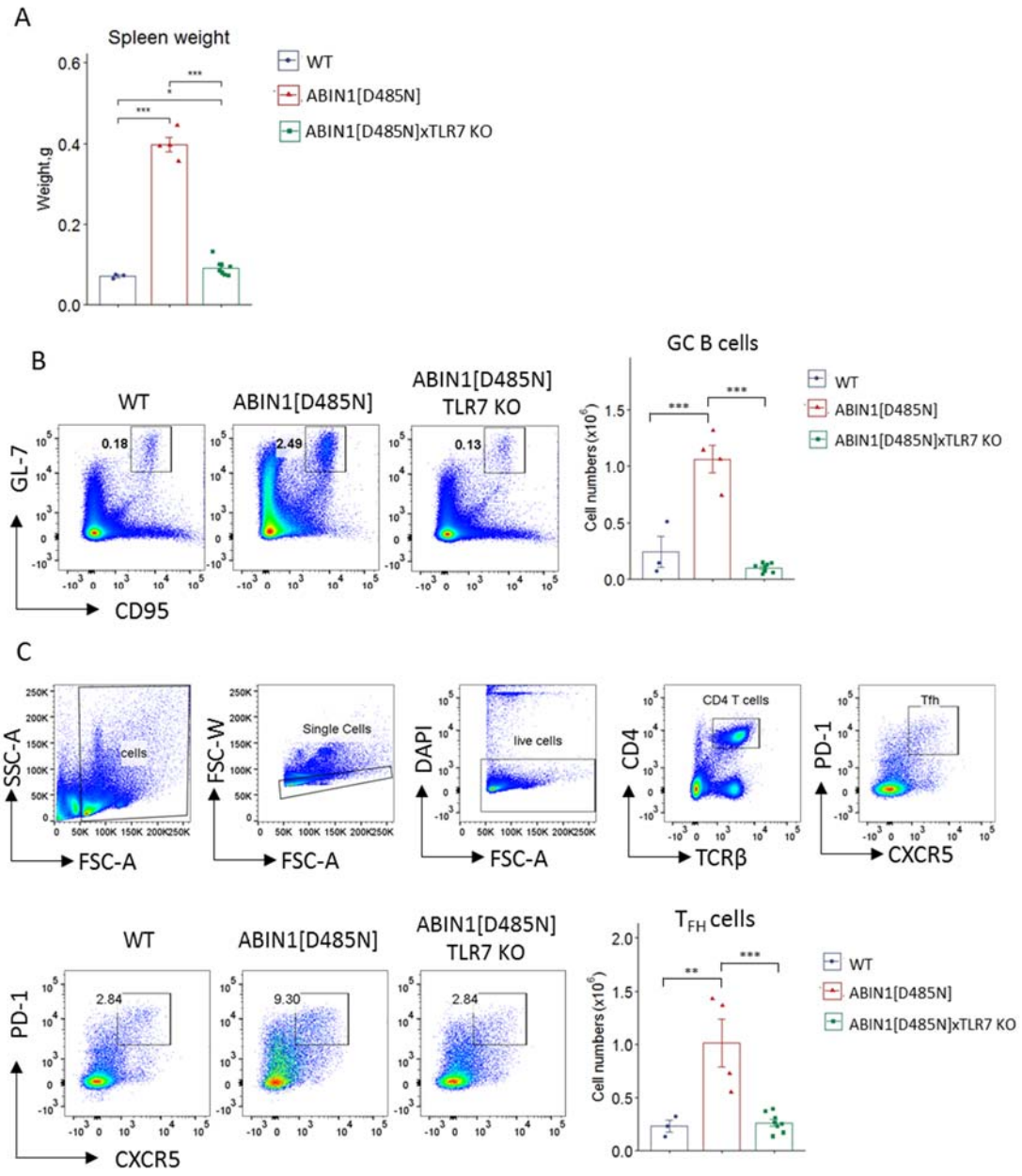

Figure 5.18 Characterisation of ABIN1[D485N]xTLR7 KO mice.
A. Average values of spleen weights of 4 month old WT, ABIN1[D485N] and ABIN1[D485N]xTLR7 KO mice B. The representative flow cytometry plots show the percentage of splenic $CD95^{+ve}GL\text{-}7^{+ve}$ germinal centre B cells from the $B220^{+ve}$ population. The bar graph show the average value of the absolute numbers of the germinal centre B cells in the spleens. C. Splenocytes were stained with DAPI, anti-CD4 (PerCP/Cy5.5), anti-TCR-β(FITC), anti-PD-1 (BV421) and anti-CXCR5(APC) to describe T follicular helper cells (T_{FH}). Flow cytometry plots show the gating strategy used for identifying T_{FH}. D. Plots show percentage of $PD\text{-}1^{+ve}CXCR5^{+ve}$ cells from the $TCR\text{-}\beta^{+ve}CD4^{+ve}$ gate and bar graph show total number of T_{FH} cells in the spleen. Statistical significance between genotypes was calculated using one-way ANOVA and Tukey HSD. * $p<0.05$, ** $p<0.01$ and *** denotes $p<0.001$.

To address the question if monocytes respond to TLR7 stimulation, I next stimulated flow cytometry sorted $Ly6C^{+ve}$ inflammatory monocytes

(DAPI^{-ve}CD45^{+ve}NK1.1^{-ve}CD11b^{+ve}Ly6C^{high}CX3CR1^{+ve}CD115^{+ve}) from spleens of WT and ABIN[D485N] mice with the TLR7 agonist R837 (imiquimod) and measured cytokine production by multiplex cytokine assay. The ABIN1[D485N] inflammatory monocytes had significantly higher production of TNF-α and MIP-β following 6 hours stimulation with TLR7 than WT monocytes (Figure 5.19). The production of IL-6 and KC also showed a trend towards upregulation in the ABIN[D485] cells, however due to the small sample number, the increase was not statistically significant and more replicates will be required to confirm these findings.

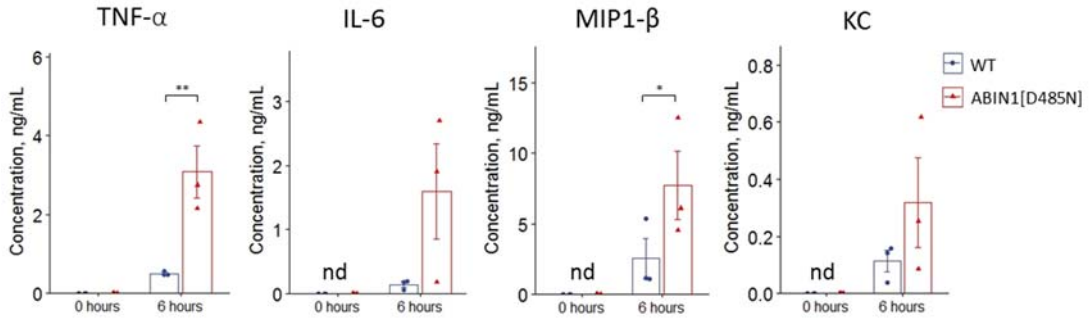

Figure 5.19 TLR7 stimulation induces cytokine production in Ly6C^{+ve} monocytes.

RBC, NK, T and B cells were magnetically depleted from spleen cells obtained from WT and ABIN1 mice and inflammatory monocytes (DAPI^{-ve}CD45^{+ve}NK1.1^{-ve}CD11b^{+ve}Ly6C^{high}CX3CR1^{+ve}CD115^{+ve}) were sorted on BD Influx™. 2.5x10^4 cells were plated in a 96 well plate and stimulated with the TLR7 agonist R837(1µg/mL) for 6 h. Culture media was collected and analysed for cytokine production by multiplex cytokine assay. Bar plots represent the average value of 3 biological replicates for each genotype. Error bars represent the standard error of the mean. Significance between the samples was calculated by two-way ANOVA followed by Tukey HSD posthoc test; * denotes $p<0.05$ and ** denotes $p<0.01$ for comparisons of ABIN1[D485N]and wild type cells. nd indicates that levels of the cytokines were below detection limit.

To further confirm these findings, I next stimulated cells from lungs and spleen of WT and ABIN1[D485N] mice with R837 and measured TNF-α and IL-6 by flow cytometry. In the spleen, induction of TNF-α was observed in both WT and ABIN[D485N] inflammatory and patrolling monocytes (Figure 5.20). There was also an upregulation of IL-6 positive inflammatory monocytes. The percentage of splenic TNF-α^{+ve} cells for both inflammatory and patrolling monocytes was higher in the ABIN1[D485N] cells compared to wild type cells (Figure 5.20A). In addition the percentage of IL-6^{+ve}TNF-α^{+ve} cells was higher in the ABIN1[D485N] inflammatory monocytes. In lungs the proportion of TNF-α^{+ve} and IL-6^{+ve}TNF-α^{+ve} cells in the stimulated Ly6C^{+ve} inflammatory monocytes was also higher in the ABIN1 knock in

mice (Figure 520B). The percentages of TNF-α^{+ve} cells patrolling monocytes in the lungs of WT and ABIN[D485N] were similar (Figure 5.20B). Interestingly, in the knock in mice the TNF-α^{+ve} cells were detected amongst the patrolling monocytes even in the absence of R837 stimulation, suggesting that these cells could produce inflammatory cytokines at steady state and therefore contribute to the inflammatory phenotype in the in ABIN1[D485N] mice.

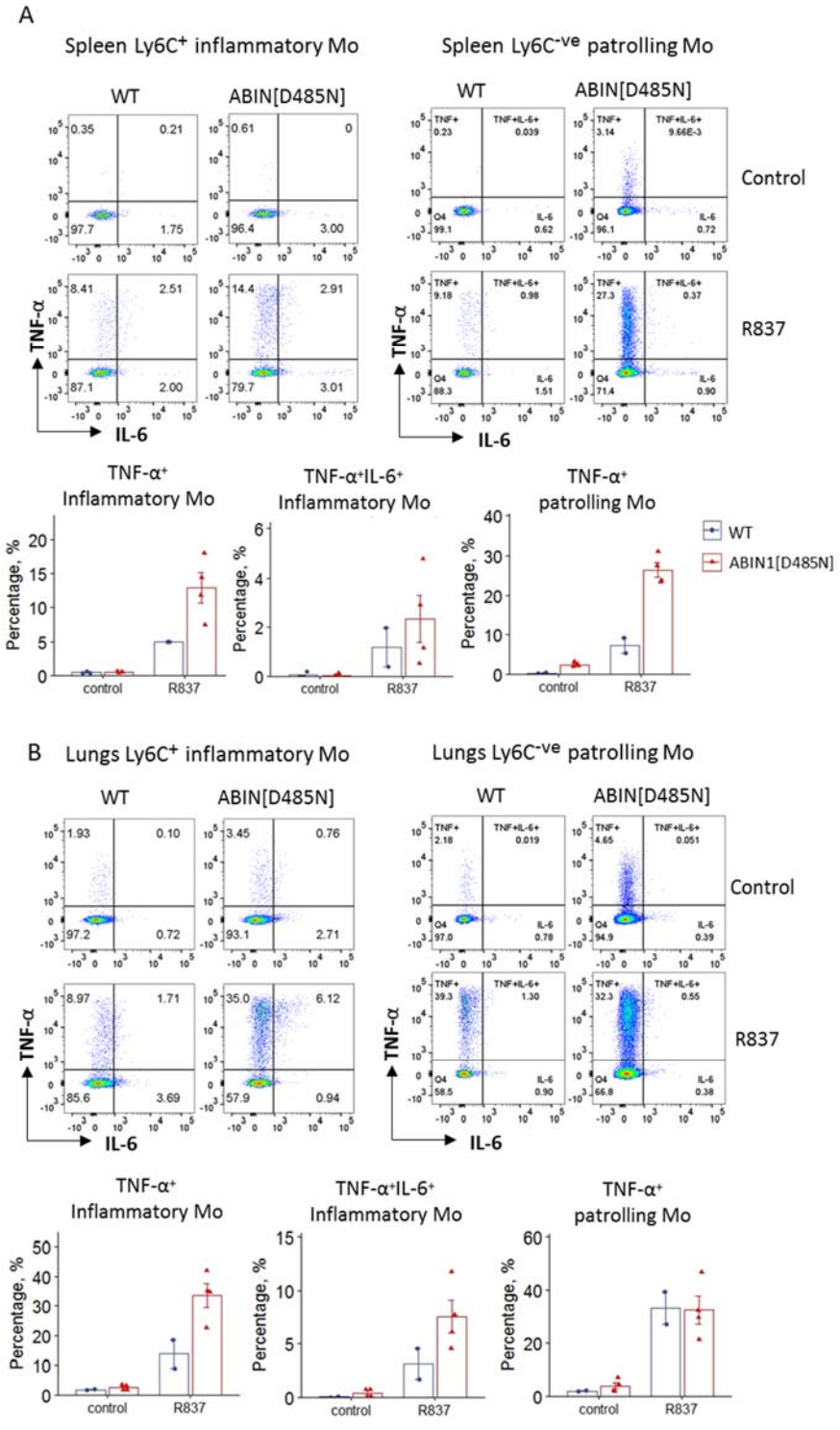

Figure 5.19 TLR7 stimulation induces TNF-α production in the inflammatory and patrolling monocytes.
$1x10^6$ spleen and lung cells from WT and ABIN1[D485N] (4 months old) mice were cultured in 1 mL of complete RPMI media with or without the TLR7 agonist R837 (1µg/mL) in the presence of Brefeldin A (5 µg/mL) and Monensin (2 µM) for 4 hours. Cells were fixed, permeabilised and stained with fluorophore conjugated antibodies against NK1.1 (APC/Cy7), CD11b (Pe/Cy7), Ly6C (FITC), CX_3CR1 (BV510), Gr-1 (PerCp/Cy5.5), MHCII (AlexaFluor700), IL-6(PE) and TNF-α(APC). Inflammatory $Ly6C^{+ve}$ monocytes were defined as $NK1.1^{-ve}CD11b^{+ve}Ly6C^{+ve}CX_3CR1^{+ve}$ and patrolling $Ly6C^{-ve}$ monocytes as $NK1.1^{-ve}CD11b^{+ve}Ly6C^{-ve}CX_3CR1^{+ve}MHCII^{-ve}$. A-B. Flow cytometry plots show expression of TNF-α and IL-6 within the corresponding monocyte populations in spleen(A) and lungs (B). Bar graphs show the average values of the percentage of $TNF\text{-}\alpha^{+ve}$, $TNF\text{-}\alpha^{+ve}$ $IL\text{-}6^{+ve}$ inflammatory monocytes and the $TNF\text{-}\alpha^{+ve}$ patrolling monocytes. Symbols represent individual biological replicates.

Epicutaneous application of the TLR7 agonist imiquimod (Aldara cream) is known to cause skin inflammation and is used as a mouse model of psoriasis (van der Fits et al., 2009). In addition, long term stimulation with imiquimod leads to systemic inflammation, splenomegaly, glomerulonephritis and production of anti-double stranded DNA antibodies (Yokogawa et al., 2014). To investigate the role of TLR7 signalling *in vivo*, Aldara cream was applied on the ears of WT mice for 2, 3, 4 or 5 days. Naïve age matched WT mice were used as a control group. Enlargement of the spleen was detected in the animals stimulated for 3, 4 and 5 days (Figure 5.21A). Although the overall proportion of the $CD115^{+ve}CD11b^{+ve}$ monocytes in the 2 day treated animals was comparable to this in the control mice, the percentage of $Ly6C^{+ve}$ inflammatory monocytes in naïve mice was 30% from all monocytes, whereas in the 2 day treated animals $Ly6C^{+ve}$ inflammatory monocytes represented more than 70% of the monocytes (Figure 5.21B). Moreover, a significant increase of the $Ly6C^{+ve}$ inflammatory monocytes was detected in the blood of 4 and 5 days simulated animals. In contrast, the patrolling monocytes were reduced initially, followed by a gradual increase. A similar trend was also observed in the spleen. These data are in line with previous studies, showing that the $Ly6C^{+ve}$ inflammatory monocytes act as a precursors for the development of the patrolling monocytes and would explain the delay in the increase of the $Ly6C^{-ve}$ monocytes.

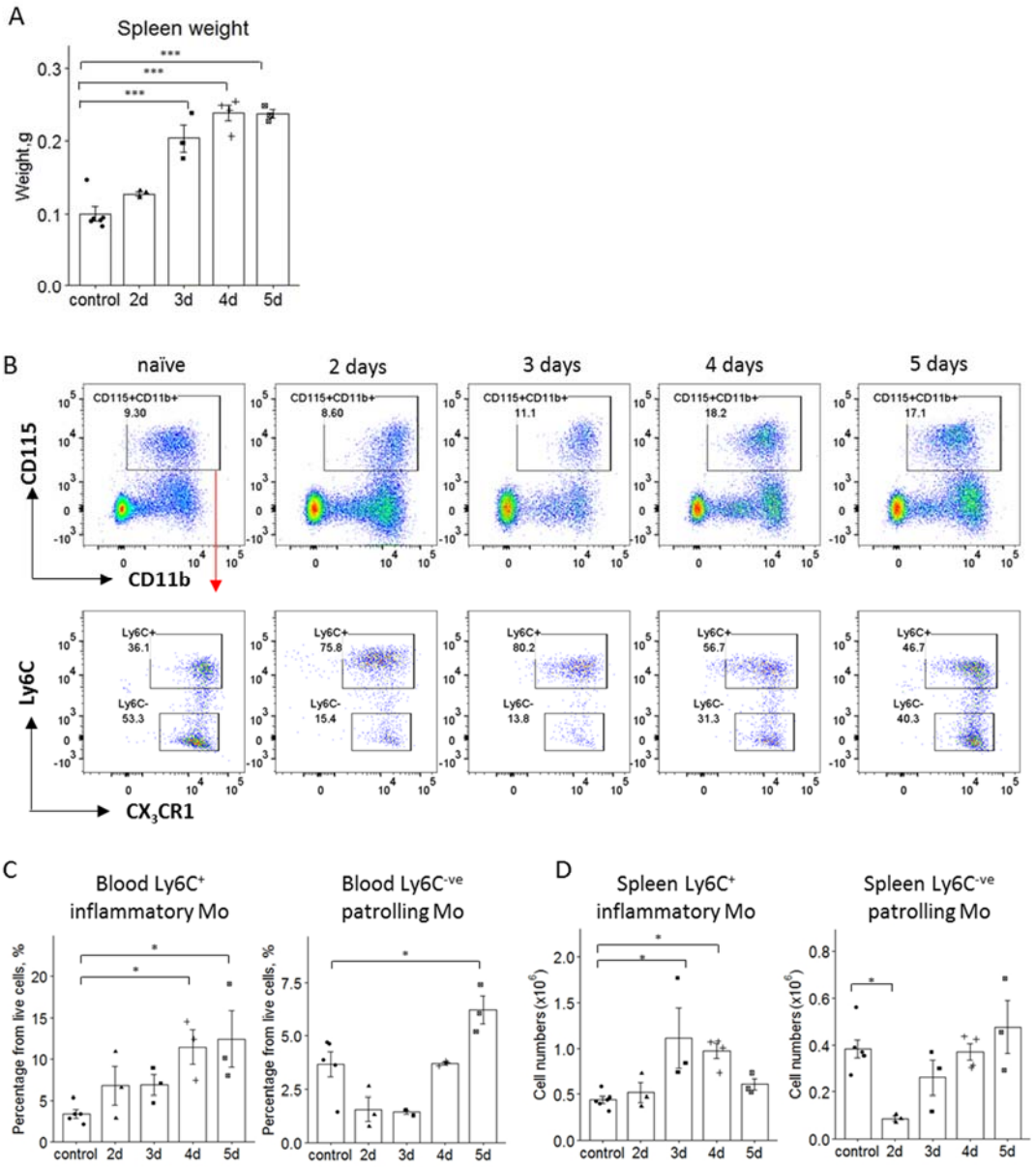

Figure 5.21 In vivo administration of the TLR7 agonist Imiquimod (Aldara) induces changes in the monocytes populations.
10-12 week old WT mice were treated with 60 mg experimental cream containing 5% of the TLR7 agonist imiquimod (Aldara) once per day on both sides of the ears for 2,3,4 or 5 days. Untreated age matched mice were used as a control group. A. Bar graphs show increase in the spleen size following treatment with imiquimod. B. Blood and spleens were analysed by flow cytometry as described in Figure 5.4. The flow cytometry plots show changes in the $CD115^{+ve}CD11b^{+ve}$, $CD115^{+ve}CD11b^{+ve}Ly6C^{+ve}CX_3CR1^{+ve}$ and $CD115^{+ve}CD11b^{+ve}Ly6C^{-ve}CX_3CR1^{+ve}$ populations in the blood. C. The bar graph represents average values (± SEM) of the percentage of $Ly6C^{+ve}$ inflammatory and $Ly6C^{-ve}$ patrolling monocytes from all live cells. D. Absolute numbers of $Ly6C^{+ve}$ inflammatory and $Ly6C^{-ve}$ patrolling monocytes in the spleen. Symbols represent individual biological replicates. Statistical significance between genotypes was calculated using one-way ANOVA followed by Tukey HSD. * $p<0.05$, **$p<0.01$ and *** $p<0.001$. *In vivo* administration of the cream was done by Dr Manuel Van Gijsel Bonnello.

5.2.5. Characterisation of ABIN1[D485N]xIL-6 KO mice

IL-6 is a pleiotropic cytokine, which has been linked to SLE development. Increased level of IL-6 is also detected in the serum samples of lupus patients (Ripley et al., 2005). IL-6 together with IL-21 is required for the expression of the B cells lymphoma 6 (Bcl6) transcription factor which promotes differentiation of T follicular helper cells (Nurieva et al., 2009). The T_{fh} cells provide signals for survival and proliferation of the B cells in the germinal centres and promote the affinity maturation of B cells (Crotty, 2014). BXSB.*Yaa* mice have increased proportion of T_{fh} cells, which is rescued when the mice are crossed to IL-6 knock out mice. Moreover, IL-6 deficiency led to a prolonged survival of BXSB.*Yaa* mice and reduction of $CD11b^{+ve}$ and $GR\text{-}1^{+ve}$ cells. The authors demonstrated that number of immune cell populations in the BXSB.*Yaa* mice including the $CD115^{+ve}$ monocytes secrete IL-6 in response to TLR7/8 stimulation with R848 (Jain et al., 2016). To understand if IL-6 plays a role in lupus development in the ABIN1[D485N] mice, ABIN1[D485N]xIL-6 KO double mutant mice were analysed for changes in the spleen size and the immune cell population. Loss of IL-6 in the ABIN1[D485N] mice led to a partial reduction of splenomegaly (Figure 5.22). The germinal centre B cells were massively reduced in the ABIN1[D485N]xIL-6 KO mice in comparison the ABIN1[D485N] mice. There was also a reduction in the Tfh in double mutant mice (Figure 5.22). However, analysis of the monocyte populations showed that the percentage increase in the $Ly6C^{+ve}$ and $Ly6C^{-ve}$ monocytes was not rescued in ABIN1[D485N]xIL-6 KO knock out mice, suggesting that IL-6 is not driving the massive expansion of the monocyte cell populations (Figure 5.23). Although monocytes were not reduced in the double mutant mice, it is possible that by producing IL-6 they contribute to the formation of germinal centres and the spontaneous auto-antibody production. Therefore, it will be interesting to understand if monocyte-derived IL-6 is required for the T_{fh} and germinal centre B cells expansion in the ABIN1[D485N] mice. Future studies will be also required to address the question, if in the ABIN1[D485N]xIL-6 KO rescues the kidney pathology and the production of autoreactive antibodies.

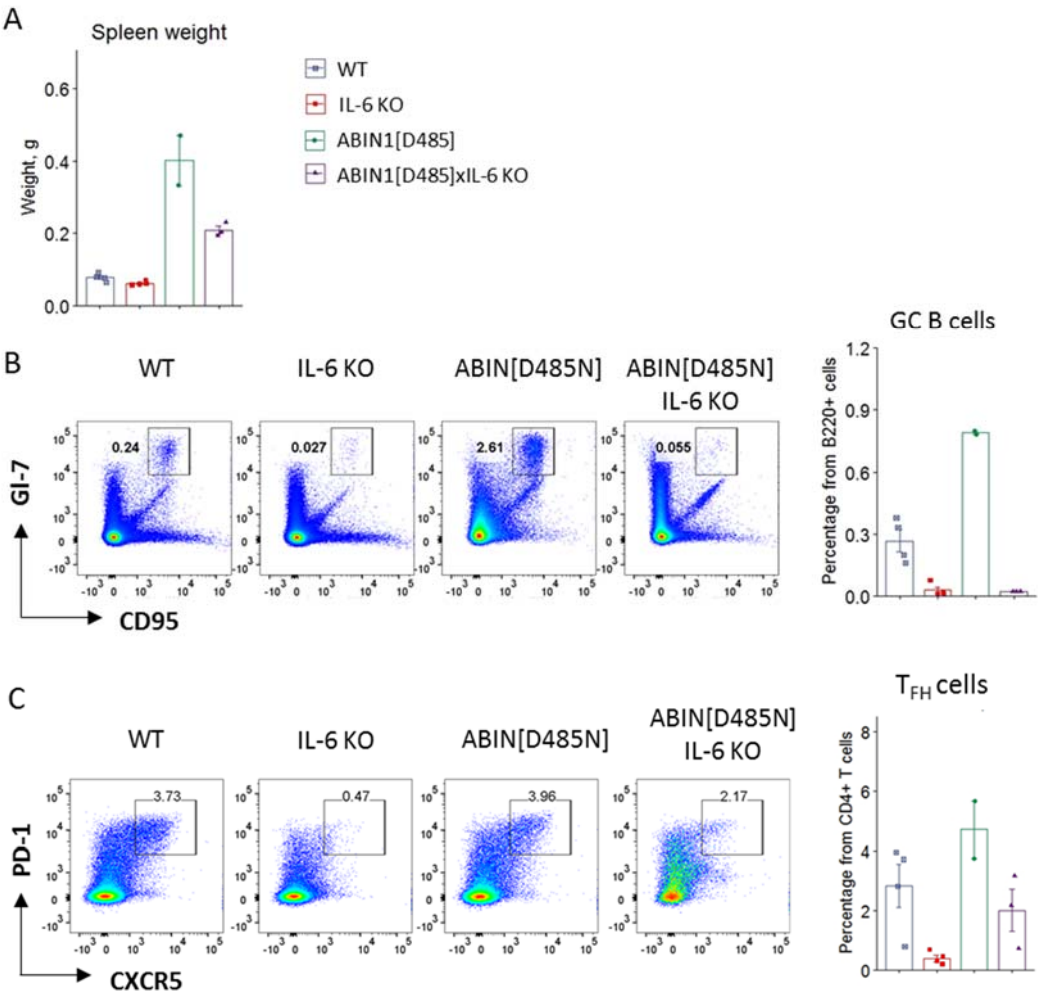

Figure 5.22 Characterisation of ABIN1[D485N]xIL-6 KO mice.
6 months old WT, IL-6 KO, ABIN1[D485N] and ABIN1[D485N]xIL-6 KO were analysed to characterise changes in the spleen size, the germinal centre B cells and T follicular helper cells. A. Average values of spleen weights (±SEM). B. The representative flow cytometry plots show the percentage of splenic $CD95^{+ve}GL\text{-}7^{+ve}$ germinal centre B cells from the $B220^{+ve}$ population. The bar graph show the average value of the percentages of the germinal centre B cells from the $B220^{+ve}$ cells. C. The representative flow cytometry plots show percentages of $PD\text{-}1^{+ve}CXCR5^{+ve}$ cells from the $TCR\text{-}\beta^{+ve}CD4^{+ve}$ gate and bar graph show the average values ±SEM.

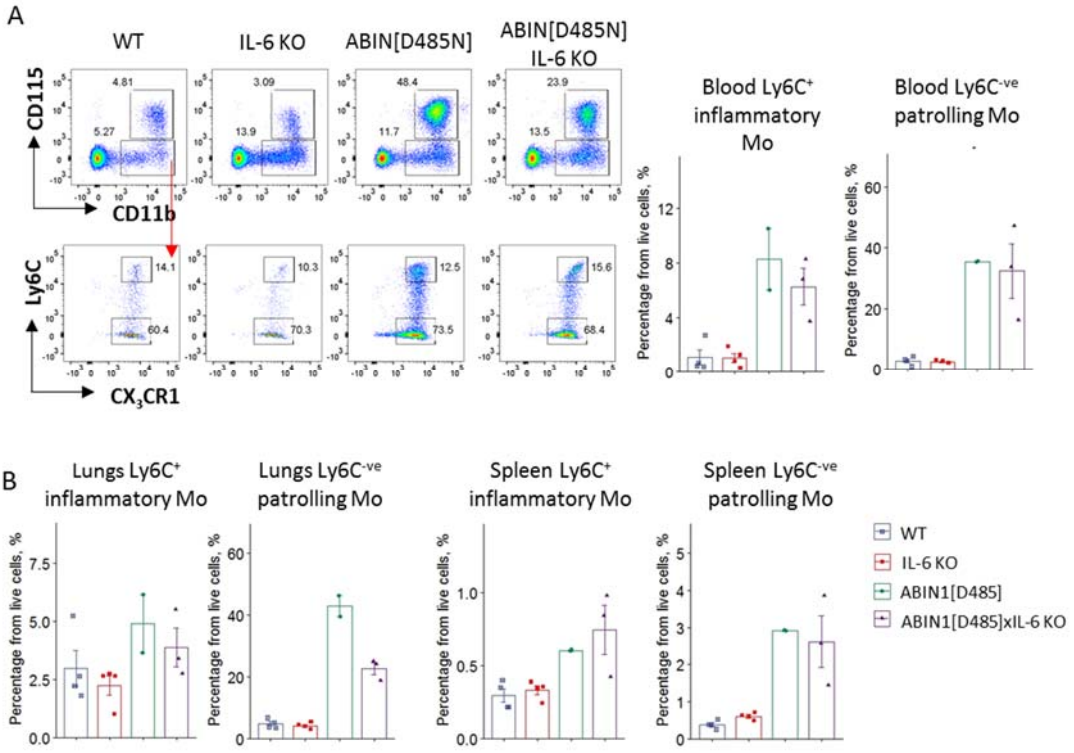

Figure 5.23 Characterisation of monocytes populations in ABIN1[D485N]xIL-6 KO mice.

Tissues from 6 months old WT, IL-6 KO, ABIN1[D485N] and ABIN1[D485N]xIL-6 KO were analysed as described in Figure 5.4 and 5.5**.** A**.** Representative plots showing changes in the $CD115^{+ve}CD11b^{+ve}$, $CD115^{+ve}CD11b^{+ve}Ly6C^{+ve}CX_3CR1^{+ve}$ and $CD115^{+ve}CD11b^{+ve}Ly6C^{-ve}CX_3CR1^{+ve}$ populations. The bar graph represents average values of the percentage of blood $Ly6C^{+ve}$ inflammatory and $Ly6C^{-ve}$ patrolling monocytes from all live cells. B. Bar graphs show percentages of $Ly6C^{+ve}$ inflammatory monocytes and $Ly6C^{-ve}$ patrolling monocytes from the live cell gate in the lungs and spleen. Symbols represent individual biological replicates. Error bars indicate standard error of the mean.

5.3. Discussion

5.3.1. Expansion of patrolling monocytes in ABIN1[D485N] mice

Here I have shown that the lupus inflammatory phenotype in ABIN1[D485N] mice is driven by the hematopoietic cells. The ABIN1[D485N] mice are characterised with changes in multiple immune cell populations including neutrophils, germinal centre B cells, follicular T helper cells. However, the most profound increase was observed in the numbers of the $Ly6C^{-ve}$ patrolling monocytes (Figures 5.7, 5.8 and 5.9). The increase in the monocytes was detected even in 4 week old animals before the appearance of autoantibody production and splenomegaly (Figure 5.7). Moreover, in 22 week old animals the patrolling monocytes represented 30-40% of the leukocytes in the blood, lungs and kidneys of ABIN1[D485N] mice (Figures 5.7, 5.8 and 5.9). An increase in the $Ly6C^{+ve}$ inflammatory monocytes was also detected in the 22 week old animals, however this increase was not as great as seen in the patrolling monocytes (Figures 5.7, 5.8 and 5.9). The $Ly6C^{+ve}$ monocytes have a short life span of approximately 20 hours, whereas $Ly6C^{-ve}$ monocytes life span is 2.2 days at steady state and in the absence of $Ly6C^{+}$ monocytes can extend to 11 days. (Yona et al., 2013, Patel et al., 2017). Adoptive transfer of $CX_3CR1^{GFP/+}Ly6C^{+ve}$ splenic inflammatory monocytes in WT mice have shown that by day 3 the $CX_3CR1^{GFP/+}Ly6C^{+ve}$ differentiate into $CX_3CR1^{GFP/+}Ly6C^{-ve}$. Similar observations were made by i.p. injection of BrdU in WT mice. BrdU staining was detected in all $Ly6C^{+ve}$ monocytes 1 day after the i.p but then gradually decreased in this population. In contrast, $BrdU^{+ve}$ $Ly6C^{-ve}$ monocytes were not detected on day 1, however by day 5 more than a third of the patrolling monocytes were positive for BrdU (Yona et al., 2013). Therefore, it is possible that in the ABIN1[D485N] mice the $Ly6C^{+ve}$ inflammatory monocytes are constantly converted into $Ly6C^{-ve}$ patrolling monocytes, which have a longer lifespan and are accumulating in the tissues.

Monocyte were originally described to develop from a common monocyte-macrophage DC progenitor (MDP) (Fogg et al., 2006). However, a more recent study has identified a common monocyte progenitor (cMoP) cells in mouse bone marrow cells, which give rise to monocytes and macrophages, but not to DCs and are characterised as $Lin^{-ve}CD117^{+ve}CD115^{+ve}CD135^{-ve}Ly6C^{+ve}CD11b^{-ve}$ (Hettinger et al., 2013). This population was found also in the spleen, but with much lower frequency (Hettinger et al., 2013). Although we have demonstrated that the monocytes

in the ABIN1[D485N] mice are increased in the peripheral tissues, it will be also interesting to understand if these mice are characterised with changes in the monocyte progenitors and this will be a subject of future work in the lab. In addition, there are some evidences suggesting that Ly6C^{-ve} monocytes can develop independently of Ly6C^{+ve} monocytes. IRF8$^{-/-}$ mice have severely reduced numbers of Ly6C^{+ve} inflammatory monocytes, however the loss of IRF8 did not have such a major effect on the patrolling monocytes, which were only partially reduced (Kurotaki et al., 2013). Therefore, it is possible that the Ly6C^{-ve} monocytes can develop directly from the cMoP.

5.3.2. Ly6C^{-ve} patrolling monocytes in other mouse models of SLE

In mice at steady state Ly6C^{-ve} monocytes crawl along the vascular endothelium and remove cellular debris from dying cells (Ginhoux and Jung, 2014). However, it has been demonstrated that during infection patrolling monocytes could extravasate into tissues. Following i.p injection of *Listeria monocytogenes,* the patrolling monocytes were rapidly recruited to the peritoneum even before neutrophils and Ly6C^{+ve} inflammatory monocytes, and were the only cells producing TNF-α at the early time point after the infection. In addition, Ly6C^{-ve} monocytes upregulated genes involved in the recruitment and activation of other immune cells such as *IL1β, CXCL1* (KC), *Eotaxin, CCL22*(Auffray et al., 2007).

Increased numbers of patrolling monocytes have been also described in the lupus prone BXSB.*Yaa* mice, which have duplication of the *tlr7* gene (Amano et al., 2005). In 8 months old BXSB.*Yaa* monocytes represented around 50% of all blood leukocytes, similar to what I have demonstrated in the ABIN1[D485N] mice (Amano et al., 2005). The patrolling monocytes in the BXSB.*Yaa* mice were also found to express high levels of the immune complex (IC) activating receptor FcγR and low levels of the inhibitory receptor FcγRIIB. Deletion of the FcγR in the BXSB.*Yaa* mice led to a significant reduction of the Gr^{-ve}CD11b^{+} monocytes (Santiago-Raber et al., 2009b). In addition to phagocytosis, FcγR receptor signalling can trigger cell activation, cell survival and cytokine production in monocytes. (Bournazos et al., 2016). A more recent study has demonstrated that the Ly6C^{-ve} monocytes are critical for IgG-mediated phagocytosis and, although many cells express FcγR, the Ly6C^{-ve}

monocytes have the highest capacity to mediate antibody-dependent cellular cytotoxicity (Biburger et al., 2011). Deficiency of FcγRIIB in C57BL/6, but not BALB/c background also leads to spontaneous autoantibody production and immune complexes-mediated lupus like autoimmunity (Bolland and Ravetch, 2000). Interestingly, a polymorphism in the gene encoding FcγRIIB has been associated with SLE in Caucasians (Su et al., 2004, Blank et al., 2005).

An increased proportion of $CD11b^{+ve}CD11c^{+ve}CX3CR1^{+ve}$ cells has also been found in the kidneys of other lupus prone strains including the MRL/lpr and NZBxNZW. These cells displayed pro-inflammatory gene signature and had the ability to promote survival and proliferation of CD4 T cells (Liao et al., 2017). Although the authors suggested that the $CD11b^{+ve}CD11c^{+ve}CX3CR1^{+ve}$ cells are renal infiltrating dendritic cells, these cells were characterised with a much lower MHCII expression than conventional dendritic cells and had higher expression of CD115 than inflammatory monocytes, suggesting they are rather patrolling monocytes and not dendritic cells (Liao et al., 2017). Interestingly, administration of anti-CX_3CR1 antibody led to a decreased body weight loss in the MRL/lpr mice, as well as reduced proteinuria, suggesting that the CX_3CR1^{+ve} cells have a pathogenic role in this model. In the ABIN1[D485N] the proportion of monocyte derived dendritic cells ($CD11b^{+ve}Ly6C^{-ve}CX3CR1^{+ve}CD11c^{+ve}MHCII^{+ve}$) was reduced in the kidneys in contrast to the patrolling monocytes($CD11b^{+ve}Ly6C^{-ve}CX3CR1^{+ve}CD11c^{+ve}MHCII^{-ve}$), which were massively increased (Figure 5.10).

5.3.3. Human monocytes and their role in SLE

In humans, a similar population of $CD14^{dim}CD16^{+ve}$ monocytes has been found to produce inflammatory cytokines such as TNF-α, IL-1β and CCL3 in response to stimulation with TLR7/8 agonists (Cros et al., 2010). Moreover, the authors demonstrated that the $CD14^{dim}CD16^{+ve}$ monocytes are observed in the IgG deposits in the glomerular vessels of patients with class IV lupus nephritis, in which more than 50% of the total number of glomeruli are affected (Cros et al., 2010) (Weening et al., 2004). Stimulation of $CD14^{dim}CD16^{+ve}$ monocytes isolated from healthy controls with sera from lupus patients induced production of inflammatory cytokines, which was reduced in the presence of RNase or DNase, and/or Ig depletion, suggesting that

$CD14^{dim}CD16^{+ve}$ monocytes respond both to nucleic acids and Fc-receptor signals (Cros et al., 2010). Another study has shown that patients with proliferative lupus nephritis have a significant induction of the CX_3CR1 ligand fractalkine in the glomeruli, which correlated with an increase in the number of $CD16^{+ve}$ monocytes expressing CX_3CR1 as well as the disease pathology (Yoshimoto et al., 2007). Similarly, another study also reported accumulation of $CD16^{+ve}$ (SlanMo) monocytes in kidney glomeruli of type III and IV lupus nephritis patients. These cells were found to produce high levels of TNF-α, IL-6 and CXCL2 following stimulation with heat-aggregated IgG. Interestingly, TNF-α production led to an upregulation of fractalkine on endothelial cells (Olaru et al., 2018).

5.3.4. TLR7 signalling in $Ly6C^{-ve}$ patrolling monocytes

Here, I have demonstrated that both $Ly6C^{+ve}$ and $Ly6C^{-ve}$ monocytes produce high levels of TNF-α upon TLR7 engagement (Figure 5.19). Moreover, the splenic $Ly6C^{+ve}$ and $Ly6C^{-ve}$ monocytes isolated from ABIN1[D485N] had significantly higher induction of TNF-α in comparison to WT monocytes when stimulated with imiquimod. Interestingly, in the knock in animals, $TNF\text{-}\alpha^{+ve}$ monocytes were detected even in non-stimulated patrolling monocytes, suggesting that they have an activated phenotype (Figure 5.19). *In vivo* stimulation with imiquimod induced rapid increase in the $Ly6C^{+ve}$ inflammatory monocytes (Figure 5.20). The kinetics of $Ly6C^{-ve}$ monocytes increase was slightly delayed and in the blood upregulation of the patrolling monocytes was detected upon 5 days stimulation (Figure 5.20). This is in line with previous studies suggesting that $Ly6C^{+ve}$ are intermediate precursors from which $Ly6C^{-ve}$ monocytes develop (Yona et al., 2013, Hettinger et al., 2013).

There is strong evidence in the literature showing that TLR7 stimulation elicits responses in patrolling monocytes. Administration of the TLR7/8 agonist R848 in mouse kidney led to a significant increase in the retention and numbers of patrolling monocytes in the kidney capillaries. In contrast, PBS or LPS treatment did not lead to changes in the recruitment of monocytes (Carlin et al., 2013). Mechanistically, the retention of monocytes was explained by the fact that treatment with R848 induced increased expression of the CX_3CR1 ligand fractalkine (CX_3CL1) in the kidney cortex leading to receptor-ligand interaction, which retained the monocytes. In addition,

$CX_3CR1^{-/-}$ deficiency abolished the monocyte increase in the kidneys (Carlin et al., 2013). The authors also demonstrated that R848 induced recruitment of neutrophils, which was dependent on the $Ly6C^{-ve}$ patrolling monocytes and led to necrosis of endothelial cells (Carlin et al., 2013). *In vivo* administration of TLR7 or TLR9 agonists also has been shown to promote maturation of inflammatory monocytes toward patrolling monocytes, which was accompanied by down regulation of the FcγRIIB inhibitory receptor on patrolling monocytes (Santiago-Raber et al., 2011). In the TLR-7 (imiquimod) or IL-23 induced psoriasis mouse model, $Ly6C^{+ve}$ inflammatory monocytes and monocyte derived dendritic cells were found to play a critical role in mediating local skin inflammation (Singh et al., 2016). Depleting monocytes and neutrophils with an anti-Ly6C antibody, but not neutrophils alone with anti-Ly6G antibody, led to a significant reduction in ear swelling and thickening and reduction of pro-inflammatory cytokines (Singh et al., 2016). Analysis of imiquimod treated $MyD88^{fl/fl}$ *LysM* $cre^{+/-}$ mice demonstrated that deletion of MyD88 in the myeloid lineage (macrophages, monocytes, neutrophils) leads to reduction of the levels of proinflammatory cytokines in the skin such as IL-23, IL-1β, IL-17A, IL-22, IL-6 and CXCL1, as well as reduction in the numbers of activated γδ-T cells both in the skin and draining lymph nodes. This reduction was not observed in *MyD88*$^{fl/fl}$*MRP8-Cre*$^{+/-}$ which results in predominant deletion in the neutrophils, suggesting that MyD88 signalling in monocytes and macrophages, but not neutrophils play a role in disease exacerbation (Costa et al., 2017). Another study showed that downregulation of ABIN1 using shRNA leads to exacerbation of imiqimod induced psoriasis, suggesting the ABIN1 plays a critical role in limiting TLR7 signalling in this model. However the authors did not look at changes in the immune cell populations and it is not clear if monocytes contributed to the exacerbated imiquimod response in this study (Chen et al., 2015b).

Consistent with the literature supporting the role of TLR7 in monocyte recruitment and activation, here I have shown that TLR7 deficiency rescues the increase in patrolling and inflammatory monocytes in ABIN1[D485N] mice (Figure 5.17). The splenomegaly and the increase in the germinal centre B cells and follicular T helper cells were also rescued in ABIN1[D485N]xTLR7[KO] mice (Figure 5.18). This would suggest that excessive TLR7 signalling is driving the autoimmunity in the ABIN1[D485N] mice. Although the exact mechanism of how ABIN1 ubiquitin

binding function prevents development of autoimmunity is not completely clear, it is possible that ABIN1 regulates this process on two levels. First, it has been demonstrated that loss of ABIN1 leads to enhanced K63 ubiquitination of RIPK1 and sensitises cells to necroptosis (Dziedzic et al., 2018). Therefore, is possible that there is an increased level of cell death in the ABIN1[D485N] mice. This in turns would lead to increased cellular debris and availability of nucleic acids which triggers TLR3/7/8/9 signalling and generation of immune complexes. Additionally, as we have demonstrated enhanced TLR7 signalling induces proliferation in the monocytes as well as production of proinflammatory cytokines such as TNF-α, which could further amplify the cell death process. The monocytes may also produce IL-6, which can promote germinal centre formation and auto-antibody production. The latter was illustrated by the fact that although cross of ABIN1[D485N] to IL-6 knock out mice did not rescue the increase in the patrolling monocytes, it led to a reduction of the spleen weight and complete loss of the germinal centre B cells and the follicular T helper cells (Figure 5.22 and 5.23). Additional experiments will be required to understand if the IL-6 KO cross to ABIN1[D485N] mice rescues the kidney pathology and increase auto-antibodies in the serum.

Excessive production of IFN-α and altered IFN gene signature has been shown to correlate with disease activity in patients with SLE (Kirou et al., 2004, Baechler et al., 2003). Plasmocytoid dendritic cells (pDCs) are a major IFN-α producing cell type and are found to accumulate in the skin lesions of lupus patients (Siegal et al., 1999) (Farkas et al., 2001). Depletion of pDC in the BXSB.*Yaa* by crossing to BDCA2-DTR Tg mice and treating mice with diphtheria toxin (DT) led to a reduction in the number of activated T cells and age associated B cells (ABCs), reduction in the anti- nuclear antibodies and IgG/C3 deposition in the kidneys, suggesting that these cells contribute to the pathology in the BXSB.*Yaa*. In contrast to these findings, suppression of type I IFN signalling by crossing ABIN1[D485N] mice to IFNAR KO did not rescue the development of autoimmunity in the ABIN1[D485N] mice (Nanda et al., 2016). In addition, the massive changes in the myeloid populations were also not rescued in the ABIN1[D485N] x IFNAR KO mice (Appendix A).

5.3.5. Targeting MyD88 signalling for treatment of SLE

Last, we investigated the role of the TLR signalling and the potential of targeting this pathway for treatment of SLE in ABIN1[D485N] mice. Ligation of TLR7 receptor leads to the recruitment of the MyD88 adaptor protein and IRAK1, IRAK2 and IRAK4. Cross of ABIN1[D485N] mice to MyD88 KO or IRAK4 and IRAK1 knock in mice completely rescued the SLE phenotype, suggesting that inhibition of IRAK1 and IRAK4 could provide a strategy for SLE treatment (Nanda et al., 2016, Nanda et al., 2011). I have shown that the increase in patrolling monocytes is also rescued in the double crosses, providing another link that these cells could be involved in the pathology of SLE (Figure 5.14).

Treatment of the ABIN1[D485N] mice with an IRAK4 inhibitor led to a significant reduction in splenomegaly and increase in the patrolling monocytes (Figure 5.15 and 5.16). These findings were in line with another study, showing that inhibition of IRAK4 with the compound BMS-986126 had a protective effect in the lupus prone mouse strains MRL/*lpr* and NZB/NZW (Dudhgaonkar et al., 2017). In both strains the IRAK4 inhibitor led to a significant reduction in proteinuria, anti-dsDNA antibodies, inflammatory cytokine production and kidney damage. Administration of BMS-986126 in combination with the glucocorticosteroid prednisolone had a synergistic effect and led to a further reduction of the auto-antibody production and proteinuria in the MRL/*lpr* mice (Dudhgaonkar et al., 2017). Furthermore, in the imiqiomod induced psoriasis model, the BMS-986126 compound also led to a significant reduction in skin thickening, erythema and splenomegaly (Dudhgaonkar et al., 2017). Taken together, our and others data have demonstrated that inhibition of IRAK4 could have beneficial effect in patients in lupus. Moreover, considering that the IRAK4 inhibitor blocked the expansion of the patrolling monocytes in the ABIN1[D485N] mice, it will be interesting to understand if inhibition of IRAK4 has a protective effect in other diseases, which are associated by deregulation of the patrolling monocytes function. In a K/BxN serum transfer induced arthritis (STIA) model patrolling monocytes were found to play a critical role in the disease initiation and progression. Depletion of monocytes with clodronate liposomes prevented disease development in the STIA model of arthritis. However, disease development was restored when Ly6C^{-ve} monocytes were adoptively transferred in to mice treated with the K/BxN serum and clodronate liposomes (Misharin et al., 2014).

Finally, I have also shown that neutrophils in the spleens of ABIN1[D485N] mice are also increased and have lower granularity, suggesting that they might have similar properties as the LDG neutrophils, described in lupus patients (Villanueva et al., 2011). Interestingly, those differences were not observed in the other tissues of the ABIN1[D485N] mice. The spleen has a specific function and acts as a filter, where altered RBC can be recognised and removed from the circulation (Pivkin et al., 2016). Damaged RBCs are phagocytosed by a specific type of macrophages called red pulp macrophages, which are described as F4/80^{high}CD68^{+ve}CD11b^{low} and have high autofluorescence (Kohyama et al., 2009). Preliminary data indicate that the ABIN1[D485N] mice have increased proportion of F4/80^{+ve}CD11b^{low} macrophages (Appendix B) in the spleen. Future studies will be required to understand if impaired function of the red pulp macrophages is driving the expansion of the neutrophils. It would be also interesting to investigate if splenic neutrophils in the ABIN1[D485N] mice have a higher production of NETs and proinflammatory cytokines than WT neutrophils.

5.3.6. Future work

The appearance of the increase in monocytes precedes the development of clinical symptoms such as auto-antibody production and kidney pathology, however it remains an open question whether the patrolling monocytes are driving the diseases in the ABIN1[D485N] mice. Therefore, a conditional knock-in mice of the ABIN1[D485N] will be generated, which will be crossed to the appropriate Cre transgenic mice such as *LysM-Cre, CD11c-Cre* or *CX$_3$CR1-Cre*. This would allow us understand the relative contribution of different immune cells to the pathology observed in the total knock in mice. Alternative strategies to deplete monocytes such as treatment with clodronate liposome will be also applied (Rooijen and Sanders, 1994).

To further characterise the monocytes populations, Ly6C^{+ve} and Ly6C^{-ve} monocytes isolated from WT and ABIN1[D485N] mice will be analysed by RNA sequencing. It will be interesting to understand if ABIN1[D485N] regulates transcription factors or proteins involved in the development of monocytes. Interestingly, hypomorphic mutation of Gfi1 in mice (referred as *Genista* mice) results

in accumulation of atypical neutrophils and expansion of $CD11b^{+ve}Ly6G^{-ve}$ cells (Ordonez-Rueda et al., 2012). The *Genista* mice were made through an N-ethyl-N-nitrosourea (ENU) mutagenesis screen, which aim was to identify mutations affecting the immune cell development. The *Genista* mice carry mutation Cys318 to Tyr in the zinc finger domain of Gfi1 (Ordonez-Rueda et al., 2012). The Genista mice also develop spontaneously lupus like autoimmunity, which is rescued by cross to TLR7 KO mice (Desnues et al., 2016). Gfi1 is a transcriptional repressor regulating expression of multiple genes. Levels of Gfi1 expression have been shown to determine the fate of granulocyte-monocyte precursors, and high Gfi1 expression determined granulocyte maturation (Vassen et al., 2012). Therefore, it is possible that, ABIN1 is involved in the regulation of Gfi1 by the ubiquitin system. Future experiments will determine if ABIN1[D485N] monocytes have changes in Gfi1 mRNA and protein levels.

5.3.7. Conclusions

Here, I have shown that the development of lupus in ABIN1[D485N] mice is a result of a defect in the immune cell compartment and loss of ABIN1 ubiquitin binding function leads to a massive increase in the patrolling monocytes. Cross of ABIN1[D485N] mice to TLR7 KO mice prevented the development of splenomegaly, germinal centre formation and monocyte expansion. Moreover, the monocytes were hypersensitive to stimulation with TLR7 and produced inflammatory cytokines. I have also demonstrated that ABIN1[D485N] mice crossed to IRAK4 or IRAK1 kinase inactive knock in mice have normal patrolling monocyte numbers. The fact that the patrolling monocytes are more than 10 times increased in the mutant mice, have pro inflammatory properties and their expansion is prevented in the double mutant mice, where the phenotype is rescued, suggests that they are most likely involved in the development of lupus pathology in the ABIN1[D485N] mice. Pharmacological inhibition of IRAK4 did rescue the expansion of the monocytes and the splenomegaly in the ABIN1[D485N] mice showing that IRAK4 inhibition has the potential to provide new therapeutic approach for lupus patients and other immune diseases which are mediated by aberrant monocyte responses.

Bibliography

ADACHI, O., KAWAI, T., TAKEDA, K., MATSUMOTO, M., TSUTSUI, H., SAKAGAMI, M., NAKANISHI, K. & AKIRA, S. 1998. Targeted disruption of the MyD88 gene results in loss of IL-1- and IL-18-mediated function. *Immunity,* 9**,** 143-50.

ADRIANTO, I., WANG, S., WILEY, G. B., LESSARD, C. J., KELLY, J. A., ADLER, A. J., GLENN, S. B., WILLIAMS, A. H., ZIEGLER, J. T., COMEAU, M. E., MARION, M. C., WAKELAND, B. E., LIANG, C., KAUFMAN, K. M., GUTHRIDGE, J. M., ALARCON-RIQUELME, M. E., ALARCON, G. S., ANAYA, J. M., BAE, S. C., KIM, J. H., JOO, Y. B., BOACKLE, S. A., BROWN, E. E., PETRI, M. A., RAMSEY-GOLDMAN, R., REVEILLE, J. D., VILA, L. M., CRISWELL, L. A., EDBERG, J. C., FREEDMAN, B. I., GILKESON, G. S., JACOB, C. O., JAMES, J. A., KAMEN, D. L., KIMBERLY, R. P., MARTIN, J., MERRILL, J. T., NIEWOLD, T. B., PONS-ESTEL, B. A., SCOFIELD, R. H., STEVENS, A. M., TSAO, B. P., VYSE, T. J., LANGEFELD, C. D., HARLEY, J. B., WAKELAND, E. K., MOSER, K. L., MONTGOMERY, C. G. & GAFFNEY, P. M. 2012. Association of two independent functional risk haplotypes in TNIP1 with systemic lupus erythematosus. *Arthritis Rheum,* 64**,** 3695-705.

AKSENTIJEVICH, I. & ZHOU, Q. 2017. NF-κB Pathway in Autoinflammatory Diseases: Dysregulation of Protein Modifications by Ubiquitin Defines a New Category of Autoinflammatory Diseases. *Frontiers in Immunology,* 8.

ALBU, D. I., VANVALKENBURGH, J., MORIN, N., CALIFANO, D., JENKINS, N. A., COPELAND, N. G., LIU, P. & AVRAM, D. 2011. Transcription factor Bcl11b controls selection of invariant natural killer T-cells by regulating glycolipid presentation in double-positive thymocytes. *Proceedings of the National Academy of Sciences,* 108**,** 6211-6216.

ALESSI, D. R., JAMES, S. R., DOWNES, C. P., HOLMES, A. B., GAFFNEY, P. R. J., REESE, C. B. & COHEN, P. 1997. Characterization of a 3-phosphoinositide-dependent protein kinase which phosphorylates and activates protein kinase Bα. *Current Biology,* 7**,** 261-269.

ALI, S., MOHS, A., THOMAS, M., KLARE, J., ROSS, R., SCHMITZ, M. L. & MARTIN, M. U. 2011a. The dual function cytokine IL-33 interacts with the transcription factor NF-kappaB to dampen NF-kappaB-stimulated gene transcription. *J Immunol,* 187**,** 1609-16.

ALLAKHVERDI, Z., SMITH, D. E., COMEAU, M. R. & DELESPESSE, G. 2007. Cutting Edge: The ST2 Ligand IL-33 Potently Activates and Drives Maturation of Human Mast Cells. *The Journal of Immunology,* 179**,** 2051-2054.

AMANO, H., AMANO, E., SANTIAGO-RABER, M. L., MOLL, T., MARTINEZ-SORIA, E., FOSSATI-JIMACK, L., IWAMOTO, M., ROZZO, S. J., KOTZIN, B. L. & IZUI, S. 2005. Selective expansion of a monocyte subset expressing the CD11c dendritic cell marker in the Yaa model of systemic lupus erythematosus. *Arthritis Rheum,* 52**,** 2790-8.

ANDERSON, K. V., BOKLA, L. & NUSSLEIN-VOLHARD, C. 1985. Establishment of dorsal-ventral polarity in the Drosophila embryo: the induction of polarity by the Toll gene product. *Cell,* 42**,** 791-8.

ANNA, B., SERENA, L., MARTINA, M., MARIA, S., RITA, M., AMATO, P., NICOLA, B. & FABIO, A. 2012. IL-33 is secreted by psoriatic keratinocytes and induces pro-inflammatory cytokines via keratinocyte and mast cell activation. *Experimental Dermatology,* 21**,** 892-894.

ANTUNES, T. T., GAGNON, A., CHEN, B., PACINI, F., SMITH, T. J. & SORISKY, A. 2006. Interleukin-6 release from human abdominal adipose cells is regulated by thyroid-stimulating hormone: effect of adipocyte differentiation and anatomic depot. *Am J Physiol Endocrinol Metab,* 290**,** E1140-4.

APEL, F., ZYCHLINSKY, A. & KENNY, E. F. 2018. The role of neutrophil extracellular traps in rheumatic diseases. *Nature Reviews Rheumatology,* 14**,** 467-475.

ARIMA, M. & FUKUDA, T. 2011. Prostaglandin D(2) and T(H)2 Inflammation in the Pathogenesis of Bronchial Asthma. *The Korean Journal of Internal Medicine,* 26**,** 8-18.

ARSHAD, M. I., GUIHARD, P., DANGER, Y., NOEL, G., LE SEYEC, J., BOUTET, M. A., RICHARDS, C. D., L'HELGOUALC'H, A., GENET, V., LUCAS-CLERC, C., GASCAN, H., BLANCHARD, F., PIQUET-PELLORCE, C. & SAMSON, M. 2015. Oncostatin M induces IL-33 expression in liver endothelial cells in mice and expands ST2+CD4+ lymphocytes. *Am J Physiol Gastrointest Liver Physiol,* 309**,** G542-53.

ARSHAD, M. I., PATRAT-DELON, S., PIQUET-PELLORCE, C., L'HELGOUALC'H, A., RAUCH, M., GENET, V., LUCAS-CLERC, C., BLEAU, C., LAMONTAGNE, L. & SAMSON, M. 2013. Pathogenic mouse hepatitis virus or poly(I:C) induce IL-33 in hepatocytes in murine models of hepatitis. *PLoS One,* 8**,** e74278.

ARTHUR, J. S. C. & LEY, S. C. 2013. Mitogen-activated protein kinases in innate immunity. *Nature Reviews Immunology,* 13**,** 679.

ASSMANN, N., O'BRIEN, K. L., DONNELLY, R. P., DYCK, L., ZAIATZ-BITTENCOURT, V., LOFTUS, R. M., HEINRICH, P., OEFNER, P. J., LYNCH, L., GARDINER, C. M., DETTMER, K. & FINLAY, D. K. 2017. Srebp-controlled glucose metabolism is essential for NK cell functional responses. *Nature Immunology,* 18**,** 1197.

AUFFRAY, C., FOGG, D., GARFA, M., ELAIN, G., JOIN-LAMBERT, O., KAYAL, S., SARNACKI, S., CUMANO, A., LAUVAU, G. & GEISSMANN, F. 2007. Monitoring of Blood Vessels and Tissues by a Population of Monocytes with Patrolling Behavior. *Science,* 317**,** 666-670.

BAECHLER, E. C., BATLIWALLA, F. M., KARYPIS, G., GAFFNEY, P. M., ORTMANN, W. A., ESPE, K. J., SHARK, K. B., GRANDE, W. J., HUGHES, K. M., KAPUR, V., GREGERSEN, P. K. & BEHRENS, T. W. 2003. Interferon-inducible gene expression signature in peripheral blood cells of patients with severe lupus. *Proceedings of the National Academy of Sciences,* 100**,** 2610-2615.

BAIN, J., MCLAUCHLAN, H., ELLIOTT, M. & COHEN, P. 2003. The specificities of protein kinase inhibitors: an update. *Biochemical Journal,* 371**,** 199-204.

BAIN, J., PLATER, L., ELLIOTT, M., SHPIRO, N., HASTIE, C. J., MCLAUCHLAN, H., KLEVERNIC, I., ARTHUR, J. S., ALESSI, D. R. & COHEN, P. 2007. The selectivity of protein kinase inhibitors: a further update. *Biochem J,* 408**,** 297-315.

BALATO, A., DI CAPRIO, R., CANTA, L., MATTII, M., LEMBO, S., RAIMONDO, A., SCHIATTARELLA, M., BALATO, N. & AYALA, F.

2014. IL-33 is regulated by TNF-alpha in normal and psoriatic skin. *Arch Dermatol Res,* 306**,** 299-304.

BANDO, J. K., NUSSBAUM, J. C., LIANG, H. E. & LOCKSLEY, R. M. 2013. Type 2 innate lymphoid cells constitutively express arginase-I in the naive and inflamed lung. *J Leukoc Biol,* 94**,** 877-84.

BANK, S., ANDERSEN, P. S., BURISCH, J., PEDERSEN, N., ROUG, S., GALSGAARD, J., TURINO, S. Y., BRODERSEN, J. B., RASHID, S., RASMUSSEN, B. K., AVLUND, S., OLESEN, T. B., HOFFMANN, H. J., THOMSEN, M. K., THOMSEN, V. O., FRYDENBERG, M., NEXO, B. A. & SODE, J. 2014. Associations between functional polymorphisms in the NFkappaB signaling pathway and response to anti-TNF treatment in Danish patients with inflammatory bowel disease. 14**,** 526-34.

BAR-PELED, L., SCHWEITZER, L. D., ZONCU, R. & SABATINI, D. M. 2012. Ragulator is a GEF for the rag GTPases that signal amino acid levels to mTORC1. *Cell,* 150**,** 1196-208.

BARLOW, J. L., PEEL, S., FOX, J., PANOVA, V., HARDMAN, C. S., CAMELO, A., BUCKS, C., WU, X., KANE, C. M., NEILL, D. R., FLYNN, R. J., SAYERS, I., HALL, I. P. & MCKENZIE, A. N. 2013. IL-33 is more potent than IL-25 in provoking IL-13-producing nuocytes (type 2 innate lymphoid cells) and airway contraction. *J Allergy Clin Immunol,* 132**,** 933-41.

BARTEMES, K. R., IIJIMA, K., KOBAYASHI, T., KEPHART, G. M., MCKENZIE, A. N. & KITA, H. 2012a. IL-33-responsive lineage- CD25+ CD44(hi) lymphoid cells mediate innate type 2 immunity and allergic inflammation in the lungs. *J Immunol,* 188**,** 1503-13.

BARTEMES, K. R., KEPHART, G. M., FOX, S. J. & KITA, H. 2014. Enhanced innate type 2 immune response in peripheral blood from patients with asthma. *Journal of Allergy and Clinical Immunology,* 134**,** 671-678.e4.

BEARDMORE, V. A., HINTON, H. J., EFTYCHI, C., APOSTOLAKI, M., ARMAKA, M., DARRAGH, J., MCILRATH, J., CARR, J. M., ARMIT, L. J., CLACHER, C., MALONE, L., KOLLIAS, G. & ARTHUR, J. S. 2005. Generation and characterization of p38beta (MAPK11) gene-targeted mice. *Mol Cell Biol,* 25**,** 10454-64.

BENNETT, L., PALUCKA, A. K., ARCE, E., CANTRELL, V., BORVAK, J., BANCHEREAU, J. & PASCUAL, V. 2003. Interferon and granulopoiesis signatures in systemic lupus erythematosus blood. *J Exp Med,* 197**,** 711-23.

BERGERS, G., REIKERSTORFER, A., BRASELMANN, S., GRANINGER, P. & BUSSLINGER, M. 1994. Alternative promoter usage of the Fos-responsive gene Fit-1 generates mRNA isoforms coding for either secreted or membrane-bound proteins related to the IL-1 receptor. *The EMBO Journal,* 13**,** 1176-1188.

BESSA, J., MEYER, C. A., DE VERA MUDRY, M. C., SCHLICHT, S., SMITH, S. H., IGLESIAS, A. & COTE-SIERRA, J. 2014. Altered subcellular localization of IL-33 leads to non-resolving lethal inflammation. *Journal of Autoimmunity,* 55**,** 33-41.

BHATTACHARYA, P., BHATTACHARJEE, S., GUPTA, G., MAJUMDER, S., ADHIKARI, A., MUKHERJEE, A., MAJUMDAR, S. B., SAHA, B. & MAJUMDAR, S. 2010. Arabinosylated lipoarabinomannan-mediated protection in visceral leishmaniasis through up-regulation of toll-like receptor 2 signaling: an immunoprophylactic approach. *J Infect Dis,* 202**,** 145-55.

BIANCHI, M. E. 2007. DAMPs, PAMPs and alarmins: all we need to know about danger. *Journal of Leukocyte Biology,* 81**,** 1-5.

BIBURGER, M., ASCHERMANN, S., SCHWAB, I., LUX, A., ALBERT, H., DANZER, H., WOIGK, M., DUDZIAK, D. & NIMMERJAHN, F. 2011. Monocyte Subsets Responsible for Immunoglobulin G-Dependent Effector Functions In Vivo. *Immunity,* 35**,** 932-944.

BIRAGYN, A., RUFFINI, P. A., LEIFER, C. A., KLYUSHNENKOVA, E., SHAKHOV, A., CHERTOV, O., SHIRAKAWA, A. K., FARBER, J. M., SEGAL, D. M., OPPENHEIM, J. J. & KWAK, L. W. 2002. Toll-like receptor 4-dependent activation of dendritic cells by beta-defensin 2. *Science,* 298**,** 1025-9.

BLANK, M. C., STEFANESCU, R. N., MASUDA, E., MARTI, F., KING, P. D., REDECHA, P. B., WURZBURGER, R. J., PETERSON, M. G., TANAKA, S. & PRICOP, L. 2005. Decreased transcription of the human FCGR2B gene mediated by the -343 G/C promoter polymorphism and association with systemic lupus erythematosus. *Hum Genet,* 117**,** 220-7.

BOLLAND, S. & RAVETCH, J. V. 2000. Spontaneous autoimmune disease in Fc(gamma)RIIB-deficient mice results from strain-specific epistasis. *Immunity,* 13**,** 277-85.

BONNERT, T. P., GARKA, K. E., PARNET, P., SONODA, G., TESTA, J. R. & SIMS, J. E. 1997. The cloning and characterization of human MyD88: a member of an IL-1 receptor related family. *FEBS Lett,* 402**,** 81-4.

BORASCHI, D., ITALIANI, P., WEIL, S. & MARTIN, M. U. 2018. The family of the interleukin-1 receptors. *Immunol Rev,* 281**,** 197-232.

BOSSINI-CASTILLO, L., MARTIN, J. E., BROEN, J., SIMEON, C. P., BERETTA, L., GORLOVA, O. Y., VONK, M. C., ORTEGO-CENTENO, N., ESPINOSA, G., CARREIRA, P., GARCIA DE LA PENA, P., OREIRO, N., ROMAN-IVORRA, J. A., CASTILLO, M. J., GONZALEZ-GAY, M. A., SAEZ-COMET, L., CASTELLVI, I., SCHUERWEGH, A. J., VOSKUYL, A. E., HOFFMANN-VOLD, A. M., HESSELSTRAND, R., NORDIN, A., LUNARDI, C., SCORZA, R., VAN LAAR, J. M., SHIELS, P. G., HERRICK, A., WORTHINGTON, J., FONSECA, C., DENTON, C., TAN, F. K., ARNETT, F. C., ASSASSI, S., KOELEMAN, B. P., MAYES, M. D., RADSTAKE, T. R. & MARTIN, J. 2013. Confirmation of TNIP1 but not RHOB and PSORS1C1 as systemic sclerosis risk factors in a large independent replication study. *Ann Rheum Dis,* 72**,** 602-7.

BOTOS, I., SEGAL, DAVID M. & DAVIES, DAVID R. 2011. The Structural Biology of Toll-like Receptors. *Structure,* 19**,** 447-459.

BOUFFI, C., ROCHMAN, M., ZUST, C. B., STUCKE, E. M., KARTASHOV, A., FULKERSON, P. C., BARSKI, A. & ROTHENBERG, M. E. 2013. IL-33 markedly activates murine eosinophils by an NF-kappaB-dependent mechanism differentially dependent upon an IL-4-driven autoinflammatory loop. *J Immunol,* 191**,** 4317-25.

BOURGEOIS, E., VAN, L. P., SAMSON, M., DIEM, S., BARRA, A., ROGA, S., GOMBERT, J. M., SCHNEIDER, E., DY, M., GOURDY, P., GIRARD, J. P. & HERBELIN, A. 2009. The pro-Th2 cytokine IL-33 directly interacts with invariant NKT and NK cells to induce IFN-gamma production. *Eur J Immunol,* 39**,** 1046-55.

BOURNAZOS, S., WANG, T. T. & RAVETCH, J. V. 2016. The Role and Function of Fcγ Receptors on Myeloid Cells. *Microbiology spectrum,* 4**,** 10.1128/microbiolspec.MCHD-0045-2016.

BOUTENS, L. & STIENSTRA, R. 2016. Adipose tissue macrophages: going off track during obesity. *Diabetologia,* 59**,** 879-894.

BOUTET, M. A. & NAJM, A. 2017. IL-38 overexpression induces anti-inflammatory effects in mice arthritis models and in human macrophages in vitro. 76**,** 1304-1312.

BRESLIN, W. L., STROHACKER, K., CARPENTER, K. C., HAVILAND, D. L. & MCFARLIN, B. K. 2013. Mouse blood monocytes: Standardizing their identification and analysis using CD115. *Journal of Immunological Methods,* 390**,** 1-8.

BRESTOFF, J. R., KIM, B. S., SAENZ, S. A., STINE, R. R., MONTICELLI, L. A., SONNENBERG, G. F., THOME, J. J., FARBER, D. L., LUTFY, K., SEALE, P. & ARTIS, D. 2014. Group 2 innate lymphoid cells promote beiging of white adipose tissue and limit obesity. *Nature,* 519**,** 242.

BRIDGEWOOD, C., FEARNLEY, G. W., BEREKMERI, A., LAWS, P., MACLEOD, T., PONNAMBALAM, S., STACEY, M., GRAHAM, A. & WITTMANN, M. 2018. IL-36γ Is a Strong Inducer of IL-23 in Psoriatic Cells and Activates Angiogenesis. *Frontiers in Immunology,* 9**,** 200.

BRUTKIEWICZ, R. R. & SRIRAM, V. 2002. Natural killer T (NKT) cells and their role in antitumor immunity. *Critical Reviews in Oncology / Hematology,* 41**,** 287-298.

BUECHLER, M. B., TEAL, T. H., ELKON, K. B. & HAMERMAN, J. A. 2013. Cutting Edge: Type I IFN Drives Emergency Myelopoiesis and Peripheral Myeloid Expansion during Chronic TLR7 Signaling. *The Journal of Immunology,* 190**,** 886-891.

BULEK, K., SWAIDANI, S., QIN, J., LU, Y., GULEN, M. F., HERJAN, T., MIN, B., KASTELEIN, R. A., ARONICA, M., KOSZ-VNENCHAK, M. & LI, X. 2009. The essential role of single Ig IL-1 receptor-related molecule/Toll IL-1R8 in regulation of Th2 immune response. *J Immunol,* 182**,** 2601-9.

BURKE, L., BUTLER, C. T., MURPHY, A., MORAN, B., GALLAGHER, W. M., O'SULLIVAN, J. & KENNEDY, B. N. 2016. Evaluation of Cysteinyl Leukotriene Signaling as a Therapeutic Target for Colorectal Cancer. *Frontiers in Cell and Developmental Biology,* 4**,** 103.

CALIFANO, D., CHO, JONATHAN J., UDDIN, MOHAMMAD N., LORENTSEN, KYLE J., YANG, Q., BHANDOOLA, A., LI, H. & AVRAM, D. 2015. Transcription Factor Bcl11b Controls Identity and Function of Mature Type 2 Innate Lymphoid Cells. *Immunity,* 43**,** 354-368.

CAMELO, A., ROSIGNOLI, G., OHNE, Y., STEWART, R. A., OVERED-SAYER, C., SLEEMAN, M. A. & MAY, R. D. 2017. IL-33, IL-25, and TSLP induce a distinct phenotypic and activation profile in human type 2 innate lymphoid cells. *Blood Advances,* 1**,** 577-589.

CANTOR, J. M. & GINSBERG, M. H. 2012. CD98 at the crossroads of adaptive immunity and cancer. *Journal of Cell Science,* 125**,** 1373-1382.

CARDOSO, V., CHESNÉ, J., RIBEIRO, H., GARCÍA-CASSANI, B., CARVALHO, T., BOUCHERY, T., SHAH, K., BARBOSA-MORAIS, N. L., HARRIS, N. & VEIGA-FERNANDES, H. 2017. Neuronal regulation of type 2 innate lymphoid cells via neuromedin U. *Nature,* 549**,** 277.

CARLIN, LEO M., STAMATIADES, EFSTATHIOS G., AUFFRAY, C., HANNA, RICHARD N., GLOVER, L., VIZCAY-BARRENA, G., HEDRICK, CATHERINE C., COOK, H. T., DIEBOLD, S. & GEISSMANN, F. 2013. Nr4a1-Dependent Ly6C^{low} Monocytes Monitor Endothelial Cells and Orchestrate Their Disposal. *Cell,* 153**,** 362-375.

CARNEIRO, P. J., CLEVELARIO, A. L., PADILHA, G. A., SILVA, J. D., KITOKO, J. Z., OLSEN, P. C., CAPELOZZI, V. L., ROCCO, P. R. & CRUZ, F. F. 2017. Bosutinib Therapy Ameliorates Lung Inflammation and Fibrosis in Experimental Silicosis. *Front Physiol,* 8**,** 159.

CARTER, E. E., BARR, S. G. & CLARKE, A. E. 2016. The global burden of SLE: prevalence, health disparities and socioeconomic impact. *Nat Rev Rheumatol,* 12**,** 605-20.

CASTER, D. J., KORTE, E. A., NANDA, S. K., MCLEISH, K. R., OLIVER, R. K., G'SELL R, T., SHEEHAN, R. M., FREEMAN, D. W., COVENTRY, S. C., KELLY, J. A., GUTHRIDGE, J. M., JAMES, J. A., SIVILS, K. L., ALARCON-RIQUELME, M. E., SCOFIELD, R. H., ADRIANTO, I., GAFFNEY, P. M., STEVENS, A. M., FREEDMAN, B. I., LANGEFELD, C. D., TSAO, B. P., PONS-ESTEL, B. A., JACOB, C. O., KAMEN, D. L., GILKESON, G. S., BROWN, E. E., ALARCON, G. S., EDBERG, J. C., KIMBERLY, R. P., MARTIN, J., MERRILL, J. T., HARLEY, J. B., KAUFMAN, K. M., REVEILLE, J. D., ANAYA, J. M., CRISWELL, L. A., VILA, L. M., PETRI, M., RAMSEY-GOLDMAN, R., BAE, S. C., BOACKLE, S. A., VYSE, T. J., NIEWOLD, T. B., COHEN, P. & POWELL, D. W. 2013. ABIN1 dysfunction as a genetic basis for lupus nephritis. *J Am Soc Nephrol,* 24**,** 1743-54.

CAUTIVO, K. M. & MOLOFSKY, A. B. 2016. Regulation of metabolic health and adipose tissue function by group 2 innate lymphoid cells. *European Journal of Immunology,* 46**,** 1315-1325.

CAYROL, C., DUVAL, A., SCHMITT, P., ROGA, S., CAMUS, M., STELLA, A., BURLET-SCHILTZ, O., GONZALEZ-DE-PEREDO, A. & GIRARD, J.-P. 2018. Environmental allergens induce allergic inflammation through proteolytic maturation of IL-33. *Nature Immunology,* 19**,** 375-385.

CAYROL, C. & GIRARD, J.-P. 2014. IL-33: an alarmin cytokine with crucial roles in innate immunity, inflammation and allergy. *Current Opinion in Immunology,* 31**,** 31-37.

CAYROL, C. & GIRARD, J. P. 2009. The IL-1-like cytokine IL-33 is inactivated after maturation by caspase-1. *Proc Natl Acad Sci U S A,* 106**,** 9021-6.

CELHAR, T. & FAIRHURST, A.-M. 2014. Toll-like receptors in systemic lupus erythematosus: potential for personalized treatment. *Frontiers in Pharmacology,* 5**,** 265.

CELLA, M., JARROSSAY, D., FACCHETTI, F., ALEBARDI, O., NAKAJIMA, H., LANZAVECCHIA, A. & COLONNA, M. 1999. Plasmacytoid monocytes migrate to inflamed lymph nodes and produce large amounts of type I interferon. *Nat Med,* 5**,** 919-23.

CHACKERIAN, A. A., OLDHAM, E. R., MURPHY, E. E., SCHMITZ, J., PFLANZ, S. & KASTELEIN, R. A. 2007. IL-1 receptor accessory protein and ST2 comprise the IL-33 receptor complex. *J Immunol,* 179**,** 2551-5.

CHEN, H., LIU, H. & QING, G. 2018. Targeting oncogenic Myc as a strategy for cancer treatment. *Signal Transduction and Targeted Therapy,* 3**,** 5.

CHEN, S., CHEN, B., WEN, Z., HUANG, Z. & YE, L. 2017. IL-33/ST2-mediated inflammation in macrophages is directly abrogated by IL-10 during rheumatoid arthritis. *Oncotarget,* 8**,** 32407-32418.

CHEN, W. Y., HONG, J., GANNON, J., KAKKAR, R. & LEE, R. T. 2015a. Myocardial pressure overload induces systemic inflammation through endothelial cell IL-33. *Proc Natl Acad Sci U S A,* 112**,** 7249-54.

CHEN, Y., YAN, H., SONG, Z., CHEN, F., WANG, H., NIU, J., SHI, X., ZHANG, D., ZHANG, N., ZHAI, Z., ZHONG, B., CHENG, L., QIAN, T. & HAO, F. 2015b. Downregulation of TNIP1 Expression Leads to Increased Proliferation of Human Keratinocytes and Severer Psoriasis-Like Conditions in an Imiquimod-Induced Mouse Model of Dermatitis. *PLoS One,* 10**,** e0127957.

CHENG, G., YU, A., DEE, M. J. & MALEK, T. R. 2013. IL-2R signaling is essential for functional maturation of regulatory T cells during thymic development. *J Immunol,* 190**,** 1567-75.

CHERRIER, M., SAWA, S. & EBERL, G. 2012. Notch, Id2, and RORgammat sequentially orchestrate the fetal development of lymphoid tissue inducer cells. *J Exp Med,* 209**,** 729-40.

CHOI, Y.-S., PARK, J. A., KIM, J., RHO, S.-S., PARK, H., KIM, Y.-M. & KWON, Y.-G. 2012. Nuclear IL-33 is a transcriptional regulator of NF-κB p65 and induces endothelial cell activation. *Biochemical and Biophysical Research Communications,* 421**,** 305-311.

CHOW, J. Y., WONG, C. K., CHEUNG, P. F. & LAM, C. W. 2010. Intracellular signaling mechanisms regulating the activation of human eosinophils by the novel Th2 cytokine IL-33: implications for allergic inflammation. *Cell Mol Immunol,* 7**,** 26-34.

CHRESTENSEN, C. A., SCHROEDER, M. J., SHABANOWITZ, J., HUNT, D. F., PELO, J. W., WORTHINGTON, M. T. & STURGILL, T. W. 2004. MAPKAP kinase 2 phosphorylates tristetraprolin on in vivo sites including Ser178, a site required for 14-3-3 binding. *J Biol Chem,* 279**,** 10176-84.

CHRISTENSEN, S. R., KASHGARIAN, M., ALEXOPOULOU, L., FLAVELL, R. A., AKIRA, S. & SHLOMCHIK, M. J. 2005. Toll-like receptor 9 controls anti-DNA autoantibody production in murine lupus. *The Journal of Experimental Medicine,* 202**,** 321-331.

CHRISTENSEN, S. R., SHUPE, J., NICKERSON, K., KASHGARIAN, M., FLAVELL, R. A. & SHLOMCHIK, M. J. 2006. Toll-like receptor 7 and TLR9 dictate autoantibody specificity and have opposing inflammatory and regulatory roles in a murine model of lupus. *Immunity,* 25**,** 417-28.

CLARK, K., NANDA, S. & COHEN, P. 2013. Molecular control of the NEMO family of ubiquitin-binding proteins. *Nat Rev Mol Cell Biol,* 14**,** 673-85.

CLEMENT, S. L., SCHECKEL, C., STOECKLIN, G. & LYKKE-ANDERSEN, J. 2011. Phosphorylation of Tristetraprolin by MK2 Impairs AU-Rich Element mRNA Decay by Preventing Deadenylase Recruitment. *Molecular and Cellular Biology,* 31**,** 256-266.

CLINICALTRIALS.GOV 2016. Effects of p38 Inhibitor AZD7624 in Corticosteroid Resistant Asthma.

COHEN, P. 2014. The TLR and IL-1 signalling network at a glance. *Journal of Cell Science,* 127**,** 2383-2390.

COHEN, P. & STRICKSON, S. 2017. The role of hybrid ubiquitin chains in the MyD88 and other innate immune signalling pathways. *Cell Death And Differentiation,* 24**,** 1153.

COHEN, S., ACHBERT-WEINER, H. & CIECHANOVER, A. 2004. Dual effects of IkappaB kinase beta-mediated phosphorylation on p105 Fate: SCF(beta-TrCP)-dependent degradation and SCF(beta-TrCP)-independent processing. *Mol Cell Biol,* 24**,** 475-86.

CORRAL, L., HANKE, T., VANCE, R. E., CADO, D. & RAULET, D. H. 2000. NK cell expression of the killer cell lectin-like receptor G1 (KLRG1), the mouse homolog of MAFA, is modulated by MHC class I molecules. *Eur J Immunol,* 30**,** 920-30.

CORREN, J. 2013. Role of interleukin-13 in asthma. *Curr Allergy Asthma Rep,* 13**,** 415-20.

COSTA, S., MARINI, O., BEVILACQUA, D., DEFRANCO, A. L., HOU, B., LONARDI, S., VERMI, W., RODEGHER, P., PANATO, A., TAGLIARO, F., LOWELL, C. A., CASSATELLA, M. A., GIROLOMONI, G. & SCAPINI, P. 2017. Role of MyD88 signaling in the imiquimod-induced mouse model of psoriasis: focus on innate myeloid cells. *J Leukoc Biol,* 102**,** 791-803.

COYLE, A. J., LEHAR, S., LLOYD, C., TIAN, J., DELANEY, T., MANNING, S., NGUYEN, T., BURWELL, T., SCHNEIDER, H., GONZALO, J. A., GOSSELIN, M., OWEN, L. R., RUDD, C. E. & GUTIERREZ-RAMOS, J. C. 2000. The CD28-related molecule ICOS is required for effective T cell-dependent immune responses. *Immunity,* 13**,** 95-105.

CROS, J., CAGNARD, N., WOOLLARD, K., PATEY, N., ZHANG, S.-Y., SENECHAL, B., PUEL, A., BISWAS, S. K., MOSHOUS, D., PICARD, C., JAIS, J.-P., D'CRUZ, D., CASANOVA, J.-L., TROUILLET, C. & GEISSMANN, F. 2010. Human CD14dim Monocytes Patrol and Sense Nucleic Acids and Viruses via TLR7 and TLR8 Receptors. *Immunity,* 33**,** 375-386.

CROTTY, S. 2014. T follicular helper cell differentiation, function, and roles in disease. *Immunity,* 41**,** 529-542.

CROW, M. K. & WOHLGEMUTH, J. 2003. Microarray analysis of gene expression in lupus. *Arthritis Res Ther,* 5**,** 279-87.

DANG, C. V., O'DONNELL, K. A., ZELLER, K. I., NGUYEN, T., OSTHUS, R. C. & LI, F. 2006. The c-Myc target gene network. *Seminars in Cancer Biology,* 16**,** 253-264.

DE, A., DAINICHI, T., RATHINAM, C. V. & GHOSH, S. 2014. The deubiquitinase activity of A20 is dispensable for NF-kappaB signaling. *EMBO Rep,* 15**,** 775-83.

DE BOER, J., WILLIAMS, A., SKAVDIS, G., HARKER, N., COLES, M., TOLAINI, M., NORTON, T., WILLIAMS, K., RODERICK, K., POTOCNIK, A. J. & KIOUSSIS, D. 2003. Transgenic mice with hematopoietic and lymphoid specific expression of Cre. *Eur J Immunol,* 33**,** 314-25.

DE BOER, J. D., YANG, J., VAN DEN BOOGAARD, F. E., HOOGENDIJK, A. J., DE BEER, R., VAN DER ZEE, J. S., ROELOFS, J. J., VAN 'T VEER, C., DE VOS, A. F. & VAN DER POLL, T. 2014. Mast cell-deficient kit mice develop house dust mite-induced lung inflammation despite impaired eosinophil recruitment. *J Innate Immun,* 6**,** 219-26.

DEANE, J. A., PISITKUN, P., BARRETT, R. S., FEIGENBAUM, L., TOWN, T., WARD, J. M., FLAVELL, R. A. & BOLLAND, S. 2007. Control of TLR7 expression is essential to restrict autoimmunity and dendritic cell expansion. *Immunity,* 27**,** 801-810.

DEGUINE, J. & BARTON, G. M. 2014. MyD88: a central player in innate immune signaling. *F1000Prime Reports,* 6**,** 97.

DENIS, O., VINCENT, M., HAVAUX, X., DE PRINS, S., TREUTENS, G. & HUYGEN, K. 2013. Induction of the specific allergic immune response is independent of proteases from the fungus Alternaria alternata. *Eur J Immunol,* 43**,** 907-17.

DENNING, D. W., O'DRISCOLL, B. R., HOGABOAM, C. M., BOWYER, P. & NIVEN, R. M. 2006. The link between fungi and severe asthma: a summary of the evidence. *Eur Respir J,* 27**,** 615-26.

DENNY, M. F., YALAVARTHI, S., ZHAO, W., THACKER, S. G., ANDERSON, M., SANDY, A. R., MCCUNE, W. J. & KAPLAN, M. J. 2010. A distinct subset of proinflammatory neutrophils isolated from patients with systemic lupus erythematosus induces vascular damage and synthesizes type I Interferons. *Journal of immunology (Baltimore, Md. : 1950),* 184**,** 3284-3297.

DESNUES, B., MACEDO, A. B., ORDONEZ-RUEDA, D., ROUSSEL-QUEVAL, A., MALISSEN, B., BRUHNS, P., MALISSEN, M. & ALEXOPOULOU, L. 2016. The transcriptional repressor Gfi1 prevents lupus autoimmunity by restraining TLR7 signaling. *Eur J Immunol,* 46**,** 2801-2811.

DIAZ-JIMENEZ, D., NUNEZ, L., DE LA FUENTE, M., DUBOIS-CAMACHO, K., SEPULVEDA, H., MONTECINO, M., TORRES-RIQUELME, A., GARCIA-GONZALEZ, P. & CHNAIDERMAN, J. 2017. A functional IL1RL1 variant regulates corticosteroid-induced sST2 expression in ulcerative colitis. 7**,** 10180.

DIEBOLD, S. S., KAISHO, T., HEMMI, H., AKIRA, S. & REIS E SOUSA, C. 2004. Innate antiviral responses by means of TLR7-mediated recognition of single-stranded RNA. *Science,* 303**,** 1529-31.

DIEPLINGER, B. & MUELLER, T. 2015. Soluble ST2 in heart failure. *Clin Chim Acta,* 443**,** 57-70.

DINARELLO, C., NOVICK, D., KIM, S. & KAPLANSKI, G. 2013. Interleukin-18 and IL-18 Binding Protein. *Frontiers in Immunology,* 4.

DINARELLO, C. A. 2011. Interleukin-1 in the pathogenesis and treatment of inflammatory diseases. *Blood,* 117**,** 3720-3732.

DIXIT, V. M., GREEN, S., SARMA, V., HOLZMAN, L. B., WOLF, F. W., O'ROURKE, K., WARD, P. A., PROCHOWNIK, E. V. & MARKS, R. M. 1990. Tumor necrosis factor-alpha induction of novel gene products in human endothelial cells including a macrophage-specific chemotaxin. *J Biol Chem,* 265**,** 2973-8.

DOHERTY, T. A., KHORRAM, N., LUND, S., MEHTA, A. K., CROFT, M. & BROIDE, D. H. 2013. Lung type 2 innate lymphoid cells express cysteinyl leukotriene receptor 1, which regulates T_H2 cytokine production. *Journal of Allergy and Clinical Immunology,* 132**,** 205-213.

DOHERTY, T. M., KASTELEIN, R., MENON, S., ANDRADE, S. & COFFMAN, R. L. 1993. Modulation of murine macrophage function by IL-13. *J Immunol,* 151**,** 7151-60.

DRAIJER, C., ROBBE, P., BOORSMA, C. E. & HYLKEMA, M. N. 2018. Dual role of YM1+ M2 macrophages in allergic lung inflammation. 8**,** 5105.

DRUBE, S., HEINK, S., WALTER, S., LOHN, T., GRUSSER, M., GERBAULET, A., BEROD, L., SCHONS, J., DUDECK, A., FREITAG, J., GROTHA, S., REICH, D., RUDESCHKO, O., NORGAUER, J., HARTMANN, K., ROERS,

A. & KAMRADT, T. 2010. The receptor tyrosine kinase c-Kit controls IL-33 receptor signaling in mast cells. *Blood,* 115**,** 3899-906.

DRUBE, S. & KRAFT, F. 2016. MK2/3 Are Pivotal for IL-33-Induced and Mast Cell-Dependent Leukocyte Recruitment and the Resulting Skin Inflammation. 197**,** 3662-3668.

DRUBE, S., KRAFT, F., DUDECK, J., MÜLLER, A.-L., WEBER, F., GÖPFERT, C., MEININGER, I., BEYER, M., IRMLER, I., HÄFNER, N., SCHÜTZ, D., STUMM, R., YAKOVLEVA, T., GAESTEL, M., DUDECK, A. & KAMRADT, T. 2016. MK2/3 Are Pivotal for IL-33–Induced and Mast Cell–Dependent Leukocyte Recruitment and the Resulting Skin Inflammation. *The Journal of Immunology,* 197**,** 3662-3668.

DUBEY, A. K., HANDU, S. S., DUBEY, S., SHARMA, P., SHARMA, K. K. & AHMED, Q. M. 2011. Belimumab: First targeted biological treatment for systemic lupus erythematosus. *Journal of Pharmacology & Pharmacotherapeutics,* 2**,** 317-319.

DUDHGAONKAR, S., RANADE, S., NAGAR, J., SUBRAMANI, S., PRASAD, D. S., KARUNANITHI, P., SRIVASTAVA, R., VENKATESH, K., SELVAM, S., KRISHNAMURTHY, P., MARIAPPAN, T. T., SAXENA, A., FAN, L., STETSKO, D. K., HOLLOWAY, D. A., LI, X., ZHU, J., YANG, W.-P., RUEPP, S., NAIR, S., SANTELLA, J., DUNCIA, J., HYNES, J., MCINTYRE, K. W. & CARMAN, J. A. 2017. Selective IRAK4 Inhibition Attenuates Disease in Murine Lupus Models and Demonstrates Steroid Sparing Activity. *The Journal of Immunology,* 198**,** 1308-1319.

DZIEDZIC, S. A., SU, Z., JEAN BARRETT, V., NAJAFOV, A., MOOKHTIAR, A. K., AMIN, P., PAN, H., SUN, L., ZHU, H., MA, A., ABBOTT, D. W. & YUAN, J. 2018. ABIN-1 regulates RIPK1 activation by linking Met1 ubiquitylation with Lys63 deubiquitylation in TNF-RSC. *Nature Cell Biology,* 20**,** 58-68.

EBERL, G., COLONNA, M., DI SANTO, J. P. & MCKENZIE, A. N. J. 2015. Innate lymphoid cells: A new paradigm in immunology. *Science,* 348.

EDER, L., CHANDRAN, V., PELLETT, F., POLLOCK, R., SHANMUGARAJAH, S., ROSEN, C. F., RAHMAN, P. & GLADMAN, D. D. 2011. IL13 gene polymorphism is a marker for psoriatic arthritis among psoriasis patients. *Ann Rheum Dis,* 70**,** 1594-8.

EMMERICH, C. H., ORDUREAU, A., STRICKSON, S., ARTHUR, J. S., PEDRIOLI, P. G., KOMANDER, D. & COHEN, P. 2013a. Activation of the canonical IKK complex by K63/M1-linked hybrid ubiquitin chains. *Proc Natl Acad Sci U S A,* 110**,** 15247-52.

ENDO, Y., HIRAHARA, K., IINUMA, T., SHINODA, K., TUMES, D. J., ASOU, H. K., MATSUGAE, N., OBATA-NINOMIYA, K., YAMAMOTO, H., MOTOHASHI, S., OBOKI, K., NAKAE, S., SAITO, H., OKAMOTO, Y. & NAKAYAMA, T. 2015. The interleukin-33-p38 kinase axis confers memory T helper 2 cell pathogenicity in the airway. *Immunity,* 42**,** 294-308.

EVERTS, B., AMIEL, E., VAN DER WINDT, G. J., FREITAS, T. C., CHOTT, R., YARASHESKI, K. E., PEARCE, E. L. & PEARCE, E. J. 2012. Commitment to glycolysis sustains survival of NO-producing inflammatory dendritic cells. *Blood,* 120**,** 1422-31.

FALLON, P. G., BALLANTYNE, S. J., MANGAN, N. E., BARLOW, J. L., DASVARMA, A., HEWETT, D. R., MCILGORM, A., JOLIN, H. E. & MCKENZIE, A. N. 2006. Identification of an interleukin (IL)-25-dependent

cell population that provides IL-4, IL-5, and IL-13 at the onset of helminth expulsion. *J Exp Med,* 203**,** 1105-16.

FAN, H., LIU, F., DONG, G., REN, D., XU, Y., DOU, J., WANG, T., SUN, L. & HOU, Y. 2014. Activation-induced necroptosis contributes to B-cell lymphopenia in active systemic lupus erythematosus. *Cell Death Dis,* 5**,** e1416.

FAN, Y., TAO, J. H., ZHANG, L. P., LI, L. H. & YE, D. Q. 2011. The association between BANK1 and TNFAIP3 gene polymorphisms and systemic lupus erythematosus: a meta-analysis. *Int J Immunogenet,* 38**,** 151-9.

FANG, M., LI, Y., HUANG, K., QI, S., ZHANG, J., ZGODZINSKI, W., MAJEWSKI, M., WALLNER, G., GOZDZ, S., MACEK, P., KOWALIK, A., PASIARSKI, M., GRYWALSKA, E., VATAN, L., NAGARSHETH, N., LI, W., ZHAO, L., KRYCZEK, I., WANG, G., WANG, Z., ZOU, W. & WANG, L. 2017. IL33 Promotes Colon Cancer Cell Stemness via JNK Activation and Macrophage Recruitment. *Cancer Research,* 77**,** 2735-2745.

FARKAS, L., BEISKE, K., LUND-JOHANSEN, F., BRANDTZAEG, P. & JAHNSEN, F. L. 2001. Plasmacytoid Dendritic Cells (Natural Interferon-α/β-Producing Cells) Accumulate in Cutaneous Lupus Erythematosus Lesions. *The American Journal of Pathology,* 159**,** 237-243.

FELTEN, R., DERVOVIC, E., CHASSET, F., GOTTENBERG, J. E., SIBILIA, J., SCHER, F. & ARNAUD, L. 2018. The 2018 pipeline of targeted therapies under clinical development for Systemic Lupus Erythematosus: a systematic review of trials. *Autoimmun Rev,* 17**,** 781-790.

FENG, C. G., SCANGA, C. A., COLLAZO-CUSTODIO, C. M., CHEEVER, A. W., HIENY, S., CASPAR, P. & SHER, A. 2003. Mice lacking myeloid differentiation factor 88 display profound defects in host resistance and immune responses to Mycobacterium avium infection not exhibited by Toll-like receptor 2 (TLR2)- and TLR4-deficient animals. *J Immunol,* 171**,** 4758-64.

FIIL, B. K., DAMGAARD, R. B., WAGNER, S. A., KEUSEKOTTEN, K., FRITSCH, M., BEKKER-JENSEN, S., MAILAND, N., CHOUDHARY, C., KOMANDER, D. & GYRD-HANSEN, M. 2013. OTULIN restricts Met1-linked ubiquitination to control innate immune signaling. *Mol Cell,* 50**,** 818-830.

FIORE, N., CASTELLANO, G., BLASI, A., CAPOBIANCO, C., LOVERRE, A., MONTINARO, V., NETTI, S., TORRES, D., MANNO, C., GRANDALIANO, G., RANIERI, E., SCHENA, F. P. & GESUALDO, L. 2008. Immature myeloid and plasmacytoid dendritic cells infiltrate renal tubulointerstitium in patients with lupus nephritis. *Mol Immunol,* 45**,** 259-65.

FITZGERALD, K. A., ROWE, D. C., BARNES, B. J., CAFFREY, D. R., VISINTIN, A., LATZ, E., MONKS, B., PITHA, P. M. & GOLENBOCK, D. T. 2003. LPS-TLR4 signaling to IRF-3/7 and NF-kappaB involves the toll adapters TRAM and TRIF. *J Exp Med,* 198**,** 1043-55.

FOGG, D. K., SIBON, C., MILED, C., JUNG, S., AUCOUTURIER, P., LITTMAN, D. R., CUMANO, A. & GEISSMANN, F. 2006. A clonogenic bone marrow progenitor specific for macrophages and dendritic cells. *Science,* 311**,** 83-7.

FORT, M. M., CHEUNG, J., YEN, D., LI, J., ZURAWSKI, S. M., LO, S., MENON, S., CLIFFORD, T., HUNTE, B., LESLEY, R., MUCHAMUEL, T., HURST, S. D., ZURAWSKI, G., LEACH, M. W., GORMAN, D. M. & RENNICK, D. M. 2001. IL-25 Induces IL-4, IL-5, and IL-13 and Th2-Associated Pathologies In Vivo. *Immunity,* 15**,** 985-995.

FOSTER, A. M., BALIWAG, J., CHEN, C. S., GUZMAN, A. M., STOLL, S. W., GUDJONSSON, J. E., WARD, N. L. & JOHNSTON, A. 2014. IL-36 promotes myeloid cell infiltration, activation and inflammatory activity in skin. *Journal of immunology (Baltimore, Md. : 1950),* 192**,** 6053-6061.

FOSTER, B. M. & ZAIDI, D. 2018. CD117/c-kit in Cancer Stem Cell-Mediated Progression and Therapeutic Resistance. 6.

FU, B., WANG, F., SUN, R., LING, B., TIAN, Z. & WEI, H. 2011. CD11b and CD27 reflect distinct population and functional specialization in human natural killer cells. *Immunology,* 133**,** 350-359.

FUNAKOSHI-TAGO, M., TAGO, K., HAYAKAWA, M., TOMINAGA, S.-I., OHSHIO, T., SONODA, Y. & KASAHARA, T. 2008. TRAF6 is a critical signal transducer in IL-33 signaling pathway. *Cellular Signalling,* 20**,** 1679-1686.

FURUKAWA, S., MORIYAMA, M., MIYAKE, K., NAKASHIMA, H., TANAKA, A., MAEHARA, T., IIZUKA-KOGA, M., TSUBOI, H., HAYASHIDA, J.-N., ISHIGURO, N., YAMAUCHI, M., SUMIDA, T. & NAKAMURA, S. 2017. Interleukin-33 produced by M2 macrophages and other immune cells contributes to Th2 immune reaction of IgG4-related disease. *Scientific Reports,* 7**,** 42413.

FURUSAWA, J.-I., MORO, K., MOTOMURA, Y., OKAMOTO, K., ZHU, J., TAKAYANAGI, H., KUBO, M. & KOYASU, S. 2013a. Critical Role of p38 and GATA3 in Natural Helper Cell Function. *The Journal of Immunology,* 191**,** 1818-1826.

G'SELL, R. T., GAFFNEY, P. M. & POWELL, D. W. 2015. Review: A20-Binding Inhibitor of NF-κB Activation 1 Is a Physiologic Inhibitor of NF-κB: A Molecular Switch for Inflammation and Autoimmunity. *Arthritis & Rheumatology,* 67**,** 2292-2302.

GAO, X., WANG, X., YANG, Q., ZHAO, X., WEN, W., LI, G., LU, J., QIN, W., QI, Y., XIE, F., JIANG, J., WU, C., ZHANG, X., CHEN, X., TURNQUIST, H., ZHU, Y. & LU, B. 2015. Tumoral Expression of IL-33 Inhibits Tumor Growth and Modifies the Tumor Microenvironment through CD8⁺ T and NK Cells. *The Journal of Immunology,* 194**,** 438-445.

GARCIA-ORTIZ, H., VELAZQUEZ-CRUZ, R., ESPINOSA-ROSALES, F., JIMENEZ-MORALES, S., BACA, V. & OROZCO, L. 2010. Association of TLR7 copy number variation with susceptibility to childhood-onset systemic lupus erythematosus in Mexican population. *Ann Rheum Dis,* 69**,** 1861-5.

GARDINER, C. M. & FINLAY, D. K. 2017. What Fuels Natural Killers? Metabolism and NK Cell Responses. *Frontiers in Immunology,* 8.

GARLANDA, C., DINARELLO, CHARLES A. & MANTOVANI, A. 2013. The Interleukin-1 Family: Back to the Future. *Immunity,* 39**,** 1003-1018.

GATEVA, V., SANDLING, J. K., HOM, G., TAYLOR, K. E., CHUNG, S. A., SUN, X., ORTMANN, W., KOSOY, R., FERREIRA, R. C., NORDMARK, G., GUNNARSSON, I., SVENUNGSSON, E., PADYUKOV, L., STURFELT, G., JONSEN, A., BENGTSSON, A. A., RANTAPAA-DAHLQVIST, S., BAECHLER, E. C., BROWN, E. E., ALARCON, G. S., EDBERG, J. C., RAMSEY-GOLDMAN, R., MCGWIN, G., JR., REVEILLE, J. D., VILA, L. M., KIMBERLY, R. P., MANZI, S., PETRI, M. A., LEE, A., GREGERSEN, P. K., SELDIN, M. F., RONNBLOM, L., CRISWELL, L. A., SYVANEN, A. C., BEHRENS, T. W. & GRAHAM, R. R. 2009. A large-scale replication

study identifies TNIP1, PRDM1, JAZF1, UHRF1BP1 and IL10 as risk loci for systemic lupus erythematosus. *Nat Genet,* 41**,** 1228-33.
GEISSMANN, F., JUNG, S. & LITTMAN, D. R. 2003. Blood monocytes consist of two principal subsets with distinct migratory properties. *Immunity,* 19**,** 71-82.
GEORGE, J., MOTSHWENE, P. G., WANG, H., KUBARENKO, A. V., RAUTANEN, A., MILLS, T. C., HILL, A. V., GAY, N. J. & WEBER, A. N. 2011. Two human MYD88 variants, S34Y and R98C, interfere with MyD88-IRAK4-myddosome assembly. *J Biol Chem,* 286**,** 1341-53.
GINHOUX, F. & JUNG, S. 2014. Monocytes and macrophages: developmental pathways and tissue homeostasis. *Nature Reviews Immunology,* 14**,** 392.
GINHOUX, F., LIU, K., HELFT, J., BOGUNOVIC, M., GRETER, M., HASHIMOTO, D., PRICE, J., YIN, N., BROMBERG, J., LIRA, S. A., STANLEY, E. R., NUSSENZWEIG, M. & MERAD, M. 2009. The origin and development of nonlymphoid tissue CD103⁺ DCs. *The Journal of Experimental Medicine,* 206**,** 3115-3130.
GLEASON, C. E., ORDUREAU, A., GOURLAY, R., ARTHUR, J. S. & COHEN, P. 2011. Polyubiquitin binding to optineurin is required for optimal activation of TANK-binding kinase 1 and production of interferon beta. *J Biol Chem,* 286**,** 35663-74.
GOH, E. T., ARTHUR, J. S., CHEUNG, P. C., AKIRA, S., TOTH, R. & COHEN, P. 2012. Identification of the protein kinases that activate the E3 ubiquitin ligase Pellino 1 in the innate immune system. *Biochem J,* 441**,** 339-46.
GOPFERT, C. & ANDREAS, N. 2018. The p38-MK2/3 Module Is Critical for IL-33-Induced Signaling and Cytokine Production in Dendritic Cells. 200**,** 1198-1206.
GÖPFERT, C., ANDREAS, N., WEBER, F., HÄFNER, N., YAKOVLEVA, T., GAESTEL, M., KAMRADT, T. & DRUBE, S. 2018. The p38-MK2/3 Module Is Critical for IL-33–Induced Signaling and Cytokine Production in Dendritic Cells. *The Journal of Immunology,* 200**,** 1198-1206.
GORSKA, M. M., LIANG, Q., STAFFORD, S. J., GOPLEN, N., DHARAJIYA, N., GUO, L., SUR, S., GAESTEL, M. & ALAM, R. 2007. MK2 controls the level of negative feedback in the NF-kappaB pathway and is essential for vascular permeability and airway inflammation. *J Exp Med,* 204**,** 1637-52.
GRAVINA, H. D., GOES, A. M., MURTA, S. M. & ROPERT, C. 2016. MyD88 Adapter-like (Mal)/TIRAP Is Required for Cytokine Production by Splenic Ly6CloTLR2hi but Not by Ly6ChiTLR2hi Monocytes during Trypanosoma cruzi Infection. *J Biol Chem,* 291**,** 23832-23841.
GREINER, E. F., GUPPY, M. & BRAND, K. 1994. Glucose is essential for proliferation and the glycolytic enzyme induction that provokes a transition to glycolytic energy production. *J Biol Chem,* 269**,** 31484-90.
GUMA, M., RONACHER, L., LIU-BRYAN, R., TAKAI, S., KARIN, M. & CORR, M. 2009. Caspase-1 Independent IL-1β Activation in Neutrophil Dependent Inflammation. *Arthritis and rheumatism,* 60**,** 3642-3650.
GUNDERSEN, M. D., GOLL, R., HOL, J., OLSEN, T., RISMO, R., SØRBYE, S. W., SUNDNES, O., HARALDSEN, G. & FLORHOLMEN, J. 2016. Loss of interleukin 33 expression in colonic crypts - a potential marker for disease remission in ulcerative colitis. *Scientific Reports,* 6**,** 35403.
GWINN, D. M., SHACKELFORD, D. B., EGAN, D. F., MIHAYLOVA, M. M., MERY, A., VASQUEZ, D. S., TURK, B. E. & SHAW, R. J. 2008. AMPK

phosphorylation of raptor mediates a metabolic checkpoint. *Mol Cell,* 30**,** 214-26.
HAASE, V. H. 2009. The VHL Tumor Suppressor: Master Regulator of HIF. *Current pharmaceutical design,* 15**,** 3895-3903.
HACKER, H., REDECKE, V., BLAGOEV, B., KRATCHMAROVA, I., HSU, L. C., WANG, G. G., KAMPS, M. P., RAZ, E., WAGNER, H., HACKER, G., MANN, M. & KARIN, M. 2006. Specificity in Toll-like receptor signalling through distinct effector functions of TRAF3 and TRAF6. *Nature,* 439**,** 204-7.
HALIM, T. Y. 2015. Group 2 innate lymphoid cells in disease. *Int Immunol*.
HALIM, TIMOTHEUS Y., STEER, CATHERINE A., MATHÄ, L., GOLD, MATTHEW J., MARTINEZ-GONZALEZ, I., MCNAGNY, KELLY M., MCKENZIE, ANDREW N. & TAKEI, F. 2014. Group 2 Innate Lymphoid Cells Are Critical for the Initiation of Adaptive T Helper 2 Cell-Mediated Allergic Lung Inflammation. *Immunity,* 40**,** 425-435.
HALIM, TIMOTHEUS Y. F., KRAUß, RAMONA H., SUN, ANN C. & TAKEI, F. 2012a. Lung Natural Helper Cells Are a Critical Source of Th2 Cell-Type Cytokines in Protease Allergen-Induced Airway Inflammation. *Immunity,* 36**,** 451-463.
HAMANN, I., UNTERWALDER, N., CARDONA, A. E., MEISEL, C., ZIPP, F., RANSOHOFF, R. M. & INFANTE-DUARTE, C. 2011. Analyses of phenotypic and functional characteristics of CX3CR1-expressing natural killer cells. *Immunology,* 133**,** 62-73.
HAMS, E., LOCKSLEY, R. M., MCKENZIE, A. N. & FALLON, P. G. 2013a. Cutting edge: IL-25 elicits innate lymphoid type 2 and type II NKT cells that regulate obesity in mice. *J Immunol,* 191**,** 5349-53.
HAMS, E., LOCKSLEY, R. M., MCKENZIE, A. N. J. & FALLON, P. G. 2013b. IL-25 elicits innate lymphoid type 2 and type II natural killer T cells that regulate obesity in mice(1). *Journal of immunology (Baltimore, Md. : 1950),* 191**,** 10.4049/jimmunol.1301176.
HAN, J. M., WU, D., DENROCHE, H. C., YAO, Y., VERCHERE, C. B. & LEVINGS, M. K. 2015. IL-33 Reverses an Obesity-Induced Deficit in Visceral Adipose Tissue ST2⁺ T Regulatory Cells and Ameliorates Adipose Tissue Inflammation and Insulin Resistance. *The Journal of Immunology,* 194**,** 4777-4783.
HARDIE, D. G., ROSS, F. A. & HAWLEY, S. A. 2012. AMPK: a nutrient and energy sensor that maintains energy homeostasis. *Nature Reviews Molecular Cell Biology,* 13**,** 251.
HARDMAN, C. S., PANOVA, V. & MCKENZIE, A. N. J. 2013. IL-33 citrine reporter mice reveal the temporal and spatial expression of IL-33 during allergic lung inflammation. *European Journal of Immunology,* 43**,** 488-498.
HARKINS, J. M., MOUSTAID-MOUSSA, N., CHUNG, Y. J., PENNER, K. M., PESTKA, J. J., NORTH, C. M. & CLAYCOMBE, K. J. 2004. Expression of interleukin-6 is greater in preadipocytes than in adipocytes of 3T3-L1 cells and C57BL/6J and ob/ob mice. *J Nutr,* 134**,** 2673-7.
HARRIS, S. G., PADILLA, J., KOUMAS, L., RAY, D. & PHIPPS, R. P. 2002. Prostaglandins as modulators of immunity. *Trends in Immunology,* 23**,** 144-150.
HAVAUX, X., ZEINE, A., DITS, A. & DENIS, O. 2005. A new mouse model of lung allergy induced by the spores of Alternaria alternata and Cladosporium herbarum molds. *Clin Exp Immunol,* 139**,** 179-88.

HAWLEY, S. A., BOUDEAU, J., REID, J. L., MUSTARD, K. J., UDD, L., MAKELA, T. P., ALESSI, D. R. & HARDIE, D. G. 2003. Complexes between the LKB1 tumor suppressor, STRAD alpha/beta and MO25 alpha/beta are upstream kinases in the AMP-activated protein kinase cascade. *J Biol,* 2**,** 28.

HAWLEY, S. A., PAN, D. A., MUSTARD, K. J., ROSS, L., BAIN, J., EDELMAN, A. M., FRENGUELLI, B. G. & HARDIE, D. G. 2005. Calmodulin-dependent protein kinase kinase-beta is an alternative upstream kinase for AMP-activated protein kinase. *Cell Metab,* 2**,** 9-19.

HAYAKAWA, M., HAYAKAWA, H., PETROVA, T., RITPRAJAK, P., SUTAVANI, R. V., JIMÉNEZ-ANDRADE, G. Y., SANO, Y., CHOO, M.-K., SEAVITT, J., VENIGALLA, R. K. C., OTSU, K., GEORGOPOULOS, K., ARTHUR, J. S. C. & PARK, J. M. 2017. Loss of Functionally Redundant p38 Isoforms in T Cells Enhances Regulatory T Cell Induction. *The Journal of Biological Chemistry,* 292**,** 1762-1772.

HAYAKAWA, M., YANAGISAWA, K., AOKI, S., HAYAKAWA, H., TAKEZAKO, N. & TOMINAGA, S. 2005. T-helper type 2 cell-specific expression of the ST2 gene is regulated by transcription factor GATA-3. *Biochim Biophys Acta,* 1728**,** 53-64.

HAYASHI, F., SMITH, K. D., OZINSKY, A., HAWN, T. R., YI, E. C., GOODLETT, D. R., ENG, J. K., AKIRA, S., UNDERHILL, D. M. & ADEREM, A. 2001. The innate immune response to bacterial flagellin is mediated by Toll-like receptor 5. *Nature,* 410**,** 1099.

HE, C. F., LIU, Y. S., CHENG, Y. L., GAO, J. P., PAN, T. M., HAN, J. W., QUAN, C., SUN, L. D., ZHENG, H. F., ZUO, X. B., XU, S. X., SHENG, Y. J., YAO, S., HU, W. L., LI, Y., YU, Z. Y., YIN, X. Y., ZHANG, X. J., CUI, Y. & YANG, S. 2010. TNIP1, SLC15A4, ETS1, RasGRP3 and IKZF1 are associated with clinical features of systemic lupus erythematosus in a Chinese Han population. *Lupus,* 19**,** 1181-6.

HE, Z., CHEN, L., SOUTO, F. O., CANASTO-CHIBUQUE, C., BONGERS, G., DESHPANDE, M., HARPAZ, N., KO, H. M., KELLEY, K., FURTADO, G. C. & LIRA, S. A. 2017. Epithelial-derived IL-33 promotes intestinal tumorigenesis in Apc Min/+ mice. *Scientific Reports,* 7**,** 5520.

HEGER, K., WICKLIFFE, K. E., NDOJA, A., ZHANG, J., MURTHY, A., DUGGER, D. L., MALTZMAN, A., DE SOUSA, E. M. F., HUNG, J., ZENG, Y., VERSCHUEREN, E., KIRKPATRICK, D. S., VUCIC, D., LEE, W. P., ROOSE-GIRMA, M., NEWMAN, R. J., WARMING, S., HSIAO, Y. C., KOMUVES, L. G., WEBSTER, J. D., NEWTON, K. & DIXIT, V. M. 2018. OTULIN limits cell death and inflammation by deubiquitinating LUBAC. *Nature,* 559**,** 120-124.

HEIL, F., HEMMI, H., HOCHREIN, H., AMPENBERGER, F., KIRSCHNING, C., AKIRA, S., LIPFORD, G., WAGNER, H. & BAUER, S. 2004. Species-specific recognition of single-stranded RNA via toll-like receptor 7 and 8. *Science,* 303**,** 1526-9.

HETTINGER, J., RICHARDS, D. M., HANSSON, J., BARRA, M. M., JOSCHKO, A.-C., KRIJGSVELD, J. & FEUERER, M. 2013. Origin of monocytes and macrophages in a committed progenitor. *Nature Immunology,* 14**,** 821.

HEYEN, L., MULLER, U., SIEGEMUND, S., SCHULZE, B., PROTSCHKA, M., ALBER, G. & PIEHLER, D. 2016. Lung epithelium is the major source of IL-33 and is regulated by IL-33-dependent and IL-33-independent mechanisms in pulmonary cryptococcosis. *Pathog Dis,* 74.

HEYNINCK, K., DE VALCK, D., BERGHE, W. V., VAN CRIEKINGE, W., CONTRERAS, R., FIERS, W., HAEGEMAN, G. & BEYAERT, R. 1999. The Zinc Finger Protein A20 Inhibits TNF-induced NF-κB–dependent Gene Expression by Interfering with an RIP- or TRAF2-mediated Transactivation Signal and Directly Binds to a Novel NF-κB–inhibiting Protein ABIN. *The Journal of Cell Biology,* 145**,** 1471-1482.

HEYNINCK, K., KREIKE, M. M. & BEYAERT, R. 2003. Structure–function analysis of the A20-binding inhibitor of NF-κB activation, ABIN-1. *FEBS Letters,* 536**,** 135-140.

HITTI, E., IAKOVLEVA, T., BROOK, M., DEPPENMEIER, S., GRUBER, A. D., RADZIOCH, D., CLARK, A. R., BLACKSHEAR, P. J., KOTLYAROV, A. & GAESTEL, M. 2006. Mitogen-Activated Protein Kinase-Activated Protein Kinase 2 Regulates Tumor Necrosis Factor mRNA Stability and Translation Mainly by Altering Tristetraprolin Expression, Stability, and Binding to Adenine/Uridine-Rich Element. *Molecular and Cellular Biology,* 26**,** 2399-2407.

HOSHINO, K., TAKEUCHI, O., KAWAI, T., SANJO, H., OGAWA, T., TAKEDA, Y., TAKEDA, K. & AKIRA, S. 1999. Cutting edge: Toll-like receptor 4 (TLR4)-deficient mice are hyporesponsive to lipopolysaccharide: evidence for TLR4 as the Lps gene product. *J Immunol,* 162**,** 3749-52.

HOYLER, T., KLOSE, C. S., SOUABNI, A., TURQUETI-NEVES, A., PFEIFER, D., RAWLINS, E. L., VOEHRINGER, D., BUSSLINGER, M. & DIEFENBACH, A. 2012a. The transcription factor GATA-3 controls cell fate and maintenance of type 2 innate lymphoid cells. *Immunity,* 37**,** 634-48.

HUANG, C.-Y., BREDEMEYER, A. L., WALKER, L. M., BASSING, C. H. & SLECKMAN, B. P. 2008. Dynamic regulation of c-Myc proto-oncogene expression during lymphocyte development revealed by a GFP-c-Myc knock-in mouse. *European Journal of Immunology,* 38**,** 342-349.

HUANG, Q., NIU, Z., TAN, J., YANG, J., LIU, Y., MA, H., LEE, V. W., SUN, S., SONG, X., GUO, M., WANG, Y. & CAO, Q. 2015. IL-25 Elicits Innate Lymphoid Cells and Multipotent Progenitor Type 2 Cells That Reduce Renal Ischemic/Reperfusion Injury. *J Am Soc Nephrol,* 26**,** 2199-211.

HUANG, Y., GUO, L., QIU, J., CHEN, X., HU-LI, J., SIEBENLIST, U., WILLIAMSON, P. R., URBAN JR, J. F. & PAUL, W. E. 2014. IL-25-responsive, lineage-negative KLRG1hi cells are multipotential 'inflammatory' type 2 innate lymphoid cells. *Nature Immunology,* 16**,** 161.

HUEBER, A. J., ALVES-FILHO, J. C., ASQUITH, D. L., MICHELS, C., MILLAR, N. L., REILLY, J. H., GRAHAM, G. J., LIEW, F. Y., MILLER, A. M. & MCINNES, I. B. 2011. IL-33 induces skin inflammation with mast cell and neutrophil activation. *Eur J Immunol,* 41**,** 2229-37.

HUNG, L.-Y., LEWKOWICH, I. P., DAWSON, L. A., DOWNEY, J., YANG, Y., SMITH, D. E. & HERBERT, D. B. R. 2013. IL-33 drives biphasic IL-13 production for noncanonical Type 2 immunity against hookworms. *Proceedings of the National Academy of Sciences of the United States of America,* 110**,** 282-287.

INDHUMATHI, S., RAJAPPA, M., CHANDRASHEKAR, L., ANANTHANARAYANAN, P. H., THAPPA, D. M. & NEGI, V. S. 2015. TNFAIP3 and TNIP1 polymorphisms confer psoriasis risk in South Indian Tamils. *Br J Biomed Sci,* 72**,** 168-73.

INOKI, K., LI, Y., XU, T. & GUAN, K. L. 2003a. Rheb GTPase is a direct target of TSC2 GAP activity and regulates mTOR signaling. *Genes Dev,* 17**,** 1829-34.

INOKI, K., LI, Y., ZHU, T., WU, J. & GUAN, K.-L. 2002. TSC2 is phosphorylated and inhibited by Akt and suppresses mTOR signalling. *Nature Cell Biology,* 4**,** 648.

INOUE, H., KATO, R., FUKUYAMA, S., NONAMI, A., TANIGUCHI, K., MATSUMOTO, K., NAKANO, T., TSUDA, M., MATSUMURA, M., KUBO, M., ISHIKAWA, F., MOON, B.-G., TAKATSU, K., NAKANISHI, Y. & YOSHIMURA, A. 2005. Spred-1 negatively regulates allergen-induced airway eosinophilia and hyperresponsiveness. *The Journal of Experimental Medicine,* 201**,** 73-82.

ITALIANI, P., MANCA, M. L., ANGELOTTI, F., MELILLO, D., PRATESI, F., PUXEDDU, I., BORASCHI, D. & MIGLIORINI, P. 2018. IL-1 family cytokines and soluble receptors in systemic lupus erythematosus. 20**,** 27.

ITO, T., SMRZ, D., JUNG, M. Y., BANDARA, G., DESAI, A., SMRZOVA, S., KUEHN, H. S., BEAVEN, M. A., METCALFE, D. D. & GILFILLAN, A. M. 2012. Stem cell factor programs the mast cell activation phenotype. *J Immunol,* 188**,** 5428-37.

JAEGER, B. N. & VIVIER, E. 2012. Natural killer cell tolerance: control by self or self-control? *Cold Spring Harb Perspect Biol,* 4.

JAIN, S., PARK, G., SPROULE, T. J., CHRISTIANSON, G. J., LEETH, C. M., WANG, H., ROOPENIAN, D. C. & MORSE, H. C., III 2016. Interleukin 6 Accelerates Mortality by Promoting the Progression of the Systemic Lupus Erythematosus-Like Disease of BXSB.Yaa Mice. *PLOS ONE,* 11**,** e0153059.

JAKUBZICK, C. V., RANDOLPH, G. J. & HENSON, P. M. 2017. Monocyte differentiation and antigen-presenting functions. *Nature Reviews Immunology,* 17**,** 349.

JANEWAY, C. A., JR. 1989. Approaching the asymptote? Evolution and revolution in immunology. *Cold Spring Harb Symp Quant Biol,* 54 Pt 1**,** 1-13.

JONES, R. G. & PEARCE, E. J. 2017. MenTORing Immunity: mTOR Signaling in the Development and Function of Tissue-Resident Immune Cells. *Immunity,* 46**,** 730-742.

JONJIC, S. 2010. Functional plasticity and robustness are essential characteristics of biological systems: lessons learned from KLRG1-deficient mice. *Eur J Immunol,* 40**,** 1241-3.

JUNG, S., ALIBERTI, J., GRAEMMEL, P., SUNSHINE, M. J., KREUTZBERG, G. W., SHER, A. & LITTMAN, D. R. 2000. Analysis of Fractalkine Receptor CX(3)CR1 Function by Targeted Deletion and Green Fluorescent Protein Reporter Gene Insertion. *Molecular and Cellular Biology,* 20**,** 4106-4114.

KAGAN, J. C., SU, T., HORNG, T., CHOW, A., AKIRA, S. & MEDZHITOV, R. 2008. TRAM couples endocytosis of Toll-like receptor 4 to the induction of interferon-beta. *Nat Immunol,* 9**,** 361-8.

KAKKAR, R., HEI, H., DOBNER, S. & LEE, R. T. 2012. Interleukin 33 as a mechanically responsive cytokine secreted by living cells. *J Biol Chem,* 287**,** 6941-8.

KAPLAN, M. J. *Nat Med*.

KAWAI, T. & AKIRA, S. 2010a. The role of pattern-recognition receptors in innate immunity: update on Toll-like receptors. *Nature Immunology,* 11**,** 373.

KAWAI, T. & AKIRA, S. 2011. Toll-like Receptors and Their Crosstalk with Other Innate Receptors in Infection and Immunity. *Immunity,* 34**,** 637-650.

KENNY, E. F., TALBOT, S., GONG, M., GOLENBOCK, D. T., BRYANT, C. E. & O'NEILL, L. A. 2009. MyD88 adaptor-like is not essential for TLR2 signaling and inhibits signaling by TLR3. *J Immunol,* 183**,** 3642-51.

KEUSEKOTTEN, K., ELLIOTT, P. R., GLOCKNER, L., FIIL, B. K., DAMGAARD, R. B., KULATHU, Y., WAUER, T., HOSPENTHAL, M. K., GYRD-HANSEN, M., KRAPPMANN, D., HOFMANN, K. & KOMANDER, D. 2013. OTULIN antagonizes LUBAC signaling by specifically hydrolyzing Met1-linked polyubiquitin. *Cell,* 153**,** 1312-26.

KIM, B. S., SIRACUSA, M. C., SAENZ, S. A., NOTI, M., MONTICELLI, L. A., SONNENBERG, G. F., HEPWORTH, M. R., VAN VOORHEES, A. S., COMEAU, M. R. & ARTIS, D. 2013. TSLP elicits IL-33–independent innate lymphoid cell responses to promote skin inflammation. *Science translational medicine,* 5**,** 170ra16-170ra16.

KIM, C. S., CHO, S. H., CHUN, H. S., LEE, S. Y., ENDOU, H., KANAI, Y. & KIM, D. K. 2008. BCH, an inhibitor of system L amino acid transporters, induces apoptosis in cancer cells. *Biol Pharm Bull,* 31**,** 1096-100.

KIROU, K. A., LEE, C., GEORGE, S., LOUCA, K., PAPAGIANNIS, I. G., PETERSON, M. G., LY, N., WOODWARD, R. N., FRY, K. E., LAU, A. Y., PRENTICE, J. G., WOHLGEMUTH, J. G. & CROW, M. K. 2004. Coordinate overexpression of interferon-alpha-induced genes in systemic lupus erythematosus. *Arthritis Rheum,* 50**,** 3958-67.

KITAGAWA, D., YOKOTA, K., GOUDA, M., NARUMI, Y., OHMOTO, H., NISHIWAKI, E., AKITA, K. & KIRII, Y. 2013. Activity-based kinase profiling of approved tyrosine kinase inhibitors. *Genes Cells,* 18**,** 110-22.

KLEIN WOLTERINK, R. G., KLEINJAN, A., VAN NIMWEGEN, M., BERGEN, I., DE BRUIJN, M., LEVANI, Y. & HENDRIKS, R. W. 2012. Pulmonary innate lymphoid cells are major producers of IL-5 and IL-13 in murine models of allergic asthma. *Eur J Immunol,* 42**,** 1106-16.

KLOSE, C. S. N. & ARTIS, D. 2016. Innate lymphoid cells as regulators of immunity, inflammation and tissue homeostasis. *Nature Immunology,* 17**,** 765.

KLOSE, C. S. N., MAHLAKÕIV, T., MOELLER, J. B., RANKIN, L. C., FLAMAR, A.-L., KABATA, H., MONTICELLI, L. A., MORIYAMA, S., PUTZEL, G. G., RAKHILIN, N., SHEN, X., KOSTENIS, E., KÖNIG, G. M., SENDA, T., CARPENTER, D., FARBER, D. L. & ARTIS, D. 2017. The neuropeptide neuromedin U stimulates innate lymphoid cells and type 2 inflammation. *Nature,* 549**,** 282.

KO, H.-J. & CHANG, S.-Y. 2015. Regulation of Intestinal Immune System by Dendritic Cells. *Immune Network,* 15**,** 1-8.

KOBAYASHI, K., HERNANDEZ, L. D., GALAN, J. E., JANEWAY, C. A., JR., MEDZHITOV, R. & FLAVELL, R. A. 2002. IRAK-M is a negative regulator of Toll-like receptor signaling. *Cell,* 110**,** 191-202.

KOHYAMA, M., ISE, W., EDELSON, B. T., WILKER, P. R., HILDNER, K., MEJIA, C., FRAZIER, W. A., MURPHY, T. L. & MURPHY, K. M. 2009. Role for Spi-C in the development of red pulp macrophages and splenic iron homeostasis. *Nature,* 457**,** 318-21.

KOMAI-KOMA, M., GILCHRIST, D. S., MCKENZIE, A. N. J., GOODYEAR, C. S., XU, D. & LIEW, F. Y. 2011. IL-33 Activates B1 Cells and Exacerbates Contact Sensitivity. *The Journal of Immunology,* 186**,** 2584-2591.

KONDO, T., KAWAI, T. & AKIRA, S. 2012. Dissecting negative regulation of Toll-like receptor signaling. *Trends Immunol,* 33**,** 449-58.

KONYA, V. & MJÖSBERG, J. 2016. Lipid mediators as regulators of human ILC2 function in allergic diseases. *Immunology Letters,* 179**,** 36-42.

KOPF, M., BAUMANN, H., FREER, G., FREUDENBERG, M., LAMERS, M., KISHIMOTO, T., ZINKERNAGEL, R., BLUETHMANN, H. & KOHLER, G. 1994. Impaired immune and acute-phase responses in interleukin-6-deficient mice. *Nature,* 368**,** 339-42.

KORENBLAT, P., KERWIN, E., LESHCHENKO, I., YEN, K., HOLWEG, C. T. J., ANZURES-CABRERA, J., MARTIN, C., PUTNAM, W. S., GOVERNALE, L., OLSSON, J. & MATTHEWS, J. G. 2018. Efficacy and safety of lebrikizumab in adult patients with mild-to-moderate asthma not receiving inhaled corticosteroids. *Respir Med,* 134**,** 143-149.

KOTLYAROV, A., NEININGER, A., SCHUBERT, C., ECKERT, R., BIRCHMEIER, C., VOLK, H.-D. & GAESTEL, M. 1999a. MAPKAP kinase 2 is essential for LPS-induced TNF-α biosynthesis. *Nature Cell Biology,* 1**,** 94.

KOTLYAROV, A., YANNONI, Y., FRITZ, S., LAAß, K., TELLIEZ, J.-B., PITMAN, D., LIN, L.-L. & GAESTEL, M. 2002. Distinct Cellular Functions of MK2. *Molecular and Cellular Biology,* 22**,** 4827-4835.

KOUZAKI, H., IIJIMA, K., KOBAYASHI, T., O'GRADY, S. M. & KITA, H. 2011. The Danger Signal, Extracellular ATP, Is a Sensor for an Airborne Allergen and Triggers IL-33 Release and Innate Th2-Type Responses. *The Journal of Immunology,* 186**,** 4375.

KOVALENKO, A., CHABLE-BESSIA, C., CANTARELLA, G., ISRAEL, A., WALLACH, D. & COURTOIS, G. 2003. The tumour suppressor CYLD negatively regulates NF-kappaB signalling by deubiquitination. *Nature,* 424**,** 801-5.

KROEGER, K. M., SULLIVAN, B. M. & LOCKSLEY, R. M. 2009. IL-18 and IL-33 elicit Th2 cytokines from basophils via a MyD88- and p38alpha-dependent pathway. *J Leukoc Biol,* 86**,** 769-78.

KUCHLER, A. M., POLLHEIMER, J., BALOGH, J., SPONHEIM, J., MANLEY, L., SORENSEN, D. R., DE ANGELIS, P. M., SCOTT, H. & HARALDSEN, G. 2008. Nuclear interleukin-33 is generally expressed in resting endothelium but rapidly lost upon angiogenic or proinflammatory activation. *Am J Pathol,* 173**,** 1229-42.

KUHN, A., HERRMANN, M., KLEBER, S., BECKMANN-WELLE, M., FEHSEL, K., MARTIN-VILLALBA, A., LEHMANN, P., RUZICKA, T., KRAMMER, P. H. & KOLB-BACHOFEN, V. 2006. Accumulation of apoptotic cells in the epidermis of patients with cutaneous lupus erythematosus after ultraviolet irradiation. *Arthritis Rheum,* 54**,** 939-50.

KUMAR, S., MINNICH, M. D. & YOUNG, P. R. 1995. ST2/T1 protein functionally binds to two secreted proteins from Balb/c 3T3 and human umbilical vein endothelial cells but does not bind interleukin 1. *J Biol Chem,* 270**,** 27905-13.

KUROTAKI, D., OSATO, N., NISHIYAMA, A., YAMAMOTO, M., BAN, T., SATO, H., NAKABAYASHI, J., UMEHARA, M., MIYAKE, N., MATSUMOTO, N., NAKAZAWA, M., OZATO, K. & TAMURA, T. 2013. Essential role of the IRF8-KLF4 transcription factor cascade in murine monocyte differentiation. *Blood,* 121**,** 1839-1849.

KUROWSKA-STOLARSKA, M., KEWIN, P., MURPHY, G., RUSSO, R. C., STOLARSKI, B., GARCIA, C. C., KOMAI-KOMA, M., PITMAN, N., LI, Y., MCKENZIE, A. N. J., TEIXEIRA, M. M., LIEW, F. Y. & XU, D. 2008. IL-33 Induces Antigen-Specific IL-5⁺ T Cells and Promotes

Allergic-Induced Airway Inflammation Independent of IL-4. *The Journal of Immunology,* 181**,** 4780-4790.

KURT-JONES, E. A., POPOVA, L., KWINN, L., HAYNES, L. M., JONES, L. P., TRIPP, R. A., WALSH, E. E., FREEMAN, M. W., GOLENBOCK, D. T., ANDERSON, L. J. & FINBERG, R. W. 2000. Pattern recognition receptors TLR4 and CD14 mediate response to respiratory syncytial virus. *Nat Immunol,* 1**,** 398-401.

LAM, M., HULL, L., IMRIE, A., SNIDVONGS, K., CHIN, D., PRATT, E., KALISH, L., SACKS, R., EARLS, P., SEWELL, W. & HARVEY, R. J. 2015. Interleukin-25 and interleukin-33 as mediators of eosinophilic inflammation in chronic rhinosinusitis. *Am J Rhinol Allergy,* 29**,** 175-81.

LAPLANTE, M. & SABATINI, D. M. 2009. mTOR signaling at a glance. *Journal of Cell Science,* 122**,** 3589-3594.

LAWLESS, S. J., KEDIA-MEHTA, N., WALLS, J. F., MCGARRIGLE, R., CONVERY, O., SINCLAIR, L. V., NAVARRO, M. N., MURRAY, J. & FINLAY, D. K. 2017. Glucose represses dendritic cell-induced T cell responses. *Nature Communications,* 8**,** 15620.

LEADBETTER, E. A., RIFKIN, I. R., HOHLBAUM, A. M., BEAUDETTE, B. C., SHLOMCHIK, M. J. & MARSHAK-ROTHSTEIN, A. 2002. Chromatin–IgG complexes activate B cells by dual engagement of IgM and Toll-like receptors. *Nature,* 416**,** 603.

LEE, E. G., BOONE, D. L., CHAI, S., LIBBY, S. L., CHIEN, M., LODOLCE, J. P. & MA, A. 2000. Failure to Regulate TNF-Induced NF-κB and Cell Death Responses in A20-Deficient Mice. *Science (New York, N.Y.),* 289**,** 2350-2354.

LEFRANCAIS, E., DUVAL, A., MIREY, E., ROGA, S., ESPINOSA, E., CAYROL, C. & GIRARD, J. P. 2014. Central domain of IL-33 is cleaved by mast cell proteases for potent activation of group-2 innate lymphoid cells. *Proc Natl Acad Sci U S A,* 111**,** 15502-7.

LEMAITRE, B., NICOLAS, E., MICHAUT, L., REICHHART, J.-M. & HOFFMANN, J. A. 1996. The Dorsoventral Regulatory Gene Cassette spätzle/Toll/cactus Controls the Potent Antifungal Response in Drosophila Adults. *Cell,* 86**,** 973-983.

LI, C., MAILLET, I., MACKOWIAK, C., VIALA, C., DI PADOVA, F., LI, M., TOGBE, D., QUESNIAUX, V., LAI, Y. & RYFFEL, B. 2017. Experimental atopic dermatitis depends on IL-33R signaling via MyD88 in dendritic cells. *Cell Death Dis,* 8**,** e2735.

LI, J., SARUTA, K., DUMOUCHEL, J. P., MAGAT, J. M., THOMAS, J. L., AJAMI, D., REBEK, M., REBEK, J. & BIGBY, T. D. 2018a. Small Molecule Mimetics of α-Helical Domain of IRAK2 Attenuate the Proinflammatory Effects of IL-33 in Asthma-like Mouse Models. *The Journal of Immunology,* 200**,** 4036-4043.

LI, R., YANG, G., YANG, R., PENG, X. & LI, J. 2015. Interleukin-33 and receptor ST2 as indicators in patients with asthma: a meta-analysis. *Int J Clin Exp Med,* 8**,** 14935-43.

LI, X.-D. & CHEN, Z. J. 2012. Sequence specific detection of bacterial 23S ribosomal RNA by TLR13. *eLife,* 1**,** e00102.

LI, Y., INOKI, K., VACRATSIS, P. & GUAN, K. L. 2003. The p38 and MK2 kinase cascade phosphorylates tuberin, the tuberous sclerosis 2 gene product, and enhances its interaction with 14-3-3. *J Biol Chem,* 278**,** 13663-71.

LIAO, X., REN, J., REIHL, A., PIRAPAKARAN, T., SREEKUMAR, B., CECERE, T. E., REILLY, C. M. & LUO, X. M. 2017. Renal-infiltrating CD11c+ cells are pathogenic in murine lupus nephritis through promoting CD4+ T cell responses. *Clinical & Experimental Immunology,* 190**,** 187-200.

LIM, S. S., BAYAKLY, A. R., HELMICK, C. G., GORDON, C., EASLEY, K. A. & DRENKARD, C. 2014. The incidence and prevalence of systemic lupus erythematosus, 2002-2004: The Georgia Lupus Registry. *Arthritis Rheumatol,* 66**,** 357-68.

LIN, J., HANDSCHIN, C. & SPIEGELMAN, B. M. 2005. Metabolic control through the PGC-1 family of transcription coactivators. *Cell Metabolism,* 1**,** 361-370.

LINGEL, A., WEISS, T. M., NIEBUHR, M., PAN, B., APPLETON, B. A., WIESMANN, C., BAZAN, J. F. & FAIRBROTHER, W. J. 2009. Structure of IL-33 and Its Interaction with the ST2 and IL-1RAcP Receptors—Insight into Heterotrimeric IL-1 Signaling Complexes. *Structure,* 17**,** 1398-1410.

LIU, T., ZHANG, L., JOO, D. & SUN, S.-C. 2017. NF-κB signaling in inflammation. *Signal Transduction And Targeted Therapy,* 2**,** 17023.

LOFTUS, R. M., ASSMANN, N., KEDIA-MEHTA, N., O'BRIEN, K. L., GARCIA, A., GILLESPIE, C., HUKELMANN, J. L., OEFNER, P. J., LAMOND, A. I., GARDINER, C. M., DETTMER, K., CANTRELL, D. A., SINCLAIR, L. V. & FINLAY, D. K. 2018. Amino acid-dependent cMyc expression is essential for NK cell metabolic and functional responses in mice. *Nature Communications,* 9**,** 2341.

LOGIE, L., RUIZ-ALCARAZ, A. J., KEANE, M., WOODS, Y. L., BAIN, J., MARQUEZ, R., ALESSI, D. R. & SUTHERLAND, C. 2007. Characterization of a protein kinase B inhibitor in vitro and in insulin-treated liver cells. *Diabetes,* 56**,** 2218-27.

LOHNING, M., STROEHMANN, A., COYLE, A. J., GROGAN, J. L., LIN, S., GUTIERREZ-RAMOS, J. C., LEVINSON, D., RADBRUCH, A. & KAMRADT, T. 1998. T1/ST2 is preferentially expressed on murine Th2 cells, independent of interleukin 4, interleukin 5, and interleukin 10, and important for Th2 effector function. *Proc Natl Acad Sci U S A,* 95**,** 6930-5.

LOOD, C., BLANCO, L. P., PURMALEK, M. M., CARMONA-RIVERA, C., DE RAVIN, S. S., SMITH, C. K. & MALECH, H. L. 2016. Neutrophil extracellular traps enriched in oxidized mitochondrial DNA are interferogenic and contribute to lupus-like disease. 22**,** 146-53.

LORK, M., VERHELST, K. & BEYAERT, R. 2017. CYLD, A20 and OTULIN deubiquitinases in NF-κB signaling and cell death: so similar, yet so different. *Cell Death and Differentiation,* 24**,** 1172-1183.

LÖSER, S., GREGORY, L. G., ZHANG, Y., SCHAEFER, K., WALKER, S. A., BUCKLEY, J., DENNEY, L., DEAN, C. H., COOKSON, W. O. C., MOFFATT, M. F. & LLOYD, C. M. 2017. Pulmonary ORMDL3 is critical for induction of Alternaria-induced allergic airways disease. *Journal of Allergy and Clinical Immunology,* 139**,** 1496-1507.e3.

LOWES, M. A., RUSSELL, C. B., MARTIN, D. A., TOWNE, J. E. & KRUEGER, J. G. 2013. The IL-23/T17 pathogenic axis in psoriasis is amplified by keratinocyte responses. *Trends in Immunology,* 34**,** 174-181.

LUCARINI, V., ZICCHEDDU, G., MACCHIA, I., LA SORSA, V., PESCHIAROLI, F., BUCCIONE, C., SISTIGU, A., SANCHEZ, M., ANDREONE, S., D'URSO, M. T., SPADA, M., MACCHIA, D., AFFERNI, C., MATTEI, F. &

SCHIAVONI, G. 2017. IL-33 restricts tumor growth and inhibits pulmonary metastasis in melanoma-bearing mice through eosinophils. *Oncoimmunology,* 6**,** e1317420.

LUND, J., SATO, A., AKIRA, S., MEDZHITOV, R. & IWASAKI, A. 2003. Toll-like Receptor 9–mediated Recognition of Herpes Simplex Virus-2 by Plasmacytoid Dendritic Cells. *The Journal of Experimental Medicine,* 198**,** 513-520.

LUND, J. M., ALEXOPOULOU, L., SATO, A., KAROW, M., ADAMS, N. C., GALE, N. W., IWASAKI, A. & FLAVELL, R. A. 2004. Recognition of single-stranded RNA viruses by Toll-like receptor 7. *Proc Natl Acad Sci U S A,* 101**,** 5598-603.

LUTHI, A. U., CULLEN, S. P., MCNEELA, E. A., DURIEZ, P. J., AFONINA, I. S., SHERIDAN, C., BRUMATTI, G., TAYLOR, R. C., KERSSE, K., VANDENABEELE, P., LAVELLE, E. C. & MARTIN, S. J. 2009. Suppression of interleukin-33 bioactivity through proteolysis by apoptotic caspases. *Immunity,* 31**,** 84-98.

MA, L., CHEN, Z., ERDJUMENT-BROMAGE, H., TEMPST, P. & PANDOLFI, P. P. 2005. Phosphorylation and Functional Inactivation of TSC2 by Erk. *Cell,* 121**,** 179-193.

MAAZI, H., PATEL, N., SANKARANARAYANAN, I., SUZUKI, Y., RIGAS, D., SOROOSH, P., FREEMAN, GORDON J., SHARPE, ARLENE H. & AKBARI, O. 2015. ICOS:ICOS-Ligand Interaction Is Required for Type 2 Innate Lymphoid Cell Function, Homeostasis, and Induction of Airway Hyperreactivity. *Immunity,* 42**,** 538-551.

MAHAPATRO, M., FOERSCH, S., HEFELE, M., HE, G.-W., GINER-VENTURA, E., MCHEDLIDZE, T., KINDERMANN, M., VETRANO, S., DANESE, S., GÜNTHER, C., NEURATH, MARKUS F., WIRTZ, S. & BECKER, C. 2016. Programming of Intestinal Epithelial Differentiation by IL-33 Derived from Pericryptal Fibroblasts in Response to Systemic Infection. *Cell Reports,* 15**,** 1743-1756.

MANTHIRAM, K., ZHOU, Q., AKSENTIJEVICH, I. & KASTNER, D. L. 2017. The monogenic autoinflammatory diseases define new pathways in human innate immunity and inflammation. *Nat Immunol,* 18**,** 832-842.

MARCHESE, F. P., AUBAREDA, A., TUDOR, C., SAKLATVALA, J., CLARK, A. R. & DEAN, J. L. 2010. MAPKAP kinase 2 blocks tristetraprolin-directed mRNA decay by inhibiting CAF1 deadenylase recruitment. *J Biol Chem,* 285**,** 27590-600.

MARIC, J., RAVINDRAN, A., MAZZURANA, L., BJORKLUND, A. K., VAN ACKER, A., RAO, A., FRIBERG, D., DAHLEN, S. E., HEINEMANN, A., KONYA, V. & MJOSBERG, J. 2018. Prostaglandin E2 suppresses human group 2 innate lymphoid cell function. *J Allergy Clin Immunol,* 141**,** 1761-1773.e6.

MARIN-HERNANDEZ, A., GALLARDO-PEREZ, J. C., RALPH, S. J., RODRIGUEZ-ENRIQUEZ, S. & MORENO-SANCHEZ, R. 2009. HIF-1alpha modulates energy metabolism in cancer cells by inducing over-expression of specific glycolytic isoforms. *Mini Rev Med Chem,* 9**,** 1084-101.

MASHIKO, S., MEHTA, H., BISSONNETTE, R. & SARFATI, M. 2017. Increased frequencies of basophils, type 2 innate lymphoid cells and Th2 cells in skin of patients with atopic dermatitis but not psoriasis. *J Dermatol Sci,* 88**,** 167-174.

MAURO, C., PACIFICO, F., LAVORGNA, A., MELLONE, S., IANNETTI, A., ACQUAVIVA, R., FORMISANO, S., VITO, P. & LEONARDI, A. 2006. ABIN-1 binds to NEMO/IKKgamma and co-operates with A20 in inhibiting NF-kappaB. *J Biol Chem,* 281**,** 18482-8.

MAYES, P. A., DEGENHARDT, Y. Y., WOOD, A., TOPOROVSKYA, Y., DISKIN, S. J., HAGLUND, E., MOY, C., WOOSTER, R. & MARIS, J. M. 2013. Mitogen-activated protein kinase (MEK/ERK) inhibition sensitizes cancer cells to centromere-associated protein E inhibition. *International journal of cancer. Journal international du cancer,* 132**,** E149-E157.

MCCARTHY, P. C., PHAIR, I. R., GREGER, C., PARDALI, K., MCGUIRE, V. A., CLARK, A. R., GAESTEL, M. & ARTHUR, J. S. C. 2018. IL-33 regulates cytokine production and neutrophil recruitment via the p38 MAPK-activated kinases MK2/3. *Immunol Cell Biol*.

MCGUIRE, V. A., GRAY, A., MONK, C. E., SANTOS, S. G., LEE, K., AUBAREDA, A., CROWE, J., RONKINA, N., SCHWERMANN, J., BATTY, I. H., LESLIE, N. R., DEAN, J. L., O'KEEFE, S. J., BOOTHBY, M., GAESTEL, M. & ARTHUR, J. S. 2013. Cross talk between the Akt and p38alpha pathways in macrophages downstream of Toll-like receptor signaling. *Mol Cell Biol,* 33**,** 4152-65.

MCGUIRE, V. A., ROSNER, D., ANANIEVA, O., ROSS, E. A., ELCOMBE, S. E., NAQVI, S., VAN DEN BOSCH, M. M., MONK, C. E., RUIZ-ZORRILLA DIEZ, T., CLARK, A. R. & ARTHUR, J. S. 2017. Beta Interferon Production Is Regulated by p38 Mitogen-Activated Protein Kinase in Macrophages via both MSK1/2- and Tristetraprolin-Dependent Pathways. *Mol Cell Biol,* 37.

MEANS, T. K., LATZ, E., HAYASHI, F., MURALI, M. R., GOLENBOCK, D. T. & LUSTER, A. D. 2005. Human lupus autoantibody-DNA complexes activate DCs through cooperation of CD32 and TLR9. *J Clin Invest,* 115**,** 407-17.

MEBIUS, R. E., RENNERT, P. & WEISSMAN, I. L. 1997. Developing Lymph Nodes Collect CD4+CD3− LTβ+ Cells That Can Differentiate to APC, NK Cells, and Follicular Cells but Not T or B Cells. *Immunity,* 7**,** 493-504.

MEDZHITOV, R., PRESTON-HURLBURT, P. & JANEWAY, C. A., JR. 1997. A human homologue of the Drosophila Toll protein signals activation of adaptive immunity. *Nature,* 388**,** 394-7.

MEIER, D., BORNMANN, C., CHAPPAZ, S., SCHMUTZ, S., OTTEN, L. A., CEREDIG, R., ACHA-ORBEA, H. & FINKE, D. 2007. Ectopic Lymphoid-Organ Development Occurs through Interleukin 7-Mediated Enhanced Survival of Lymphoid-Tissue-Inducer Cells. *Immunity,* 26**,** 643-654.

MENON, M. B., GROPENGIESSER, J., FISCHER, J., NOVIKOVA, L., DEURETZBACHER, A., LAFERA, J., SCHIMMECK, H., CZYMMECK, N., RONKINA, N., KOTLYAROV, A., AEPFELBACHER, M. & GAESTEL, M. 2017. p38(MAPK)/MK2-dependent phosphorylation controls cytotoxic RIPK1 signalling in inflammation and infection. 19**,** 1248-1259.

MICHALEK, R. D., GERRIETS, V. A., JACOBS, S. R., MACINTYRE, A. N., MACIVER, N. J., MASON, E. F., SULLIVAN, S. A., NICHOLS, A. G. & RATHMELL, J. C. 2011. Cutting edge: distinct glycolytic and lipid oxidative metabolic programs are essential for effector and regulatory CD4+ T cell subsets. *J Immunol,* 186**,** 3299-303.

MILLER, A. M., ASQUITH, D. L., HUEBER, A. J., ANDERSON, L. A., HOLMES, W. M., MCKENZIE, A. N., XU, D., SATTAR, N., MCINNES, I. B. & LIEW,

F. Y. 2010a. IL-33 induces protective effects in adipose tissue inflammation during obesity in mice. *Circulation research,* 107**,** 650-658.
MILLER, A. M., ASQUITH, D. L., HUEBER, A. J., ANDERSON, L. A., HOLMES, W. M., MCKENZIE, A. N., XU, D., SATTAR, N., MCINNES, I. B. & LIEW, F. Y. 2010b. Interleukin-33 induces protective effects in adipose tissue inflammation during obesity in mice. *Circ Res,* 107**,** 650-8.
MISHARIN, A. V., CUDA, C. M., SABER, R., TURNER, J. D., GIERUT, A. K., HAINES, G. K., BERDNIKOVS, S., FILER, A., CLARK, A. R., BUCKLEY, C. D., MUTLU, G. M., BUDINGER, G. R. S. & PERLMAN, H. 2014. Non-classical Ly6C(−) monocytes drive the development of inflammatory arthritis in mice. *Cell reports,* 9**,** 591-604.
MISHARIN, A. V., MORALES-NEBREDA, L., MUTLU, G. M., BUDINGER, G. R. S. & PERLMAN, H. 2013. Flow Cytometric Analysis of Macrophages and Dendritic Cell Subsets in the Mouse Lung. *American Journal of Respiratory Cell and Molecular Biology,* 49**,** 503-510.
MISTRY, P. & KAPLAN, M. J. 2017. Cell death in the pathogenesis of systemic lupus erythematosus and lupus nephritis. *Clinical Immunology,* 185**,** 59-73.
MJÖSBERG, J., BERNINK, J., GOLEBSKI, K., KARRICH, JULIEN J., PETERS, CHARLOTTE P., BLOM, B., TE VELDE, ANJE A., FOKKENS, WYTSKE J., VAN DRUNEN, CORNELIS M. & SPITS, H. 2012. The Transcription Factor GATA3 Is Essential for the Function of Human Type 2 Innate Lymphoid Cells. *Immunity,* 37**,** 649-659.
MJOSBERG, J. M., TRIFARI, S., CRELLIN, N. K., PETERS, C. P., VAN DRUNEN, C. M., PIET, B., FOKKENS, W. J., CUPEDO, T. & SPITS, H. 2011. Human IL-25- and IL-33-responsive type 2 innate lymphoid cells are defined by expression of CRTH2 and CD161. *Nat Immunol,* 12**,** 1055-62.
MOLOFSKY, A. B., SAVAGE, A. K. & LOCKSLEY, R. M. 2015. Interleukin-33 in Tissue Homeostasis, Injury, and Inflammation. *Immunity,* 42**,** 1005-19.
MONTICELLI, L. A., BUCK, M. D., FLAMAR, A.-L., SAENZ, S. A., TAIT WOJNO, E. D., YUDANIN, N. A., OSBORNE, L. C., HEPWORTH, M. R., TRAN, S. V., RODEWALD, H.-R., SHAH, H., CROSS, J. R., DIAMOND, J. M., CANTU, E., CHRISTIE, J. D., PEARCE, E. L. & ARTIS, D. 2016. Arginase 1 is an innate lymphoid-cell-intrinsic metabolic checkpoint controlling type 2 inflammation. *Nature Immunology,* 17**,** 656.
MOODIE, S. A., WILLUMSEN, B. M., WEBER, M. J. & WOLFMAN, A. 1993. Complexes of Ras.GTP with Raf-1 and mitogen-activated protein kinase kinase. *Science,* 260**,** 1658-61.
MORIMOTO, Y., HIRAHARA, K., KIUCHI, M., WADA, T., ICHIKAWA, T., KANNO, T., OKANO, M., KOKUBO, K., ONODERA, A., SAKURAI, D., OKAMOTO, Y. & NAKAYAMA, T. 2018. Amphiregulin-Producing Pathogenic Memory T Helper 2 Cells Instruct Eosinophils to Secrete Osteopontin and Facilitate Airway Fibrosis. *Immunity,* 49**,** 134-150.e6.
MORITA, H., ARAE, K., UNNO, H., MIYAUCHI, K., TOYAMA, S., NAMBU, A., OBOKI, K., OHNO, T., MOTOMURA, K., MATSUDA, A., YAMAGUCHI, S., NARUSHIMA, S., KAJIWARA, N., IIKURA, M., SUTO, H., MCKENZIE, ANDREW N. J., TAKAHASHI, T., KARASUYAMA, H., OKUMURA, K., AZUMA, M., MORO, K., AKDIS, CEZMI A., GALLI, STEPHEN J., KOYASU, S., KUBO, M., SUDO, K., SAITO, H., MATSUMOTO, K. & NAKAE, S. 2015. An Interleukin-33-Mast Cell-

Interleukin-2 Axis Suppresses Papain-Induced Allergic Inflammation by Promoting Regulatory T Cell Numbers. *Immunity,* 43**,** 175-186.

MORITZ, D. R., RODEWALD, H.-R., GHEYSELINCK, J. & KLEMENZ, R. 1998. The IL-1 Receptor-Related T1 Antigen Is Expressed on Immature and Mature Mast Cells and on Fetal Blood Mast Cell Progenitors. *The Journal of Immunology,* 161**,** 4866-4874.

MORIYAMA, S., BRESTOFF, J. R., FLAMAR, A.-L., MOELLER, J. B., KLOSE, C. S. N., RANKIN, L. C., YUDANIN, N. A., MONTICELLI, L. A., PUTZEL, G. G., RODEWALD, H.-R. & ARTIS, D. 2018. β₂-adrenergic receptor–mediated negative regulation of group 2 innate lymphoid cell responses. *Science,* 359**,** 1056-1061.

MORO, K., EALEY, K. N., KABATA, H. & KOYASU, S. 2015a. Isolation and analysis of group 2 innate lymphoid cells in mice. *Nat Protoc,* 10**,** 792-806.

MORO, K., YAMADA, T., TANABE, M., TAKEUCHI, T., IKAWA, T., KAWAMOTO, H., FURUSAWA, J.-I., OHTANI, M., FUJII, H. & KOYASU, S. 2009. Innate production of TH2 cytokines by adipose tissue-associated c-Kit+Sca-1+ lymphoid cells. *Nature,* 463**,** 540.

MORO, K., YAMADA, T., TANABE, M., TAKEUCHI, T., IKAWA, T., KAWAMOTO, H., FURUSAWA, J., OHTANI, M., FUJII, H. & KOYASU, S. 2010. Innate production of T(H)2 cytokines by adipose tissue-associated c-Kit(+)Sca-1(+) lymphoid cells. *Nature,* 463**,** 540-4.

MORTON, S., HESSON, L., PEGGIE, M. & COHEN, P. 2008. Enhanced binding of TBK1 by an optineurin mutant that causes a familial form of primary open angle glaucoma. *FEBS Letters,* 582**,** 997-1002.

MOTAMEDI, M., XU, L. & ELAHI, S. 2016. Correlation of transferrin receptor (CD71) with Ki67 expression on stimulated human and mouse T cells: The kinetics of expression of T cell activation markers. *J Immunol Methods,* 437**,** 43-52.

MOUREY, R. J., BURNETTE, B. L., BRUSTKERN, S. J., DANIELS, J. S., HIRSCH, J. L., HOOD, W. F., MEYERS, M. J., MNICH, S. J., PIERCE, B. S., SAABYE, M. J., SCHINDLER, J. F., SOUTH, S. A., WEBB, E. G., ZHANG, J. & ANDERSON, D. R. 2010. A benzothiophene inhibitor of mitogen-activated protein kinase-activated protein kinase 2 inhibits tumor necrosis factor alpha production and has oral anti-inflammatory efficacy in acute and chronic models of inflammation. *J Pharmacol Exp Ther,* 333**,** 797-807.

MOUSSION, C., ORTEGA, N. & GIRARD, J.-P. 2008a. The IL-1-Like Cytokine IL-33 Is Constitutively Expressed in the Nucleus of Endothelial Cells and Epithelial Cells In Vivo: A Novel 'Alarmin'? *PLOS ONE,* 3**,** e3331.

MOUSSION, C., ORTEGA, N. & GIRARD, J. P. 2008b. The IL-1-like cytokine IL-33 is constitutively expressed in the nucleus of endothelial cells and epithelial cells in vivo: a novel 'alarmin'? *PLoS One,* 3**,** e3331.

MUNOZ, L. E., CHAURIO, R. A., GAIPL, U. S., SCHETT, G. & KERN, P. 2009. MoMa from patients with systemic lupus erythematosus show altered adhesive activity. *Autoimmunity,* 42**,** 269-71.

MURN, J., MLINARIC-RASCAN, I., VAIGOT, P., ALIBERT, O., FROUIN, V. & GIDROL, X. 2009. A Myc-regulated transcriptional network controls B-cell fate in response to BCR triggering. *BMC Genomics,* 10**,** 323.

NABEKURA, T., GIRARD, J.-P. & LANIER, L. L. 2015. IL-33 Receptor ST2 Amplifies the Expansion of NK Cells and Enhances Host Defense during

Mouse Cytomegalovirus Infection. *The Journal of Immunology,* 194**,** 5948-5952.

NAIR, R. P., DUFFIN, K. C., HELMS, C., DING, J., STUART, P. E., GOLDGAR, D., GUDJONSSON, J. E., LI, Y., TEJASVI, T., FENG, B. J., RUETHER, A., SCHREIBER, S., WEICHENTHAL, M., GLADMAN, D., RAHMAN, P., SCHRODI, S. J., PRAHALAD, S., GUTHERY, S. L., FISCHER, J., LIAO, W., KWOK, P. Y., MENTER, A., LATHROP, G. M., WISE, C. A., BEGOVICH, A. B., VOORHEES, J. J., ELDER, J. T., KRUEGER, G. G., BOWCOCK, A. M. & ABECASIS, G. R. 2009. Genome-wide scan reveals association of psoriasis with IL-23 and NF-kappaB pathways. *Nat Genet,* 41**,** 199-204.

NAKAMURA, E., SATO, M., YANG, H., MIYAGAWA, F., HARASAKI, M., TOMITA, K., MATSUOKA, S., NOMA, A., IWAI, K. & MINATO, N. 1999. 4F2 (CD98) heavy chain is associated covalently with an amino acid transporter and controls intracellular trafficking and membrane topology of 4F2 heterodimer. *J Biol Chem,* 274**,** 3009-16.

NANDA, S. K., LOPEZ-PELAEZ, M., ARTHUR, J. S. C., MARCHESI, F. & COHEN, P. 2016. Suppression of IRAK1 or IRAK4 catalytic activity, but not type1 IFN signaling, prevents lupus nephritis in mice expressing a ubiquitin binding-defective mutant of ABIN1. *J Immunol,* 197**,** 4266-73.

NANDA, S. K., VENIGALLA, R. K. C., ORDUREAU, A., PATTERSON-KANE, J. C., POWELL, D. W., TOTH, R., C. ARTHUR, J. S. & COHEN, P. 2011. Polyubiquitin binding to ABIN1 is required to prevent autoimmunity. *The Journal of Experimental Medicine,* 208**,** 1215-1228.

NAWIJN, M. C., DINGJAN, G. M., FERREIRA, R., LAMBRECHT, B. N., KARIS, A., GROSVELD, F., SAVELKOUL, H. & HENDRIKS, R. W. 2001. Enforced expression of GATA-3 in transgenic mice inhibits Th1 differentiation and induces the formation of a T1/ST2-expressing Th2-committed T cell compartment in vivo. *J Immunol,* 167**,** 724-32.

NECHAMA, M., KWON, J., WEI, S., KYI, A. T., WELNER, R. S., BEN-DOV, I. Z., ARREDOUANI, M. S., ASARA, J. M., CHEN, C.-H., TSAI, C.-Y., NELSON, K. F., KOBAYASHI, K. S., ISRAEL, E., ZHOU, X. Z., NICHOLSON, L. K. & LU, K. P. 2018. The IL-33-PIN1-IRAK-M axis is critical for type 2 immunity in IL-33-induced allergic airway inflammation. *Nature Communications,* 9**,** 1603.

NEILL, D. R., WONG, S. H., BELLOSI, A., FLYNN, R. J., DALY, M., LANGFORD, T. K., BUCKS, C., KANE, C. M., FALLON, P. G., PANNELL, R., JOLIN, H. E. & MCKENZIE, A. N. 2010. Nuocytes represent a new innate effector leukocyte that mediates type-2 immunity. *Nature,* 464**,** 1367-70.

NEUMANN, D., KOLLEWE, C., RESCH, K. & MARTIN, M. U. 2007. The death domain of IRAK-1: an oligomerization domain mediating interactions with MyD88, Tollip, IRAK-1, and IRAK-4. *Biochem Biophys Res Commun,* 354**,** 1089-94.

NEVEU, W. A., ALLARD, J. B., DIENZ, O., WARGO, M. J., CILIBERTO, G., WHITTAKER, L. A. & RINCON, M. 2009. IL-6 is required for airway mucus production induced by inhaled fungal allergens. *J Immunol,* 183**,** 1732-8.

NEVEU, W. A., ALLARD, J. L., RAYMOND, D. M., BOURASSA, L. M., BURNS, S. M., BUNN, J. Y., IRVIN, C. G., KAMINSKY, D. A. & RINCON, M. 2010. Elevation of IL-6 in the allergic asthmatic airway is independent of

inflammation but associates with loss of central airway function. *Respir Res,* 11**,** 28.
NEWLAND, S. A., MOHANTA, S., CLÉMENT, M., TALEB, S., WALKER, J. A., NUS, M., SAGE, A. P., YIN, C., HU, D., KITT, L. L., FINIGAN, A. J., RODEWALD, H.-R., BINDER, C. J., MCKENZIE, A. N. J., HABENICHT, A. J. & MALLAT, Z. 2017. Type-2 innate lymphoid cells control the development of atherosclerosis in mice. *Nature Communications,* 8**,** 15781.
NICKERSON, K. M., CHRISTENSEN, S. R., SHUPE, J., KASHGARIAN, M., KIM, D., ELKON, K. & SHLOMCHIK, M. J. 2010. TLR9 Regulates TLR7- and MyD88-Dependent Autoantibody Production and Disease in a Murine Model of Lupus. *Journal of immunology (Baltimore, Md. : 1950),* 184**,** 1840-1848.
NICKLIN, P., BERGMAN, P., ZHANG, B., TRIANTAFELLOW, E., WANG, H., NYFELER, B., YANG, H., HILD, M., KUNG, C., WILSON, C., MYER, V. E., MACKEIGAN, J. P., PORTER, J. A., WANG, Y. K., CANTLEY, L. C., FINAN, P. M. & MURPHY, L. O. 2009. Bidirectional transport of amino acids regulates mTOR and autophagy. *Cell,* 136**,** 521-34.
NILE, C. J., BARKSBY, E., JITPRASERTWONG, P., PRESHAW, P. M. & TAYLOR, J. J. 2010. Expression and regulation of interleukin-33 in human monocytes. *Immunology,* 130**,** 172-180.
NUMATA, T., ITO, T., MAEDA, T., EGUSA, C. & TSUBOI, R. 2016. IL-33 promotes ICAM-1 expression via NF-kB in murine mast cells. *Allergology International,* 65**,** 158-165.
NURIEVA, R. I., CHUNG, Y., MARTINEZ, G. J., YANG, X. O., TANAKA, S., MATSKEVITCH, T. D., WANG, Y.-H. & DONG, C. 2009. Bcl6 Mediates the Development of T Follicular Helper Cells. *Science,* 325**,** 1001-1005.
O'NEILL, L. A. J., KISHTON, R. J. & RATHMELL, J. 2016. A guide to immunometabolism for immunologists. *Nature Reviews Immunology,* 16**,** 553.
OBAID, R., WANI, S. E., AZFER, A., HURD, T., JONES, R., COHEN, P., RALSTON, S. H. & ALBAGHA, O. M. E. 2015. Optineurin Negatively Regulates Osteoclast Differentiation by Modulating NF-κB and Interferon Signaling: Implications for Paget's Disease. *Cell Reports,* 13**,** 1096-1102.
OLARU, F., DOBEL, T., LONSDORF, A. S., OEHRL, S., MAAS, M., ENK, A. H., SCHMITZ, M., GRONE, E. F., GRONE, H. J. & SCHAKEL, K. 2018. Intracapillary immune complexes recruit and activate slan-expressing CD16+ monocytes in human lupus nephritis. *JCI Insight,* 3.
OLIPHANT, CHRISTOPHER J., HWANG, YOU Y., WALKER, JENNIFER A., SALIMI, M., WONG, SEE H., BREWER, JAMES M., ENGLEZAKIS, A., BARLOW, JILLIAN L., HAMS, E., SCANLON, SETH T., OGG, GRAHAM S., FALLON, PADRAIC G. & MCKENZIE, ANDREW N. J. 2014. MHCII-Mediated Dialog between Group 2 Innate Lymphoid Cells and CD4+ T Cells Potentiates Type 2 Immunity and Promotes Parasitic Helminth Expulsion. *Immunity,* 41**,** 283-295.
OPIPARI, A. W., JR., BOGUSKI, M. S. & DIXIT, V. M. 1990. The A20 cDNA induced by tumor necrosis factor alpha encodes a novel type of zinc finger protein. *J Biol Chem,* 265**,** 14705-8.
ORDONEZ-RUEDA, D., JONSSON, F., MANCARDI, D. A., ZHAO, W., MALZAC, A., LIANG, Y., BERTOSIO, E., GRENOT, P., BLANQUET, V., SABRAUTZKI, S., DE ANGELIS, M. H., MERESSE, S., DUPREZ, E., BRUHNS, P., MALISSEN, B. & MALISSEN, M. 2012. A hypomorphic

mutation in the Gfi1 transcriptional repressor results in a novel form of neutropenia. *Eur J Immunol,* 42**,** 2395-408.

ORDUREAU, A., SMITH, H., WINDHEIM, M., PEGGIE, M., CARRICK, E., MORRICE, N. & COHEN, P. 2008. The IRAK-catalysed activation of the E3 ligase function of Pellino isoforms induces the Lys63-linked polyubiquitination of IRAK1. *Biochem J,* 409**,** 43-52.

ORIAN, A., GONEN, H., BERCOVICH, B., FAJERMAN, I., EYTAN, E., ISRAEL, A., MERCURIO, F., IWAI, K., SCHWARTZ, A. L. & CIECHANOVER, A. 2000. SCF(beta)(-TrCP) ubiquitin ligase-mediated processing of NF-kappaB p105 requires phosphorylation of its C-terminus by IkappaB kinase. *Embo j,* 19**,** 2580-91.

OSHIKAWA, K., KUROIWA, K., TAGO, K., IWAHANA, H., YANAGISAWA, K., OHNO, S., TOMINAGA, S. I. & SUGIYAMA, Y. 2001. Elevated soluble ST2 protein levels in sera of patients with asthma with an acute exacerbation. *Am J Respir Crit Care Med,* 164**,** 277-81.

OSHIMA, S., TURER, E. E., CALLAHAN, J. A., CHAI, S., ADVINCULA, R., BARRERA, J., SHIFRIN, N., LEE, B., BENEDICT YEN, T. S., WOO, T., MALYNN, B. A. & MA, A. 2009. ABIN-1 is a ubiquitin sensor that restricts cell death and sustains embryonic development. *Nature,* 457**,** 906-9.

P., L., H., M., D., H. & K., M. 2015. Interleukin-33 affects cytokine production by keratinocytes in vitiligo. *Clinical and Experimental Dermatology,* 40**,** 163-170.

PACLIK, D., STEHLE, C., LAHMANN, A., HUTLOFF, A. & ROMAGNANI, C. 2015. ICOS regulates the pool of group 2 innate lymphoid cells under homeostatic and inflammatory conditions in mice. *Eur J Immunol,* 45**,** 2766-72.

PAN, Y., TIAN, T., PARK, C. O., LOFFTUS, S. Y., MEI, S., LIU, X., LUO, C., O'MALLEY, J. T., GEHAD, A., TEAGUE, J. E., DIVITO, S. J., FUHLBRIGGE, R., PUIGSERVER, P., KRUEGER, J. G., HOTAMISLIGIL, G. S., CLARK, R. A. & KUPPER, T. S. 2017. Survival of tissue-resident memory T cells requires exogenous lipid uptake and metabolism. *Nature,* 543**,** 252-256.

PANCER, Z. & COOPER, M. D. 2006. THE EVOLUTION OF ADAPTIVE IMMUNITY. *Annual Review of Immunology,* 24**,** 497-518.

PAPOUTSOPOULOU, S., SYMONS, A., THARMALINGHAM, T., BELICH, M. P., KAISER, F., KIOUSSIS, D., O'GARRA, A., TYBULEWICZ, V. & LEY, S. C. 2006. ABIN-2 is required for optimal activation of Erk MAP kinase in innate immune responses. *Nature Immunology,* 7**,** 606.

PARIS, G., POZHARSKAYA, T., ASEMPA, T. & LANE, A. P. 2014. Damage-associated molecular patterns stimulate interleukin-33 expression in nasal polyp epithelial cells. *Int Forum Allergy Rhinol,* 4**,** 15-21.

PARK, B. S., SONG, D. H., KIM, H. M., CHOI, B.-S., LEE, H. & LEE, J.-O. 2009. The structural basis of lipopolysaccharide recognition by the TLR4–MD-2 complex. *Nature,* 458**,** 1191.

PARK, I. H., PARK, J. H., SHIN, J. M. & LEE, H. M. 2016. Tumor necrosis factor-alpha regulates interleukin-33 expression through extracellular signal-regulated kinase, p38, and nuclear factor-kappaB pathways in airway epithelial cells. *Int Forum Allergy Rhinol,* 6**,** 973-80.

PASTORELLI, L., GARG, R. R., HOANG, S. B., SPINA, L., MATTIOLI, B., SCARPA, M., FIOCCHI, C., VECCHI, M. & PIZARRO, T. T. 2010.

Epithelial-derived IL-33 and its receptor ST2 are dysregulated in ulcerative colitis and in experimental Th1/Th2 driven enteritis. *Proceedings of the National Academy of Sciences,* 107**,** 8017-8022.

PATEL, A. A., ZHANG, Y., FULLERTON, J. N., BOELEN, L., RONGVAUX, A., MAINI, A. A., BIGLEY, V., FLAVELL, R. A., GILROY, D. W., ASQUITH, B., MACALLAN, D. & YONA, S. 2017. The fate and lifespan of human monocyte subsets in steady state and systemic inflammation. *The Journal of Experimental Medicine*.

PATEL, N. R., CUNOOSAMY, D. M., FAGERAS, M., TAIB, Z., ASIMUS, S., HEGELUND-MYRBACK, T., LUNDIN, S., PARDALI, K., KURIAN, N., ERSDAL, E., KRISTENSSON, C., KORSBACK, K., PALMER, R., BROWN, M. N., GREENAWAY, S., SIEW, L., CLARKE, G. W., RENNARD, S. I., MAKE, B. J., WISE, R. A. & JANSSON, P. 2018. The development of AZD7624 for prevention of exacerbations in COPD: a randomized controlled trial. *Int J Chron Obstruct Pulmon Dis,* 13**,** 1009-1019.

PATTISON, M. J., MITCHELL, O., FLYNN, H. R., CHEN, C. S., YANG, H. T., BEN-ADDI, H., BOEING, S., SNIJDERS, A. P. & LEY, S. C. 2016. TLR and TNF-R1 activation of the MKK3/MKK6-p38alpha axis in macrophages is mediated by TPL-2 kinase. *Biochem J,* 473**,** 2845-61.

PAULS, E., NANDA, S. K., SMITH, H., TOTH, R., ARTHUR, J. S. C. & COHEN, P. 2013a. Two phases of inflammatory mediator production defined by the study of IRAK2 and IRAK1 knock-in mice. *J Immunol,* 191**,** 2717-30.

PEARCE, E. L. 2010. Metabolism in T cell activation and differentiation. *Current Opinion in Immunology,* 22**,** 314-320.

PEARCE, E. L. & PEARCE, E. J. 2013. Metabolic Pathways In Immune Cell Activation And Quiescence. *Immunity,* 38**,** 633-643.

PERERA, P. Y., MAYADAS, T. N., TAKEUCHI, O., AKIRA, S., ZAKS-ZILBERMAN, M., GOYERT, S. M. & VOGEL, S. N. 2001. CD11b/CD18 acts in concert with CD14 and Toll-like receptor (TLR) 4 to elicit full lipopolysaccharide and taxol-inducible gene expression. *J Immunol,* 166**,** 574-81.

PERRY, A. K., CHOW, E. K., GOODNOUGH, J. B., YEH, W.-C. & CHENG, G. 2004. Differential Requirement for TANK-binding Kinase-1 in Type I Interferon Responses to Toll-like Receptor Activation and Viral Infection. *The Journal of Experimental Medicine,* 199**,** 1651-1658.

PETERS-GOLDEN, M., GLEASON, M. M. & TOGIAS, A. 2006. Cysteinyl leukotrienes: multi-functional mediators in allergic rhinitis. *Clinical and Experimental Allergy,* 36**,** 689-703.

PETERSON, T. R., LAPLANTE, M., THOREEN, C. C., SANCAK, Y., KANG, S. A., KUEHL, W. M., GRAY, N. S. & SABATINI, D. M. 2009. DEPTOR is an mTOR inhibitor frequently overexpressed in multiple myeloma cells and required for their survival. *Cell,* 137**,** 873-86.

PICHERY, M., MIREY, E., MERCIER, P., LEFRANCAIS, E., DUJARDIN, A., ORTEGA, N. & GIRARD, J. P. 2012. Endogenous IL-33 is highly expressed in mouse epithelial barrier tissues, lymphoid organs, brain, embryos, and inflamed tissues: in situ analysis using a novel Il-33-LacZ gene trap reporter strain. *J Immunol,* 188**,** 3488-95.

PISITKUN, P., DEANE, J. A., DIFILIPPANTONIO, M. J., TARASENKO, T., SATTERTHWAITE, A. B. & BOLLAND, S. 2006. Autoreactive B cell

responses to RNA-related antigens due to TLR7 gene duplication. *Science,* 312**,** 1669-72.

PIVKIN, I. V., PENG, Z., KARNIADAKIS, G. E., BUFFET, P. A., DAO, M. & SURESH, S. 2016. Biomechanics of red blood cells in human spleen and consequences for physiology and disease. *Proceedings of the National Academy of Sciences of the United States of America,* 113**,** 7804-7809.

POLTORAK, A., HE, X., SMIRNOVA, I., LIU, M. Y., VAN HUFFEL, C., DU, X., BIRDWELL, D., ALEJOS, E., SILVA, M., GALANOS, C., FREUDENBERG, M., RICCIARDI-CASTAGNOLI, P., LAYTON, B. & BEUTLER, B. 1998. Defective LPS signaling in C3H/HeJ and C57BL/10ScCr mice: mutations in Tlr4 gene. *Science,* 282**,** 2085-8.

PONCET, N., MITCHELL, F. E., IBRAHIM, A. F., MCGUIRE, V. A., ENGLISH, G., ARTHUR, J. S., SHI, Y. B. & TAYLOR, P. M. 2014. The catalytic subunit of the system L1 amino acid transporter (slc7a5) facilitates nutrient signalling in mouse skeletal muscle. *PLoS One,* 9**,** e89547.

POPOSKI, J. A., KLINGLER, A. I., TAN, B. K., SOROOSH, P., BANIE, H., LEWIS, G., HULSE, K. E., STEVENS, W. W., PETERS, A. T., GRAMMER, L. C., SCHLEIMER, R. P., WELCH, K. C., SMITH, S. S., CONLEY, D. B., RAVIV, J. R., KARRAS, J. G., AKBARI, O., KERN, R. C. & KATO, A. 2017. Group 2 innate lymphoid cells are elevated and activated in chronic rhinosinusitis with nasal polyps. 5**,** 233-243.

POWELL, N., LO, J. W., BIANCHERI, P., VOSSENKAMPER, A., PANTAZI, E., WALKER, A. W., STOLARCZYK, E., AMMOSCATO, F., GOLDBERG, R., SCOTT, P., CANAVAN, J. B., PERUCHA, E., GARRIDO-MESA, N., IRVING, P. M., SANDERSON, J. D., HAYEE, B., HOWARD, J. K., PARKHILL, J., MACDONALD, T. T. & LORD, G. M. 2015. Interleukin 6 Increases Production of Cytokines by Colonic Innate Lymphoid Cells in Mice and Patients With Chronic Intestinal Inflammation. *Gastroenterology,* 149**,** 456-67.e15.

POWIS, K. & DE VIRGILIO, C. 2016. Conserved regulators of Rag GTPases orchestrate amino acid-dependent TORC1 signaling. *Cell Discovery,* 2**,** 15049.

PRÉFONTAINE, D., LAJOIE-KADOCH, S., FOLEY, S., AUDUSSEAU, S., OLIVENSTEIN, R., HALAYKO, A. J., LEMIÈRE, C., MARTIN, J. G. & HAMID, Q. 2009. Increased Expression of IL-33 in Severe Asthma: Evidence of Expression by Airway Smooth Muscle Cells. *The Journal of Immunology,* 183**,** 5094-5103.

PRESTON, G. C., SINCLAIR, L. V., KASKAR, A., HUKELMANN, J. L., NAVARRO, M. N., FERRERO, I., MACDONALD, H. R., COWLING, V. H. & CANTRELL, D. A. 2015. Single cell tuning of Myc expression by antigen receptor signal strength and interleukin-2 in T lymphocytes. *The EMBO Journal,* 34**,** 2008-2024.

PRICE, A. E., LIANG, H. E., SULLIVAN, B. M., REINHARDT, R. L., EISLEY, C. J., ERLE, D. J. & LOCKSLEY, R. M. 2010. Systemically dispersed innate IL-13-expressing cells in type 2 immunity. *Proc Natl Acad Sci U S A,* 107**,** 11489-94.

RADDATZ, R., WILSON, A. E., ARTYMYSHYN, R., BONINI, J. A., BOROWSKY, B., BOTEJU, L. W., ZHOU, S., KOURANOVA, E. V., NAGORNY, R., GUEVARRA, M. S., DAI, M., LERMAN, G. S., VAYSSE, P. J., BRANCHEK, T. A., GERALD, C., FORRAY, C. & ADHAM, N. 2000. Identification and Characterization of Two Neuromedin U Receptors

Differentially Expressed in Peripheral Tissues and the Central Nervous System. *Journal of Biological Chemistry,* 275**,** 32452-32459.

RAES, G., DE BAETSELIER, P., NOEL, W., BESCHIN, A., BROMBACHER, F. & HASSANZADEH GH, G. 2002. Differential expression of FIZZ1 and Ym1 in alternatively versus classically activated macrophages. *J Leukoc Biol,* 71**,** 597-602.

RAES, G., VAN DEN BERGH, R., DE BAETSELIER, P. & GHASSABEH, G. H. 2005. Arginase-1 and Ym1 Are Markers for Murine, but Not Human, Alternatively Activated Myeloid Cells. *The Journal of Immunology,* 174**,** 6561-6562.

RAETZ, M., KIBARDIN, A., STURGE, C. R., PIFER, R., LI, H., BURSTEIN, E., OZATO, K., LARIN, S. & YAROVINSKY, F. 2013. Cooperation of TLR12 and TLR11 in the IRF8-dependent IL-12 response to Toxoplasma gondii profilin. *Journal of immunology (Baltimore, Md. : 1950),* 191**,** 4818-4827.

RAO, H., ZENG, Q., LIANG, Y., XIAO, C., XIE, S. & XU, X. 2015. Correlation between TLR9 Expression and Cytokine Secretion in the Clinical Diagnosis of Systemic Lupus Erythematosus. *Mediators Inflamm,* 2015**,** 710720.

RATH, M., MÜLLER, I., KROPF, P., CLOSS, E. I. & MUNDER, M. 2014. Metabolism via Arginase or Nitric Oxide Synthase: Two Competing Arginine Pathways in Macrophages. *Frontiers in Immunology,* 5**,** 532.

REES, F., DOHERTY, M., GRAINGE, M., DAVENPORT, G., LANYON, P. & ZHANG, W. 2016. The incidence and prevalence of systemic lupus erythematosus in the UK, 1999-2012. *Ann Rheum Dis,* 75**,** 136-41.

RHYASEN, G. W. & STARCZYNOWSKI, D. T. 2014. IRAK signalling in cancer. *British Journal Of Cancer,* 112**,** 232.

RINCON, M. & IRVIN, C. G. 2012. Role of IL-6 in asthma and other inflammatory pulmonary diseases. *Int J Biol Sci,* 8**,** 1281-90.

RIPLEY, B., GONCALVES, B., ISENBERG, D., LATCHMAN, D. & RAHMAN, A. 2005. Raised levels of interleukin 6 in systemic lupus erythematosus correlate with anaemia. *Annals of the Rheumatic Diseases,* 64**,** 849-853.

ROBINETTE, M. L., FUCHS, A., CORTEZ, V. S., LEE, J. S., WANG, Y., DURUM, S. K., GILFILLAN, S., COLONNA, M. & THE IMMUNOLOGICAL GENOME, C. 2015. Transcriptional programs define molecular characteristics of innate lymphoid cell classes and subsets. *Nature Immunology,* 16**,** 306.

RODRÍGUEZ-ESPINOSA, O., ROJAS-ESPINOSA, O., MORENO-ALTAMIRANO, M. M. B., LÓPEZ-VILLEGAS, E. O. & SÁNCHEZ-GARCÍA, F. J. 2015. Metabolic requirements for neutrophil extracellular traps formation. *Immunology,* 145**,** 213-224.

ROEDIGER, B., KYLE, R., TAY, S. S., MITCHELL, A. J., BOLTON, H. A., GUY, T. V., TAN, S.-Y., FORBES-BLOM, E., TONG, P. L., KÖLLER, Y., SHKLOVSKAYA, E., IWASHIMA, M., MCCOY, K. D., LE GROS, G., FAZEKAS DE ST GROTH, B. & WENINGER, W. 2015. IL-2 is a critical regulator of group 2 innate lymphoid cell function during pulmonary inflammation. *Journal of Allergy and Clinical Immunology,* 136**,** 1653-1663.e7.

RONKINA, N., KOTLYAROV, A., DITTRICH-BREIHOLZ, O., KRACHT, M., HITTI, E., MILARSKI, K., ASKEW, R., MARUSIC, S., LIN, L.-L., GAESTEL, M. & TELLIEZ, J.-B. 2007a. The Mitogen-Activated Protein Kinase (MAPK)-Activated Protein Kinases MK2 and MK3 Cooperate in

Stimulation of Tumor Necrosis Factor Biosynthesis and Stabilization of p38 MAPK. *Molecular and Cellular Biology,* 27**,** 170-181.

ROOIJEN, N. V. & SANDERS, A. 1994. Liposome mediated depletion of macrophages: mechanism of action, preparation of liposomes and applications. *Journal of Immunological Methods,* 174**,** 83-93.

ROSKOSKI, R. 2005. Signaling by Kit protein-tyrosine kinase—The stem cell factor receptor. *Biochemical and Biophysical Research Communications,* 337**,** 1-13.

ROSS, E. A., SMALLIE, T., DING, Q., O'NEIL, J. D., CUNLIFFE, H. E., TANG, T., ROSNER, D. R., KLEVERNIC, I., MORRICE, N. A., MONACO, C., CUNNINGHAM, A. F., BUCKLEY, C. D., SAKLATVALA, J., DEAN, J. L. & CLARK, A. R. 2015. Dominant Suppression of Inflammation via Targeted Mutation of the mRNA Destabilizing Protein Tristetraprolin. *The Journal of Immunology,* 195**,** 265-276.

ROUSE, J., COHEN, P., TRIGON, S., MORANGE, M., ALONSO-LLAMAZARES, A., ZAMANILLO, D., HUNT, T. & NEBREDA, A. R. 1994. A novel kinase cascade triggered by stress and heat shock that stimulates MAPKAP kinase-2 and phosphorylation of the small heat shock proteins. *Cell,* 78**,** 1027-37.

RUBEN, S. M., KLEMENT, J. F., COLEMAN, T. A., MAHER, M., CHEN, C. H. & ROSEN, C. A. 1992. I-Rel: a novel rel-related protein that inhibits NF-kappa B transcriptional activity. *Genes Dev,* 6**,** 745-60.

RUSSI, A. E., WALKER-CAULFIELD, M. E., EBEL, M. E. & BROWN, M. A. 2015. Cutting Edge: c-Kit Signaling Differentially Regulates Type 2 Innate Lymphoid Cell Accumulation and Susceptibility to Central Nervous System Demyelination in Male and Female SJL Mice. *The Journal of Immunology,* 194**,** 5609-5613.

RYSECK, R. P., BULL, P., TAKAMIYA, M., BOURS, V., SIEBENLIST, U., DOBRZANSKI, P. & BRAVO, R. 1992. RelB, a new Rel family transcription activator that can interact with p50-NF-kappa B. *Molecular and Cellular Biology,* 12**,** 674-684.

S., H. C., VEERA, P. & J., M. A. N. 2013. IL-33 citrine reporter mice reveal the temporal and spatial expression of IL-33 during allergic lung inflammation. *European Journal of Immunology,* 43**,** 488-498.

SABÒ, A., KRESS, T. R., PELIZZOLA, M., DE PRETIS, S., GORSKI, M. M., TESI, A., MORELLI, M. J., BORA, P., DONI, M., VERRECCHIA, A., TONELLI, C., FAGÀ, G., BIANCHI, V., RONCHI, A., LOW, D., MÜLLER, H., GUCCIONE, E., CAMPANER, S. & AMATI, B. 2014. Selective transcriptional regulation by Myc in cellular growth control and lymphomagenesis. *Nature,* 511**,** 488.

SAENZ, S. A., SIRACUSA, M. C., MONTICELLI, L. A., ZIEGLER, C. G., KIM, B. S., BRESTOFF, J. R., PETERSON, L. W., WHERRY, E. J., GOLDRATH, A. W., BHANDOOLA, A. & ARTIS, D. 2013. IL-25 simultaneously elicits distinct populations of innate lymphoid cells and multipotent progenitor type 2 (MPPtype2) cells. *J Exp Med,* 210**,** 1823-37.

SAENZ, S. A., SIRACUSA, M. C., PERRIGOUE, J. G., SPENCER, S. P., URBAN JR, J. F., TOCKER, J. E., BUDELSKY, A. L., KLEINSCHEK, M. A., KASTELEIN, R. A., KAMBAYASHI, T., BHANDOOLA, A. & ARTIS, D. 2010. IL25 elicits a multipotent progenitor cell population that promotes TH2 cytokine responses. *Nature,* 464**,** 1362.

SAKURAI, H., CHIBA, H., MIYOSHI, H., SUGITA, T. & TORIUMI, W. 1999. IkappaB kinases phosphorylate NF-kappaB p65 subunit on serine 536 in the transactivation domain. *J Biol Chem,* 274**,** 30353-6.

SALIMI, M., BARLOW, J. L., SAUNDERS, S. P., XUE, L., GUTOWSKA-OWSIAK, D., WANG, X., HUANG, L.-C., JOHNSON, D., SCANLON, S. T., MCKENZIE, A. N. J., FALLON, P. G. & OGG, G. S. 2013. A role for IL-25 and IL-33–driven type-2 innate lymphoid cells in atopic dermatitis. *The Journal of Experimental Medicine,* 210**,** 2939-2950.

SALMOND, R. J., MIRCHANDANI, A. S., BESNARD, A.-G., BAIN, C. C., THOMSON, N. C. & LIEW, F. Y. 2012. IL-33 induces innate lymphoid cell–mediated airway inflammation by activating mammalian target of rapamycin. *Journal of Allergy and Clinical Immunology,* 130**,** 1159-1166.e6.

SANADA, S., HAKUNO, D., HIGGINS, L. J., SCHREITER, E. R., MCKENZIE, A. N. & LEE, R. T. 2007. IL-33 and ST2 comprise a critical biomechanically induced and cardioprotective signaling system. *J Clin Invest,* 117**,** 1538-49.

SANCAK, Y., BAR-PELED, L., ZONCU, R., MARKHARD, A. L., NADA, S. & SABATINI, D. M. 2010. Ragulator-Rag complex targets mTORC1 to the lysosomal surface and is necessary for its activation by amino acids. *Cell,* 141**,** 290-303.

SANDIG, H., JOBBINGS, C. E., ROLDAN, N. G., WHITTINGHAM-DOWD, J. K., ORINSKA, Z., TAKEUCHI, O., AKIRA, S. & BULFONE-PAUS, S. 2013. IL-33 causes selective mast cell tolerance to bacterial cell wall products by inducing IRAK1 degradation. *Eur J Immunol,* 43**,** 979-88.

SANTIAGO-RABER, M.-L., BAUDINO, L., ALVAREZ, M., VAN ROOIJEN, N., NIMMERJAHN, F. & IZUI, S. 2011. TLR7/9-mediated monocytosis and maturation of Gr-1hi inflammatory monocytes towards Gr-1lo resting monocytes implicated in murine lupus. *Journal of Autoimmunity,* 37**,** 171-179.

SANTIAGO-RABER, M.-L., BAUDINO, L. & IZUI, S. 2009a. Emerging roles of TLR7 and TLR9 in murine SLE. *Journal of Autoimmunity,* 33**,** 231-238.

SARBASSOV, D. D., GUERTIN, D. A., ALI, S. M. & SABATINI, D. M. 2005. Phosphorylation and regulation of Akt/PKB by the rictor-mTOR complex. *Science,* 307**,** 1098-101.

SARMA, J. V. & WARD, P. A. 2011. The complement system. *Cell and Tissue Research,* 343**,** 227-235.

SAVINKO, T., MATIKAINEN, S., SAARIALHO-KERE, U., LEHTO, M., WANG, G., LEHTIMÄKI, S., KARISOLA, P., REUNALA, T., WOLFF, H., LAUERMA, A. & ALENIUS, H. 2012. IL-33 and ST2 in Atopic Dermatitis: Expression Profiles and Modulation by Triggering Factors. *Journal of Investigative Dermatology,* 132**,** 1392-1400.

SAXTON, R. A. & SABATINI, D. M. 2017. mTOR Signaling in Growth, Metabolism, and Disease. *Cell,* 168**,** 960-976.

SCHIERING, C., KRAUSGRUBER, T., CHOMKA, A., FRÖHLICH, A., ADELMANN, K., WOHLFERT, E. A., POTT, J., GRISERI, T., BOLLRATH, J., HEGAZY, A. N., HARRISON, O. J., OWENS, B. M. J., LÖHNING, M., BELKAID, Y., FALLON, P. G. & POWRIE, F. 2014. The alarmin IL-33 promotes regulatory T-cell function in the intestine. *Nature,* 513**,** 564.

SCHMITZ, J., OWYANG, A., OLDHAM, E., SONG, Y., MURPHY, E., MCCLANAHAN, T. K., ZURAWSKI, G., MOSHREFI, M., QIN, J., LI, X., GORMAN, D. M., BAZAN, J. F. & KASTELEIN, R. A. 2005a. IL-33, an

Interleukin-1-like Cytokine that Signals via the IL-1 Receptor-Related Protein ST2 and Induces T Helper Type 2-Associated Cytokines. *Immunity,* 23**,** 479-490.

SCOTT, I. C., MAJITHIYA, J. B., SANDEN, C., THORNTON, P., SANDERS, P. N., MOORE, T., GUSCOTT, M., CORKILL, D. J., ERJEFÄLT, J. S. & COHEN, E. S. 2018. Interleukin-33 is activated by allergen- and necrosis-associated proteolytic activities to regulate its alarmin activity during epithelial damage. *Scientific Reports,* 8**,** 3363.

SEDGER, L. M. & MCDERMOTT, M. F. 2014. TNF and TNF-receptors: From mediators of cell death and inflammation to therapeutic giants – past, present and future. *Cytokine & Growth Factor Reviews,* 25**,** 453-472.

SEEHUS, C. R., KADAVALLORE, A., TORRE, B. D. L., YECKES, A. R., WANG, Y., TANG, J. & KAYE, J. 2017. Alternative activation generates IL-10 producing type 2 innate lymphoid cells. *Nature Communications,* 8**,** 1900.

SEIDELIN, J. B., BJERRUM, J. T., COSKUN, M., WIDJAYA, B., VAINER, B. & NIELSEN, O. H. 2010. IL-33 is upregulated in colonocytes of ulcerative colitis. *Immunology Letters,* 128**,** 80-85.

SEILLET, C., BELZ, G. T. & HUNTINGTON, N. D. 2016. Development, Homeostasis, and Heterogeneity of NK Cells and ILC1. *Curr Top Microbiol Immunol,* 395**,** 37-61.

SEO, D. H., CHE, X., KWAK, M. S., KIM, S., KIM, J. H., MA, H. W., KIM, D. H., KIM, T. I., KIM, W. H., KIM, S. W. & CHEON, J. H. 2017. Interleukin-33 regulates intestinal inflammation by modulating macrophages in inflammatory bowel disease. *Sci Rep,* 7**,** 851.

SERBULEA, V., UPCHURCH, C. M., SCHAPPE, M. S., VOIGT, P., DEWEESE, D. E., DESAI, B. N., MEHER, A. K. & LEITINGER, N. 2018. Macrophage phenotype and bioenergetics are controlled by oxidized phospholipids identified in lean and obese adipose tissue. *Proceedings of the National Academy of Sciences*.

SHEN, H., TESAR, B. M., WALKER, W. E. & GOLDSTEIN, D. R. 2008. Dual Signaling of MyD88 and TRIF are Critical for Maximal TLR4-Induced Dendritic Cell Maturation. *Journal of immunology (Baltimore, Md. : 1950),* 181**,** 1849-1858.

SHI, L. J., LIU, C., LI, J. H., ZHU, X. Y., LI, Y. N. & LI, J. T. 2018. Elevated Levels of Soluble ST2 were Associated with Rheumatoid Arthritis Disease Activity and Ameliorated Inflammation in Synovial Fibroblasts. *Chin Med J (Engl),* 131**,** 316-322.

SHIGEHARA, K., SHIJUBO, N., OHMICHI, M., TAKAHASHI, R., KON, S.-I., OKAMURA, H., KURIMOTO, M., HIRAGA, Y., TATSUNO, T., ABE, S. & SATO, N. 2001. IL-12 and IL-18 Are Increased and Stimulate IFN-γ Production in Sarcoid Lungs. *The Journal of Immunology,* 166**,** 642-649.

SIEDNIENKO, J., HALLE, A., NAGPAL, K., GOLENBOCK, D. T. & MIGGIN, S. M. 2010. TLR3-mediated IFN-beta gene induction is negatively regulated by the TLR adaptor MyD88 adaptor-like. *Eur J Immunol,* 40**,** 3150-60.

SIEGAL, F. P., KADOWAKI, N., SHODELL, M., FITZGERALD-BOCARSLY, P. A., SHAH, K., HO, S., ANTONENKO, S. & LIU, Y.-J. 1999. The Nature of the Principal Type 1 Interferon-Producing Cells in Human Blood. *Science,* 284**,** 1835-1837.

SILVA, A., MAGALHÃES, R., BRANCO, V., SILVA, J., CRUZ, F., MARQUES, P., FERREIRA, T., MORALES, M., MARTINS, M., OLSEN, P. & ROCCO,

P. 2016. The tyrosine kinase inhibitor dasatinib reduces lung inflammation and remodelling in experimental allergic asthma. *British Journal of Pharmacology,* 173**,** 1236-1247.

SINCLAIR, L. V., NEYENS, D., RAMSAY, G., TAYLOR, P. M. & CANTRELL, D. A. 2018. Single cell analysis of kynurenine and System L amino acid transport in T cells. *Nature Communications,* 9**,** 1981.

SINCLAIR, L. V., ROLF, J., EMSLIE, E., SHI, Y.-B., TAYLOR, P. M. & CANTRELL, D. A. 2013a. Control of amino-acid transport by antigen receptors coordinates the metabolic reprogramming essential for T cell differentiation. *Nature Immunology,* 14**,** 500.

SINGH, T. P., ZHANG, H. H., BOREK, I., WOLF, P., HEDRICK, M. N., SINGH, S. P., KELSALL, B. L., CLAUSEN, B. E. & FARBER, J. M. 2016. Monocyte-derived inflammatory Langerhans cells and dermal dendritic cells mediate psoriasis-like inflammation. *Nat Commun,* 7**,** 13581.

SKAUG, B., CHEN, J., DU, F., HE, J., MA, A. & CHEN, ZHIJIAN J. 2011. Direct, Noncatalytic Mechanism of IKK Inhibition by A20. *Molecular Cell,* 44**,** 559-571.

SMITH, K. D., ANDERSEN-NISSEN, E., HAYASHI, F., STROBE, K., BERGMAN, M. A., BARRETT, S. L. R., COOKSON, B. T. & ADEREM, A. 2003. Toll-like receptor 5 recognizes a conserved site on flagellin required for protofilament formation and bacterial motility. *Nature Immunology,* 4**,** 1247.

SMITHGALL, M. D., COMEAU, M. R., PARK YOON, B.-R., KAUFMAN, D., ARMITAGE, R. & SMITH, D. E. 2008. IL-33 amplifies both Th1- and Th2-type responses through its activity on human basophils, allergen-reactive Th2 cells, iNKT and NK Cells. *International Immunology,* 20**,** 1019-1030.

SNELGROVE, R. J., GREGORY, L. G., PEIRÓ, T., AKTHAR, S., CAMPBELL, G. A., WALKER, S. A. & LLOYD, C. M. 2014. Alternaria-derived serine protease activity drives IL-33–mediated asthma exacerbations. *The Journal of Allergy and Clinical Immunology,* 134**,** 583-592.e6.

SOMERS, E. C., MARDER, W., CAGNOLI, P., LEWIS, E. E., DEGUIRE, P., GORDON, C., HELMICK, C. G., WANG, L., WING, J. J., DHAR, J. P., LEISEN, J., SHALTIS, D. & MCCUNE, W. J. 2014. Population-based incidence and prevalence of systemic lupus erythematosus: the Michigan Lupus Epidemiology and Surveillance program. *Arthritis Rheumatol,* 66**,** 369-78.

SONI, C., WONG, E. B., DOMEIER, P. P., KHAN, T. N., SATOH, T., AKIRA, S. & RAHMAN, Z. S. M. 2014. B Cell–Intrinsic TLR7 Signaling Is Essential for the Development of Spontaneous Germinal Centers. *The Journal of Immunology,* 193**,** 4400-4414.

SOUMELIS, V. & LIU, Y. J. 2004. Human thymic stromal lymphopoietin: a novel epithelial cell-derived cytokine and a potential key player in the induction of allergic inflammation. *Springer Semin Immunopathol,* 25**,** 325-33.

SPITS, H., ARTIS, D., COLONNA, M., DIEFENBACH, A., DI SANTO, J. P., EBERL, G., KOYASU, S., LOCKSLEY, R. M., MCKENZIE, A. N. J., MEBIUS, R. E., POWRIE, F. & VIVIER, E. 2013. Innate lymphoid cells — a proposal for uniform nomenclature. *Nature Reviews Immunology,* 13**,** 145.

SPONHEIM, J., POLLHEIMER, J., OLSEN, T., BALOGH, J., HAMMARSTRÖM, C., LOOS, T., KASPRZYCKA, M., SØRENSEN, D. R., NILSEN, H. R., KÜCHLER, A. M., VATN, M. H. & HARALDSEN, G. 2010. Inflammatory Bowel Disease-Associated Interleukin-33 Is Preferentially Expressed in

Ulceration-Associated Myofibroblasts. *The American Journal of Pathology,* 177**,** 2804-2815.

SPOONER, C. J., LESCH, J., YAN, D., KHAN, A. A., ABBAS, A., RAMIREZ-CARROZZI, V., ZHOU, M., SORIANO, R., EASTHAM-ANDERSON, J., DIEHL, L., LEE, W. P., MODRUSAN, Z., PAPPU, R., XU, M., DEVOSS, J. & SINGH, H. 2013. Specification of type 2 innate lymphocytes by the transcriptional determinant Gfi1. *Nat Immunol,* 14**,** 1229-36.

STEGMANN, K. A., DE SOUZA, J. B. & RILEY, E. M. 2015. IL-18-induced expression of high-affinity IL-2R on murine NK cells is essential for NK-cell IFN-gamma production during murine Plasmodium yoelii infection. *Eur J Immunol,* 45**,** 3431-40.

STEIN, M., KESHAV, S., HARRIS, N. & GORDON, S. 1992. Interleukin 4 potently enhances murine macrophage mannose receptor activity: a marker of alternative immunologic macrophage activation. *J Exp Med,* 176**,** 287-92.

STETSON, D. B. & MEDZHITOV, R. 2006. Recognition of Cytosolic DNA Activates an IRF3-Dependent Innate Immune Response. *Immunity,* 24**,** 93-103.

STIER, M. T., ZHANG, J., GOLENIEWSKA, K., CEPHUS, J. Y., RUSZNAK, M., WU, L., VAN KAER, L., ZHOU, B., NEWCOMB, D. C. & PEEBLES, R. S. 2017. IL-33 promotes the egress of group 2 innate lymphoid cells from the bone marrow. *The Journal of Experimental Medicine*.

STRICKSON, S., EMMERICH, C. H., GOH, E. T. H., ZHANG, J. & KELSALL, I. R. 2017a. Roles of the TRAF6 and Pellino E3 ligases in MyD88 and RANKL signaling. 114**,** E3481-e3489.

SU, K., WU, J., EDBERG, J. C., LI, X., FERGUSON, P., COOPER, G. S., LANGEFELD, C. D. & KIMBERLY, R. P. 2004. A promoter haplotype of the immunoreceptor tyrosine-based inhibitory motif-bearing FcgammaRIIb alters receptor expression and associates with autoimmunity. I. Regulatory FCGR2B polymorphisms and their association with systemic lupus erythematosus. *J Immunol,* 172**,** 7186-91.

SUN, S. C. 2009. CYLD: a tumor suppressor deubiquitinase regulating NF-κB activation and diverse biological processes. *Cell Death And Differentiation,* 17**,** 25.

SUNDNES, O., PIETKA, W., LOOS, T., SPONHEIM, J., RANKIN, A. L., PFLANZ, S., BERTELSEN, V., SITEK, J. C., HOL, J., HARALDSEN, G. & KHNYKIN, D. 2015. Epidermal Expression and Regulation of Interleukin-33 during Homeostasis and Inflammation: Strong Species Differences. *Journal of Investigative Dermatology,* 135**,** 1771-1780.

SUWARA, M. I., GREEN, N. J., BORTHWICK, L. A., MANN, J., MAYER-BARBER, K. D., BARRON, L., CORRIS, P. A., FARROW, S. N., WYNN, T. A., FISHER, A. J. & MANN, D. A. 2013. IL-1α released from damaged epithelial cells is sufficient and essential to trigger inflammatory responses in human lung fibroblasts. *Mucosal Immunology,* 7**,** 684.

SUZUKI, M., MORITA, R., HIRATA, Y., SHICHITA, T. & YOSHIMURA, A. 2015. Spred1, a Suppressor of the Ras–ERK Pathway, Negatively Regulates Expansion and Function of Group 2 Innate Lymphoid Cells. *The Journal of Immunology,* 195**,** 1273-1281.

TAIT WOJNO, E. D., MONTICELLI, L. A., TRAN, S. V., ALENGHAT, T., OSBORNE, L. C., THOME, J. J., WILLIS, C., BUDELSKY, A., FARBER, D. L. & ARTIS, D. 2015. The prostaglandin D2 receptor CRTH2 regulates

accumulation of group 2 innate lymphoid cells in the inflamed lung. *Mucosal Immunology,* 8**,** 1313.

TAKATORI, H., KANNO, Y., WATFORD, W. T., TATO, C. M., WEISS, G., IVANOV, I. I., LITTMAN, D. R. & O'SHEA, J. J. 2009. Lymphoid tissue inducer–like cells are an innate source of IL-17 and IL-22. *The Journal of Experimental Medicine,* 206**,** 35-41.

TAKEUCHI, O. & AKIRA, S. 2010. Pattern Recognition Receptors and Inflammation. *Cell,* 140**,** 805-820.

TAKEUCHI, O., HOSHINO, K. & AKIRA, S. 2000. Cutting edge: TLR2-deficient and MyD88-deficient mice are highly susceptible to Staphylococcus aureus infection. *J Immunol,* 165**,** 5392-6.

TANISHIMA, M., TAKASHIMA, S., HONDA, A., YASUDA, D., TANIKAWA, T., ISHII, S. & MARUYAMA, T. 2017. Identification of optineurin as an interleukin-1 receptor-associated kinase 1-binding protein and its role in regulation of MyD88-dependent signaling. *J Biol Chem,* 292**,** 17250-17257.

TAS, S. W., QUARTIER, P., BOTTO, M. & FOSSATI-JIMACK, L. 2006. Macrophages from patients with SLE and rheumatoid arthritis have defective adhesion in vitro, while only SLE macrophages have impaired uptake of apoptotic cells. *Ann Rheum Dis,* 65**,** 216-21.

TAYLOR, M. L. & METCALFE, D. D. 2000. Kit signal transduction. *Hematol Oncol Clin North Am,* 14**,** 517-35.

TEJASVI, T., STUART, P. E., CHANDRAN, V., VOORHEES, J. J., GLADMAN, D. D., RAHMAN, P., ELDER, J. T. & NAIR, R. P. 2012. TNFAIP3 gene polymorphisms are associated with response to TNF blockade in psoriasis. *J Invest Dermatol,* 132**,** 593-600.

TIEDJE, C., RONKINA, N., TEHRANI, M., DHAMIJA, S., LAASS, K., HOLTMANN, H., KOTLYAROV, A. & GAESTEL, M. 2012. The p38/MK2-driven exchange between tristetraprolin and HuR regulates AU-rich element-dependent translation. *PLoS Genet,* 8**,** e1002977.

TOMINAGA, S. 1989. A putative protein of a growth specific cDNA from BALB/c-3T3 cells is highly similar to the extracellular portion of mouse interleukin 1 receptor. *FEBS Lett,* 258**,** 301-4.

TRABANELLI, S., GOMEZ-CADENA, A., SALOME, B., MICHAUD, K., MAVILIO, D., LANDIS, B. N., JANDUS, P. & JANDUS, C. 2018. Human innate lymphoid cells (ILCs): Toward a uniform immune-phenotyping. *Cytometry B Clin Cytom,* 94**,** 392-399.

TRAUTMANN, A., ALTZNAUER, F., AKDIS, M., SIMON, H. U., DISCH, R., BROCKER, E. B., BLASER, K. & AKDIS, C. A. 2001. The differential fate of cadherins during T-cell-induced keratinocyte apoptosis leads to spongiosis in eczematous dermatitis. *J Invest Dermatol,* 117**,** 927-34.

TRIANTAFILOU, M., MANUKYAN, M., MACKIE, A., MORATH, S., HARTUNG, T., HEINE, H. & TRIANTAFILOU, K. 2004. Lipoteichoic acid and toll-like receptor 2 internalization and targeting to the Golgi are lipid raft-dependent. *J Biol Chem,* 279**,** 40882-9.

TSAI, Y. R., WANG, Y. J., LEE, M. R., HSU, M. F. & WANG, J. P. 2013. p38 Mitogen-activated protein kinase and extracellular signal-regulated kinase signaling pathways are not essential regulators of formyl peptide-stimulated p47(phox) activation in neutrophils. *Eur J Pharmacol,* 701**,** 96-105.

TSOKOS, G. C., LO, M. S., REIS, P. C. & SULLIVAN, K. E. 2016. New insights into the immunopathogenesis of systemic lupus erythematosus. *Nature Reviews Rheumatology,* 12**,** 716.

TSUJI-TAKAYAMA, K., SUZUKI, M., YAMAMOTO, M., HARASHIMA, A., OKOCHI, A., OTANI, T., INOUE, T., SUGIMOTO, A., TORAYA, T., TAKEUCHI, M., YAMASAKI, F., NAKAMURA, S. & KIBATA, M. 2008. The production of IL-10 by human regulatory T cells is enhanced by IL-2 through a STAT5-responsive intronic enhancer in the IL-10 locus. *J Immunol,* 181**,** 3897-905.

TUNG, H. Y., PLUNKETT, B., HUANG, S. K. & ZHOU, Y. 2014. Murine mast cells secrete and respond to interleukin-33. *J Interferon Cytokine Res,* 34**,** 141-7.

TURVEY, S. E. & BROIDE, D. H. 2010. Chapter 2: Innate Immunity. *The Journal of allergy and clinical immunology,* 125**,** S24-S32.

TZANAVARI, T., GIANNOGONAS, P. & KARALIS, K. P. 2010. TNF-alpha and obesity. *Curr Dir Autoimmun,* 11**,** 145-56.

UMEBASHI, K., TOKITO, A., YAMAMOTO, M. & JOUGASAKI, M. 2018. Interleukin-33 induces interleukin-8 expression via JNK/c-Jun/AP-1 pathway in human umbilical vein endothelial cells. 13**,** e0191659.

VAN DE VEERDONK, F. L., STOECKMAN, A. K., WU, G., BOECKERMANN, A. N., AZAM, T., NETEA, M. G., JOOSTEN, L. A. B., VAN DER MEER, J. W. M., HAO, R., KALABOKIS, V. & DINARELLO, C. A. 2012. IL-38 binds to the IL-36 receptor and has biological effects on immune cells similar to IL-36 receptor antagonist. *Proceedings of the National Academy of Sciences,* 109**,** 3001-3005.

VAN DER FITS, L., MOURITS, S., VOERMAN, J. S., KANT, M., BOON, L., LAMAN, J. D., CORNELISSEN, F., MUS, A. M., FLORENCIA, E., PRENS, E. P. & LUBBERTS, E. 2009. Imiquimod-induced psoriasis-like skin inflammation in mice is mediated via the IL-23/IL-17 axis. *J Immunol,* 182**,** 5836-45.

VANDEN BERGHE, T., VANLANGENAKKER, N., PARTHOENS, E., DECKERS, W., DEVOS, M., FESTJENS, N., GUERIN, C. J., BRUNK, U. T., DECLERCQ, W. & VANDENABEELE, P. 2010. Necroptosis, necrosis and secondary necrosis converge on similar cellular disintegration features. *Cell Death Differ,* 17**,** 922-30.

VASANTHAKUMAR, A., MORO, K., XIN, A., LIAO, Y., GLOURY, R., KAWAMOTO, S., FAGARASAN, S., MIELKE, L. A., AFSHAR-STERLE, S., MASTERS, S. L., NAKAE, S., SAITO, H., WENTWORTH, J. M., LI, P., LIAO, W., LEONARD, W. J., SMYTH, G. K., SHI, W., NUTT, S. L., KOYASU, S. & KALLIES, A. 2015. The transcriptional regulators IRF4, BATF and IL-33 orchestrate development and maintenance of adipose tissue–resident regulatory T cells. *Nature Immunology,* 16**,** 276.

VASSEN, L., DÜHRSEN, U., KOSAN, C., ZENG, H. & MÖRÖY, T. 2012. Growth factor independence 1 (Gfi1) regulates cell-fate decision of a bipotential granulocytic-monocytic precursor defined by expression of Gfi1 and CD48. *American Journal of Blood Research,* 2**,** 228-242.

VATS, D., MUKUNDAN, L., ODEGAARD, J. I., ZHANG, L., SMITH, K. L., MOREL, C. R., WAGNER, R. A., GREAVES, D. R., MURRAY, P. J. & CHAWLA, A. 2006. Oxidative metabolism and PGC-1beta attenuate macrophage-mediated inflammation. *Cell Metab,* 4**,** 13-24.

VERMI, W., LONARDI, S., MORASSI, M., ROSSINI, C., TARDANICO, R., VENTURINI, M., SALA, R., TINCANI, A., POLIANI, P. L., CALZAVARA-PINTON, P. G., CERRONI, L., SANTORO, A. & FACCHETTI, F. 2009. Cutaneous distribution of plasmacytoid dendritic cells in lupus erythematosus. Selective tropism at the site of epithelial apoptotic damage. *Immunobiology,* 214**,** 877-86.

VERSTREPEN, L., CARPENTIER, I., VERHELST, K. & BEYAERT, R. 2009. ABINs: A20 binding inhibitors of NF-κB and apoptosis signaling. *Biochemical Pharmacology,* 78**,** 105-114.

VILLANUEVA, E., YALAVARTHI, S., BERTHIER, C. C., HODGIN, J. B., KHANDPUR, R., LIN, A. M., RUBIN, C. J., ZHAO, W., OLSEN, S. H., KLINKER, M., SHEALY, D., DENNY, M. F., PLUMAS, J., CHAPEROT, L., KRETZLER, M., BRUCE, A. T. & KAPLAN, M. J. 2011. Netting Neutrophils Induce Endothelial Damage, Infiltrate Tissues, and Expose Immunostimulatory Molecules in Systemic Lupus Erythematosus. *The Journal of Immunology,* 187**,** 538-552.

VON MOLTKE, J., JI, M., LIANG, H.-E. & LOCKSLEY, R. M. 2015. Tuft-cell-derived IL-25 regulates an intestinal ILC2–epithelial response circuit. *Nature,* 529**,** 221.

VON MOLTKE, J., O'LEARY, C. E., BARRETT, N. A., KANAOKA, Y., AUSTEN, K. F. & LOCKSLEY, R. M. 2017. Leukotrienes provide an NFAT-dependent signal that synergizes with IL-33 to activate ILC2s. *The Journal of Experimental Medicine,* 214**,** 27-37.

WALKER, J. A., OLIPHANT, C. J., ENGLEZAKIS, A., YU, Y., CLARE, S., RODEWALD, H.-R., BELZ, G., LIU, P., FALLON, P. G. & MCKENZIE, A. N. J. 2015. Bcl11b is essential for group 2 innate lymphoid cell development. *The Journal of Experimental Medicine,* 212**,** 875-882.

WALLACE, D. J., STRAND, V., MERRILL, J. T., POPA, S., SPINDLER, A. J., EIMON, A., PETRI, M., SMOLEN, J. S., WAJDULA, J., CHRISTENSEN, J., LI, C., DIEHL, A., VINCENT, M. S., BEEBE, J., HEALEY, P. & SRIDHARAN, S. 2017. Efficacy and safety of an interleukin 6 monoclonal antibody for the treatment of systemic lupus erythematosus: a phase II dose-ranging randomised controlled trial. *Annals of the Rheumatic Diseases,* 76**,** 534-542.

WALLRAPP, A., RIESENFELD, S. J., BURKETT, P. R., ABDULNOUR, R.-E. E., NYMAN, J., DIONNE, D., HOFREE, M., CUOCO, M. S., RODMAN, C., FAROUQ, D., HAAS, B. J., TICKLE, T. L., TROMBETTA, J. J., BARAL, P., KLOSE, C. S. N., MAHLAKÕIV, T., ARTIS, D., ROZENBLATT-ROSEN, O., CHIU, I. M., LEVY, B. D., KOWALCZYK, M. S., REGEV, A. & KUCHROO, V. K. 2017. The neuropeptide NMU amplifies ILC2-driven allergic lung inflammation. *Nature,* 549**,** 351.

WANG, C.-H., ENG, H.-L., LIN, K.-H., CHANG, C.-H., HSIEH, C.-A., LIN, Y.-L. & LIN, T.-M. 2011a. TLR7 and TLR8 Gene Variations and Susceptibility to Hepatitis C Virus Infection. *PLOS ONE,* 6**,** e26235.

WANG, J. P., ASHER, D. R., CHAN, M., KURT-JONES, E. A. & FINBERG, R. W. 2007. Cutting Edge: Antibody-Mediated TLR7-Dependent Recognition of Viral RNA. *The Journal of Immunology,* 178**,** 3363-3367.

WANG, K., BALDASSANO, R., ZHANG, H., QU, H. Q., IMIELINSKI, M., KUGATHASAN, S., ANNESE, V., DUBINSKY, M., ROTTER, J. I., RUSSELL, R. K., BRADFIELD, J. P., SLEIMAN, P. M., GLESSNER, J. T.,

WALTERS, T., HOU, C., KIM, C., FRACKELTON, E. C., GARRIS, M., DORAN, J., ROMANO, C., CATASSI, C., VAN LIMBERGEN, J., GUTHERY, S. L., DENSON, L., PICCOLI, D., SILVERBERG, M. S., STANLEY, C. A., MONOS, D., WILSON, D. C., GRIFFITHS, A., GRANT, S. F., SATSANGI, J., POLYCHRONAKOS, C. & HAKONARSON, H. 2010. Comparative genetic analysis of inflammatory bowel disease and type 1 diabetes implicates multiple loci with opposite effects. *Hum Mol Genet,* 19**,** 2059-67.

WANG, S., XIA, P., CHEN, Y., QU, Y., XIONG, Z., YE, B., DU, Y., TIAN, Y., YIN, Z., XU, Z. & FAN, Z. 2017. Regulatory Innate Lymphoid Cells Control Innate Intestinal Inflammation. *Cell,* 171**,** 201-216.e18.

WANG, T., TOWN, T., ALEXOPOULOU, L., ANDERSON, J. F., FIKRIG, E. & FLAVELL, R. A. 2004. Toll-like receptor 3 mediates West Nile virus entry into the brain causing lethal encephalitis. *Nat Med,* 10**,** 1366-73.

WATANABE-FUKUNAGA, R., BRANNAN, C. I., COPELAND, N. G., JENKINS, N. A. & NAGATA, S. 1992. Lymphoproliferation disorder in mice explained by defects in Fas antigen that mediates apoptosis. *Nature,* 356**,** 314.

WEAVER, B. K., BOHN, E., JUDD, B. A., GIL, M. P. & SCHREIBER, R. D. 2007. ABIN-3: a Molecular Basis for Species Divergence in Interleukin-10-Induced Anti-Inflammatory Actions. *Molecular and Cellular Biology,* 27**,** 4603-4616.

WEENING, J. J., D'AGATI, V. D., SCHWARTZ, M. M., SESHAN, S. V., ALPERS, C. E., APPEL, G. B., BALOW, J. E., BRUIJN, J. A., COOK, T., FERRARIO, F., FOGO, A. B., GINZLER, E. M., HEBERT, L., HILL, G., HILL, P., JENNETTE, J. C., KONG, N. C., LESAVRE, P., LOCKSHIN, M., LOOI, L. M., MAKINO, H., MOURA, L. A. & NAGATA, M. 2004. The classification of glomerulonephritis in systemic lupus erythematosus revisited. *J Am Soc Nephrol,* 15**,** 241-50.

WERENSKIOLD, A. K., HOFFMANN, S. & KLEMENZ, R. 1989. Induction of a mitogen-responsive gene after expression of the Ha-ras oncogene in NIH 3T3 fibroblasts. *Molecular and Cellular Biology,* 9**,** 5207-5214.

WEST, A. P., KOBLANSKY, A. A. & GHOSH, S. 2006. Recognition and Signaling by Toll-Like Receptors. *Annual Review of Cell and Developmental Biology,* 22**,** 409-437.

WILHELM, C., HARRISON, O. J. & SCHMITT, V. 2016. Critical role of fatty acid metabolism in ILC2-mediated barrier protection during malnutrition and helminth infection. 213**,** 1409-18.

WILHELM, C., HIROTA, K., STIEGLITZ, B., VAN SNICK, J., TOLAINI, M., LAHL, K., SPARWASSER, T., HELMBY, H. & STOCKINGER, B. 2011. An IL-9 fate reporter demonstrates the induction of an innate IL-9 response in lung inflammation. *Nature Immunology,* 12**,** 1071.

WILLEBRAND, R. & VOEHRINGER, D. 2016. IL-33-Induced Cytokine Secretion and Survival of Mouse Eosinophils Is Promoted by Autocrine GM-CSF. *PLOS ONE,* 11**,** e0163751.

WOLFSON, R. L., CHANTRANUPONG, L., SAXTON, R. A., SHEN, K., SCARIA, S. M., CANTOR, J. R. & SABATINI, D. M. 2016. Sestrin2 is a leucine sensor for the mTORC1 pathway. *Science,* 351**,** 43-48.

WONG, S. H., WALKER, J. A., JOLIN, H. E., DRYNAN, L. F., HAMS, E., CAMELO, A., BARLOW, J. L., NEILL, D. R., PANOVA, V., KOCH, U., RADTKE, F., HARDMAN, C. S., HWANG, Y. Y., FALLON, P. G. &

MCKENZIE, A. N. 2012. Transcription factor RORalpha is critical for nuocyte development. *Nat Immunol,* 13**,** 229-36.

WU, C., WU, Y., CHENG, C., HONG, Z., SHI, Z., LIN, S., LI, J., HE, X. & ZHU, A. 2018. Interleukin-33 Predicts Poor Prognosis and Promotes Renal Cell Carcinoma Cell Growth Through its Receptor ST2 and the JNK Signaling Pathway. *Cellular Physiology and Biochemistry,* 47**,** 191-200.

XIAO, D., PALANI, A., HUANG, X., SOFOLARIDES, M., ZHOU, W., CHEN, X., ASLANIAN, R., GUO, Z., FOSSETTA, J., TIAN, F., TRIVEDI, P., SPACCIAPOLI, P., WHITEHURST, C. E. & LUNDELL, D. 2013. Conformation constraint of anilides enabling the discovery of tricyclic lactams as potent MK2 non-ATP competitive inhibitors. *Bioorganic & Medicinal Chemistry Letters,* 23**,** 3262-3266.

XU, D., JIANG, H.-R., KEWIN, P., LI, Y., MU, R., FRASER, A. R., PITMAN, N., KUROWSKA-STOLARSKA, M., MCKENZIE, A. N. J., MCINNES, I. B. & LIEW, F. Y. 2008. IL-33 exacerbates antigen-induced arthritis by activating mast cells. *Proceedings of the National Academy of Sciences,* 105**,** 10913-10918.

XU, F., LIN, S., YAN, X., WANG, C., TU, H., YIN, Y. & CAO, J. 2018. Interleukin 38 Protects Against Lethal Sepsis. *The Journal of Infectious Diseases,* 218**,** 1175-1184.

XUE, L., SALIMI, M., PANSE, I., MJÖSBERG, J. M., MCKENZIE, A. N. J., SPITS, H., KLENERMAN, P. & OGG, G. 2014. Prostaglandin D₂ activates group 2 innate lymphoid cells through chemoattractant receptor-homologous molecule expressed on T_H2 cells. *Journal of Allergy and Clinical Immunology,* 133**,** 1184-1194.e7.

YAMAMOTO, Y. & GAYNOR, R. B. 2004. IκB kinases: key regulators of the NF-κB pathway. *Trends in Biochemical Sciences,* 29**,** 72-79.

YAMASHITA, M., UKAI-TADENUMA, M., KIMURA, M., OMORI, M., INAMI, M., TANIGUCHI, M. & NAKAYAMA, T. 2002. Identification of a conserved GATA3 response element upstream proximal from the interleukin-13 gene locus. *J Biol Chem,* 277**,** 42399-408.

YANG, Z., SUN, R., GRINCHUK, V., FERNANDEZ-BLANCO, J. A., NOTARI, L., BOHL, J. A., MCLEAN, L. P., RAMALINGAM, T. R., WYNN, T. A., URBAN, J. F., JR., VOGEL, S. N., SHEA-DONOHUE, T. & ZHAO, A. 2013. IL-33-induced alterations in murine intestinal function and cytokine responses are MyD88, STAT6, and IL-13 dependent. *Am J Physiol Gastrointest Liver Physiol,* 304**,** G381-9.

YE, H., ARRON, J. R., LAMOTHE, B., CIRILLI, M., KOBAYASHI, T., SHEVDE, N. K., SEGAL, D., DZIVENU, O. K., VOLOGODSKAIA, M., YIM, M., DU, K., SINGH, S., PIKE, J. W., DARNAY, B. G., CHOI, Y. & WU, H. 2002. Distinct molecular mechanism for initiating TRAF6 signalling. *Nature,* 418**,** 443-7.

YOKOGAWA, M., TAKAISHI, M., NAKAJIMA, K., KAMIJIMA, R., FUJIMOTO, C., KATAOKA, S., TERADA, Y. & SANO, S. 2014. Epicutaneous application of toll-like receptor 7 agonists leads to systemic autoimmunity in wild-type mice: a new model of systemic Lupus erythematosus. *Arthritis Rheumatol,* 66**,** 694-706.

YOKOTA, Y., MANSOURI, A., MORI, S., SUGAWARA, S., ADACHI, S., NISHIKAWA, S. & GRUSS, P. 1999. Development of peripheral lymphoid

organs and natural killer cells depends on the helix-loop-helix inhibitor Id2. *Nature,* 397**,** 702-6.

YONA, S., KIM, K.-W., WOLF, Y., MILDNER, A., VAROL, D., BREKER, M., STRAUSS-AYALI, D., VIUKOV, S., GUILLIAMS, M., MISHARIN, A., HUME, DAVID A., PERLMAN, H., MALISSEN, B., ZELZER, E. & JUNG, S. 2013. Fate Mapping Reveals Origins and Dynamics of Monocytes and Tissue Macrophages under Homeostasis. *Immunity,* 38**,** 79-91.

YOON, B. R., OH, Y. J., KANG, S. W., LEE, E. B. & LEE, W. W. 2018. Role of SLC7A5 in Metabolic Reprogramming of Human Monocyte/Macrophage Immune Responses. *Front Immunol,* 9**,** 53.

YOSHIMOTO, S., NAKATANI, K., IWANO, M., ASAI, O., SAMEJIMA, K.-I., SAKAN, H., TERADA, M., HARADA, K., AKAI, Y., SHIIKI, H., NOSE, M. & SAITO, Y. 2007. Elevated Levels of Fractalkine Expression and Accumulation of CD16+ Monocytes in Glomeruli of Active Lupus Nephritis. *American Journal of Kidney Diseases,* 50**,** 47-58.

YU, Y.-R. A., O'KOREN, E. G., HOTTEN, D. F., KAN, M. J., KOPIN, D., NELSON, E. R., QUE, L. & GUNN, M. D. 2016. A Protocol for the Comprehensive Flow Cytometric Analysis of Immune Cells in Normal and Inflamed Murine Non-Lymphoid Tissues. *PLOS ONE,* 11**,** e0150606.

ZAISS, D. M. W., GAUSE, W. C., OSBORNE, L. C. & ARTIS, D. 2015. Emerging functions of amphiregulin in orchestrating immunity, inflammation and tissue repair. *Immunity,* 42**,** 216-226.

ZANDI, E., ROTHWARF, D. M., DELHASE, M., HAYAKAWA, M. & KARIN, M. 1997. The IkappaB kinase complex (IKK) contains two kinase subunits, IKKalpha and IKKbeta, necessary for IkappaB phosphorylation and NF-kappaB activation. *Cell,* 91**,** 243-52.

ZARU, R., EDGAR, A. J., HANAUER, A. & WATTS, C. 2015. Structural and functional basis for p38-MK2-activated Rsk signaling in toll-like receptor-stimulated dendritic cells. *Mol Cell Biol,* 35**,** 132-40.

ZARU, R., RONKINA, N., GAESTEL, M., ARTHUR, J. S. & WATTS, C. 2007. The MAPK-activated kinase Rsk controls an acute Toll-like receptor signaling response in dendritic cells and is activated through two distinct pathways. *Nat Immunol,* 8**,** 1227-35.

ZHANG, S.-Y., JOUANGUY, E., UGOLINI, S., SMAHI, A., ELAIN, G., ROMERO, P., SEGAL, D., SANCHO-SHIMIZU, V., LORENZO, L., PUEL, A., PICARD, C., CHAPGIER, A., PLANCOULAINE, S., TITEUX, M., COGNET, C., VON BERNUTH, H., KU, C.-L., CASROUGE, A., ZHANG, X.-X., BARREIRO, L., LEONARD, J., HAMILTON, C., LEBON, P., HÉRON, B., VALLÉE, L., QUINTANA-MURCI, L., HOVNANIAN, A., ROZENBERG, F., VIVIER, E., GEISSMANN, F., TARDIEU, M., ABEL, L. & CASANOVA, J.-L. 2007. TLR3 Deficiency in Patients with Herpes Simplex Encephalitis. *Science,* 317**,** 1522-1527.

ZHANG, T., INESTA-VAQUERA, F., NIEPEL, M., ZHANG, J., FICARRO, S. B., MACHLEIDT, T., XIE, T., MARTO, J. A., KIM, N., SIM, T., LAUGHLIN, J. D., PARK, H., LOGRASSO, P. V., PATRICELLI, M., NOMANBHOY, T. K., SORGER, P. K., ALESSI, D. R. & GRAY, N. S. 2012. Discovery of potent and selective covalent inhibitors of JNK. *Chemistry & biology,* 19**,** 140-154.

ZHAO, J., WEI, J., BOWSER, R. K., TRAISTER, R. S., FAN, M.-H. & ZHAO, Y. 2015. Focal adhesion kinase-mediated activation of glycogen synthase kinase

3β regulates IL-33 receptor internalization and IL-33 signaling. *Journal of immunology (Baltimore, Md. : 1950),* 194**,** 795-802.

ZHAO, J., WEI, J., MIALKI, R. K., MALLAMPALLI, D. F., CHEN, B. B., COON, T., ZOU, C., MALLAMPALLI, R. K. & ZHAO, Y. 2012. F-box protein FBXL19–mediated ubiquitination and degradation of the receptor for IL-33 limits pulmonary inflammation. *Nature immunology,* 13**,** 651-658.

ZHOU, J., WU, R., HIGH, A. A., SLAUGHTER, C. A., FINKELSTEIN, D., REHG, J. E., REDECKE, V. & HÄCKER, H. 2011. A20-binding inhibitor of NF-κB (ABIN1) controls Toll-like receptor-mediated CCAAT/enhancer-binding protein β activation and protects from inflammatory disease. *Proceedings of the National Academy of Sciences,* 108**,** E998-E1006.

ZHOU, Q., YU, X., DEMIRKAYA, E., DEUITCH, N., STONE, D., TSAI, W. L., KUEHN, H. S., WANG, H., YANG, D., PARK, Y. H., OMBRELLO, A. K., BLAKE, M., ROMEO, T., REMMERS, E. F., CHAE, J. J., MULLIKIN, J. C., GÜZEL, F., MILNER, J. D., BOEHM, M., ROSENZWEIG, S. D., GADINA, M., WELCH, S. B., ÖZEN, S., TOPALOGLU, R., ABINUN, M., KASTNER, D. L. & AKSENTIJEVICH, I. 2016. Biallelic hypomorphic mutations in a linear deubiquitinase define otulipenia, an early-onset autoinflammatory disease. *Proceedings of the National Academy of Sciences of the United States of America,* 113**,** 10127-10132.

ZHOU, Y., JI, Y., WANG, H., ZHANG, H. & ZHOU, H. 2018a. IL-33 Promotes the Development of Colorectal Cancer Through Inducing Tumor-Infiltrating ST2L(+) Regulatory T Cells in Mice. 17**,** 1533033818780091.

ZHOU, Y., WANG, W., ZHAO, C., WANG, Y., WU, H., SUN, X., GUAN, Y. & ZHANG, Y. 2018b. Prostaglandin E2 Inhibits Group 2 Innate Lymphoid Cell Activation and Allergic Airway Inflammation Through E-Prostanoid 4-Cyclic Adenosine Monophosphate Signaling. *Frontiers in Immunology,* 9.

ZONCU, R., EFEYAN, A. & SABATINI, D. M. 2010. mTOR: from growth signal integration to cancer, diabetes and ageing. *Nature Reviews Molecular Cell Biology,* 12**,** 21.

ZUO, X., SUN, L., YIN, X., GAO, J., SHENG, Y., XU, J., ZHANG, J., HE, C., QIU, Y., WEN, G., TIAN, H., ZHENG, X., LIU, S., WANG, W., LI, W., CHENG, Y., LIU, L., CHANG, Y., WANG, Z., LI, Z., LI, L., WU, J., FANG, L., SHEN, C., ZHOU, F., LIANG, B., CHEN, G., LI, H., CUI, Y., XU, A., YANG, X., HAO, F., XU, L., FAN, X., LI, Y., WU, R., WANG, X., LIU, X., ZHENG, M., SONG, S., JI, B., FANG, H., YU, J., SUN, Y., HUI, Y., ZHANG, F., YANG, R., YANG, S. & ZHANG, X. 2015. Whole-exome SNP array identifies 15 new susceptibility loci for psoriasis. *Nat Commun,* 6**,** 6793.

ZYKOVA, S. N., SEREDKINA, N., BENJAMINSEN, J. & REKVIG, O. P. 2008. Reduced fragmentation of apoptotic chromatin is associated with nephritis in lupus-prone (NZB x NZW)F(1) mice. *Arthritis Rheum,* 58**,** 813-25.

Appendices

Appendix A:

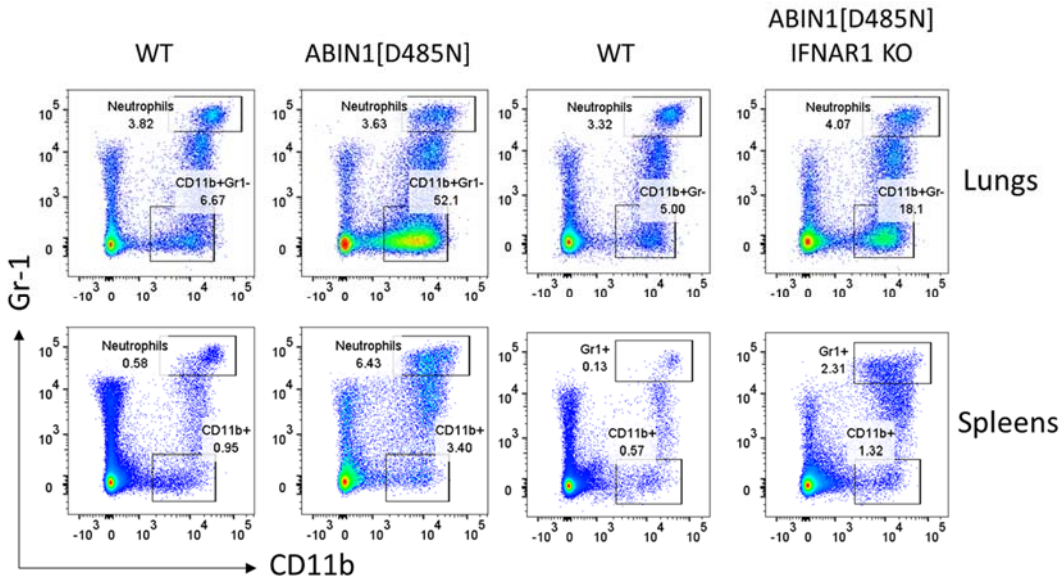

Figure 6.1
Spleen and lungs cells isolated from 4 months old WT, ABIN1[D485N], IFNAR1 KO, and ABIN1[D485N]xIFNAR1 were analysed for expression of CD45 (APC/Efluor780), NK1.1 (FITC), Gr-1 (PerCp/.Cy5.5),CD11b (Pe/Cy7) and CD11c(APC) and DAPI. Cells were first gated on FSC-A and SSC-A, DAPI negative live cells were gated for further characterisation. Cells were then analysed for expression of CD45 and NK1.1. $CD45^{+ve}NK1.1^{+ve}$ population was further gated for expression of Gr-1 and CD11b. The representative FACS plots show $CD45^{+ve}NK1.1^{+ve}Gr\text{-}1^{high}$ and $CD45^{+ve}NK1.1^{+ve}Gr\text{-}1^{-ve}$ populations in the spleen and lungs of the corresponding genotypes.

Appendix B:

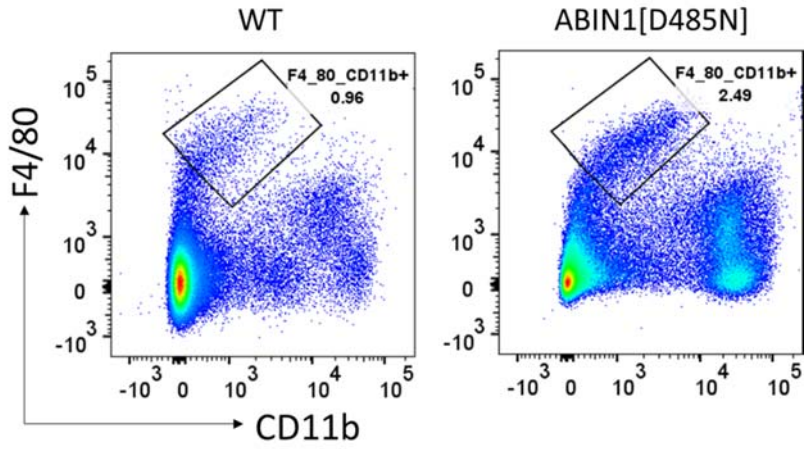

Figure 6.2
Spleen cell susprensions from 6 months old WT and ABIN1[D485N were stained with antibodies against F4/80 (APC), CD11b (Pe/Cy7), CD72 (PE), CX_3CR1 (BV510) and Ly6C(BV421) and DAPI. Cells were first gated on FSC-A and SSC-A, DAPI negative live cells were gated for further characterisation. The representative FACS plots show expression of percentages of $F4/80^{+ve}CD11b^{+ve}$ cells from all live cells.